

2015

**Rehabilitation of contaminated surface and groundwater for selected sites in the Illawarra and Sydney regions utilising carbon nanotube technology, nanofiltration system and reverse osmosis**

Hamad Nasser Altalyan

Follow this and additional works at: <https://ro.uow.edu.au/theses>

**University of Wollongong**

**Copyright Warning**

You may print or download ONE copy of this document for the purpose of your own research or study. The University does not authorise you to copy, communicate or otherwise make available electronically to any other person any copyright material contained on this site.

You are reminded of the following: This work is copyright. Apart from any use permitted under the Copyright Act 1968, no part of this work may be reproduced by any process, nor may any other exclusive right be exercised, without the permission of the author. Copyright owners are entitled to take legal action against persons who infringe their copyright. A reproduction of material that is protected by copyright may be a copyright infringement. A court may impose penalties and award damages in relation to offences and infringements relating to copyright material.

Higher penalties may apply, and higher damages may be awarded, for offences and infringements involving the conversion of material into digital or electronic form.

Unless otherwise indicated, the views expressed in this thesis are those of the author and do not necessarily represent the views of the University of Wollongong.

---

**Recommended Citation**

Altalyan, Hamad Nasser, Rehabilitation of contaminated surface and groundwater for selected sites in the Illawarra and Sydney regions utilising carbon nanotube technology, nanofiltration system and reverse osmosis, Doctor of Philosophy thesis, School of Earth and Environmental Sciences, University of Wollongong, 2015. <https://ro.uow.edu.au/theses/4533>

## **UNIVERSITY OF WOLLONGONG**

### **COPYRIGHT WARNING**

You may print or download ONE copy of this document for the purpose of your own research or study. The University does not authorise you to copy, communicate or otherwise make available electronically to any other person any copyright material contained on this site. You are reminded of the following:

Copyright owners are entitled to take legal action against persons who infringe their copyright. A reproduction of material that is protected by copyright may be a copyright infringement. A court may impose penalties and award damages in relation to offences and infringements relating to copyright material. Higher penalties may apply, and higher damages may be awarded, for offences and infringements involving the conversion of material into digital or electronic form.



**Faculty of Science, Medicine and Health**

**Rehabilitation of contaminated surface and groundwater for  
selected sites in the Illawarra and Sydney regions utilising carbon  
nanotube technology, nanofiltration system and reverse osmosis**

**Hamad Nasser Altalyan**

**This thesis is presented as part of the requirements for the  
award of the Degree of the Doctor of Philosophy**

**University of Wollongong**

**Nov, 2015**

## ***DECLARATION***

I, Hamad Nasser Altalyan, declare that this thesis, submitted in fulfilment of the requirements for awarding the degree of Doctor of Philosophy, in the School of Science, Medicine and Health, University of Wollongong, is wholly my own work unless otherwise referenced or acknowledged. This document has not been submitted for qualifications at any other academic institution. Any contribution made to the research by others, with whom I have worked at University of Wollongong or elsewhere is explicitly acknowledged in the thesis.

Hamad Nasser Altalyan

November, 2015



## ***ABSTRACT***

The occurrence and fate of both organic and inorganic contaminants in the aquatic environment has been recognised as a critical issue of public health and environmental concern. Treated contaminated surface and groundwater is a valuable water source that can be reclaimed for diverse purposes. However, with the intention of minimizing health and environmental risks and maintaining sufficient levels of sustainable water sources, advanced treatment is required. Membrane technology can be used for better treatment of contaminated surface and groundwater and it can be said that membrane technology is a promising technology for removal of trace organic and inorganic contaminants for environmental friendly water reuse. A comprehensive study was conducted to examine the removal of two main contaminant groups that are of concern in aquatic resources namely volatile organic compounds (VOCs) and cations and anions which exist in surface and groundwater in the Illawarra and Sydney regions. The ability of nanofiltration (NF) or reverse osmosis (RO) and carbon nanotube (CNT) systems as advanced treatment was investigated using two commercially available NF or RO membranes and multi-walled carbon nanotube (MWNT) buckypapers. Laboratory-scale tests were used with both cross-flow cell and dead-end stirred-cell filtration; tests were conducted with 21 ubiquitous compounds that represented the significant volatile organic compounds and 10 inorganic compounds representing cations and anions commonly found in contaminated surface and groundwater.

The results reported in this study indicate that the removal efficiency of reverse osmosis (RO) was better than NF and MWNT in rejecting both organic and inorganic contaminants detected in surface and groundwater. This study revealed that the removal efficiency of RO in rejecting organic contaminants ranged between 43.4 - 100 %, whereas the removal efficiency of RO in rejecting inorganic contaminants ranged between 76 - 100 %. Also this study concluded that the removal efficiency of NF in rejecting organic contaminants ranged between 27.6 - 98.4 %. In contrast, the removal efficiency of NF-90 in rejecting inorganic contaminants ranged between 60 - 100 %. It is notable that the removal efficiency of MWNT in rejecting organic and inorganic contaminants was the lowest compared to the removal efficiency of RO and NF. This study showed that the removal efficiency of MWNT in rejecting

organic contaminants ranged between 33.1 - 88.5 %. On the other hand, the removal efficiency of MWNT in rejecting inorganic contaminants ranged between 1.3 - 69.2%. Consequently, it can be concluded that RO is considered the best and most effective system to retain contaminants from surface and groundwater.

Additionally, this study revealed that the performance of NF and RO membranes in rejecting hydrophilic volatile organic compounds was higher than that for hydrophobic compounds and the highest rejection achieved by NF and RO membranes amounted 98.4 % and 100 %, respectively. Hydrophilic compounds can be effectively rejected by NF/RO membranes using the size exclusion mechanism (steric hindrance), whereas hydrophobic compounds can be adsorbed into NF/RO membranes and then diffuse through the dense polymeric matrix, resulting in the lower removal for these compounds compared to hydrophilic compounds. Furthermore, the findings in this study indicate that the performance of the NF and RO membranes in rejecting divalent ions was higher than that for monovalent ion rejection and this can be attributed to multivalent ions with large hydrated radii (e.g.  $Mg^{2+}$ ,  $Ca^{2+}$  and  $SO_4^{2-}$ ) being retained more than monovalent ions with smaller hydrated radii (e.g.  $K^+$  and  $Na^+$ ). The removal efficiency of the NF membrane ranged from 85.9 to 98.3 % for cations, compared with anions, which showed a lower rejection ranging from 71.4 to 99 %. On the other hand, the removal efficiency of the RO membrane ranged from 94.1 to 98.4 % for cations while anion rejection ranged from 89.5 to 99.7 %.

The electrical, mechanical and morphological properties of MWNT buckypaper membranes have been characterised and are compared to those of the corresponding buckypaper membranes containing the same surfactant Triton X-100. Analysis of scanning electron microscopic images of the surfaces of MWNT/Triton X-100 buckypapers revealed that the diameter of their surface pores ( $65.6 \pm 2$  nm) was marginally smaller than that of the corresponding materials prepared using MWNTs ( $80 \pm 2$  nm). In contrast, the average internal pore diameter of MWNT buckypapers ( $27.7 \pm 2$  nm) was found to be slightly higher than that of their MWNT counterparts ( $24 \pm 1$  nm), after analysis of binding isotherms derived from nitrogen adsorption/desorption measurements performed on the materials. The performance of MWNT buckypaper membranes in rejecting hydrophilic compounds was higher than

hydrophobic compounds and the highest rejection reached 88.5 %, however it remained less efficient than NF and RO membranes in rejecting VOCs. Also the results revealed that phosphate recorded the highest value of rejection achieved by MWNT buckypaper membranes for cations and anions and amounted 69.2% and this can be attributed to the charge repulsion mechanism.

The relationship of seasonal effects using membrane technology was also investigated in this study. Results indicate that flux was good for samples which were collected from contaminated surface and groundwater in all seasons except samples which were collected from the leachate pond at Russell Vale, specifically in the summer season due to fouling. High temperatures and light intensity as well as nutrient availability in this season enhance the growth and photosynthesis process and result in high release of extracellular organic matter (EOM). Accordingly, the existence of EOM in the reservoir frequently clogs the pores of membranes, leading to permeate flux decline.

## ***DEDICATION***

I dedicate this work to my best and greatest people who have touched my life and reached me to this level of knowledge...

*My father*

*My mother*

*My wife*

The sacrifices you have taught me the meaning of unconditional love. I love you all and I appreciate your guidance and your support. This work is a simple gift for you.

## ***ACKNOWLEDGEMENTS***

This thesis has proven that there is no impossible in the world of knowledge if there is enthusiasm, determination and the availability of academic competencies, capabilities and advanced technologies, and that's really what I found at the University of Wollongong. Throughout my studies for a PhD I have got tremendous support and encouragement, and currently it has ended and will be the start of a new life research.

First of all, I am grateful to the almighty Allah [God] for granting me health and guidance through my life and gracing me with his uncountable blessing, so I can reach 'finish line' of my thesis completion.

Many people have contributed directly or indirectly in the completion of this thesis and for this reason, they deserve credit and appreciation.

I would like to express my considerable gratitude to my supervisors, Assoc. Prof. Brian Jones and Principal Honorary Fellow Dr John Bradd, for their guidance, extensive support, inspiration and for having me in their research world since I have gained knowledge and experience which I would not have received without their distinguished understanding and support.

I also would like to thank the Ministry Defence in Saudi Arabia and the Royal Saudi Naval Forces for providing me a PhD scholarship with generous financial support for me and my family.

I would like to offer my blessings and regards to my parents, may God bless them and give them his mercy. I wish they were both alive to share with me this a wonderful moment, both of whom are the reason for my success in this life.

A special thank to my brothers and sisters for their moral support and infinite love during the difficult times, while always pushing me to succeed with my studies.

I extend special thanks to all staff and students at the Environmental Engineering and Strategic Water Infrastructure Laboratories, in particular Assoc. Prof. Long Duc Nghiem, Abdulhakeem Alturki, Ling Tie, Takahiro Fujioka, Rajab Abousnina, and

Le Kha Tu for all the support and exchange of knowledge in a very friendly environment.

Big thanks to all staff and students in the Soft Materials group for their help and guidance in carrying out the research. In particular I would like to thank Assoc. Prof. Marc in het Panhuis, Assoc. Prof. Stephen Ralph, Ahmed Alshahrani, Holly and Leighton.

I would also like to thank our collaborators, James Stening, Sylvia Huo and Ivan Ward from Orica and thanks also go to Carl Hopley from Wollongong City Council for their continuous support for my research.

I am greatly indebted to Mr Tony Romeo in the Electron Microscopy Centre, University of Wollongong for his assistance and support with scanning electron microscope (SEM) images.

Finally, from the depth of my heart I would like to thank my wife for her time, caring, patience and understanding throughout the course of this research, particularly when I was spending most of my time in the University while she was looking after our children. Special thanks to my daughters and sons: Sara, Ammgad, Norah, Nasser, Abdullah, Reham and Rand for their patience and understanding during the times of hard work.

## ***TABLE OF CONTENTS***

DECLARATION .....	i
ABSTRACT .....	ii
DEDICATION .....	v
ACKNOWLEDGEMENTS .....	vi
LIST OF FIGURES .....	i
LIST OF TABLES .....	ix
LIST OF ABBREVIATIONS .....	xii
CHAPTER 1: Introduction .....	1
1.1 The importance of alternative water sources .....	1
1.2 Australian surface and groundwater .....	1
1.3 Organic and inorganic contaminants in surface and groundwater .....	4
1.4 The removal of organic and inorganic contaminants by membrane technology .....	6
1.5 Statement of the problem .....	7
1.6 Research objectives .....	8
1.7 Significance .....	8
1.8 Dissertation structure .....	9
CHAPTER 2: Literature review .....	11
2.1 Introduction .....	11
2.2 Organic and inorganic contaminants, definition and types .....	11
2.3 Occurrence of organic and inorganic contaminants in the aquatic environment .....	15
2.4 Effects of organic and inorganic compounds on human health and the environment .....	17
2.5 Fate and transport of contaminants to aquatic sources .....	20
2.6 Conventional treatment processes .....	21
2.6.1 Coagulation .....	21
2.6.2 Sedimentation .....	22
2.6.3 Chemical precipitation .....	23
2.6.4 Adsorption .....	23
2.6.5 Ion exchange .....	24
2.7 Membrane technology .....	25

2.7.1	Nanofiltration (NF) system .....	30
2.7.2	Reverse osmosis (RO) system.....	33
2.7.3	Carbone nanotube (CNTs) technology .....	35
2.8	Factors affecting the removal of organic and inorganic compounds by membrane technology.....	40
2.9	Factors affecting the rejection of organic and inorganic compounds by NF/RO.....	41
2.10	Factors affecting the adsorption of organic and inorganic compounds by CNTs.....	56
2.11	Development of antifouling membranes for water treatment .....	59
2.11.1	Surface modification of membranes .....	60
2.13	Summary .....	64
CHAPTER 3: Materials and Methods .....		66
3.1	Introduction .....	66
3.2	Study area.....	66
3.2.1	Russell Vale Golf Course.....	67
3.2.2	Botany Industrial Park groundwater .....	69
3.3	Weather data for Russell Vale and Botany areas .....	72
3.4	Laboratory-scale set-ups .....	73
3.4.1	Pressure driven membrane filtration system.....	74
3.4.2	Dead-end filtration cell setup.....	75
3.5	Membranes and membrane modules.....	78
3.5.1	Nanofiltration and reverse osmosis (NF/RO) membranes .....	78
3.5.2	Carbon nanotube (CNT) membrane.....	78
3.6	Membrane characterization technique .....	82
3.6.1	Membrane characterization techniques for NF/RO membranes....	82
3.6.2	Membrane characterization techniques for CNT membrane .....	83
3.7	Water permeability experiments of CNT.....	86
3.8	Model contaminated water .....	87
3.9	Model organic and inorganic contaminants .....	88
3.10	Analytical techniques .....	95
3.10.1	Analysis of basic water parameters.....	95
3.10.2	Organic and inorganic component analysis .....	98



3.11	Experimental protocols .....	102
3.11.1	Pressure driven membrane filtration experimental protocol.....	102
3.11.2	The dead-end filtration experimental protocol.....	103
CHAPTER 4: The removal of organic contaminants by using NF/RO filtration system.....		104
4.1	Introduction .....	104
4.2	Materials and methods .....	106
4.2.1	Model organic contaminants .....	106
4.3	Results and discussion .....	107
4.3.1	Characterization of NF-90 and ESPA2 membranes.....	107
4.4	Removal of organic contaminants (volatile organic compounds) by the NF/RO system .....	119
4.4.2	Performance of the NF/RO membranes.....	124
4.5	Conclusion .....	128
CHAPTER 5: The removal of organic contaminants by using MWNT buckypaper membrane.....		130
5.1	Introduction .....	130
5.2	Materials and methods .....	131
5.2.1	Model organic contaminants .....	132
5.3	Results and discussion .....	132
5.3.1	Optimisation of sonication time .....	132
5.3.2	AFM, SEM-EDS and BET analysis.....	134
5.3.3	Physical properties of MWNT buckypapers .....	143
5.3.4	Hydrophobicity of MWNT buckypapers .....	147
5.3.5	Water permeability experiments of MWNT buckypapers .....	148
5.3.6	Removal of organic contaminants by MWNT buckypaper membrane.....	149
5.3.7	Performance of MWNT buckypaper membrane.....	155
5.4	Conclusion .....	157
CHAPTER 6: The removal of inorganic contaminants by using NF/RO filtration system.....		159
6.1	Introduction .....	159
6.2	Materials and methods .....	161

6.2.1	Model inorganic contaminants .....	161
6.3	Results and discussion .....	162
6.3.1	Characterization of NF-90 and ESPA2 membranes.....	162
6.3.1.1	SEM-EDS analysis.....	162
6.3.2	Removal of inorganic contaminants by the NF/RO system.....	168
6.3.3	Performance of the NF/RO membranes .....	171
6.4	Conclusion .....	180
CHAPTER 7: The removal of inorganic contaminants by using MWNT buckypaper membrane .....		181
7.1	Introduction .....	181
7.2	Materials and methods .....	182
7.3	Results and discussion .....	182
7.3.1	Characterization of MWNT buckypapers .....	182
7.3.2	Removal of inorganic contaminants by MWNT buckypaper membrane.....	185
7.3.3	Performance of The MWNT buckypaper membrane.....	191
7.4	Flux decline .....	194
7.5	Conclusion .....	195
CHAPTER 8: Further discussion: The critical and fundamental findings .....		197
8.1	Introduction .....	197
8.2	The efficiency of membrane technology to treat different kinds of water..... .....	198
8.3	Separation mechanisms .....	203
8.4	Flux decline and roughness .....	206
8.5	SEM-EDS analysis .....	208
8.6	Mitigation of flux decline effects .....	210
8.6.1	Pretreatment .....	211
8.6.2	Membrane modification .....	213
8.6.3	Membrane cleaning.....	214
8.7	Characterisation of MWNT buckypaper membranes .....	216
8.8	The relationship between seasonal effects using membrane technology.	218
8.9	Comparison of common NF/RO membranes widely used in purification..... .....	220

8.10	The comparison among the performance of RO, NF and MWNT membranes for removal of organic and inorganic contaminants.....	223
8.11	Summary .....	224
CHAPTER 9: Conclusions and Recommendations for Future Studies.....		227
REFERENCES .....		234
Thesis related publication.....		260
Appendix A : Illustrates weather data for Russell Vale and Botany Bay areas..		261
Appendix B : Images of the NF-90 and ESPA2 membranes fouled by leachate pond at Russell Vale and WGB32 at Botany Bay in different seasons.....		269
Appendix C : Images of Field Emission Scanning Electron Microscopy (SEM). ...		275

## ***LIST OF FIGURES***

<b>Figure 1-1:</b> Schematic description of the Rehabilitation of contaminated surface and groundwater for selected sites in Illawarra and Sydney regions utilising nanofiltration (NF), reverse osmosis (RO) and carbon nanotube technology (CNT).....	10
<b>Figure 2-1:</b> Schematic diagrams of principal types of membranes (Baker, 2012). ..	25
<b>Figure 2-2:</b> The family of membrane processes (driving forces and applicable size ranges; Fane et al., 2011). .....	26
<b>Figure 2-3:</b> The basic concept of membrane separation process adopted from (Ismail et al., 2009).....	27
<b>Figure 2-4:</b> structure representations of (a) SWCNT and (b) MWNT (Ismail et al., 2009) .....	36
<b>Figure 2-5:</b> Schematic diagram showing how a hexagonal sheet of graphite is ‘rolled’ to form a carbon nanotube (Thostenson et al., 2001).....	37
<b>Figure 2-6:</b> Illustrations of the atomic structure of (a) an armchair and (b) a zigzag nanotube (Paradise and Goswami, 2007).....	37
<b>Figure 2-7:</b> Schematic illustration of the arc-discharge technique (Paradise and Goswami, 2007). .....	38
<b>Figure 2-8:</b> Schematic of the laser ablation process (Paradise and Goswami, 2007). .....	39
<b>Figure 2-9:</b> Major parameters affecting the performance and production of most of membranes. ....	41
<b>Figure 2-10:</b> Pore size distributions of the membrane samples at 8 bar (Košutić et al., 2007). ....	44
<b>Figure 2-11:</b> Streaming potential measurements in the pH range 4.0–8.3: (a) along the surface and through the pores for clean membranes, (b) along the surface in the presence of divalent cations $\text{Ca}^{2+}$ and $\text{Mg}^{2+}$ , (c) through the pores in the presence of divalent cations $\text{Ca}^{2+}$ and $\text{Mg}^{2+}$ , and (d) along the surface in the presence of two concentrations of $\text{CaCl}_2$ (Teixeira et al., 2005). ....	50
<b>Figure 2-12:</b> Conceptual sketch of the swollen membrane matrix for different ionic environments (a: thick electrical double layer at high pH and low ionic strength and b: thin electrical double layer at high ionic strength and low pH; Al-Amoudi, 2010). ....	53

<b>Figure 2-13:</b> Factors affecting the adsorption of organic and inorganic compounds by CNTs * (Ismail et al., 2009).....	57
<b>Figure 3-1:</b> Image illustrates samples sites in the Illawarra (Russell Vale) and Sydney (Botany Bay) regions. ....	67
<b>Figure 3-2:</b> (A) Aerial image for Russell Vale Golf Course Club. (B) Photograph of the leachate pond at Russell Vale Golf Course.....	69
<b>Figure 3-3:</b> Aerial image for Botany Industrial Park (BIP) and nearby areas. ....	70
<b>Figure 3-4:</b> Aerial image of the Botany Industrial Park showing sample collection sites.....	71
<b>Figure 3-5:</b> Photographs of sample sites at Botany Bay. (A) Photograph of EWB13D at Southlands. (B) Photograph of EWB10D at Southlands. (C) Photograph of WGB32 located near the tennis courts.....	72
<b>Figure 3-6:</b> Schematic diagram and photograph of the laboratory-scale pressure driven membrane filtration system.....	75
<b>Figure 3-7:</b> Schematic diagram and photograph of the laboratory-scale dead end filtration cell setup.....	77
<b>Figure 3-8:</b> Structure of surfactant that has been used as CNT dispersant (Triton X-100). ....	79
<b>Figure 3-9:</b> Schematic illustration of the experimental set-up used to disperse MWNTs. Adapted from (Branson, 2013). ....	80
<b>Figure 3-10:</b> Photograph of MWNT buckypaper.....	81
<b>Figure 3-11:</b> Photograph of the vacuum filtration unit used to produce MWNT buckypapers.....	82
<b>Figure 3-12:</b> Photograph of the filter (Stericup Durapore™ 0.45 µm) used for separation of colloidal and suspended materials.....	88
<b>Figure 3-13:</b> Photograph of Water Quality Analyser (MODEL 516).....	98
<b>Figure 3-14:</b> Perkin Elmer Optima 7000 DV ICP-OES (from PerkinElmer, 2013 ). ....	99
<b>Figure 3-15:</b> Metrohm 881 Compact IC Pro Suppression Ion Chromatography (from Metrohm, 2013). ....	100
<b>Figure 3-16:</b> PerkinElmer FIMS 400 (Flow injection mercury system; from PerkinElmer, 2013). ....	101

<b>Figure 3-17:</b> Shimadzu purge and trap/Gas Chromatography/Mass Spectrometer Detector (from Shimadzu, 2013).....	102
<b>Figure 4-1:</b> Zeta potential of the selected membranes (measured at 25 °C, in a background electrolyte solution containing NaCl, CaCl <sub>2</sub> and NaHCO <sub>3</sub> at concentrations of 10 mM, 1 mM, and 1 mM, respectively; pH was adjusted using HCl or KOH solutions).....	108
<b>Figure 4-2:</b> Surface topography image of ESPA2 membrane.....	110
<b>Figure 4-3:</b> Section graph of ESPA2 membrane. ....	110
<b>Figure 4-4:</b> Surface topography image of NF-90 membrane. ....	111
<b>Figure 4-5:</b> Section graph of NF-90 membrane.....	111
<b>Figure 4-6:</b> Plan view images of SIM membrane surfaces reconstructed from AFM roughness statistics for a NF-90 membrane.....	112
<b>Figure 4-7:</b> Plan view images of SIM membrane surfaces reconstructed from AFM roughness statistics for an ESPA2 membrane.....	113
<b>Figure 4-8:</b> SEM images of the (A) virgin ESPA2 membrane, (B) ESPA2 membrane surface fouled by EWB10D and (C) ESPA2 membrane surface fouled by EWB13D at Southlands-Botany Bay. ....	114
<b>Figure 4-9:</b> SEM images of the (A) virgin NF-90 membrane, (B) NF-90 membrane surface fouled by EWB10D and (C) NF-90 membrane surface by fouled EWB13D at Southlands-Botany Bay. ....	115
<b>Figure 4-10:</b> EDS data of the virgin ESPA2 membrane (A), ESPA2 membrane fouled by EWB10D (B) and ESPA2 membrane fouled by EWB13D (C) at Southlands-Botany Bay.....	117
<b>Figure 4-11:</b> EDS data of the virgin NF-90 membrane (A), NF-90 membrane fouled by EWB10D (B) and NF-90 membrane fouled by EWB13D (C) at Southlands-Botany Bay.....	118
<b>Figure 4-12:</b> Overall removal efficiency of the volatile organic compounds which were detected in the contaminated groundwater EWB10D. The NF/RO membrane filtration experiment was conducted at an initial permeate flux of 41 L/m <sup>2</sup> h and temperature of 4 °C, with a cross-flow velocity of 30.4 cm/s. Samples were collected after 1 and 8 hours of filtration.....	121
<b>Figure 4-13:</b> Overall removal efficiency of the selected volatile organic compounds which were detected in the contaminated groundwater EWB13D. The NF/RO	

membrane filtration experiment was conducted at an initial permeate flux of 41 L/m <sup>2</sup> h and temperature of 4 °C, with a cross-flow velocity of 30.4 cm/s. Samples were collected after 1 and 8 hours of filtration.....	123
<b>Figure 4-14:</b> Permeate flux of the NF-90 and ESPA2 as a function of filtration time. Experiments were conducted at an initial permeate flux of 41 L/m <sup>2</sup> h and temperature of 4 °C, with a cross-flow velocity of 30.4 cm/s. Samples were collected after 1 and 8 hours of filtration. Samples were collected from EWB10D-Botany Bay.....	125
<b>Figure 4-15:</b> Permeate flux of the NF-90/ESPA2 membranes as a function of filtration time. Experiments were conducted at an initial permeate flux of 41 L/m <sup>2</sup> h and temperature of 4 °C, with a cross-flow velocity of 30.4 cm/s. Samples were collected after 1 and 8 hours of filtration. Samples were collected from EWB13D-Botany Bay.....	127
<b>Figure 5-1:</b> (a) Absorption spectra of a 0.1% (w/v) MWNT/1% (w/v) Triton-X dispersion taken at different sonication times. (b) Effect of increasing sonication time on the absorbance at 660 nm of the MWNT/Triton X-100 dispersion. ...	133
<b>Figure 5-2:</b> Surface topography image of MWNT/Triton X-100 buckypaper.....	134
<b>Figure 5-3:</b> Section graph of MWNT/Triton X-100 buckypaper.....	135
<b>Figure 5-4:</b> Plan view image of SIM membrane surfaces reconstructed from AFM roughness statistics for MWNT/Triton X-100 buckypaper. ....	135
<b>Figure 5-5:</b> SEM images of the (A) virgin MWNT buckypaper; (B) MWNT buckypaper membrane fouled by EWB10D and (C) MWNT buckypaper membrane fouled by EWB13D at Sutherland Botany Bay.....	136
<b>Figure 5-6:</b> SEM images cross-section (A) virgin MWNT buckypaper; (B) MWNT buckypaper membrane fouled by EWB10D and (C) MWNT buckypaper membrane fouled by EWB13D at Sutherland Botany Bay.....	137
<b>Figure 5-7:</b> EDS data of the virgin MWNT/Triton X-100 buckypaper membrane.	138
<b>Figure 5-8:</b> EDS data of the MWNT/Triton X-100 buckypaper membrane fouled by EWB10D. ....	139
<b>Figure 5-9:</b> EDS data of the MWNT/Triton X-100 buckypaper membrane fouled by EWB13D. ....	139
<b>Figure 5-10:</b> Nitrogen adsorption (blue)/desorption (red) isotherms for MWNT/Triton X-100.....	140

<b>Figure 5-11:</b> Pore size distributions for MWNT buckypaper derived by applying the HK method (blue line) and BJH method (brown line) to data obtained from nitrogen adsorption/desorption isotherms.....	142
<b>Figure 5-12:</b> Current-voltage plots obtained using five different lengths of a strip of gellan gum. The buckypaper was prepared from an 80 mL dispersion using 24 minutes sonication time and filtration through a 0.45 $\mu\text{m}$ nylon membrane.....	144
<b>Figure 5-13:</b> Effect of length on the resistance of buckypapers prepared from a dispersion containing 0.1% (w/v) MWNT and 1% (w/v) Triton X-100.....	145
<b>Figure 5-14:</b> Images of 2 $\mu\text{L}$ water droplets added to the surface of Buckypaper MWNT/Triton X-100 0.6% w/v, Sonicator time 24min final volume 500 ml.	147
<b>Figure 5-15:</b> Effect of pressure on the mass of water permeating across a MWNT/Triton X-100 buckypaper. The slopes of the individual plots give the permeation flux. Data for only selected pressures are shown.....	148
<b>Figure 5-16:</b> Effect of applied pressure on the permeation flux of a MWNT/Triton-X buckypaper. ....	149
<b>Figure 5-17:</b> Overall removal efficiency of the selected VOCs which were detected in contaminated groundwater at EWB10D. MWNT/Triton X-100 buckypaper membrane filtration experiment was conducted at 140 Kpa. Samples were collected after 8 hours of filtration.....	152
<b>Figure 5-18:</b> Overall removal efficiency of the selected VOCs which were detected in contaminated groundwater at EWB13D. MWNT-Triton-X-100 buckypaper membrane filtration experiment was conducted at 140 Kpa. Samples were collected after 8 hours of filtration.....	154
<b>Figure 5-19:</b> Permeate flux of MWNT buckypaper membrane as a function of filtration time. Experiment was conducted at 140 Kpa. Samples were collected after 8 hours of filtration. ....	156
<b>Figure 5-20:</b> Permeate flux of MWNT buckypaper membrane as a function of filtration time. Experiment was conducted at 140 Kpa. Samples were collected after 8 hours of filtration. ....	157
<b>Figure 6-1:</b> SEM images of the (A) virgin ESPA2 membrane, (B) ESPA2 membrane surface fouled by leachate pond-autumn, (C) ESPA2 membrane surface fouled	



by WGB32-spring and (D) ESPA2 membrane surface fouled by WGB32-winter.....	163
<b>Figure 6-2:</b> SEM images of the (A) virgin NF-90 membrane, (B) NF-90 membrane surface fouled by leachate pond-autumn, (C) NF-90 membrane surface fouled by WGB32-spring and (D) NF-90 membrane surface fouled by leachate pond-summer.....	164
<b>Figure 6-3:</b> EDS data of the virgin ESPA2 membrane (A-1 and A-2) and ESPA2 membrane fouled by leachate pond at Russell Vale-autumn (B-1, B-2 and B-3). .....	166
<b>Figure 6-4:</b> EDS data of virgin NF-90 membrane (A-1, A-2 and A-3) and NF-90 membrane fouled by WGB32 at Botany Bay-spring (B-1, B-2 and B-3).....	167
<b>Figure 6-5:</b> Overall removal efficiency of the selected inorganic compounds which were detected in contaminated surface water at Russell Vale. NF/RO membrane filtration experiment was conducted at an initial permeate flux of 41 L/m <sup>2</sup> h at a temperature of 20 °C and a cross-flow velocity of 30.4 cm/s. Samples were collected after 1 and 8 hours of filtration. ....	169
<b>Figure 6-6:</b> Overall removal efficiency of the selected inorganic compounds which were detected in contaminated groundwater at Orica (Botany Bay). NF/RO membrane filtration experiment was conducted at an initial permeate flux of 41 L/m <sup>2</sup> h at a temperature of 20 °C and a cross-flow velocity of 30.4 cm/s. Samples were collected after 1 and 8 hours of filtration. ....	171
<b>Figure 6-7:</b> Permeate flux of (A) the NF-90 and (B) the ESPA2 membranes as a function of filtration time. Experiments were conducted at an initial permeate flux of 41 L/m <sup>2</sup> h, temperature of 20 °C and cross-flow velocity of 30.4 cm/s. Permeate were collected after 8 hours of filtration. Data for samples collected from the leachate pond at Russell Vale.....	173
<b>Figure 6-8:</b> Images demonstrating water samples collected from the leachate pond at Russell Vale before and after using NF-90 (a) and ESPA2 (b) membranes....	174
<b>Figure 6-9:</b> Permeate flux of (A) the NF-90 and (B) the ESPA2 membranes as a function of filtration time. Experiments were conducted at an initial permeate flux of 41 L/m <sup>2</sup> h, temperature of 20 °C and cross-flow velocity of 30.4 cm/s. Permeate were collected after 8 hours of filtration. Data for samples were collected from WGB32 at Botany Bay. ....	177

<b>Figure 6-10:</b> Image demonstrates a water sample, which was collected from WGB32 at Botany Bay, before and after using a NF-90 membrane. ....	178
<b>Figure 7-1:</b> SEM images of the (A) virgin MWNT buckypaper and (B) MWNT buckypaper fouled by leachate pond-winter. ....	183
<b>Figure 7-2:</b> SEM images of the (A) virgin MWNT buckypaper and (B) MWNT buckypaper fouled by leachate pond-winter. ....	184
<b>Figure 7-3:</b> EDS data of the virgin MWNT-Triton X-100 membrane (A and B)...	185
<b>Figure 7-4:</b> EDS data of the MWNT-Triton X-100 membrane fouled by leachate from the pond at Russell Vale in spring (A and B).....	185
<b>Figure 7-5:</b> Overall removal efficiency of the selected inorganic compounds which were detected in contaminated surface water at Russell Vale. MWNT-Triton-X-100 buckypaper membrane filtration experiment was conducted at 140 Kpa and temperature of 20 °C. Samples were collected after 24 hours of filtration.....	188
<b>Figure 7-6:</b> Overall removal efficiency of the selected inorganic compounds which were detected in contaminated groundwater water in WGB32 at Botany Bay. Experiments were conducted at 140 Kpa and temperature of 20 °C. Samples were collected after 24 hours of filtration. ....	190
<b>Figure 7-7:</b> Permeate flux of The MWNT buckypaper membrane as a function of filtration time. Experiment was conducted at 140 Kpa and temperature of 20 °C. Samples used in this experiment were collected from the leachate pond at Russell Vale. ....	192
<b>Figure 7-8:</b> Permeate flux of The MWNT buckypaper membrane as a function of filtration time. Experiment was conducted at 140 Kpa and temperature of 20 °C. Samples were collected from WGB32 at Botany Bay. ....	194
<b>Figure 8-1:</b> Process of membrane fouling (adapted from Wang et al., 2014).....	210
<b>Figure 8-2:</b> Explanation a possible mechanism when <i>Chlorella</i> release EOM in matrix during filtration process (Babel and Takizawa, 2010).....	220
<b>Figure A-1:</b> Illustrates monthly maximum temperature for Russell Vale area [Bellambi AWS (68228) - 2012]. ....	264
<b>Figure A-2:</b> Illustrates monthly maximum temperature for Botany Bay area [Sydney Airport AMO (66037) -2012]. ....	264
<b>Figure A-3:</b> Illustrates monthly rainfall for Russell Vale area [Bellambi AWS (68228) - 2012]. ....	268

<b>Figure A-4:</b> Illustrates monthly rainfall for Botany Bay area [Sydney Airport AMO (66037) -201.....	268
<b>Figure B-1:</b> Image of the NF-90 membrane surface fouled by leachate pond at Russell Vale-autumn.....	269
<b>Figure B-2:</b> Image of the ESPA2 membrane surface fouled by leachate pond at Russell Vale-autumn.....	269
<b>Figure B-3:</b> Image of the NF-90 membrane surface fouled by leachate pond at Russell Vale-winter.....	270
<b>Figure B-4:</b> Image of the ESPA2 membrane surface fouled by leachate pond at Russell Vale-winter.....	270
<b>Figure B-5:</b> Image of the NF-90 membrane surface fouled by leachate pond at Russell Vale-spring.....	271
<b>Figure B-6:</b> Image of the ESPA2 membrane surface fouled by leachate pond at Russell Vale-spring.....	271
<b>Figure B-7:</b> Image of the NF-90 membrane surface fouled by WG32 at Botany Bay-summer.....	272
<b>Figure B-8:</b> Image of the NF-90 membrane surface fouled by WG32 at Botany Bay-autumn.....	272
<b>Figure B-9:</b> Image of the ESPA2 membrane surface fouled by WG32 at Botany Bay-autumn.....	273
<b>Figure B-10:</b> Image of the NF-90 membrane surface fouled by WG32 at Botany Bay-winter.....	273
<b>Figure B-11:</b> Image of the ESPA2 membrane surface fouled by WG32 at Botany Bay-winter.....	274
<b>Figure B-12:</b> Image of the ESPA2 membrane surface fouled by WG32 at Botany Bay-summer.....	274
<b>Figure C-1:</b> Images of Field Emission Scanning Electron Microscopy (SEM) using a JEOL JSM-7500FA - (BRUKER-QUANTAX 400). ....	275

## ***LIST OF TABLES***

<b>Table 1-1:</b> Australian Guidelines for Drinking Water, Livestock and Irrigation Water.....	3
<b>Table 2-1:</b> Production levels and physical-chemical properties for the most common chlorinated solvents.....	13
<b>Table 2-2:</b> The average of two selected locations in Australia comparing with the World Health Organization drinking water guideline.....	20
<b>Table 2-3:</b> Examples of wastewater and water treatment plants using NF/RO membranes. ....	28
<b>Table 2-4:</b> Comparison of membranes (NF/RO).....	30
<b>Table 2-5:</b> Summary of reported inorganic contaminants removal efficiency by various NF membranes. ....	32
<b>Table 2-6:</b> Summary of reported inorganic contaminants removal efficiency by various RO membranes. ....	34
<b>Table 2-7:</b> Expected application areas of carbon nanotubes in the future. ....	35
<b>Table 3-1:</b> Illustrates weather data for Russell Vale area <sup>a</sup> . ....	73
<b>Table 3-2:</b> Illustrates weather data for Botany Bay area <sup>a</sup> .....	73
<b>Table 3-3:</b> Properties of the selected NF/RO membranes.....	78
<b>Table 3-4:</b> Summary of relevant physiochemical properties of selected chlorinated solvents.....	89
<b>Table 3-5:</b> Molecular weight, ionic and hydrated radii for relevant cations and anions. ....	94
<b>Table 3-6:</b> Water quality parameters for samples which were collected from Leachate pond-Russell Vale Golf Course <sup>a</sup> .....	96
<b>Table 3-7:</b> Water quality parameters for samples which were collected from WGB32 located near the tennis courts outside the fenceline-Orica <sup>a</sup> .....	97
<b>Table 4-1:</b> Overall removal efficiency of the volatile organic compounds which were detected in EWB10D at Southlands-Botany Bay. ....	121
<b>Table 4-2:</b> Overall removal efficiency of the volatile organic compounds which were detected in EWB13D at Southlands-Botany Bay. ....	123
<b>Table 4-3:</b> Conductivity, flux, pH, pressure and temperature values measured after 1 hour and 8 hours of filtration for samples which were collected from EWB10D located at Southlands-Orica. ....	126

<b>Table 4-4:</b> Conductivity, flux, pH, pressure and temperature values measured after 1 hour and 8 hours of filtration for samples which were collected from EWB13D located at Southlands-Orica. ....	128
<b>Table 5-1:</b> $^aD_{SEM}$ surface pore diameter derived by Image Analysis of SEM micrographs. All other parameters determined through analysis of results obtained from nitrogen adsorption/desorption isotherms, and compared to findings obtained by Sweetman et al. (2013) for the same type. ....	142
<b>Table 5-2:</b> Physical properties of buckypapers. Values shown are the average of at least 3 samples, with the errors reported determined from the standard deviation obtained from all measurements. ....	146
<b>Table 5-3:</b> Average membrane fluxes determined for MWNT/Triton X-100 compared to the average membrane fluxes obtained by Alcock (2010) and Wise (2011) for the same type. ....	149
<b>Table 5-4:</b> Overall removal efficiency of the selected volatile organic compounds (VOCs) which were detected in EWB10D at Sutherland-Botany Bay.....	151
<b>Table 5-5:</b> Overall removal efficiency of the selected organic compounds (VOCs) which were detected in EWB13D at Sutherland Botany Bay.....	154
<b>Table 6-1:</b> Comparison between permeate flux decline (%) of the NF-90 and ESPA2 membranes for samples collected from the leachate pond at Russell Vale after 8 hours of filtration.....	173
<b>Table 6-2:</b> Conductivity, flux, pH, pressure and temperature values measured after 1 hour and 8 hours of filtration for samples collected from the leachate pond at Russell Vale. ....	175
<b>Table 6-3:</b> Comparison between permeate flux decline (%) of the NF-90 and ESPA2 membranes for samples collected from WGB32 at Botany Bay after 8 hours of filtration.....	176
<b>Table 6-4:</b> Conductivity, flux, pH, pressure and temperature values measured after 1 hour and 8 hours of filtration for samples collected from WGB32 located near the tennis courts outside the Botany Industrial Park (BIP) fenceline at Orica. ....	179
<b>Table 7-1:</b> Overall removal efficiency of the selected inorganic compounds which were detected in contaminated surface water from the leachate pond in Russell Vale. ....	187

<b>Table 7-2:</b> Overall removal efficiency of the selected inorganic compounds which were detected in contaminated groundwater water from WGB32 in Botany Bay. ....	190
<b>Table 7-3:</b> Comparison between permeate flux decline of MWNT membranes for samples collected from the leachate pond at Russell Vale and WGB32 at Botany Bay. ....	195
<b>Table 8-1:</b> Comparison of morphological and mechanical properties of MWNT buckypaper prepared in this study to those of corresponding buckypaper membranes containing same surfactant Triton X-100. ....	218
<b>Table 8-2:</b> Comparison of properties for four NF/RO membranes. ....	221
<b>Table 8-3:</b> The recommended treatment for contaminated waters collected from sites at Russell Vale and Botany Bay. ....	222
<b>Table 8-4:</b> The comparison among the performance of RO, NF and MWNT membranes for removal of organic/inorganic contaminants. ....	224
<b>Table A-1:</b> Illustrates daily maximum temperature for Russell Vale area [Bellambi AWS (68228)] <sup>a</sup> . ....	261
<b>Table A-2:</b> Illustrates area daily maximum temperature for Botany Bay [Sydney Airport AMO (66037) -2011] <sup>a</sup> . ....	262
<b>Table A-3:</b> Illustrates area daily maximum temperature for Botany Bay [Sydney Airport AMO (66037) -2012] <sup>a</sup> . ....	263
<b>Table A-4:</b> Illustrates daily rainfall for Russell Vale area [Bellambi AWS (68228)] <sup>a</sup> . ....	265
<b>Table A-5:</b> Illustrates daily rainfall for Botany Bay area [Sydney Airport AMO (66037) -2011] <sup>a</sup> . ....	266
<b>Table A-6:</b> Illustrates daily rainfall for Botany Bay area [Sydney Airport AMO (66037) -2012] <sup>a</sup> . ....	267

## ***LIST OF ABBREVIATIONS***

Å	Angstrom
A <sub>BET</sub>	Membrane surface area (determined by BET)
AOM	Algal organic matter
APHA	American Public Health Association
AWWA	American Water Works Association
BET	Brunauer, Emmett, and Teller
BIP	Botany Industrial Park
BJH	Barrett, Joyner and Halenda
BP	Buckypaper
BPA	Bisphenol A
CHCs	Chlorinated hydrocarbons
CNT	Carbon nanotube
CNTs	Carbon nanotubes
CVD	Chemical vapour deposition
ρ	Density
d <sub>BET</sub>	Internal pore size (determined by BET)
D <sub>bun</sub>	Carbon nanotube bundle diameter
DBP	Disinfection by product
DNAPLs	Dense non-aqueous phase liquids
DOM	Dissolved organic matter
D <sub>SEM</sub>	Average surface pore diameter
EE2	17α-ethinyl estradiol
EDC	Endocrine distributed compounds
EDTA	Ethylene diamine tetra acetic acid
EDX	Energy dispersive X-ray spectroscopy
EOM	Extracellular organic matter
g	Gram
GAC	Granulated activated carbon
GC-MSD	Gas Chromatography/Mass Spectrometer Detector
Gl	Gigalitres
GTP	Groundwater Treatment Plant

HCs	Hydrocarbons
Hg	Mercury
h	Hour
IC	Ion chromatography
ICI Australia	Imperial Chemical Industries of Australia
ICP-MS	Inductively coupled plasma-mass spectrometry
ICP-OES	Inductively coupled plasma optical emission spectrometry
L	Litre
Log $D$	Effective log water-octanol partitioning coefficient
Log $K_{ow}$	Log octanol-water partitioning coefficient
LNAPLs	Light non-aqueous phase liquids
m	Metre
Me-Hg	Methylmercury
MEMS	Microelectro-mechanical systems
min	Minute
MF	Microfiltration
mol	Mole
MWCO	Molecular weight cut-off
MWNT	Multi-walled carbon nanotube
NAPLs	Non-aqueous phase liquids
NF	Nanofiltration
NOM	Natural organic matter
$\Omega$	Ohm
PA	Polyamide
Pa	Pascal
PCE	Perchloroethene
PEI	Polyethyleneimine
PEO	Poly ethylene oxide
PTFE	Polytetrafluoroethylene
PSD	Pore size distribution
PVA	Polyvinyl alcohol
Ref.	References
RO	Reverse osmosis



s	Second
SAR	Specific adsorption rate
SDI	Silt density index
SDS	Sodium dodecyl sulfate
SEM	Scanning electron microscopy
SVOCs	Semi-volatile organic compounds
SWNT	Single-walled carbon nanotube
R <sub>T</sub>	Total resistance
T	Toughness
TCE	Trichloroethene
TDS	Total dissolved solids
TFC	Thin-film composite
THMs	Trihalomethanes
THg	Total mercury
TOC	Total organic carbon
Trix	Triton X-100
UF	Ultrafiltration
US-EPA	U.S. Environmental Protection Agency
VOCs	Volatile organic compounds
W	Watt
WEF	Water Environment Federation
WWTP	Wastewater treatment plant
(w/v)	Weight per volume
wt. %	Weight percent
E	Young's modulus

## **CHAPTER 1: INTRODUCTION**

### **1.1 The importance of alternative water sources**

Since the world population is gradually increasing, there is a rising demand for water. The world is facing formidable challenges in meeting increasing demands for clean water as the available supplies of freshwater decrease because of extended droughts, population growth, more stringent health-based regulations, and competing demands from industrial users (Savage, 2005). The rates of water consumption in 118 countries demonstrate that one third of the world's population will experience severe water scarcity by 2025 because the supply of fresh water to wells, lakes and rivers is decreasing universally (Higgins et al., 2002). Recently, several issues can be linked to the lack of clean fresh water. For instance, 1.2 billion people lack access to safe drinking water, 2.6 billion do not have adequate sanitation, and millions of people die yearly (3,900 children a day) from diseases transferred through unsafe water or human waste (Shannon et al., 2008).

Traditional fresh water resources such as lakes, rivers, aquifers, rainwater and groundwater are overused or misused; as a result, available water resources (e.g. industrial wastewater, runoff water and municipal wastewater) could be used or managed more effectively to sustain future generations across the globe. For facing increasing domestic, tourist and industrial demand and sustaining growing future generations, intense efforts need to be undertaken towards development of all alternative water sources in order to minimise environmental and health risks, maintain sustainable production and prevent political conflicts (Toze, 2006).

### **1.2 Australian surface and groundwater**

Water is a crucial resource in every society; however in Australia water is scarcer than on any other continent except for Antarctica. Australia is considered to be a country with one of the highest water consumptions at an individual level; almost three quarters of this water's being utilised for irrigated agriculture. The consumption rates are such that more than a quarter of Australia's river basins and more than third

of groundwater organisational units are approaching or exceeding sustainable extraction limits (Higgins et al., 2002).

Australia is a large country (approximately 7.7 million square kilometres) and extends over almost 33° of latitude. It has the highest year to year variability in rainfall of all the continents, and droughts are common. Mean yearly run-off for Australia is 387,000 gigalitres (Gl), but almost half (46%) is in the practically inhabited north of the country (Vardon et al., 2007). Australia has 25,780 Gl of groundwater appropriate for potable, stock and household use and irrigated agriculture that needs to be sustained each year (Thiruvengkatachari et al., 2008). Groundwater is widely used for urban water supplies, agriculture, irrigation, industry and mining. In Australia, some regions, like the drier zones of South Australia, the Northern Territory and the Pilbara, are totally dependent on groundwater. Because of the limits on surface water extraction in the Murray-Darling Basin and the scarcity of surface water resources in other areas, groundwater use across Australia has increased considerably in the last 10 years (Thiruvengkatachari et al., 2008). South Australia, New South Wales and Victoria use more than 60% of the groundwater for irrigation, while Western Australia uses 72% for urban and industrial purposes (Thiruvengkatachari et al., 2008).

Increased demand for water in Australia was identified by (Brodie et al., 2007). They concluded that the incompatibility between growing water demand and decline in water availability is the most significant resource problem in Australia. This can be attributed to population growth, intensive agricultural development, urbanisation, industrial growth and environment requirements. Since groundwater resources support many urban, rural and remote communities around Australia, the Australian government has established many guidelines. These guidelines set significant steps about the quality of water that is anticipated for particular uses. The objective of groundwater protection is to save the groundwater resources in order that they can support their identified beneficial uses and principles in an economically, socially, and environmentally sustainable and acceptable manner. The national guidelines are summarized in Table 1-1 (Sundaram et al., 2009).

**Table 1-1:** Australian Guidelines for Drinking Water, Livestock and Irrigation Water.

PARAMETER	DRINKING WATER (mg/L)		LIVESTOCK	IRRIGATION LTV <sup>a</sup>	IRRIGATION STV <sup>b</sup>
	Health	AESTHETIC	(mg/L)	(mg/L)	(mg/L)
Thermotolerant Coliforms	0 CFU/100 mL	-	100 CFU/100 mL	<10-10000 CFU/100 mL	
Aluminium	NAD	0.2	5	5	20
Antimony	0.003	-	-	-	-
Arsenic	0.007	-	0.55 <sup>c</sup>	0.1	2
Barium	0.7	-	-	-	-
Beryllium	NAD	NAD	-	0.1	0.5
Boron	4	-	5	0.5	Crop dependent
Calcium	-	-	1000	-	-
Cadmium	0.002	-	0.01	0.01	0.05
Chloride	-	250	-	Crop dependent	Crop dependent
Chromium (as VI)	0.05	-	1	0.1	0.2
Cobalt	2	1	0.4 (sheep) 1 (cattle) 5 (pigs/poultry)	0.2	5
Fluoride	1.5	-	2.0	1.0	2.0
Iodide	0.1	-	-	-	-
Iron	-	0.3	-	0.2	10
Lead	0.01	-	0.1	2	5
Lithium	-	-	-	2.5 (0.075 on citrus)	-
Magnesium	-	-	-	-	-
Manganese	0.5	0.1	-	0.2	10
Mercury	0.001	-	0.002	0.002	0.002
Molybdenum	0.05	-	0.15	0.01	0.05
Nickel	0.02	-	2	0.2	2
Selenium	0.01	-	0.02	0.02	0.05
Silver	0.1	-	-	-	-
Sodium	1	180	1	Crop dependent	Crop dependent
Uranium	0.02	-	0.2	0.01	0.1
Vanadium	-	-	-	0.1	0.5
Zinc	-	3	20	2	5
Ammonia (as N)	-	0.41	-	-	-
Nitrite (as N)	0.9	-	9.12	-	-
Nitrate (as N)	11.3	-	90.3	-	-
pH	-	6.5-8.5	-	6-8.5	
Sulfate	500	250	1000	-	-
TDS	-	500	Stock dependent	Site specific	Site specific

<sup>a</sup> LTV denotes long-term trigger value.

<sup>b</sup> STV denotes short-term trigger value.

<sup>c</sup> May be tolerated if not provided as a food additive and natural levels in the diet are low.  
NAD denotes No Available Data.

### **1.3 Organic and inorganic contaminants in surface and groundwater**

Contaminated groundwater with non-aqueous phase liquids (NAPLs), such as volatile organic compounds (VOCs), hydrocarbons (HCs), and polyaromatic hydrocarbons (PAHs), has received growing interest in the last decade (Kamon et al., 2003). Because of their low solubility, NAPLs in contact with environmental waters dissolve slowly, acting as long-term sources of water pollution. Due to their naturally high toxicity, a small amount of NAPL can pollute very large volumes of groundwater (Weiner, 2007). Relative to water density, NAPLs can be classified into dense NAPLs (DNAPLs) and light NAPLs (LNAPLs). Removal of DNAPLs is difficult because they are less water soluble and denser than LNAPLs. When a spill happens, DNAPLs are primarily trapped in the form of immobile blobs or ganglia by capillary forces (Lee et al., 2007). DNAPLs such as trichloroethylene (TCE) and tetrachloroethylene or perchloroethene (PCE) have been extensively used in industry since early in the 20th century (e.g. TCE and PCE are used as extracting solvents, dry cleaning fluids and chemical intermediates; Lee et al., 2007). An extensive use of these petroleum hydrocarbons and chlorinated solvents has caused contamination of huge valuable groundwater resources and has become an urgent environmental issue (Qin et al., 2007). In particular, chlorinated solvents are suspected carcinogens, and for that reason their existence in groundwater is of significant concern (Lee et al., 2007). Because they move readily in subsurface systems and they are resistant to the usual degradation processes, concentrated research efforts should be made to discover effective ways for the exclusion of these compounds (Schüth et al., 2004). The conventional treatment technology for chlorinated hydrocarbon (CHC) polluted sites includes pumping groundwater to the surface and remediating the extracted water by granulated activated carbon (GAC) adsorption or air stripping. This process is inefficient because it usually takes decades to extract the CHCs from the subsurface and requires treatment and removal of large quantities of water. Furthermore, GAC is a non-destructive process, and spent GAC needs disposal or regeneration. Therefore, there is an urgent need for new technologies that remove contaminants in situ (Schüth et al., 2000).

Membrane technology has emerged as a technology of choice in water treatment. It has several advantages over conventional treatment technologies. Currently, many studies have shown that nanofiltration (NF)/reverse osmosis (RO) are considered effective technology to remove chlorinated hydrocarbons from contaminated aquatic resources particularly the semi-volatile organic compounds (SVOCs; Ducom and Cabassud, 1999; Agenson et al., 2003; Agenson and Urase, 2007; Kim et al., 2007).

One of the most recognised examples of inorganic contaminants in aquatic systems is mercury (Hg). Environmental contamination caused by mercury is a vital issue universally. Mercury has been stated to cause numerous neurodegenerative diseases, for instance amyotrophic lateral sclerosis, Alzheimer's disease and Parkinson's disease (Mutter et al., 2004). Both elemental and inorganic mercury compounds have been described as damaging the immune system and kidneys (Holmes et al., 2009). For example, methylmercury (Me-Hg) has been stated to pose dangerous consequences to the cardiovascular and nervous systems (Stern, 2005; Wang et al., 2012b).

Mercury can be transformed to Me-Hg and subsequently accumulated in the food chain, causing a threat to human health. The greatest concern about Hg contamination is the consumption of Me-Hg by fish and marine products and it eventually reaches human as the final consumer for these products (Clarkson, 1993; Li et al., 2009). Hg exists in the environment through natural, anthropogenic and re-emitted sources, while the key anthropogenic sources of Hg contamination in the atmosphere are metropolitan discharges, agricultural materials, mining, combustion and industrial discharges. Also atmospheric deposition is the main pathway for mercury deposition into the environment (Zhang and Wong, 2007).

It is important to remove Hg, particularly from aquatic systems. Traditional treatment processes for Hg, including precipitation, ion exchange; and adsorption, could be effective particularly when the compound is in the soluble and ionic forms. On the other hand, these methods may not be effective when the Hg is in the particulate/colloidal form. The affinity of Hg for particulates makes the use of membrane technology a good choice to remove Hg from wastewater even at low

levels (ng Hg/L; Urgun-Demirtas et al., 2012). Even so, this type treatment is not sufficient to allow reuse of the treated water for potable purposes. Hence, more advanced treatment processes are necessary to get water of better quality.

#### **1.4 The removal of organic and inorganic contaminants by membrane technology**

High pressure membrane filtration such as NF or RO is being increasingly utilized in water and wastewater decontamination, since they represent an exceptionally broad decontamination technology that can deal with a wide range of organic and inorganic pollutants. NF and RO membranes can provide an effective barrier for rejection of these contaminants (Gur-Reznik et al., 2011). Several researchers have studied the effectiveness of membrane technology for eliminating different types of contaminants. For example, Kiso et al. (2001b) reported that high pressure membranes rejected most aromatic pesticides at >92.4%, except tricyclazole. Agenson et al. (2003) also examined the retention of a broad range of organic contaminants by various nanofiltration/reverse osmosis processes and concluded that the retention of all the semi-volatile organic compounds (SVOCs) by the tight membranes (NTR729HF, LF10, UTC70, ES10C) was more than 90% except 2-hydrobenzothiazole that frequently had a lower retention. Radjenovic et al. (2008) reported that the maximum rejections in NF/RO processes were recorded for negatively charged pharmaceuticals ketoprofen, diclofenac and sulfamethoxazole ( $R > 95\%$ ). Additionally, Urgun-Demirtas et al. (2012) reported that both NF and RO were able to remove the target mercury concentration at lower operating pressures (20.7 bars).

Carbon nanotubes (CNTs) have been recognized to play a crucial role as better adsorbents for eliminating various kinds of organic and inorganic contaminants such as dioxin (Richard and Yang, 2001), volatile organic compounds (Agnihotri et al., 2005; Gauden et al., 2006), 1,2-dichlorobenzene (Peng et al., 2003), trihalomethanes (Lu et al., 2005) and many divalent metal ions can be removed from aqueous solution (Rao et al., 2007). For example, Zhang et al. (2011) reported that the adsorption efficiency of olaquinox (OLA) by multi-walled carbon nanotube

(MWNT) could reach 99.7% and, therefore, it can be recommended that MWNT is an exceptional adsorbent for removing this compound from water. Because CNTs show effective removal of natural organic matter (NOM) from water (Lu and Su, 2007), they are considered to have a good potential application to maintain water of high quality. Joseph et al. (2011a) conducted a study to investigate the adsorption of bisphenol A (BPA) and 17 $\alpha$ -ethinyl estradiol (EE2) on single walled carbon nanotubes from seawater and brackish water. They found that the removal efficiency for EE2 (95–98%) was greater than for BPA (75–80%), probably because of its higher  $\log K_{ow}$  value. Additionally, Dumée et al. (2010) investigated the characterization and evaluation of carbon nanotube buckypaper membranes for direct contact membrane distillation and they concluded that the best results gave 99% salt rejection at a flux rate of 12 kg/m<sup>2</sup> h at a water vapour partial pressure difference of 22.7 kPa.

## **1.5 Statement of the problem**

Leachate at many sites in the Illawarra region is completely unsuitable for turfgrass use. For example, the leachate pond at Russell Vale Golf Club has nutrient augmentation, high salinity; excessive bicarbonates and high pH. The sodium level in the dam water is high, indicated by the ratio of sodium to all other cations (specific adsorption rate), and the adapted SAR to Ca and Mg only (Cooper, 2005a). Lawns irrigated with this water could have adverse effects for both turfgrass and the soil environment. Amongst the possible risks associated with irrigation utilising this leachate is degradation to the soil structure. The high dissolved organic matter, suspended solids and total salt concentrations in the leachate can result in the devastation of aggregate stability contributing of reduced soil hydraulic conductivity, elevated susceptibility to surface sealing, runoff and soil erosion issues, soil compaction and reduced soil ventilation (Loncnar et al., 2010).

On the other hand, the groundwater below and close to the Botany Industrial Park (BIP) in Sydney and nearby areas has been polluted with various chemical compounds including chlorinated hydrocarbons (CHCs). This pollution is an inevitable result of industrial activities which have been carried out in these areas for



several decades by Orica's predecessor, Imperial Chemical Industries of Australia (ICI Australia). ICI Australia and other companies carried out many industrial operations using CHCs at the Botany site and spills have seeped into the ground and have gradually leaked through the soil and dissolved, making large plumes of contaminated groundwater (ORICA, 2011). Since most CHCs of environmental concern have very low solubilities in water, the duration of residual and pooled CHCs underneath the water table could take many decades or centuries to dissipate. This depends on local groundwater flow velocities and solubility of the CHCs (Yu and Chou, 2000).

## **1.6 Research objectives**

The objectives of this study are to examine removal mechanisms for contaminants from surface and groundwater, which will be selected from different sites in the Illawarra and Sydney regions utilizing, CNTs and RO/NF systems. Therefore, this study aims to:

1. Investigate the potential of RO/NF and CNT systems in the removal of contaminants from surface and groundwater in different sites in the Illawarra and Sydney regions;
2. Compare these treatment systems and determine the best treatment in terms of cost and effectiveness in the removal of contaminants;
3. Assess the efficiency of these systems in the removal of contaminants compared with conventional treatment systems.

## **1.7 Significance**

The unique and significant contribution this research undertakes is in relation to the collection and analysis of data associated with new materials technology for water treatment purposes. This is achieved by testing different types of polluted surface and groundwater containing a wide range of organic and inorganic contaminants. It provides original scientific research result with direct potential applications for

treating polluted water. The most effective water treatment method will contribute to the removal of organic and inorganic contaminants, and thus improve the beneficial uses of the treated water.

## **1.8 Dissertation structure**

The structure of this dissertation is schematically described in Figure 1-1. The body of the dissertation consists of 9 chapters. Chapter 1 involves a simplified introduction for this dissertation. Chapter 2 presents a comprehensive literature review on the current state of knowledge about contaminated surface and groundwater and how to remove these contaminants by utilising NF/RO filtration systems and CNT technology. This chapter includes recent findings resulting from other studies, which were conducted prior to this dissertation. Detailed descriptions of the selected membranes, organic and inorganic contaminants, as well as the filtration system and protocol used in this research are illustrated in Chapter 3. This is followed by critical evaluation of the three filtration systems which are used in this study: the removal of organic contaminants by using NF/RO filtration system (Chapter 4), the removal of organic contaminants by using CNT technology (Chapter 5), the removal of inorganic contaminants by using NF/RO filtration system (Chapter 6) and the removal of inorganic contaminants by using CNT technology (Chapter 7). Critical and fundamental findings of this study are summarized in the Chapter 8 further discussion: the critical and fundamental findings. This dissertation is finished with various conclusions (Chapter 9) on research outlook with respect to this topic and recommendations for future research to further improve the potential of membrane technology in dealing with organic and inorganic contaminants.

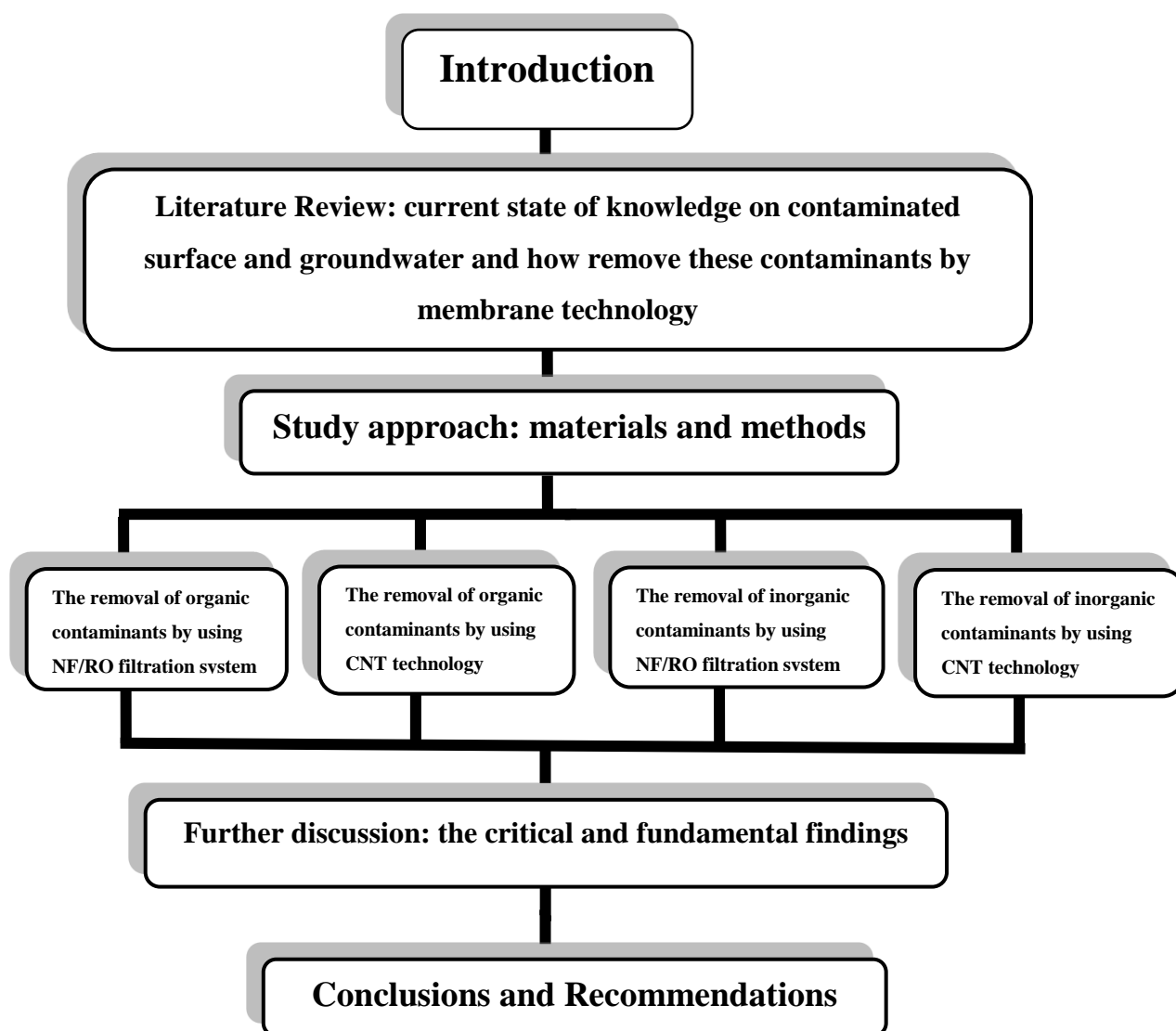


**Figure 1-1:** Schematic description of the Rehabilitation of contaminated surface and groundwater for selected sites in Illawarra and Sydney regions utilising nanofiltration (NF), reverse osmosis (RO) and carbon nanotube technology (CNT).

## **CHAPTER 2: LITERATURE REVIEW**

### **2.1 Introduction**

The occurrence and fate of both organic and inorganic contaminants in the aquatic environment has been documented as a significant issue of public health and environmental concern. A broad range of these contaminants, of either anthropogenic origin or biogenic origin, have been detected and recognised as significant contaminants in water sources, including surface and groundwater. Many organic and inorganic contaminants have a negative effect on aquatic sources; however the most common of these contaminants are non-aqueous phase liquids (e.g. volatile organic compounds, semi-volatile organic compounds and hydrocarbons), cations (e.g. mercury, sodium and calcium) and anions (e.g. phosphate, nitrate, chloride and sulphate).

### **2.2 Organic and inorganic contaminants, definition and types**

Surface and groundwater contaminated with organic and inorganic components have received increasing attention from many scientists in the last few decades. The most common example of organic contaminant that exists in aquatic environments is non-aqueous phase liquids (NAPLs). This group includes, for example, but is not limited to volatile organic compounds (VOCs), semi-volatile organic compounds (SVOCs) and hydrocarbons (HCs). Volatile organic compounds are very important organic contaminants, due to their common use and high toxicity (Jakubowska et al., 2009). Volatile organic compounds in the environment are mostly of anthropogenic origin; however, they could be of biogenic origin but anthropogenic sources cause more concern than natural sources (Chary and Fernandez-Alba, 2012). The Environmental Protection Agency (EPA) definition is “Volatile organic compounds are organic chemical compounds whose composition makes it possible for them to evaporate under normal indoor atmospheric conditions of temperature and pressure” (Ni et al., 2012; USEPA, 2011). On the other hand, the US EPA Terminology Reference System has defined semi-volatile organic compounds as compounds which vaporise comparatively slowly at normal temperature (20 °C) and pressure (1 atm). The most

significant volatile organic compounds are trihalomethanes (THMs) tetrachloromethane, dichloromethane, trichloroethene, dichloroethanes, dichloroethenes, tetrachloroethanes and trichloroethanes. Semi-volatile organic compounds are utilised extensively in industry as solvents, cleaning and degreasing agents. Moreover, semi-volatile organic compounds are used for polymerisation, as blowing agents as well as disinfecting agents (Jakubowska et al., 2009). Semi-volatile organic compounds contain an extensive range of significant contaminants, for instance polycyclic aromatic hydrocarbons (PAHs), organochlorine pesticides (OCPs) and polychlorinated biphenyls (PCBs); they widely exist in air, water, soil as well as biota. Furthermore, these compounds can also be found in remote areas such as the Arctic (Zi-wei et al., 2002; Riget et al., 2004). Production levels and physical-chemical properties for the most common chlorinated solvents are illustrated in Table 2-1.

**Table 2-1:** Production levels and physical-chemical properties for the most common chlorinated solvents.

Compound	CAS number <sup>a</sup>	Molecular weight (g/mol) <sup>a</sup>	Chemical formula <sup>a</sup>	Class <sup>c</sup>	Annual production (10 <sup>6</sup> kg/yr)	Molar Volume cm <sup>3</sup> /mol <sup>a</sup>	Solubility (in water) (10 <sup>-6</sup> kg/L) <sup>b</sup>	Density (g/cm <sup>3</sup> ) at 20° C <sup>a</sup>	EPA MCL (10 <sup>-6</sup> kg/L) <sup>b</sup>	Vapor pressure (Torr) <sup>b</sup>	Boiling point (°C) <sup>a</sup>
1,2-Dichloroethane	107-06-2	98.96	C <sub>2</sub> H <sub>4</sub> Cl <sub>2</sub>	VOC	5871	84.3	8690	1.173	0.005	64	83.5
1,1,1-Trichloroethane	71-55-6	133.40	C <sub>2</sub> H <sub>3</sub> Cl <sub>3</sub>	VOC	294	95.7	1360	1.393	0.2	90	74.1
Carbon tetrachloride	56-23-5	153.82	CCl <sub>4</sub>	VOC	284	90.6	800	1.697	0.005	90	76.0
Methylene chloride	75-09-2	84.93	CH <sub>2</sub> Cl <sub>2</sub>	VOC	255	67.8	20000	1.252	0.005	348	39.6
Chloroform	67-66-3	119.38	CHCl <sub>3</sub>	VOC	191	79.5	8000	1.500	0.01	160	61.2
Tetrachloroethylene	127-18-4	165.83	C <sub>2</sub> Cl <sub>4</sub>	VOC	184	100.3	150	1.653	0.005	14.2	119.1
Trichloroethylene	79-01-6	131.39	C <sub>2</sub> HCl <sub>3</sub>	VOC	75	89.1	1100	1.474	0.005	57.8	87.2
Benzene	71-43-2	78.11	C <sub>6</sub> H <sub>6</sub>	VOC	–	89.4	1780	0.873	0.005	76	78.8
Toluene	108-88-3	92.14	C <sub>7</sub> H <sub>8</sub>	VOC	–	105.7	515	0.871	1	22	110.6

<sup>a</sup> Predicted values from the SciFinder Scholar (ACS) database.<sup>b</sup> (Ajo-Franklin et al., 2006).<sup>c</sup> (Agenson et al., 2003).

In contrast, the most common examples of inorganic contaminants in aquatic environments are cations (e.g. mercury, sodium and manganese). For example, mercury is considered as one of the main hazardous materials by the Agency for Toxic Substances and Disease Registry (ATSDR) due to its toxicity, mobility and long residence time in the atmosphere (Wang et al., 2012b). Because of its remarkable physical and chemical properties, mercury has been broadly utilized in many fields such as industry (e.g., electrical equipment and control devices, the electrolytic preparation of chlorine and alkalis), agriculture (e.g., as pesticides, fungicides and bactericides), dental applications, and products such as thermometers, barometers, bulbs, batteries, paints and cosmetics etc. (Cairns et al., 2011). Sodium has a high solubility in aqueous solutions, where it can reach concentration as high as 15000 mg/L in balance with bicarbonate and or chloride (Franson, 1998). The ratio of sodium to total cations in a soil is important for agriculture and human physiology. In large concentrations it may lead to a negative effect on persons with cardiac difficulties (Franson, 1998). Manganese is an important trace metal for human brains, and it is supplied to the brain through the blood–brain and the blood-cerebrospinal fluid barriers. In industry, manganese has been utilized widely in metallurgy, dry-cell batteries, glass, ceramics, dyes, pigments, soil and food supplements, and medicine for at least 100 years; nevertheless, public concern about environmental contamination in addition to new uses of manganese compounds for magnetic resonance imaging, antiknock agents and fungicides have directed attention to the potential contribution of manganese compounds in causing cancer or malformations (Gerber et al., 2002).

Anions are also common inorganic contaminants that exist in aquatic sources (e.g. chloride, nitrate and sulphate). For example, chloride is a main anionic component of groundwater and it typically exists at concentrations above 5 mg/L. Chloride concentrations above 150 mg/L are toxic to crops and usually inappropriate for irrigation. High chloride concentrations will cause rusty pipes. Water containing more than 350 mg/L chloride is inappropriate for most industrial uses (Hudak, 2000). Nitrate is a compound of nitrogen which exists in reasonable concentrations in many environments. Since it is very soluble, it can be used significantly by plants. The

principal source of all nitrates is atmospheric nitrogen gas. This is transformed to organic nitrogen by some plant species by a process called nitrogen fixation. On the death of the plants the organic compounds are degraded by micro-organisms to inorganic ammonium salts. These are subsequently transformed to nitrates by a process called nitrification (Hounslow, 1995). Sulfate is considered useful in irrigation water, particularly in the presence of calcium. Nevertheless, high levels of sulfate with calcium cause a hard scale in steam boilers. Moreover, sulfate concentrations higher than 500 mg/L can have a laxative consequence on humans (Hudak, 2000).

### **2.3 Occurrence of organic and inorganic contaminants in the aquatic environment**

The occurrence of volatile and semi-volatile organic compounds in the aquatic environment has been a subject of intense scientific investigations over the last decades. Most anthropogenic sources of VOCs to the aquatic environment are paints and coatings, gasoline, solvents, industrial and urban wastewaters, urban and rural run-offs, and atmospheric deposition (Chary and Fernandez-Alba, 2012). VOCs can be present in the environment as pollutants of wastewater, tap water and as vapours (Jakubowska et al., 2009). For example, trichloroethylene (TCE) can reach surface water through direct discharges and groundwater by leaching from waste disposal operation sites (Berkowitz et al., 2008). The concentrations of VOCs in waters and air are very changeable and depend significantly upon atmospheric conditions as a result of washing by rain and evaporation from water through long periods of warm weather (Biziuk and Przyjazny, 1996).

Volatile and semi-volatile organic compounds occur not only in aquatic environments, but they are also present in the atmosphere. Volatile organic compounds reach the atmosphere via evaporation and subsequently they can be returned to the soil and surface waters but in a different form (wet or dry deposition). From water and soil, organic contaminants can go into living organisms either directly or through the food chain (Biziuk and Przyjazny, 1996). The crucial step is when these compounds reach the human body by inhalation, dermal contact or



unintentional ingestion through handmouth contact (Rutkiewicz et al., 2010). SVOCs can occur in the environment via the atmosphere. For instance, in the emissions of incomplete combustion of carbon-based fuels (e.g. PAHs), outgassing from contaminant-containing products previously used in transformers and capacitors (e.g. PCBs) and by spraying onto soils and vegetation (e.g. OCPs; He and Balasubramanian, 2010).

The main anthropogenic sources of mercury as an inorganic contaminant in aquatic systems are through atmospheric deposition, erosion, municipal discharges, agricultural substances, mining, and combustion and industrial discharges (Wang et al., 2004). Furthermore, mercury can be added to the atmosphere through a number of natural processes, including volcanoes and geothermal activities, derivation from surficial soils, water bodies, vegetation surfaces and wild fires as well as the re-emission of deposited mercury (Li et al., 2009). Mercury which is emitted to the atmosphere can be held for between 6 and 24 months and be transported over tens of thousands of kilometres before ultimate re-deposition on the Earth's surface (Dastoor and Larocque, 2004; Wang et al., 2012b). Nitrate is soluble and negatively charged and therefore has a high mobility and is likely to be lost from the unsaturated zone by leaching (Chowdary et al., 2005; Almasri, 2007). Numerous studies have demonstrated a close relationship and connection between agriculture and nitrate concentration in groundwater (Harter et al., 2002; Dunn et al., 2005; Jordan and Smith, 2005; Liu et al., 2005). The wide use of fertilizers is considered to be a key non-point source of nitrate that leaches into groundwater (Chowdary et al., 2005). Additionally, point sources of nitrogen, for example septic systems, are revealed to contribute to nitrate contamination of groundwater (MacQuarrie et al., 2001; Almasri, 2007).

## **2.4 Effects of organic and inorganic compounds on human health and the environment**

Due to adverse effects of volatile and semi-volatile organic compounds on human health and the environment, these compounds are the subject of substantial concern. In particular, volatile organohalogen compounds are suspected of being carcinogenic, mutagenic and/or teratogenic. Their toxicity differs based on their chemical structure, chlorine content and physicochemical properties (Polkowska et al., 2003). For instance, tetrachloroethene or perchloroethene (PCE) is identified to be toxic to the central nervous system, liver and kidneys of humans. Moreover, PCE could inflame the upper respiratory tracts, eyes and skin (Räisänen et al., 2001; Rutkiewicz et al., 2010). Exposure to high vapor concentrations of trichloroethene (TCE) may lead to headache, vertigo, tremors, nausea and vomiting, fatigue, intoxication, unconsciousness and even death (Berkowitz et al., 2008). Also Zhang et al. (2012) reported that benzene is a carcinogenic compound inducing leukemia. The International Agency for Research on Cancer (IARC, 2004) has documented that benzene and formaldehyde are human carcinogens (Ohura et al., 2006). Additionally, trihalomethanes (THMs) are common volatile organic compounds (VOCs) that are known to be carcinogenic to humans (Villanueva et al., 2004). Many researchers have reported that using chlorinated surface waters has been linked to rising risks of bladder, stomach, large intestine and rectal cancer as well as adverse reproductive effects (Nieuwenhuijsen et al., 2000; Ikem, 2010). Furthermore, consumption of drinking water including VOCs such as trihalomethanes (THMs) could cause liver and kidney damage, immune system, nervous system and reproductive system disorders in addition to numerous types of cancers.

Mercury poses a hazardous environmental contaminant that can easily enter the human body via inhalation, ingestion and other pathways, and can cause adverse effects to human health. The U.S. Environmental Protection Agency (US-EPA) has stated that high levels of methylmercury in the bloodstream of fetuses and young children can damage their development of cognitive systems, creating a child less able to think and learn (Zheng et al., 2007). For example, epidemics of mercury poisoning following high-dose exposures to methylmercury in Japan and Iraq have

illustrated that neurotoxicity is the health consequence of highest concern when methylmercury exposure occurs to the developing fetus (Pirrone and Wichmann-Fiebig, 2003). On the other hand, the contamination of soil with mercury has caused environmental concerns. Mercury can easily be absorbed by plants and subsequently be accumulated in the human body via the food chain. It has been confirmed that crops grown in mercury contaminated soil have an increased total mercury (THg) concentration in their tissues. For instance, Qian et al. (2009) concluded that the total mercury concentration in vegetables grown in mercury-contaminated soil (0.09–0.54 mg kg<sup>-1</sup>) ranged from 0.05 to 0.13 mg kg<sup>-1</sup> (Wang et al., 2012b).

Soil permeability can be harmed by high sodium ratios caused by extended irrigation. Such water is specifically rich in cations nevertheless the high sodium percentage constitutes a significant issue because continued use of this water will cause accumulation of sodium and later reduction in pore spaces. Consequently, it raises the potential of forming a black layer which constitutes a major problem for agriculture (Cooper, 2005a). Because calcium is a main soil cation, it is responsible for the displacement of sodium and maintenance of open and dispersed soil pore spaces. When bicarbonates control the availability of calcium, issues such as black layer formation and accumulation of sodium salts need to be controlled (Cooper, 2005b).

Sulfate and chloride are the main anionic components of groundwater. Both solutes typically exist at concentrations above 5 mg/L. Sodium and chloride in surface water are generally linked to urbanization and population density and can have a vital impact on drinking water sources and the consequent salinity of aquatic ecosystems. In particular human health may be influenced by high salt absorption leading to hypertension and other issues such as stroke and cardiovascular disease (Steele and Aitkenhead-Peterson, 2011). Nitrate is also considered to be one of the most important surface and groundwater contaminants that can cause health issues in infants and animals and the eutrophication of water bodies (Wakida and Lerner, 2005). High nitrate concentrations in drinking water can lead to *methemoglobinemia* in infants and stomach cancer in adults (Wolfe and Patz, 2002; Ward, 2005).

Furthermore, nitrates in surface water can cause eutrophication and water contamination because of heavy algal growth (Zhan et al., 2011). Even though the bromide ion does not have a negative effect on the human body, it can be transformed to bromate ( $\text{BrO}_3^-$ ) which is suspected to have carcinogenic potential in drinking water treatment particularly during oxidation and disinfection with ozone (Lv et al., 2008). An overview of average feed water composition at two locations in Australia (Pine Hill and Ti Tree), their detection limits, and both Australian and World Health Organization drinking water guidelines are illustrated in Table 2-2 (Richards et al., 2011).

**Table 2-2:** The average of two selected locations in Australia comparing with the World Health Organization drinking water guideline.

Solute	Pine Hill concentration (mg/L)	Ti Tree concentration (mg/L)	Detection limit (mg/L)	Australian guideline (mg/L)	WHO guideline (mg/L) (2)
Aluminium	<0.01	0.107	0.01	0.2 <sup>a</sup>	–
Arsenic	0.005	0.003	0.001	0.007	0.01 <sup>b</sup>
Barium	0.016	0.040	0.001	0.7	0.7
Beryllium	<0.001	<0.001	0.001	–	–
Calcium	60.1	30.4	0.01	–	–
Chloride	2000	437	0.1	250 <sup>a</sup>	–
Chromium	<0.001	<0.001	0.001	0.05	0.05 <sup>b</sup>
Copper	0.021	0.096	0.001	1 <sup>a</sup> ; 2	2
Fluoride	1.10	0.464	0.01	1.5	1.5
Iron	0.225	0.055	0.001	0.3 <sup>a</sup>	–
Lead	0.004	0.005	0.001	0.01	0.01
Lithium	0.060	0.007	0.001	–	–
Magnesium	149	38.1	0.1	–	–
Manganese	0.007	0.002	0.001	0.1 <sup>a</sup> ; 0.5	0.4 <sup>a</sup>
Molybdenum	0.005	<0.001	0.001	0.05	0.07
Nickel	0.003	0.005	0.001	0.02	0.07
Nitrate 50c	19.0	58.4	0.1	50 <sup>c</sup>	50 <sup>c</sup>
Potassium	15.0	26.0	0.03	–	–
Selenium	0.015	0.004	0.001	0.01	0.01
Sodium	1650	173	0.1	180 <sup>a</sup>	–
Strontium	1.30	0.475	0.001	–	–
Sulfur	272	33.2	0.001	–	–
Sulfate	889	116	1.0	250 <sup>a</sup> ; 500	–
Titanium	<0.001	<0.001	0.001	–	–
Uranium	0.295	0.025	0.001	0.02	0.015 <sup>b</sup>
Vanadium	0.022	0.0009	0.001	–	–
Zinc	0.222	0.0008	0.001	3 <sup>a</sup>	–
TDS	5700	1080	–	500 <sup>a</sup>	600 <sup>a</sup>

<sup>a</sup> Aesthetic-based guideline.<sup>b</sup> Provisional guideline due to scientific uncertainties regarding toxicology/epidemiology and/or due to difficulties regarding technical achievability.<sup>c</sup> Guideline recommended protecting against methaemoglobinaemia in bottle-fed infants (short term exposure).

## 2.5 Fate and transport of contaminants to aquatic sources

Sources of groundwater contamination can be classified as: point source contamination and non-point source contamination. Point source contamination refers to pollution from discrete locations that can be easily identified with a single discharge source (e.g. municipal sewage treatment plant discharges, industrial

discharges, accidental spills and landfills; Dolar et al., 2011b; Jurado et al., 2012). On the other hand, non-point source contamination is produced by contamination over a wide area and often cannot be easily identified as coming from a single or certain source. Important examples include agriculture, runoff from urban and agricultural areas and leakage from urban sewage systems (Chowdary et al., 2005; Jurado et al., 2012). The existence and fate of both organic and inorganic contaminants in the aquatic environment has long been known as a significant issue of public health and environmental concern. A wide range of these contaminants, both of anthropogenic and natural origin, have been detected and identified as significant pollutants in sewage and wastewater affected water bodies, including both surface and groundwater (Nghiem and Schäfer, 2004). The fate of any contaminant in aquatic sources relies on both its physicochemical properties, such as its solubility in water,  $K_{ow}$  and  $D_{ow}$  (Fakhru'l-Razi et al., 2009; Lapworth et al., 2012). Particularly, the fate and transport of the trace contaminants depends on several factors such as the depth to the watertable, sediment porosity, permeability and ground water flow control as well as geochemical and nutrient conditions (Díaz-Cruz and Barcelo', 2008).

## **2.6 Conventional treatment processes**

### **2.6.1 Coagulation**

Historically, coagulation is one of the main processes has been used in water treatment to decrease turbidity and colour as well as to eliminate pathogens. Essentially, coagulation involves equalisation of the charges on colloidal particles so they can agglomerate in a following flocculation step, or by adding materials that can also connect between like-charged particles or enmesh them (Huck and Sozański, 2011). Many coagulants are broadly used in the traditional wastewater remediation processes such as alumina, ferrous sulfate and ferric chloride, contributing to the successful removal of wastewater particulates and contaminants by charge equalisation of particles or by adsorption of contaminants on amorphous metal hydroxide precipitates (Fu and Wang, 2011). Selection of an appropriate coagulant

depends upon the nature of the particles, particularly their affinity to adsorb water, and their electrical charge (Gray, 2010). The efficiency of coagulation to eliminate natural organic matter (Ba and Economy, 2010) and particles relies on a number of factors, including coagulant type and dosage, integration conditions, pH, temperature, particle and NOM properties (such as size, functionality, charge and hydrophobicity) besides the occurrence of divalent cations and concentrations of destabilizing anions (bicarbonate, chloride, and sulfate; Matilainen et al., 2010).

### **2.6.2 Sedimentation**

Sedimentation is considered to be one of the most significant operational units which is used in water and wastewater treatment. Sedimentation can be classified as a solid–liquid separation process, in which particles precipitate under the force of gravity (Al-Sammarraee et al., 2009). Particles with density greater than water are removed from suspension by allowing these particles to gravitate to bottom of a tank to form sludge under inactive conditions. The process is used in primary water treatment to remove settleable organic and inorganic material to reduce the organic load in the secondary treatment process (Gray, 2010).

At the present time a good understanding of sedimentation tank behaviour is important for appropriate tank design and operation. Usually, sedimentation tanks are described by interesting hydrodynamic phenomena, for instance density waterfalls, bottom currents and surface return currents, and are similarly sensitive to temperature fluctuations and wind effects. Numerous factors obviously impact the capacity and efficiency of a sedimentation tank, such as surface and solids loading rates, tank type, solids elimination mechanism, inlet design and weir placement (Goula et al., 2008).

### **2.6.3 Chemical precipitation**

Chemical precipitation is more broadly recognized as precipitation softening. It is used mostly to remove or reduce the solid materials in potable waters resulting from excessive salts of calcium and magnesium (Gray, 2010). Precipitation softening changes the soluble salts into insoluble ones that can be removed by following flocculation and sedimentation. Furthermore, chemical precipitation can be used to recuperate metals from industrial effluents. For instance, hexavalent chromium ( $\text{Cr}^{6+}$ ), which is found in wastewater from metal plating and anodizing processes, is extremely toxic. The most important use of chemical precipitation in wastewater treatment is the removal of phosphate as a precipitate of calcium, magnesium or iron (Gray, 2010).

Some studies have concluded that the combination of chemical precipitation and ion-exchange gave high rejection for contaminants, in particular heavy metals. Papadopoulos et al. (2004) used ion-exchange processes individually and then combined with chemical precipitation to investigate the removal of nickel from wastewater streams from a rinse bath of aluminium parts. They concluded that the individual use of ion exchange resulted in the removal of up to 74.8% nickel, whereas using the combination of ion exchange and precipitation processes achieved higher rejection ranged between 94.2% and 98.3% (Papadopoulos et al., 2004).

### **2.6.4 Adsorption**

Adsorption is a key process that can be employed for the elimination of chemical pollutants. Simply, the process of adsorption includes separation of a material from one phase followed by its accumulation or concentration at the surface of another (Choong et al., 2007). Particularly, it is used in water treatment for the removal of organic contaminants. It is appropriate to both groundwater and surface waters; nevertheless, it can be a comparatively costly process depending on the levels of contaminants to be removed and the occurrence of other elements in the water (such



as background TOC) that are also adsorbed, reducing the capacity of the process for the contaminants of attention (Huck and Sozański, 2011).

Adsorption is a physical process where soluble molecules (adsorbate) are eliminated by attachment to the surface of a solid substrate (absorbent). Adsorbents should have a very high surface area and they include activated alumina, clay colloids, hydroxides and adsorbent resins, with the most extensively used being activated carbon (Gray, 2010). In water remediation adsorption is used to treat taste and odour caused by trace organic compounds, in addition to colour and other organic residuals, particularly chlorination disinfection by products, such as trihalomethanes (THM). In wastewater remediation adsorption is used to develop settleability of activated sludge and to eliminate toxic compounds (Gray, 2010).

#### **2.6.5 Ion exchange**

Ion exchange is an adsorption process that replaces ions of the same charge between a solid ion-exchange medium and a solution. This technique is mainly used for softening. Furthermore, ion exchange is used to remove cations such as chromium, barium, strontium and radium, and anions such as nitrate, fluoride, cyanide and humates (Gray, 2010). Recently, ion-exchange has been extensively used to remove heavy metals from wastewater because it has many advantages, such as high treatment capacity, high removal effectiveness and fast kinetics. Ion-exchange resin, whether synthetic or natural solid resin, has the particular capability to exchange its cations with the metals in the wastewater. Among the materials used in ion-exchange processes, synthetic resins are usually favoured as they are most useful for removing heavy metals from solutions (Fu and Wang, 2011). The influence of ion exchange on water quality is subject to the ion used to regenerate the resin. For instance if an ion exchanger used for water softening is regenerated with sodium chloride, as is usually the case in home units, the sodium concentration of the water will increase (Huck and Sozański, 2011).

## 2.7 Membrane technology

A membrane can be defined fundamentally as a barrier, which isolates two phases and prevents transport of numerous chemicals in a selective approach. A membrane can be considered homogenous or heterogeneous, symmetric or asymmetric in structure, solid or liquid; it can carry a positive or negative charge or be neutral or bipolar (Takht Ravanchi et al., 2009). The main types of membrane are illustrated schematically in (Figure 2-1).

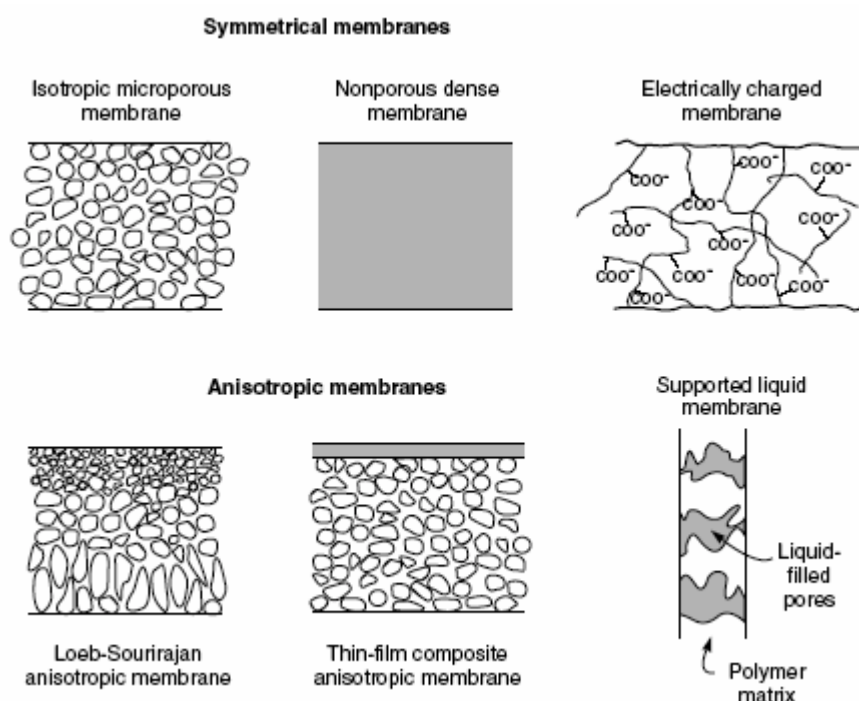


**Figure 2-1:** Schematic diagrams of principal types of membranes (Baker, 2012).

Environmental pollution and health risks need careful consideration when reusing treated wastewater. Water shortages have resulted in a wide range of exploitation of groundwater from aquifers and other water sources, some of which may need treatment before they can be used. This has reinforced the search for advanced high level and reliable wastewater treatment processes. Membrane treatment could play a

crucial role to alleviate water shortage problems and provide better environmental control. This technology includes microfiltration (MF), ultrafiltration (UF), nanofiltration (NF) and reverse osmosis (RO; Oron et al., 2006) as well as carbon nanotubes (CNTs; Liu et al., 2013b). Figure 2-2 illustrates the family of membrane processes (driving forces and applications size range).

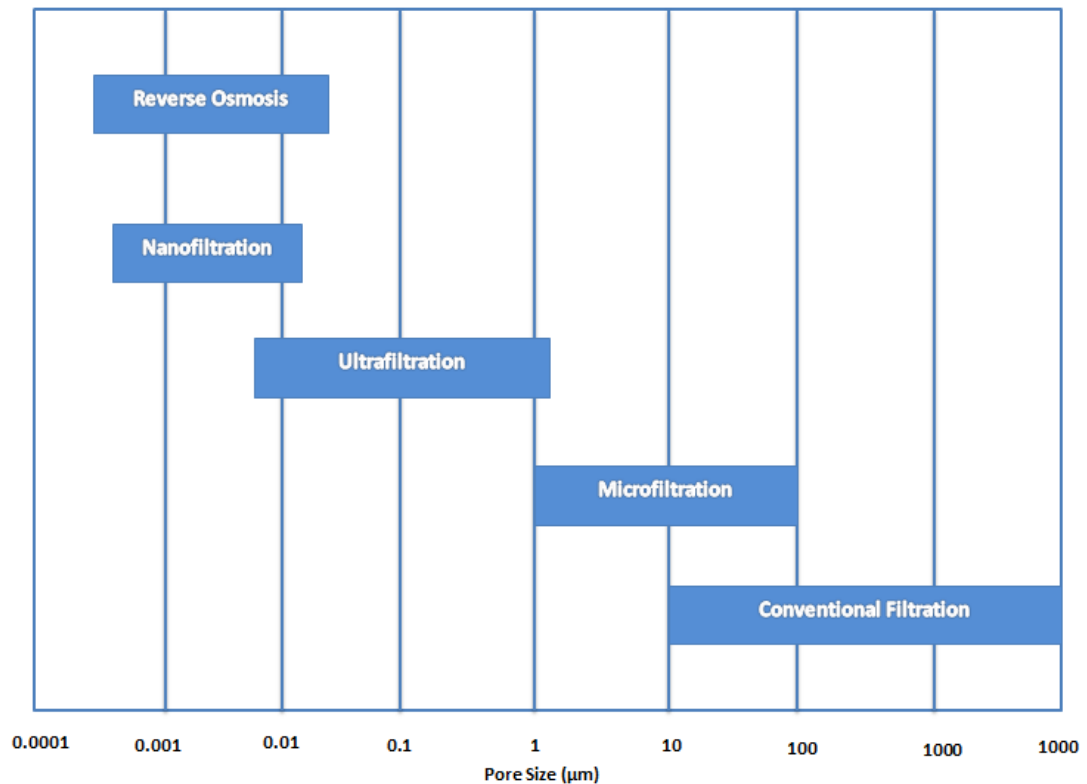


**Figure 2-2:** The family of membrane processes (driving forces and applicable size ranges; Fane et al., 2011).

Membrane technology is a very effective method of separating the liquid and solid portions contained in an effluent (Figure 2-3). Furthermore, membrane technology is commonly applied as part of the biological treatment process for the removal of suspended substances and pathogens from wastewater. Membrane technology can be used for better treatment of industrial wastewater and the removal of dangerous components. Consequently, it can be concluded that membrane remediation is a promising technology for removal of pathogens and the total dissolved solids (TDS) for environmental friendly water reuse (Oron et al., 2007).

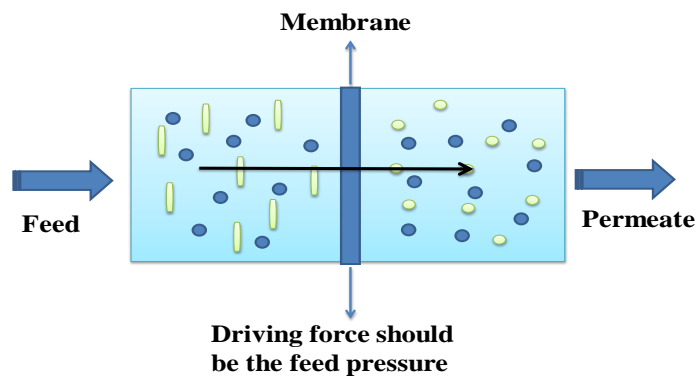


**Figure 2-3:** The basic concept of membrane separation process adopted from (Ismail et al., 2009).

Due to declining freshwater availability, wastewater reclamation and reuse is becoming economically attractive for preserving water resources. Currently, membrane technology is widely used in various aspects of life. One of the most important applications of membrane technology is water and wastewater treatment. The benefits of the application of membrane technology over other technologies which do not offer an absolute barrier are extensively recognised, and evident from Table 2-3.

**Table 2-3:** Examples of wastewater and water treatment plants using NF/RO membranes.

Site	Final water use	Capacity ( $'000 \text{ s m}^3/\text{d}$ )	Commissioning year	Reference
Israel	Drinking water production	330,000	2005	(Greenlee et al., 2009)
Fujairah desalination plant (UAE)	Drinking water production	454,000	2005	(Greenlee et al., 2009)
Algeria's capital city,	Drinking water production	200,000	2007	(Greenlee et al., 2009)
Wadi Ma'in in Jordan,	Drinking water production	129,000	2006	(Greenlee et al., 2009)
Hedekoga landfill in southern Sweden	leachate treatment for irrigation uses	3000	NA	(Gupta and Ali, 2013)
Sydney Olympic Park	Non-potable reuse	7,500	NA	(Wintgens et al., 2005)
Illawarra Waste Water Strategy in Wollongong, Australia	Non-potable water reuse	20,000	2005	(Wintgens et al., 2005)
Wulpen, Belgium/Flemish coast of Belgium	Indirect potable reuse via groundwater recharge	2,500,000	NA	(Wintgens et al., 2005)
The NEWater Project, Singapore	Indirect potable reuse	91,000	2004	(Wintgens et al., 2005)
Doha North, Qatar	Irrigation	440	2012	(Garcia et al., 2013)
Orange County, USA	Groundwater replenishment	328	2008	(Garcia et al., 2013)
Changi, Singapore	Industry, indirect potable reuse	232	2010	(Garcia et al., 2013)
Gwinnet County, GA, USA	Irrigation	289	2005	(Garcia et al., 2013)
Qinghe Phase II China	Industry, irrigation, municipal non-potable reuse	180	2010	(Garcia et al., 2013)
Sulaibiya, Kuwait	Irrigation	375	2004	(Garcia et al., 2013)
Botany Groundwater Cleanup Project, Sydney	Irrigation	6,000	2006	(2011)

NA: Not available.

Membranes used in water and wastewater industry can be generally classified into two main categories: porous membranes and non-porous membranes. Porous membranes separate particles on the basis of sieving, straining or size exclusion. Microfiltration, ultrafiltration and loose membranes are examples of porous membranes. Non-porous membranes separate molecules on the basis of the variations in solubility or diffusivity between the solvent and the solute in the membranes. Tight end nanofiltration and reverse osmosis membranes are usually non-porous membranes (Shirazi et al., 2010). Microfiltration membranes usually have pore sizes ranging from 1 to 10  $\mu\text{m}$ . According to their comparatively large pore sizes, microfiltration membranes have great permeability ( $>500 \text{ l}^{-1} \text{ m}^{-2} \text{ h}^{-1} \text{ bar}^{-1}$ ) and therefore they can be used in a low-pressure range (normally from 0.1 to 2.0 bars). Microfiltration membranes are used to reject particulates whose size is higher than membrane pore size. On the other hand, the pore sizes of ultrafiltration membranes are much smaller than microfiltration membranes and range from 1 to 100 nm. This characteristic lets them be used for removing bacteria, viruses, colloids and macromolecules from a feedwater. In construct, RO membranes can retain small organic molecules and dissolved ions, including monovalent ions for instance  $\text{Na}^+$  and  $\text{Cl}^-$ . These membranes have sub-nanometre pores and their separation properties are typically stated in terms of water permeability and sodium chloride rejection. Nanofiltration membranes are like reverse osmosis membranes in terms of their ability of remove dissolved ions in addition to some small organic molecules. Because of their capability to effectively retain calcium and magnesium ions, nanofiltration membranes can be applied for water softening. Nanofiltration membranes can be operated at remarkably low pressure levels ( $<10 \text{ bar}$ ) compared to those for reverse osmosis membranes because of their greater water permeabilities ( $5\text{--}50 \text{ l}^{-1} \text{ m}^{-2} \text{ h}^{-1} \text{ bar}^{-1}$ ; Fane et al., 2011). Characteristics of the systems (NF/RO) are presented in Table 2-4.

**Table 2-4:** Comparison of membranes (NF/RO).

Characteristic	NF	RO
Pore size, $\mu\text{m}$ <sup>a</sup>	0.0001– 0.001	< 0.0001
Molecular weight cutoff (MWCO) <sup>a</sup>	300–1,000	100–300
Suspended solids removal <sup>a</sup>	Yes	Yes
Dissolved Organics Removal <sup>a</sup>	Organics >300 mol.wt. Simple sugars and trihalomethane compounds.	Organics >100 mol.wt.
Dissolved inorganics Removal <sup>a</sup>	20–85% rejection.	All dissolved salts to 95–99% rejection.
Water permeability ( $\text{lm}^{-1} \text{h}^{-1} \text{bar}^{-1}$ ) <sup>c</sup>	5–50	0.5–10
Common applications <sup>a</sup>	Has water softening capabilities, i.e. rejection of divalent salts (Ca and Mg) and some rejection of monovalent salts such NaCl; decolorizing. Used to separate sugars.	Used as pre-treatment for demineralization ion exchange and where low dissolved solids effluent is required.
Separation mechanism <sup>b</sup>	Solution–diffusion and Donnan exclusion	Solution–diffusion
Membrane materials <sup>c</sup>	Thin-film composite polyamide, cellulose acetate, other materials.	Thin-film composite polyamide, cellulose acetate
Strengths <sup>b</sup>	Excellent rejection of divalent solutes. Lower pressure than RO. Selective separation possible.	Excellent rejection of all ionic solutes
Weaknesses <sup>b</sup>	Low rejection of some monovalent solutes Limited to dilute solutions Pretreatment	Higher energy requirement Large retentate volume Pretreatment

<sup>a</sup> (Al-Rifai et al., 2010).

<sup>b</sup> (Ritchie and Bhattacharyya, 2002).

<sup>c</sup> (Fane et al., 2011).

### 2.7.1 Nanofiltration (NF) system

Historically, the first appearance of nanofiltration (NF) was in the nineteen seventies, when reverse osmosis membranes with a logical water flux that operated at comparatively low pressures were developed. The high pressures now conventionally

used in reverse osmosis caused a substantial energy cost. In contrast, the quality of permeate in most cases was very good. Consequently, membranes with a lower rejection of dissolve components, but with a higher water permeability would be an excellent improvement for separation or purification technology (Van der Bruggen and Vandecasteele, 2003). Accordingly, it can be concluded that this technology will become more interesting for using in many applications in the future (Mohammad et al., 2015).

The removal of natural organic matter (Ba and Economy, 2010) is essential for most water treatment production units, particularly when surface water is treated, and this can be done competently by nanofiltration. Moreover, experimental studies and full-scale plants demonstrate that NF is a reliable process for the removal of an extensive range of components from surface water as well as from groundwater (Van der Bruggen and Vandecasteele, 2003). Agenson and Urase (2007) conducted a study to examine the retention of a wide range of trace organic contaminants as a function of molecular weight by using a nanofiltration membrane (UTC20). They found that the size-exclusion mechanism is dominant to retain these contaminants and the rejection was >99%. Also Yangali-Quintanilla et al. (2009) reported that the clean NF-90 membrane (virgin) rejected almost all of the hydrophobic neutral compounds (95-98%) mainly because of size exclusion. However, electrostatic repulsion was the key mechanism of rejection of ionic compounds by NF-90 (99%). Nghiem et al. (2005) concluded that carbamazepine was rejected at approximately 85% by NF-270 and approximately 96% by NF-90 membranes at pH 8. Chen et al. (2004) found that the NF membrane can remove 46% to 100 % of pesticides and rejection increased with molecular weight. In Paris at a large NF plant, removal of organics (up to 96%) was achieved by utilising a novel NF membrane (NF-200; Hilal et al., 2004). Remarkably, the removal of trihalomethanes with the NF-200 membrane was 95% for 80g/l feed concentration at all pressure levels, except 15 bar the removal of trihalomethanes was less than 95% (Uyak et al., 2008).

NF membranes are not only effective for removal of organic contaminants but also effective for removal of inorganic contaminants in particular; they are used to



remove divalent ions, such as calcium and magnesium, as well as monovalent ions but with a lower rate (Table 2-5). Liikanen et al. (2003) found that the NF-70 membrane achieved 99% calcium rejection, 96% magnesium rejection and 89% sodium rejection. Hong et al. (2009) concluded that the NF-90 exhibited 99% rejection of phosphate and 79% rejection of chloride. Harrison et al. (2007) reported that the NF-90 membrane achieved 94-96% bromide rejection and 84-91% iodide rejection. The removal efficiency of various NF membranes is illustrated in Table 2-5.

**Table 2-5:** Summary of reported inorganic contaminants removal efficiency by various NF membranes.

Contaminant	NF membrane used	Removal efficiency (%)	Ref.
Na <sup>+</sup>	NF-270	89	(Liikanen et al., 2003)
K <sup>+</sup>	NF-270	>95	(Ortega et al., 2008)
SO <sub>4</sub> <sup>2-</sup>	NF-270	>95	(Ortega et al., 2008)
Ca <sup>2+</sup>	NF-70	99	(Liikanen et al., 2003)
Mg <sup>2+</sup>	NF-70	96	(Liikanen et al., 2003)
Hg <sup>+</sup> <sup>a</sup>	NF-90	97.38	(Dolar et al., 2011a)
Cl <sup>-</sup>	NF-90	>79	(Hong et al., 2009)
PO <sub>4</sub> <sup>3-</sup>	NF-90	>98	(Hong et al., 2009)
NO <sub>3</sub> <sup>-</sup>	NF-90	90	(Voorthuizen et al., 2005)
Br <sup>-</sup>	NF-90	94-96	(Harrison et al., 2007)

<sup>a</sup> Element mercury.

Based on their estimated pore size, the NF-90 membrane could be classified as a tight nano-filtration membrane (0.68 nm) compared to NF270 membrane (0.84 nm) and thus it can give high removal efficiency for contaminants.

### **2.7.2 Reverse osmosis (RO) system**

Reverse osmosis (RO) membranes exhibit the best overall removal of total dissolved solids (TDS) and organic constituents. Therefore, RO membranes can be exploited to produce high quality water used for agricultural and industrial purposes, and particularly for drinking water (Belkacem et al., 2007). In the last few decades, many studies at both pilot and industrial scales, have already illustrated the effectiveness of RO with respect to the isolation of contaminants from landfill leachate (e.g., Renou et al., 2008). Moreover, RO is a very effective method for quick collection of dissolved organic matter (DOM) from both surface and ground waters (Sun et al., 1995). However, the efficiency of RO regarding rejection of trace contaminants depends on many factors, namely the dipole moment of the components, the hydrophobicity of the components and the component's molecular size (Al-Rifai et al., 2010).

RO was able to retain more than 90% of the target organics, irrespective of their chemical properties. These results recommend that RO treatment is effective in removing organic micropollutants in natural water where their molecular weights are greater than the molecular weight cut-off of the membrane (Huang et al., 2011). A study conducted by Li et al. (2004) on the treatment of wastewater from a pharmaceutical manufacturing industry revealed that RO treatment effectively reduced oxytetracycline concentration from 1000 mg L<sup>-1</sup> to below 80 mg L<sup>-1</sup> (>92% removal). High rejection was achieved after using the RO stage (>99% for macrolides, pharmaceuticals, cholesterol and BPA, 95% for diclofenac, and >93% removal of sulphonamides; Sahar et al., 2011). All photodegradation products were removed totally (>99.99%) with RO membranes (LFC-1, XLE), except FEBA1 which had rejections of approximately 70% (Dolar et al., 2012b). The removal of triclosan by RO membrane was almost 100% since the molecular width of this compound was greater than the estimated mean effective membrane pore size (Xie et al., 2012). RO membrane exhibited high rejection (always higher than 99%) for pharmaceutical compounds which were found in municipal wastewater of a coastal wastewater treatment plant (Castell-Platja d'Aro, Spain; Dolar et al., 2012a). The

removal of primidone by TFC-HR and XLE RO membranes was also high, 92.2% and 91.3% respectively (Xu et al., 2006).

RO membranes can retain small organic molecules and dissolved ions, including monovalent ions such as sodium and chloride (Table 2-6). Tu et al. (2011) reported that the removal of calcium and sodium using RO membrane (WB30) was 97.7% and 96.2% respectively. RO membrane (SWC4+) was used and achieved a high rejection of bromide (>99%0; Bartels et al., 2009). Removal of phosphates was investigated by Dolar et al. (2011a) and they reported a high rejection (>97%) of phosphate by RO membrane (XLE). Hilal et al. (2004) stated that the removal of nitrate was high (94%) after using a RO membrane. The removal efficiency of various RO membranes is illustrated in Table 2-6.

**Table 2-6:** Summary of reported inorganic contaminants removal efficiency by various RO membranes.

Contaminant	RO membrane used	Removal efficiency (%)	Ref.
Na <sup>+</sup>	BW30	96.2	(Tu et al., 2011)
K <sup>+</sup>	BW30	94.9	(Richards et al., 2011)
SO <sub>4</sub> <sup>2-</sup>	BW30	81	(Alzahrani et al., 2013b)
Ca <sup>2+</sup>	BW30	97.7	(Tu et al., 2011)
Mg <sup>2+</sup>	TW30-4021	96.1	(Malamis et al., 2012)
Hg <sup>+</sup> <sup>a</sup>	LFC-1	99.73	(Dolar et al., 2011a)
Cl <sup>-</sup>	BW30	77	(Alzahrani et al., 2013b)
PO <sub>4</sub> <sup>3-</sup>	XLE	>97	(Dolar et al., 2011a)
NO <sub>3</sub> <sup>-</sup>	NA	94	(Hilal et al., 2004)
Br <sup>-</sup>	SWC4+	99.8	(Bartels et al., 2009)

<sup>a</sup> Element mercury.

NA: Not available.

### 2.7.3 Carbone nanotube (CNTs) technology

The first appearance of CNTs was 1991, when they were discovered by Iijima (1991). Since CNTs were discovered, they have been widely used in most areas of science and engineering due to their unique physical and chemical properties. CNTs have exhibited a combination of exceptional mechanical, thermal and electronic properties that make them superlative materials for a broad range of applications (Coleman et al., 2006; Thostenson et al., 2001) such as field-emission materials (Liu et al., 2010), scanning probe microscopy tips, microelectronic devices (Thostenson et al., 2001), electrochemical devices (Baughman et al., 2002) and hydrogen storage devices (Oriňáková and Oriňák, 2011). Table 2-7 lists CNT application areas expected in the future, as reported in the literature (Köhler et al., 2008).

**Table 2-7:** Expected application areas of carbon nanotubes in the future.

Industry sector	Application/material
Materials and chemistry	Ceramic and metallic CNT composites. Polymer CNT composites (heat conducting polymers). Coatings (e.g. conductive surfaces). Membranes and catalysis. Tips of scanning probe microscopes (SPM).
Medicine and life science	Medical diagnosis (e.g. lab on a chip). Medical applications (e.g. drug delivery). Cosmetics (anti-ageing creams). Chemical sensors. Filters for water and food treatment.
Electronics and ICT	Lighting elements, CNT-based field emission displays. Microelectronic: single electron transistor. Molecular computing and data storage. Ultra-sensitive electromechanical sensors. Microelectro-mechanical systems (MEMS).
Energy	Hydrogen storage, energy storage (super capacitors). Solar cells. Fuel cells. Superconductive materials.

As the name indicates, carbon nanotubes can be imagined as a sheet of graphite that has been rolled into a tube (Thostenson et al., 2001). Carbon nanotubes exist in two main types: single-walled nanotubes (SWNTs) composed of a single graphite sheet seamlessly wrapped into a cylindrical tube (Figure 2-4A). Multiwalled nanotubes (MWNTs) include an array of such nanotubes that are concentrically nested like rings of a tree trunk (Figure 2-4B; Baughman et al., 2002).

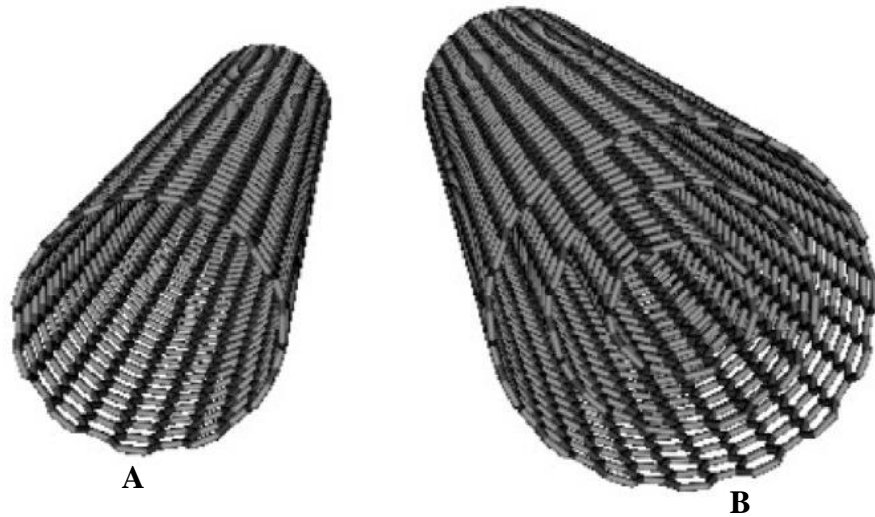


**Figure 2-4:** structure representations of (a) SWCNT and (b) MWNT (Ismail et al., 2009)

Depending on the rolling, CNTs can be additionally classified as armchair, zigzag and chiral types (Figure 2-5). These categories are distinguished by their unit cells which are defined by the chiral vector given by the equation:  $\vec{C}_h = n\vec{a}_1 + m\vec{a}_2$  where  $\vec{a}_1$  and  $\vec{a}_2$  are unit vectors in the two-dimensional hexagonal lattice, and  $n$  and  $m$  are integers. An additional significant parameter is the chiral angle  $\theta$ , which is the angle between  $\vec{C}_h$  and  $\vec{a}_1$  (Figure 2-6A-B). When  $n = m$  and the chiral angle is 30 degrees it is identified as an armchair type. When  $m$  or  $n$  are zero and the chiral angle is equal to zero the nanotube is identified as zigzag (Paradise and Goswami, 2007).

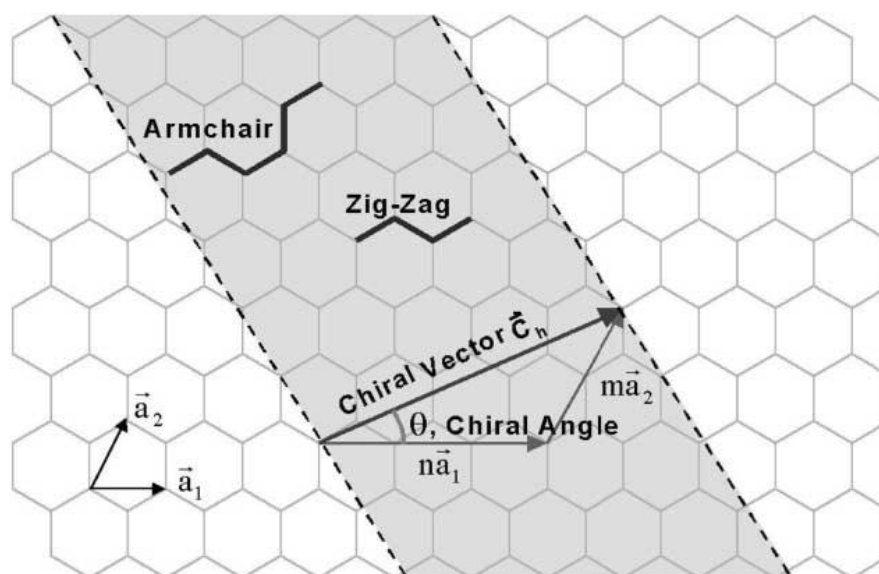


**Figure 2-5:** Schematic diagram showing how a hexagonal sheet of graphite is ‘rolled’ to form a carbon nanotube (Thostenson et al., 2001).

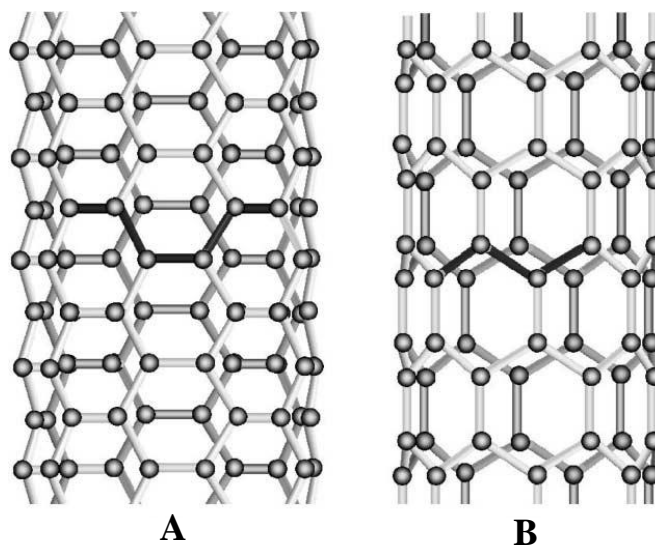


**Figure 2-6:** Illustrations of the atomic structure of (a) an armchair and (b) a zigzag nanotube (Paradise and Goswami, 2007).

Currently, CNTs are produced fundamentally by three techniques: arc discharge, laser ablation and chemical vapour deposition (CVD; Oriňáková and Oriňák, 2011; Popov, 2004). The first technique that was utilised to produce CNTs is the arc discharge (Figure 2-7). In this technique two high-purity graphite rods are used as the anode and cathode. The rods are transported together under a helium atmosphere and

a voltage is utilised until a steady arc is attained. The exact process variables depend on the size of the graphite rods. As the anode is consumed, a constant gap between the anode and cathode is kept by regulating the position of the anode. The material deposits on the cathode to form a build-up containing of an outside shell of fused material and a softer fibrous core involving nanotubes and other carbon particles (Thostenson et al., 2001).

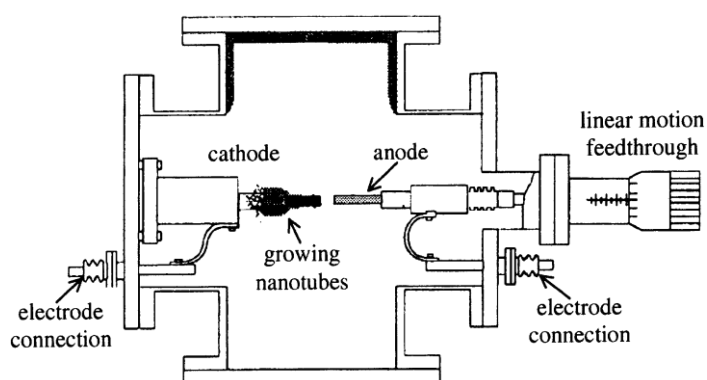


**Figure 2-7:** Schematic illustration of the arc-discharge technique (Paradise and Goswami, 2007).

Laser ablation is considered the first technique that was used to generate fullerenes in clusters. In this technique, a piece of graphite is evaporated by laser irradiation under an inert atmosphere. This leads to soot containing nanotubes which are cooled at the walls of a quartz tube (Figure 2-8). Two kinds of CNTs (multiwalled carbon nanotubes and single walled carbon nanotubes) can be synthesised by this technique. For this technique a purification step by gasification is also required to remove carbonaceous substance (Paradise and Goswami, 2007).

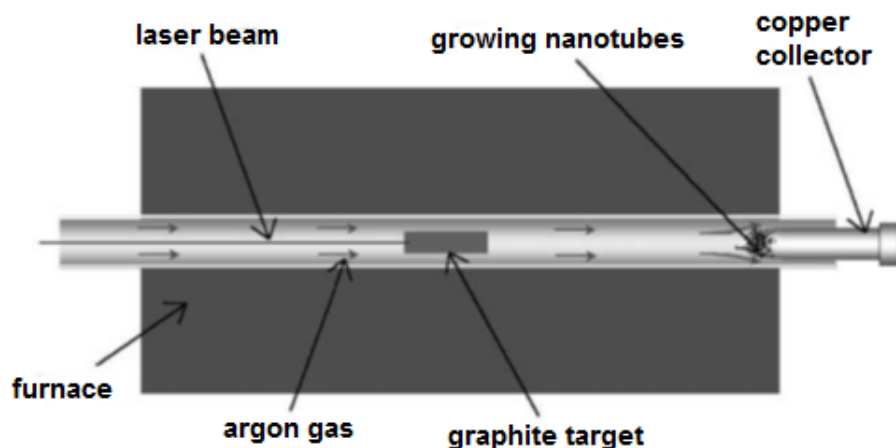


**Figure 2-8:** Schematic of the laser ablation process (Paradise and Goswami, 2007).

The both above techniques, theoretically, cannot synthesize CNTs continuously; therefore, the product yield is limited. Additionally, purification steps are essential to separate the tubes from unwanted by-products. These limitations have motivated the development of gas-phase techniques, such as chemical vapour deposition (CVD), where nanotubes are formed by the decomposition of a carbon-containing gas. The gas-phase techniques are amenable to continuous processes meanwhile the carbon source is continually replaced by flowing gas. Furthermore, the final purity of the as-produced nanotubes can be fairly high, minimizing following purification steps (Thostenson et al., 2001).

In recent years, nanotechnology has provided various kinds of nanomaterials which can be used in water treatment and can give promising results. Nanoparticles such as CNTs have exceptional absorption properties and can be applied to remove chemical and biological pollutants. CNTs met with special attention because of their capabilities for water treatment and their effectiveness against chemical and biological pollutants (Upadhyayula et al., 2009). In environmental engineering, CNTs are regarded as an excellent media for different adsorbent applications, including: heavy metals (Tofighy and Mohammadi, 2011); organic compounds inclusive of herbicides (Yuan et al., 2008), chlorinated compounds (Yang and Xing, 2007); disinfection byproducts (Lu et al., 2005); endocrine disruptors (Pan et al., 2010); biological contaminants including microorganisms (Upadhyayula et al.,



2009); natural organic matter (Lu and Su, 2007); and cyanobacterial (e.g. microcystin) toxins (Yan et al., 2006).

CNTs, as a new member of the carbon family, have displayed high abilities as a remarkable adsorbent in waste water treatment (Li et al., 2003; Pillay et al., 2009). It has been documented that CNTs are effective for the removal of the herbicide diuron (Deng et al., 2012), roxarsone (Hu et al., 2012), atrazine (Yan et al., 2008) and divalent metal ions from aqueous solution (Rao et al., 2007; Tofighy and Mohammadi, 2011). Rashid et al. (2014) concluded that the removal of bisphenol A (BPA) using multi-walled carbon nanotube (MWNT) buckypapers remained constant at roughly 90% throughout the experiment. Peng et al. (2003) stated that CNTs were excellent adsorbents for the removal of 1, 2-dichlorobenzene and Fagan et al. (2004) reported that CNTs as a membrane were able to remove this component effectively. Lu et al. (2005) have concluded that CNTs have potential applications for removal of trihalomethanes (THMs) during drinking water treatment. Pillaya et al. (2009) found that the functionalised MWNTs exhibited the greatest adsorption ability with up to 98% of a 100 ppb Cr (VI) solution being adsorbed. Chen et al. (2011) reported that CNTs showed excellent adsorption efficiency for lead.

## **2.8 Factors affecting the removal of organic and inorganic compounds by membrane technology**

Membrane technology such as NF/RO, ultrafiltration (UF), microfiltration (MF) and CNTs are becoming progressively used in water treatment and wastewater recovery, as well as in recycle applications. Membrane technology is able to attain high removals of components such as dissolved solids, organic carbon, inorganic ions, and regulated and unregulated organic compounds (Bellona et al., 2004). To estimate the rejection of a solute by membrane technology, many factors should be taken into account, such as properties of the membrane (the molecular weight cut-offs, desalting degree, porosity, membrane morphology, charge, and hydrophobicity) and properties of the solute (the molecular weight, molecular size, charge, and hydrophobicity) in addition to the feedwater chemistry (Figure 2-9; Bellona et al., 2004; Chang et al., 2012).

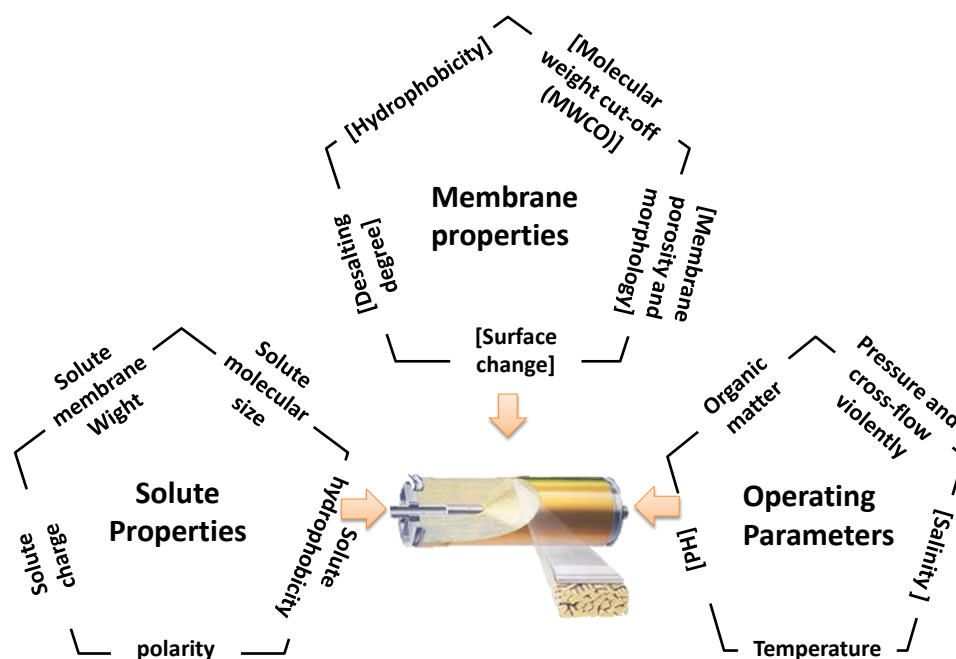


**Figure 2-9:** Major parameters affecting the performance and production of most of membranes.

## 2.9 Factors affecting the rejection of organic and inorganic compounds by NF/RO

Many studies have reported that the rejection of solutes by NF/RO membranes is influenced by properties of the membrane, properties of the solute and operating parameters (Ozaki and Li, 2002; Chang et al., 2012; Plakas and Karabelas, 2012). Furthermore, these studies have documented that the membrane operating environment, for instance feed pressure and reclamation, may influence the rejection of target solutes. Ozaki and Li (2002) mentioned that the rejection of organic solutes by RO membranes relies on the membrane substance and solute structure. Jarusutthirak et al. (2007) reported that the rejection of natural organic matter by a nanofiltration membrane was affected by ionic strength, natural organic matter (NOM) concentration and solution pH. This study showed that the increase of NOM concentration from  $0 \text{ mg L}^{-1}$  to  $25 \text{ mg L}^{-1}$  led to higher NOM rejection, membrane fouling, and greater flux decline, because of NOM accumulation on membrane surface.

#### 2.9.1.1 Membrane properties and their effect on the rejection

One of the most important properties that has to be taken into consideration when selecting a membrane is the molecular weight cut-off, which is defined as the molecular weight of a solute that was rejected at 90 percent (Van der Bruggen et al., 1999). The molecular weight cut-off notion is derived from the observation that molecules usually become larger as their mass increases. As molecules become larger, sieving effects because of steric hindrance augmentation increase and the molecule is rejected by the membrane more frequently than a smaller molecule. It is striking to note that the molecular weight cut-off could also be related to diffusion, as a bigger molecule will diffuse more slowly than a smaller molecule (Bellona et al., 2004). For example, Salveson et al. (2000) carried out laboratory-scale RO studies in combination with a comprehensive analytical monitoring program. Authors in this study concluded that RO treatment was extremely efficient for elimination of total organic carbon and regulated organic compounds; nevertheless,  $17\beta$ -estradiol with a molecular weight of 279 g/mol was still detected at 0.3ng/L in the product water. Another study was conducted by Reinhard et al. (1986) who examined the removal of trace organics by RO utilizing cellulose acetate and polyamide membranes; all membranes successfully rejected split, composite molecules but were diverse in their rejection characteristics for smaller molecules, for instance chlorinated solvents, base neutrals and low molecular weight acids.

On the other hand, some studies have used different approaches. For example, Van der Bruggen et al. (1998) found that the molecular weight cut-off for the used NF membranes was poorly connected with the removal of two categories of herbicides; i.e. triazines (atrazine and simazine) and phenyl-ureas (isoproturon and diuron). Particularly, the NF-70 membrane, with a molecular weight cut-off of 200 Dalton, showed better retention ability than the apparently rather tighter UTC-20 membrane (molecular weight cut-off 180 Da). Conversely, a NTR-7450 membrane (MWCO 600–800 Da) showed the worst performance (by 20% retention) because of its larger pore size. These observations have been reached by another study (Mohammad and Ali, 2002), where the rejection of uncharged solutes and salts did not agree with the

anticipated approach of low rejection with rising molecular weight cut-off of the NF membranes employed. Furthermore, some studies reported a limited rejection of compounds of concern to humans and the environment with molecular weight below the molecular weight cut-off of the membranes. These compounds include disinfection by-products, e.g., N-nitrosodimethylamine, trihalomethanes and haloacetic acids (Bellona et al., 2004).

When choosing a membrane both the molecular weight cut-off and desalting degree should be borne in mind, for the reason that membranes with the same molecular weight cut-off can have critically different desalting degrees. The desalination degree of a membrane is defined as the constant salt rejection of a 2000 mg/L sodium chloride or magnesium sulfate solution, and/or a 500 mg/L calcium chloride solution (Plakas and Karabelas, 2012). Kiso et al. (2001a) have documented a positive correlation between desalting degree and rejection for polysaccharides and alcohols. A number of studies reported that membranes with the highest desalting degree showed the highest pesticide rejection (Kiso et al., 2001a; Kiso et al., 2001b). Agenson et al. (2003) studied the retention of a wide range of organic contaminants by different nanofiltration/reverse osmosis process and reported that the high desalting membranes efficiently retained more than 90% of the semi-volatile organic compounds, except 2-hydroxybenzothiazole, whereas the retention of volatile organic compounds in most cases was greater than 80%. In contrast, the low desalting membrane UTC60 retained less than 20% of the volatile organic compounds whilst the majority of the semi-volatile organic compounds were retained in the range of 20–80%.

Membrane porosity is considered a useful parameter to estimate the rejection of compounds in membrane processes. Košutić et al. (2000) defined the porosity as pore density, pore size distribution (PSD), or effective number of pores in the skin layer of a membrane. Also they studied the porosity of some commercial RO and NF polyamide membranes and concluded that the membranes porous structure was the most significant factor in determining the membrane performance, and solute rejection could be elucidated by membrane porosity parameters (for instance PSD

and N). Increasing the effective number of pores in the membrane's upper layer of RO and NF membranes is affected by increasing pressure, and pore size distribution can be changed under higher pressure (Košutić et al., 2000). For example, the rejection of uncharged pesticide molecules was extremely connected with membrane porosity parameters (pore size distribution and effective number of pores; Košutić and Kunst, 2002; Košutić et al., 2005). This was confirmed by another study (Košutić et al., 2007). In this later study, the researchers examined the rejection of antibiotics for a model wastewater by many NF/RO membranes. They concluded that the pore size distribution of the RO membranes, HR95 and XLE are unimodal and have centered on the size 0.67 nm (Figure 2-10). On the other side, the pore size distribution of the tight NF membrane (e.g. NF-90) is unimodal as well; however the higher value of the size was 0.82 nm. Also the pore size distribution of the RO water softening TFC-S type membrane is represented by wider pores with the peak at 0.84 nm indicating a similar porosity to that of the nanofiltration NF-90 type. In contrast, the pore size distribution of a loose nanofiltration membrane such as the HL type (bimodal) differed from all the membranes which were mentioned previously and recorded two separated peaks. The pores with the maximum occurrence in this study are those of 1.02 nm, followed by noteworthy incidence of larger pores, sized between 1.3 and 2.0 nm.

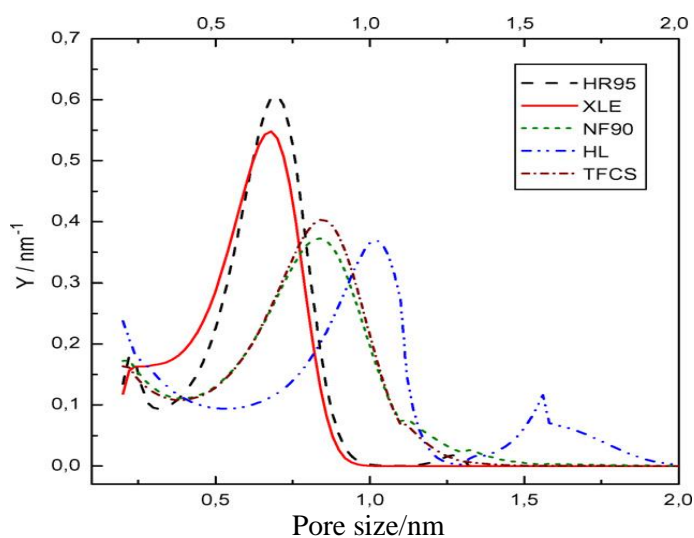


**Figure 2-10:** Pore size disions of the membrane samples at 8 bar (Košutić et al., 2007).

Developments in microscope technology resulted in determining the characterization of the surface and performance of membranes. Both scanning electron microscopy (SEM) and atomic force microscopy (AFM) could give a good description of membrane pore size and subsequently assist in the study of morphological characteristics of the membrane. Studying the surface morphology of membranes could aid in elucidating the separation process in these membranes, for instance the properties of pore structure (pore diameter, pore density and pore size distribution) could define their filtration properties (Hilal et al., 2004). As an example, Hirose et al. (1996) investigated the effect of surface structure on the flux of polyamide composite RO membranes. The authors concluded that the membranes with a rougher skin layer had high fluxes and the flux of RO membranes was approximately comparative to the surface roughness parameters determined by AFM. Also Stamatialis et al. (1999) examined the surface structure of cellulose acetate and cellulose acetate butyrate membranes. The membranes investigated in this study exhibited a broad range of NF and RO permeation characteristics that were associated with surface roughness parameters of the active layers.

#### 2.9.1.2 Solute properties and their effect on the rejection

The rejection  $R$  (%) of a solute is calculated as follows (Equation 2-1; Lin et al., 2007):

$$R = \left(1 - \frac{C_p}{C_f}\right) \times 100\% \quad (2-1)$$

where  $C_p$  is the concentration of permeate and  $C_f$  is the average concentration of feed.

There is no doubt that size exclusion plays a crucial role in the mechanism of solute retention. Many researchers have utilized size parameters to associate with solute rejection and molecular weight, the stokes diameter, the diameter based on the molar volume, the molecular length and molecular width (calculations according to molecular STERIMOL parameters; Van der Bruggen et al., 1999; Agenson et al., 2003; Braeken et al., 2005; Chang et al., 2012).

The Stokes radius according to Kiso et al. (2005) is determined as follows (Equation 2-2):

$$r_d = kT / (6\pi\eta D_w) \quad (2-2)$$

Where  $r_d$  is the molecular radius or Stokes radii (m),  $D_w$  is the diffusion coefficient of the organic compound in water ( $\text{m}^2/\text{s}$ ),  $k$  is the Boltzman constant (J/K),  $T$  is the absolute temperature (K),  $\eta$  is the viscosity of water ( $\text{N s/m}^2$ ).

Bruggen et al. (1999) conducted a comprehensive study to investigate the influence of molecular size on the retention of organic molecules by nanofiltration. Four different membrane types were used in this study (NF-70, NTR-7450, UTC-20 and Zirfon). Four size parameters of the molecules: molecular weight, Stokes diameter, equivalent molar diameter, and a calculated molecular diameter were investigated in detailed. They concluded that there is a good relationship between retention and the four different size parameters. Chen et al. (2004) also investigated the rejection of aromatic pesticides by NF membranes. They reported that some pesticides were completely rejected but some pesticides were partly rejected in this study, in addition the rejection ranges were from 46% to 100% depending on their molecular weight, length, flux and recovery. Bentazone, pirimicarb and vinclozolin were totally rejected in all pilot-scale experiments for the NF membrane. The molecular weights of bentazone, pirimicarb and vinclozolin are 238, 240 and 286, respectively, and they were highest molecular weight pesticides in this study. On the other hand, the average rejection of cyanazine and diuron for the four bench experiments was 93% and 66%. The molecular weights of cyanazine and diuron are 240 and 233, which means that size and other parameters influenced pesticide rejection in the NF experiments. Also Agenson and Urase (2007) examined (20) volatile organic compounds, including low molecular weight contaminants that may are concern such as toluene and trichloroethylene, and (16) semi-volatile organic compounds including plastic additives like organic phosphoric acid esters and phthalate esters. They concluded that the size-exclusion mechanism is dominant for the semi-volatile organic compound molecules too large to pass through the active membrane film

(rejected at >99%). On the other hand, the mechanism of other contaminants which were partly rejected could be characterized as diffusion controlled and depended on the solute type. A few solutes such as 1,1-dichloroethylene, *cis*-1,2-dichloroethylene, *trans*-1,2 dichloroethene displayed insignificant interaction with the membrane surface, achieving nearly complete rejection with separation dominantly convective.

To calculate solute hydrophobicity/hydrophilicity it is common to use the octanol/water partition coefficient ( $\log K_{ow}$  or  $\log P$ ) which is defined as:

$$\text{Log } K_{ow} = \log \frac{C_o}{C_w} \quad (2-3)$$

where  $C_o$  and  $C_w$  are the concentrations of solute in *n*-octanol and water layers, respectively (Kiso et al., 2001b).

On the other hand, the sorption amount of solute can be calculated by Equation 2-4 (Kiso et al., 2001b):

$$K = \frac{Q}{C_b} \quad (2-4)$$

where  $Q$  is the adsorption amount per unit area ( $\mu\text{g cm}^{-2}$ ),  $C_b$  the concentration of solute in bulk solution ( $\text{mg l}^{-1}$ ), and the unit of  $K$  ( $\mu\text{g cm}^{-2}/(\text{mg l}^{-1})$ ).

$\text{Log } K_{ow}$  values of trace organic molecules range between -3 and 7, with the higher values describing hydrophobic components (generally for  $\log K_{ow} > 2$ ; Plakas and Karabelas, 2012). Bruggen et al. (2002) reported that the logarithm of the octanol-water partition coefficient ( $\log K_{ow}$ ) strongly correlated with adsorption on the membrane for molecules with a similar molecular weight below the molecular weight cut-off of the membrane. This clearly indicates that hydrophobicity of the compounds affects the development of the permeate concentration over time. Braeken et al. (2005) examined the correlation between the hydrophobicity of organic compounds, expressed by  $\log P$ , and their retention in nanofiltration. They



found that the retention of compounds with a molecular weight between 146 and 154 is known as a function of  $\log P$  for both membranes UTC-20 and Desal-51-HL. This was clearly evident through a close linear correlation between  $\log P$  and retention for both membranes. In other words, it can be said that a molecule with a high value of  $\log P$  (hydrophobic compound) permeates comparatively easily through the membranes, whereas a compound with a high affinity for the water phase (negative value of  $\log P$ ) will be rejected.

Jung et al. (2005) examined the rejection properties of a variety of aromatic pesticides by using a hollow fiber NF membrane (HNF-1). The findings of this study showed that the rejection of pesticides varied between 41.0% and 88.3%, and the rejection according to the primary feed concentration varied between 45.0 and 93.8%. The authors found that all of the pesticides were adsorbed on the membrane and the adsorption property was affected by hydrophobicity as well as by the molecular planarity of the solute. Yangali-Quintanilla et al. (2009) investigated the rejection of pharmaceutically active compounds and endocrine disrupting compounds by clean and contaminated nanofiltration membranes. They reported that the rejection of hydrophilic neutral compounds by the clean NF-200 membrane varied from 35 to 70% under stable conditions whereas the NF-90 membrane was in the range between 62–96%. The clean NF-90 membrane rejected roughly all of the hydrophobic neutral compounds (95–98%) mainly because of size exclusion. However, electrostatic repulsion was the key mechanism of rejection of ionic compounds by both membranes (71–94% by NF-200 and 99% by NF-90). Another study by Agenson et al. (2003), which examined the retention of a wide range of organic contaminants by different nanofiltration/reverse osmosis processes, concluded that solutes with larger widths, larger lengths and higher logarithmic octanol-water partition coefficients ( $\log K_{ow}$ ) will have higher retentions for all the membranes used. Therefore, it can be said the retention by membranes gave the best correlation with these three parameters.

### 2.9.1.3 Solute and membrane charge

Separation of organic contaminants in aqueous solution through NF/RO is controlled by many significant parameters; one of the most important parameters is electrostatic interactions between charged solutes and a porous membrane (Košutić and Kunst, 2002; Dalton et al., 2005; Teixeira et al., 2005; Ahmad et al., 2008; Arsuaga et al., 2008). Most of the commercial thin-film composite membranes are distinguished by a negative charge which reduces the adsorption of negatively charged foulants, which frequently exist in membrane feed waters, and to improve the rejection of dissolved salts (Teixeira et al., 2005; Jarusutthirak et al., 2007; Plakas and Karabelas, 2012).

The negative charge on the membrane skin is typically due to the presence of sulfonic and/or carboxylic acid groups that are deprotonated at neutral pH. Generally, membrane surface charge is calculated by zeta potential measurements. Many literatures (Teixeira et al., 2005; Lin et al., 2007; Ahmad et al., 2008) have concluded that pH had an influence upon the charge of a membrane because of the disassociation of functional groups. Zeta potentials for the majority of membranes examined in many studies have been shown to become increasingly negative as pH is increased and functional groups deprotonate (Teixeira et al., 2005; Lin et al., 2007; Al-Amoudi, 2010). Teixeira et al. (2005) investigated the role of membrane charge on nanofiltration performance. This study found that the highest flux and lowest retention for uncharged membranes were obtained at an isoelectric point ( $4.2 \pm 0.2$ ). It is noteworthy, when the pH was increased, the membrane negative charge increased, consequently the flux decreased while the retention increased. In the case of divalent hardness ions ( $\text{CaCl}_2$  and  $\text{MgSO}_4$ ), the membrane was less negatively charged and therefore the flux decreased more (Figure 2-11).

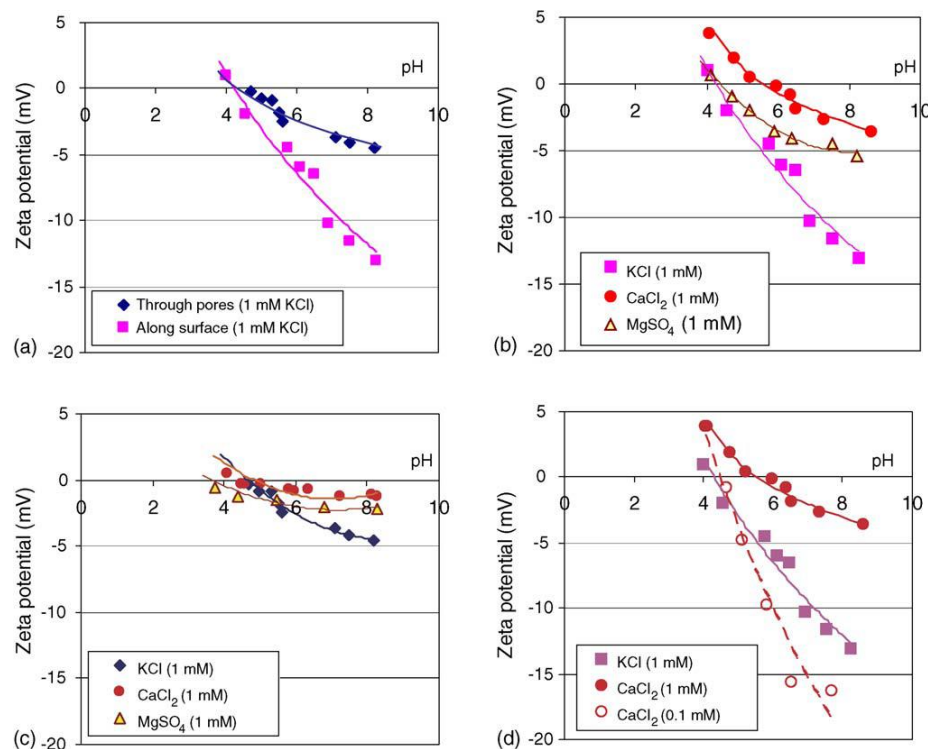


**Figure 2-11:** Streaming potential measurements in the pH range 4.0–8.3: (a) along the surface and through the pores for clean membranes, (b) along the surface in the presence of divalent cations  $\text{Ca}^{2+}$  and  $\text{Mg}^{2+}$ , (c) through the pores in the presence of divalent cations  $\text{Ca}^{2+}$  and  $\text{Mg}^{2+}$ , and (d) along the surface in the presence of two concentrations of  $\text{CaCl}_2$  (Teixeira et al., 2005).

Jarusutthirak et al. (2007) also confirmed that there is a relationship between membrane charge and nanofiltration performance when they conducted a comprehensive study for various factors (i.e. different natural organic matter concentrations, ionic strength and solution pH) affecting cross-flow nanofiltration performances for natural organic matter rejection and flux decline. They concluded that the rejections of salt varied between 16.0%, 25.5% and 37.3% with increased solution pH of 4, 7 and 10 respectively. Solutions having a solution pH of 7 and 10 illustrated higher salt rejection than those having low solution pH. Thus, it can be concluded that increased salt rejection increased permeate flux decline, and that means increased charge repulsion between the negatively charged NF membrane and functional groups in the natural organic matter molecules for high solution pH. Radjenovic et al. (2008) studied the rejection of a wide range of pharmaceuticals during nanofiltration (NF) and reverse osmosis (RO) utilized in a full-scale drinking water treatment plant using groundwater. The results of this study have illustrated

that the maximum rejections in NF/RO processes were recorded for negatively charged pharmaceuticals ketoprofen, diclofenac and sulfamethoxazole ( $R > 95\%$ ). In contrast, negatively charged gemfibrozil and mefenamic acid were rejected on NF and RO membranes with comparatively poor efficiency (i.e., 50–70% and 30–50%, respectively), for which no reasonable elucidation was found. Furthermore, this study demonstrated that positively charged sotalol and metoprolol were rejected on the membranes with very high efficiency ( $R > 90\%$ ).

#### 2.9.1.4 Effect of membrane fouling

One significant issue facing membrane processes is fouling. Mostly, membrane fouling is the result of the existence of dissolved inorganics ( $\text{BaSO}_4$ ,  $\text{CaCO}_3$ ) or organic constituents (humic acids), colloids (suspended particles), bacteria or suspended solids (Hilal et al., 2004). According to Al-Amoudi (2010) membrane fouling poses a key obstacle which has an extreme effect on membrane performance because it causes higher operation costs, higher energy consumption, increased need of cleaning and reduced life-time expectancy.

Flux is considered a parameter for investigation of membrane performance and can be calculated by using Equation 2-5 where  $J$  was flux ( $\text{L}/\text{m}^2\cdot\text{h}$ ),  $V$  is permeate volume (L),  $A$  is membrane area in  $\text{m}^2$  and  $t$  is filtration time (h; Neale, 2009).

$$J \equiv \frac{1dV}{A \cdot dt} \quad (2-5)$$

On the other hand, flux decline, which is an indicator of membrane fouling, could be calculated by using Equation (2-6) where  $J_0$  is the initial permeate flux taken at filtration time of 30 min and  $J$  is the permeate flux at a later filtration time ( $\text{L}/\text{m}^2\cdot\text{h}$ ; Xu et al., 2006).

$$\text{Flux Decline (\%)} = \left(1 - \frac{J}{J_0}\right) \times 100 \quad (2-6)$$

Fouling can be classified into three categories: inorganic fouling as a result of deposition on the membrane surface of inorganic scales (e.g. metal hydroxides, carbonates and colloidal substances), organic fouling due to the presence of natural organic matter such as the derivatives of humic acid or humic matter and biofouling caused by microbial attachment to the membrane surface, followed afterward by their growth and increase if there is enough supply of organic nutrients in the pretreated feed or organic nutrients deposited on membrane surfaces such as bacteria and fungi (Al-Amoudi and Farooque, 2005; Al-Amoudi, 2010; Kang and Cao, 2012).

Xu et al. (2006) reported that surface membrane properties constitute an important factor in membrane fouling through examining the influence of membrane fouling on transport of organic contaminants in NF/RO membrane applications. In this study, membrane fouling was significantly dependent upon the hydrophobicity and roughness of the skin layer of the membrane. For instance hydrophilic and smooth membrane surfaces (TFCHR, CTA and NF-200) are anticipated to interact less with the hydrophobic organics in effluent, therefore dropping the adsorption of organics on the membrane surface.

Xu et al. (2010) also confirmed in another study that membrane surface characteristics play a vital role in membrane fouling by investigating fouling of nanofiltration and reverse osmosis membranes during municipal wastewater reclamation. They found that rough and hydrophobic membranes with high permeability, for instance the NF-90 membrane, mostly show more extreme initial temperature corrected specific flux decline (60%) during filtration as a result of membrane compaction and adsorption of hydrophobic organic matter. On the other hand, the smooth and hydrophilic NF-4040 membrane displayed high and steady temperature corrected specific flux through the filtration of nitrified/denitrified effluent when biofouling was under management. Additionally, Al-Amoudi (2010) conducted a comprehensive review to examine factors affecting natural organic matter and scaling fouling in NF membranes and concluded that membrane surface structure in the solution depends heavily on pH and ionic strength. This review demonstrated that at high ionic strength, the membrane was found to display larger

pore size. Conversely, at low ionic strength, the membrane was found to exhibit a smaller pore size. Consequently, it can be said that membrane fouling is significantly associated with pH and ionic strength (Figure 2-12).

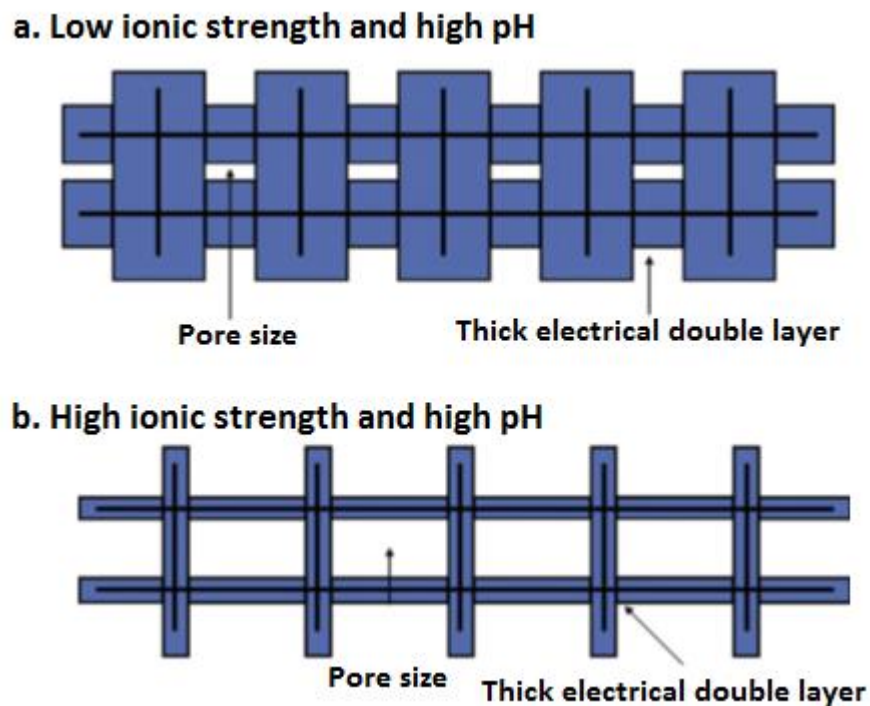


**Figure 2-12:** Conceptual sketch of the swollen membrane matrix for different ionic environments (a: thick electrical double layer at high pH and low ionic strength and b: thin electrical double layer at high ionic strength and low pH; Al-Amoudi, 2010).

Tu et al. (2011) also found that all membrane fouling experiments which they examined seemed to be dependent on the cake-enhanced concentration polarisation phenomenon which not only led to severe permeate flux decline, but also reduced the rejection efficiency of boron and inorganic salts. Moreover, the fouling layer might play the role of a physical barrier that inhibited the effect of solution pH alterations on membrane surface charged properties. As a result, the impact of high solution pH to augment membrane surface negative charge that encouraged boron rejection was inhibited

#### 2.9.1.5 Influence of the filtration system operating parameters

Operating conditions such as solution pH, salinity, organic matter, temperature, pressure and cross-flow velocity could affect the rejection of organic and inorganic contaminants by NF/RO membranes.

The effect of pH as a water quality parameter has been investigated in several papers. For instance, Jarusutthirak et al. (2007) found that the increase of solution pH from 4 to 10 exhibited greater flux decline due to increased salt concentrations on the membrane surface and/or pores. Furthermore Nghiem et al. (2006) found that the rejection of pharmaceutically active compounds increase significantly as the compound converts from a neutral to a negatively charged species because solution pH increases higher than its pKa value. Moreover Zazouli et al. (2009) concluded that the increase of both permeate flux and solute rejection was adapted to the increase of pH solution value. Ballet et al. (2007) reported that the rejection of phosphate increased from 40% to 95% as a result of an increase in pH of the solution from 2.8 to 6. Saitúa et al. (2012) also reported that rejection increased from 72.5 to 92.5% when pH altered from 4 to 8.5.

Many studies have reported that natural organic matter could affect the rejection of organic and inorganic contaminants. For instance, Hu et al. (2007) found that the existence of humic acid in feed solution seemed to improve both the estrone adsorption on a membrane and estrone rejection. Also Schafer et al. (2010) reported that the existence of organic matter in the feed solution has an extreme influence on the rejection of trace contaminants by NF. Furthermore, Jarusutthirak et al. (2007) found the same finding and concluded that increased natural organic matter concentration caused increased permeate flux decline, salt rejection and promoted natural organic matter accumulation on the membrane surface. Other studies have confirmed that natural organic matter may affect the rejection of inorganic contaminants. Comerton et al. (2009) found that natural organic matter contributed to a substantial reduction in effective molecular weight cut-off (from  $385 \pm 13$  Dalton to  $343 \pm 12$  Dalton) while neither the effect of cations nor the interaction of natural organic matter and cations were significant. Also Comerton et al. (2008) in another

study concluded that the existence of organic matter may cause higher rejections of endocrine disrupting chemicals (EDCs) and pharmaceutically active compounds (PhACs) whereas higher concentrations of divalent ions seemed to cause lower endocrine disrupting chemical and pharmaceutically active compound rejection by the membranes.

Salinity of feed solution can cause the effective radius of a charged pore of the membrane to increase as the ionic strength of the feed solution increases. As a result, the rejection of monovalent ions will decrease as their concentration in the feed solution increases (Bolong et al., 2009). Also Teixeira et al. (2005) concluded that higher salt concentrations (higher ionic strength) will decrease flux and rejection, this decrease being more noticeable for the greatly rejected  $\text{MgSO}_4$  salt. Furthermore, Zazouli et al. (2009) reported that transformation of ionic content (from 10 to 20 mM) cause an increase (from 89 to 93% for SR 3) or decrease (from 100 to 91% for SR2) of cephalixin rejection based on the membrane used.

Temperature of the feed solution also affects the rejection efficiency. An increase in temperature of the feed solution leads to an increase in both diffusivity and convective flux of solutes. This situation results in high permeability and water flux which at the same time reduces retention (Mänttari et al., 2006). Fujioka et al. (2012) reported that an increase in the feed temperature between 20 °C and 30 °C lead to a considerable decline in the rejection of all N-nitrosamines (NDMA, NMEA and NPYR) from 49 to 24%, 81 to 62% and 90 to 74%, respectively. Also Arsuaga et al. (2008) examined the concentration, temperature and pH dependences on retention for phenol and malonic acid single solutions and their mixtures. The findings of this study showed that phenol retention was much reduced with temperature increase. On the contrary, malonic acid retention, which broadly depends on solute concentration, displayed a somewhat constant behaviour against temperature.

Operating pressure is considered to be a significant factor that could affect water flux as well as the rejection of contaminants. For instance, high operating pressures would cause high rejections; while a high quantity of permeate produced per unit feed will result in a reduction in rejection (Verliefde et al., 2007a). Uyak et al. (2008) reported



that increasing operating pressure causes a higher flux but does not have a considerable influence on trihalomethane rejection. Also, Figoli et al. (2010) reported that an increase of pH and a decrease of feed temperature and arsenic concentration caused higher arsenic rejection for both membranes used. In contrast, higher operating pressure values somewhat decreased the removal efficiency of the N30F membrane. On the other side, Agenson et al. (2003) found that at a low pressure of 0.3MPa, the high desalting membranes successfully retained practically all of the semi-volatile organic compounds at (more than 90%) but this did not occur for the volatile organic compounds.

Also cross-flow velocity could positively or negatively affect the permeate flux. For instance when the cross-flow velocity was changed from  $4.0 \times 10^{-2}$  to  $3.2 \times 10^{-3}$  m/s, the permeate flux decline because concentration polarization increased from 23% to 43% (Lin et al., 2006).

## **2.10 Factors affecting the adsorption of organic and inorganic compounds by CNTs**

Adsorption by CNTs is considered an effective and economic technology that could be used for the removal of trace organic contaminants from aquatic sources (Chen et al., 2011; Joseph et al., 2011a; Deng et al., 2012). To achieve the removal by this method, contaminants of concern are transferred from the water phase to the solid phase (adsorbent). The adsorption of organic and inorganic compounds by CNTs depends on: CNT properties (adsorption site, surface area, surface function group, purity and porosity), solute properties (hydrophobicity, electron polarizability, polarity, functional groups) and environmental conditions (pH, ionic strength; Figure 2-13; Ren et al., 2011).

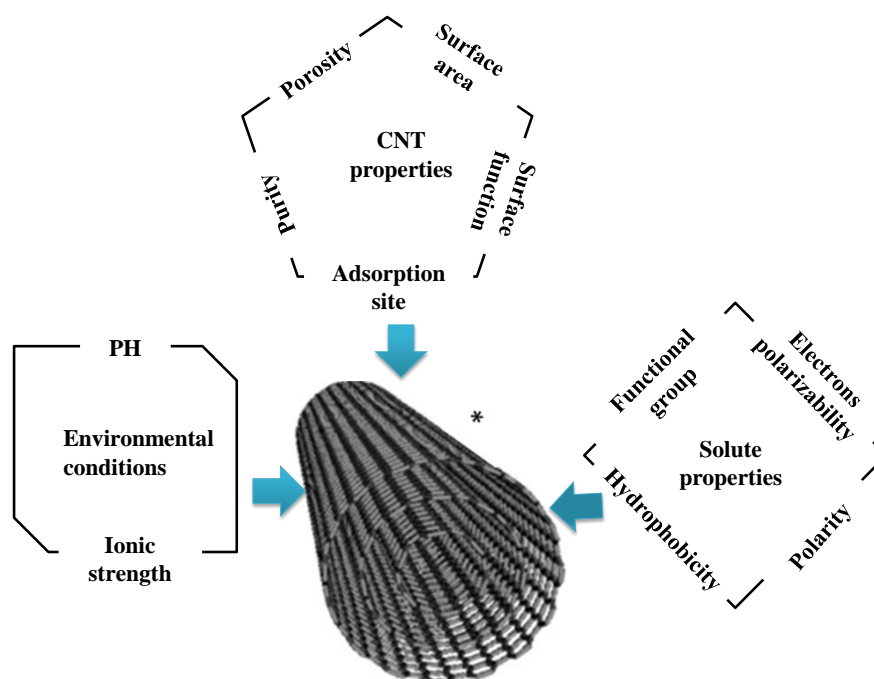


**Figure 2-13:** Factors affecting the adsorption of organic and inorganic compounds by CNTs  
\* (Ismail et al., 2009).

The properties of CNTs such as purity, structure and nature of the surface play a fundamental role in influencing adsorption performance of CNTs. In particular, functionalisation of CNTs in solution could significantly increase the interaction of CNTs with contaminants, and thus could increase the removal capacity of CNTs in the preconcentration of contaminants (Ren et al., 2011). Lu and Chiu (2006) reported that the properties of CNTs, for instance purity, structure and nature of the surface were significantly enhanced after functionalisation by sodium hypochlorite solutions which made CNTs more hydrophilic and appropriate for adsorption of  $\text{Zn}^{2+}$  from water. Also Adolph et al. (2012) conducted a study to investigate phosphine functionalised multiwalled carbon nanotubes as an adsorbent for the removal of nickel from aqueous solution. They concluded that the phosphine functionalised multiwalled carbon nanotubes (MWNTs) gave a greater adsorption capacity compared with purified multiwalled carbon nanotubes. It can be explained that triphenylphosphine connected multiwalled carbon nanotubes adsorbed more  $\text{Ni}^{2+}$  from aqueous solution than the purified multiwalled carbon nanotubes. Furthermore, Shao and Wang (2012) reported that the modified polyaniline on MWNT surfaces

resulted in an improved MWNT adsorption capacity. This is attributed to the amine and imine functional groups of polyaniline having a strong affinity with  $\text{Pb}^{2+}$  ions.

Surface area and porosity of CNTs could play an important role in affecting adsorption of contaminants onto CNTs. Upadhyayula et al. (2009) reported that the adsorption in CNTs depends on available surface area and, therefore, the high molecular weight portion of natural organic matter is adsorbed somewhat strongly. Furthermore, they reported that the greater adsorption capacities of CNTs compared to other adsorbents is fundamentally due to their fibrous shape with high aspect ratio, availability of large external surface area which can be easily accessed by biological pollutants, and existence of well-developed mesopores. Also Yan et al. (2006) concluded that increased adsorption of cyanobacterial toxins (microcystins) was a result of the decreased outside diameter of CNTs. This indicates that the size of CNT pores that fit the molecular dimension of microcystins represented a fundamental role. Moreover, the surface area of CNTs can be considered another factor affecting the adsorption of microcystins through CNTs. Yan et al. (2008) reported that the adsorption of atrazine on CNTs was clearly changeable, as a result of external surface adsorption. Moreover, interstitial spaces within CNT aggregates are not closed. Li et al. (2003) concluded that the sorption for three heavy metals ( $\text{Pb}^{2+}$ ,  $\text{Cu}^{2+}$  and  $\text{Cd}^{2+}$ ) increased with an increase in CNT mass, which can be attributed to the availability of more sorption sites. Rao et al. (2007) reported that a decreased rejection of divalent metal ions from aqueous solution by CNTs could be due to the increase in activity coefficients of these metal ions, which delays their transmission to the surface site of CNTs.

The pH and ionic strength play a significant role in affecting adsorption efficiency as does the degree of ionization of adsorbate and the surface charge of adsorbent. For instance, Hu et al. (2012) reported that the adsorption of roxarsone on MWNTs declines significantly with a raise in pH value from 2.0 to 11.7 and declines dramatically with a rise in ionic strength value from 0 to 1.0 mol/L KCl. Also Lu and Su (2007) concluded that the adsorption of natural organic matter onto CNTs increased with increased natural organic matter concentration and solution ionic

strength. However, natural organic matter concentration and solution ionic strength decreased with increased solution pH. This obviously indicates that adsorption, of more natural organic matter onto CNTs leads to the release of more  $\text{OH}^-$  from the CNT surface into the solution, thus increasing the solution pH. In addition Deng et al. (2012) concluded that the adsorption capacity for MWNTs was much superior at pH 7 than at pH 3 and 5 and then remained constant between pH 7 and pH 10. This phenomenon could be elucidated by comparing the pH of the solution, the  $\text{pK}_a$  of diuron and the  $\text{pH}_{\text{pzc}}$  of MWNTs. When solution pH is less than 4, the cationic species of diuron ( $\text{DH}^+$ ) are dominant in solution and the complete surface charge on as-prepared and oxidized MWNTs are both positive. Consequently, the electrostatic repulsion forces predominate, causing the lower adsorption capacity.

On the other hand, temperature could affect the adsorption of contaminants onto CNTs. Hong et al. (2007) found that the average length of MWNTs is affected significantly with a rise in both temperature and oxidation time. Also Kuo et al. (2008) concluded that the adsorption ratio of direct dyes increased as a result of the amount of CNTs, NaCl addition and as temperature increased. In contrast, the adsorption ratio of direct dyes decreased as dye concentration increased.

## **2.11 Development of antifouling membranes for water treatment**

Membrane filtration is considered a significant technology that can participate in the sustainability of water supplies. NF/RO have been widely used for the removal of organic and inorganic compounds, however, membrane fouling is a key constraint to the further application of the NF/RO (Freger et al., 2002; Xu et al., 2010). Fouling either raises the transmembrane pressure or decreases the flux, depending on whether the system is operated at constant flux or constant pressure, respectively (Mondal and Wickramasinghe, 2012).

Several significant factors such as hydrophilicity, surface roughness, pore size and surface charge could influence the membrane antifouling properties (Zularisam et al., 2007). It is notable that higher hydrophilicity and smoother surface give the membrane better fouling resistance. Hydrophilic materials are less prone to

biofouling due to hydration through hydrogen bonding (Tu et al., 2011). Higher surface roughness offers higher surface area, which could endow more binding sites for foulants to attach. Also, as surface roughness increases, the formation of defects increases, which can augment the formation of biofilms (Misdan et al., 2012). The effect of the surface charge relies on the composition of the feed matrix. If there are contaminants of opposite charge to that of the membrane charge in the feed matrix, higher surface charge density will increase the membrane fouling because of the deposition of the particles (Wang et al., 2012a; Xu et al., 2013). Consequently, many efforts have been made to alleviate this issue, including the combination with pretreatment processes (Shon et al., 2004), finding a new generation of membranes (Chen et al., 2004) and the development of antifouling membranes. Among these efforts, the last one is a fundamental way and has been paid much attention by many scientists and membrane manufacturers (Kang and Cao, 2012).

Many efforts are made to improve the hydrophilicity and antifouling properties of membranes however most of these efforts focused on surface modification of membranes.

### **2.11.1 Surface modification of membranes**

Surface modification of current membranes is considered as a potential and effective method to improve antifouling membranes. There are many methods to modify the surface of membranes however, the most effective surface modification methods are surface adsorption, surface coating, plasma treatment, radical grafting and chemical reactions.

The surface adsorption means that the hydrophobic portion of the surfactant has a favourable free energy of attraction for the polymeric surface leads to a modification in membrane surface character. Several scientists adopted this method to modify the surface properties of water filtration membranes (Xie et al., 2007). For example, Zhou et al. (2009) investigated the modification of a polyamide RO membrane by electrostatic self-assembly of polyethyleneimine (PEI) on the membrane surface.

They found that the charge reversal on the membrane surface because of using the PEI layer was shown to increase the fouling resistance to cationic foulants due to the improved electrostatic repulsion and increased surface hydrophilicity as well. Also, Ba and Economy (2010) enhanced the charged NF membrane by adsorption of a layer of negatively charged sulfonated poly (ether-ether ketone) onto the surface of a positively charged NF membrane using bovine serum albumin (BSA), humic acid and sodium alginate as the model foulants. This study revealed that the modified membrane displayed much better fouling resistance than both the positively and the negatively charged membranes. Additionally, the foulants would less likely deposit onto the membrane because of the removal of the charge interaction between the membrane and the foulants.

Surface coating is a simple method and easily applied, therefore it has attracted the attention of many researchers and membrane manufacturers up to now. The coating acts as a protective layer to reduce or eliminate the adsorption and deposition of foulants onto the membrane surface. Hachisuka and Ikeda, (2001) coated hydrophilic and electric neutral polyvinyl alcohol onto a polyamide RO membrane to develop the antifouling properties. After coating, the hydrophilicity of membrane surface was improved. Furthermore, the surface zeta potential ( $\zeta$ ) at pH 6 changed from 25 mV to 0 mV. Consequently, the coated RO membrane showed a superior antifouling property in industrial wastewater and cationic surfactant feed solution. Also Kim and Lee (2006) conducted a study to examine surface coating of the RO and NF membranes using polyvinyl alcohol (PVA). They concluded that the polyvinyl alcohol coated RO and NF membranes led to decreasing surface charge and surface roughness and consequently the coating reduced fouling significantly.

Madaeni et al. (2013) studied fouling resistance of nanofiltration membranes by deposition of multi-walled carbon nanotubes (MWNTs) on the surface of a polyvinylidene fluoride microfiltration membrane followed by polydimethylsiloxane coating. This study revealed that the flux recovery ratio for a membrane coated with 5wt.% polydimethylsiloxane was 82%. This displays that the fabricated superhydrophobic NF membrane possesses a better antibiofouling property. Hernadi

et al. (2003) conducted a study to examine synthesis of MWNT-based composite materials with inorganic coating. This study recommend that an effective interfacial bonding between the carbon nanotube surface and forerunners offers a constant reinforcement composite fiber, which provides a favourable wettability for dispersion in either polymer or metal matrices.

Plasma treatment is considered one of the most promising technologies for the surface modification of polymer materials to enhance the surface properties. The exceptional advantage of plasma modification is that the surface properties and biocompatibility can be improved selectively whereas the bulk attributes of the membrane remain unchanged (Xu et al., 2009). Indeed, this technique includes two categories, plasma polymerization and plasma-induced polymerization. Plasma polymerization is a one-step process as the plasma is utilized to deposit the polymer onto membrane surfaces, whereas the plasma-induced polymerization employs plasma to activate the surface to produce oxide or hydroxide groups, which can then be used in conventional polymerization methods (Zou et al., 2011). For example Shi et al. (2011) used cold plasma treatment for the surface modification of porous polytetrafluoroethylene (PTFE) film to improve the hydrophilicity. In this study contact angle measurements revealed that the hydrophilicity of the PTFE film surface was significantly improved because of the surface roughness and changes of chemical elements on the polytetrafluoroethylene surface. Also, Zou et al. (2011) conducted a study to investigate surface hydrophilic modification of RO membranes by plasma polymerization. This study reported that the modified membranes offered an exceptional maintenance of flux compared to the unmodified membranes. It was observed that after 210 min of filtration, no flux decline was found for the modified membranes, whereas there was a 27% reduction of the initial flux for the unmodified membrane. The surface hydrophilic modification of RO membranes by plasma polymerization has exhibited a clear enhancement in membrane anti-fouling performance. Kim et al. (2011) applied plasma surface modification of nanofiltration (NF) thin-film composite (TFC) membranes to improve anti-organic fouling. The results showed higher salt rejection and this can be attributed to the plasma-induced surface cross-linking, and less adsorption of bovine serum albumin (BSA) and humic

acid due to the enhanced surface hydrophilicity and more negatively charged surfaces.

Radical grafting is an effective technique for the polymer surface modification. In this method, the free radicals are created from the initiators and transferred to the polymer to react with a monomer. Wei et al. (2010) conducted a radical grafting study. In this study the authors used 2,20-azobis-isobutyramidine dihydrochloride as an initiator, which can be thermally decomposed to produce free radicals. Also they used 3-allyl-5,5-dimethylhydantoin as a grafting monomer. This study concluded that 3-allyl-5,5-dimethylhydantoin-grafted RO membranes had lower contact angles than those of the raw membranes, demonstrating the increase of surface hydrophilicity. After exposures to microbial cell suspension, the modified membranes exhibited a smaller decrease in pure water flux and less adsorption of microbial colonies on the surface, which confirmed the enhancement of anti-biofouling properties.

Chemical reaction treatment is the dominant means for chemically modified reactions. Carboxylic acid and primary amine groups provide the possibility of surface modification by means of chemical reactions (Kang and Cao, 2012). Van Wagner et al. (2011) investigated surface modification of commercial polyamide RO membranes using the reaction of primary amine groups with the epoxy end groups of polyethylene glycol diglycidyl ether, and the resultants displayed improved fouling resistance to charged surfactants and emulsions containing *n*-decane and a charged surfactant

## **2.12 Integrated/Hybrid membrane systems**

A combination of two technologies in a hybrid process is a promising way of improving the overall membrane operation. To get high quality water and good performance of the membrane, it has to be combined with other processes such as coagulation, adsorption or even coupled with another membrane (Ang et al., 2015). In the last decade, many scientists and researchers recommended combining membrane systems with one another rather, than combined with other processes such as coagulation and adsorption. For example, the combined membrane bioreactor



(MBR) and RO systems resulted in above 99 % removal of metronidazole, hydrocodone, codeine and ranitidine through size exclusion, steric hindrance, electrostatic interaction, and hydrophobic interaction between the contaminants and the membrane (Dolar et al., 2012a). Alturki et al. (2010) concluded that the combination of NF/RO membranes and a MBR system resulted in a removal rate of higher than 99% for most of the 40 trace organic contaminants selected in their study. High water quality was obtained using the integrated treatments MBR–NF and MBR RO, with removal efficiencies higher than 97% for salinity, 96% for total organic carbon (TOC), 91% for  $\text{NO}_3^-$  and 99% for total phosphorous TP (Cartagena et al., 2013). Additionally, the combination between forward osmosis (FO) and membrane bioreactor (MBR) achieved more than 99% and 98% removal of total organic carbon and ammonium-nitrogen, respectively (Achilli et al., 2009).

### **2.13 Summary**

This chapter describes clearly the types of contamination in surface and groundwater, with special reference to the effects of both organic and inorganic contaminants. This includes their classification, their presence in aquatic environments and their adverse effects on the environment and human health as well as the fate and transport of these contaminants to surface and groundwater.

Surface and groundwater remediation has been reviewed in this chapter whether conventional treatment or advanced treatment. However, membrane technology received more attention, because this study is based on the use of NF/RO membrane and CNT technology to rehabilitate contaminated surface and groundwater. Effectiveness of this technology in the removal of both trace organic and inorganic contaminants has also been discussed.

Membrane fouling is a main limitation to using NF/RO and CNTs as well. By reducing or removing fouling, the range, type and economics of membrane applications can increase significantly. Many efforts are made to improve the hydrophilicity and antifouling properties of membranes, however most of these

efforts concentrated on surface modification of membranes. Methods used to modify the surface of membranes have been also discussed in this chapter.

## **CHAPTER 3: MATERIALS AND METHODS**

### **3.1 Introduction**

Membrane technology has become a promising technology that can be relied upon in water treatment techniques. In light of this, membrane technology could play a significant role for removal of organic and inorganic contaminants and consequently solving water shortage problems as well as providing better environmental control. Among this technology, nanofiltration (NF), reverse osmosis (RO) and carbon nanotube (CNTs) have become increasingly important. This thesis investigates the use of the membrane technologies in treating contaminated surface and groundwater sites. The various analytical methods, laboratory scale set-ups, and experimental protocols used in this study are described and a model of selected organic and inorganic contaminants with their physicochemical properties is proposed. Weather data was also collected, analysed and discussed in this chapter. More information concerning materials and methods are given in following chapters as required.

### **3.2 Study area**

In this study contaminated surface and groundwater for selected sites in the Illawarra and Sydney regions have been examined. At the Illawarra region samples have been collected from the Russell Vale Golf Course specifically from the leachate pond. On the other hand, at Sydney region samples have been collected from Botany Bay. In the Botany area samples have been collected from three contaminated areas, namely EWB10D, EWB13D and WGB32. Figure 3-1 illustrates samples sites in the Illawarra (Russell Vale) and Sydney (Botany Bay) regions.

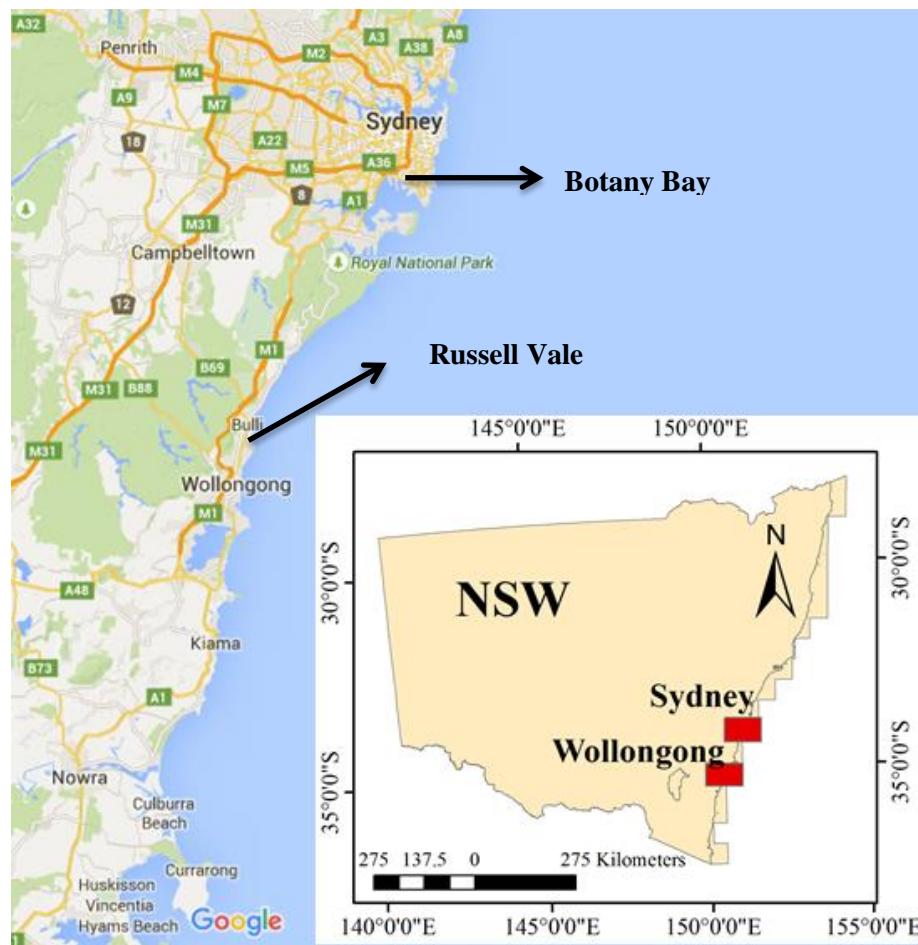


**Figure 3-1:** Image illustrates samples sites in the Illawarra (Russell Vale) and Sydney (Botany Bay) regions.

### 3.2.1 Russell Vale Golf Course

#### 3.2.1.1 A brief history of the Russell Vale Golf Course site

In the 1960's Wollongong City Council recognised the requirement for a public golf course in the northern suburbs of Wollongong. Numerous potential sites were recognized and the Russell Vale waste disposal site, surrounded by Hicks St, Princes Highway and Rixon's Pass Road was ultimately selected as the most appropriate site. In February 1978 Council established a Golf Course Committee, under the chairmanship of Alderman Jack Parker, to examine, report on and organize the staged improvement of a golf course at Russell Vale (Wollongong City Council, 2011).

In the 1980's the first stage of the landfill operation was achieved and there was adequate land to develop a 9 hole par 3 golf course. In April 1981, Council determined to proceed with the establishment of an 18 hole par 3 golf course in a staged growth on the landfill site. The course was formally opened by John Brown MHR Federal Minister for Sport, Recreation and Tourism on 31 October 1986 (Wollongong City Council, 2011). Endorsement for the second stage of the course development was obtained from Wollongong City Council in 1987. The next most important course developments, following the end of the tip use in December 1995, was the expansion of the 2nd and 18th holes to par 4's, the construction of the par 4 14th, a new par 3 15th and the gem in the crown the par 5 16th. These holes came into play on Feb 6th 1999 (Wollongong City Council, 2011). In late 2002 Council established fairway watering on the 14th, 16th and 18th holes. The design of the course has produced a very demanding par 59 layout. The course has great greens which are recognised as among the best in the Illawarra region (Wollongong City Council, 2011).

#### 3.2.1.2 Sample sites at the Russell Vale Golf Course

At the Russell Vale Golf Course samples have been collected from the leachate pond as shown in Figure 3-2A-B. The leachate pond receives surface runoff from the golf course as well as leachate from the buried waste disposal landfill beneath the golf course.

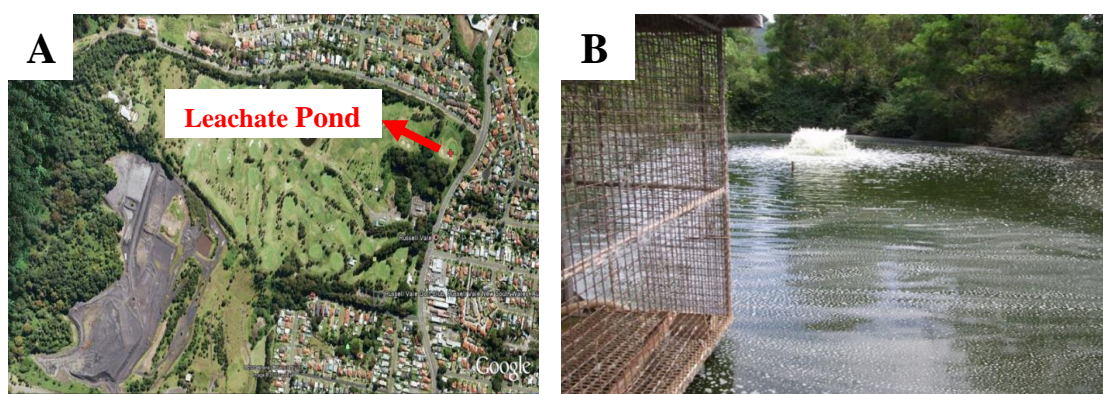


**Figure 3-2:** (A) Aerial image for Russell Vale Golf Course Club. (B) Photograph of the leachate pond at Russell Vale Golf Course.

### 3.2.2 Botany Industrial Park groundwater

#### 3.2.2.1 Background

The environmental issues at what is now identified as the Botany Industrial Park (BIP) and adjacent areas (Figure 3-3) date back to the early 1940s when manufacturing began in this area. The 1960s saw the commencement of huge manufacturing plants that produced an extensive range of chemicals. This was before the implementation of strict government legislative environmental regulations, particularly in understanding the consequence of chemical use and storage in soil and in groundwater. Through this time, chlorinated hydrocarbons (CHCs) were stored on-site in tanks and drums. Some of these stored materials have leaked into the ground and the groundwater. It is expected that contamination resulted from accidental spills as well. Since CHCs are denser than water, they usually dissolve gradually in water. This means that the greatest contamination has a tendency to be found in deep rather than shallow groundwater. The CHCs are toxic and some are related to cancer (ORICA, 2011).

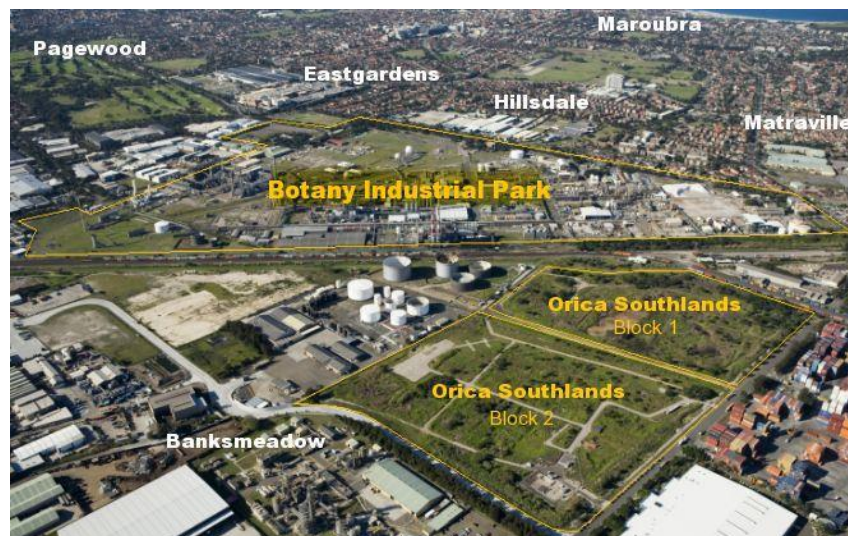


**Figure 3-3:** Aerial image for Botany Industrial Park (BIP) and nearby areas.

If no response is taken to control, rehabilitate and treat the pollutants in the groundwater, they will increasingly contaminate Penrhyn Estuary and probably Botany Bay. This will have possible risks for the health of humans who use recreational areas in these locations, and adversely affect the important feeding and nesting habitats of sheltered migratory shorebirds in Penrhyn Estuary. Orica is now accountable for controlling the groundwater contamination and is entrusted with cleaning it up to avoid long-term environmental deterioration. Orica created the Botany Groundwater Cleanup Project to hydraulically enclose the polluted groundwater, in order to prevent it from entering Botany Bay and to treat the groundwater to usable standard at a Groundwater Treatment Plant (GTP; ORICA, 2011).

#### 3.2.2.2 Sample sites at Botany Industrial Park

In the Botany area samples have been collected from three contaminated areas, namely EWB10D and EWB13D at Southlands and WGB32 located near the tennis courts outside the Botany Industrial Park fence line as illustrated in Figure 3-4 and Figure 3-5 respectively.



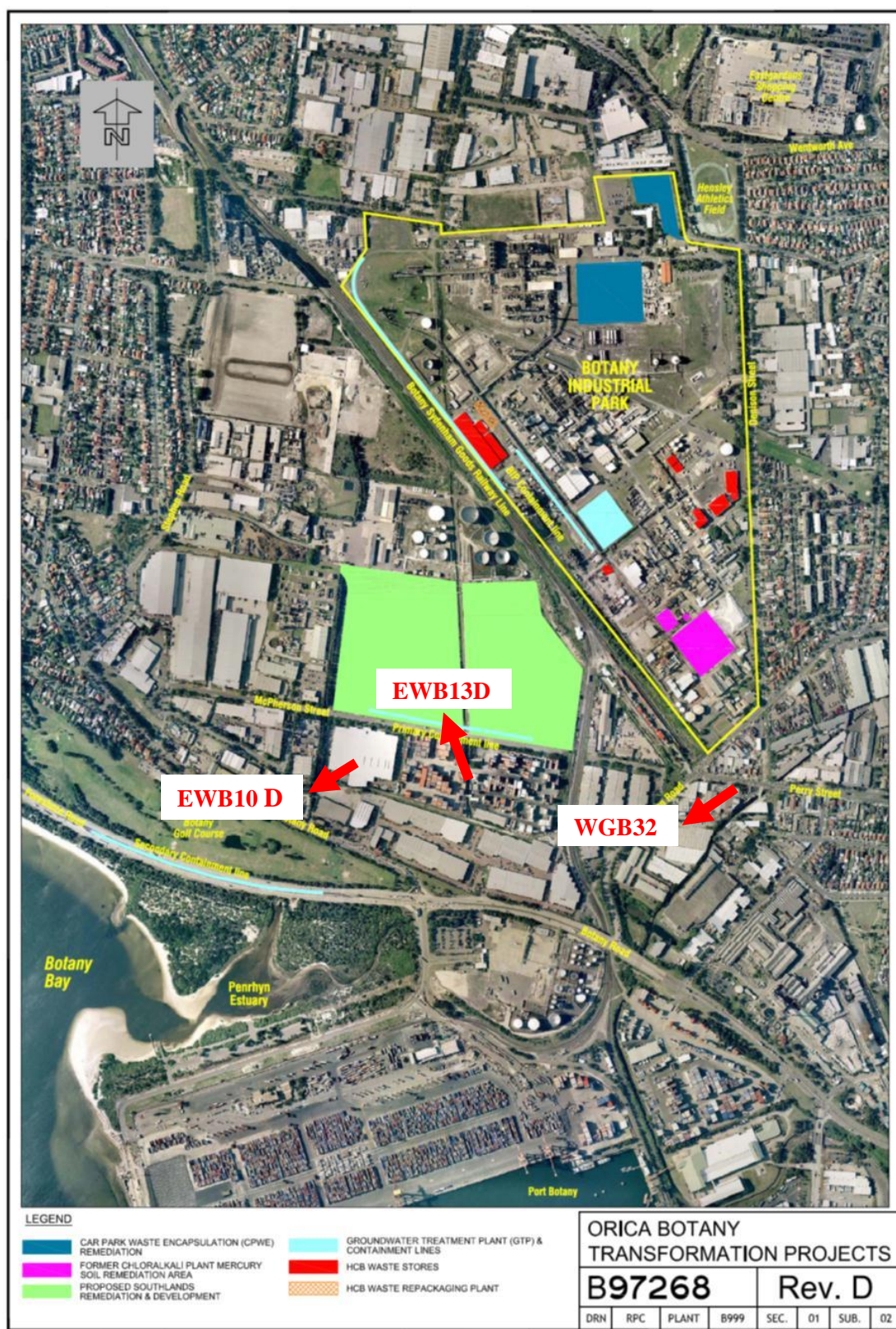
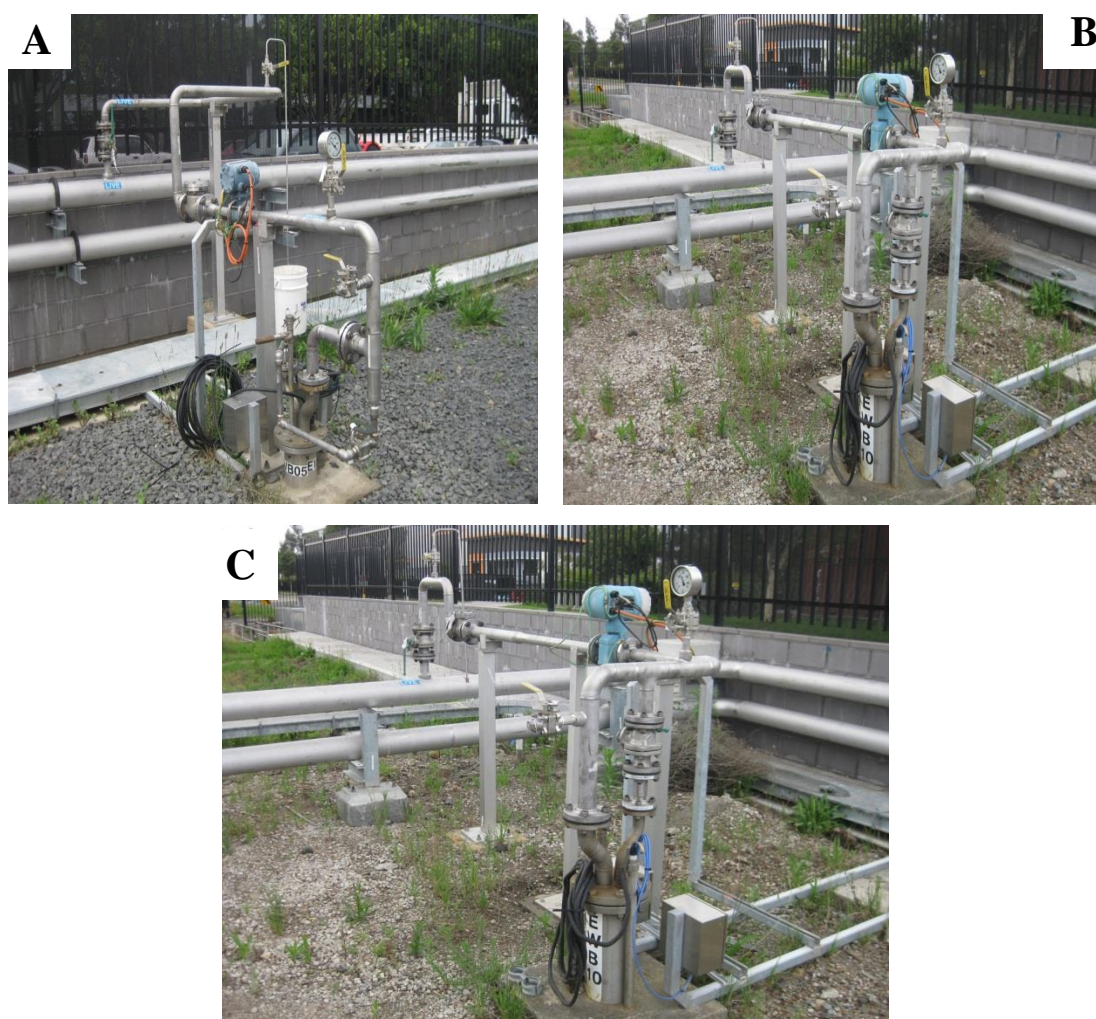


Figure 3-4: Aerial image of the Botany Industrial Park showing sample collection sites.





**Figure 3-5:** Photographs of sample sites at Botany Bay. (A) Photograph of EWB13D at Southlands. (B) Photograph of EWB10D at Southlands. (C) Photograph of WGB32 located near the tennis courts.

### 3.3 Weather data for Russell Vale and Botany areas

All weather data for Russell Vale and Botany Bay areas have been obtained from Australian Government-Bureau of Meteorology (Two stations) as shown in Table 3-1, Table 3-2 and Appendix A. This information is very significant in particular when used them to investigate the relationship between seasonal effects and using membrane technology.

**Table 3-1:** Illustrates weather data for Russell Vale area <sup>a</sup>.

Season	(A) Russell Vale - 068228 Bellambi AWS NSW			
	Date of sampling	Temperature ( c° )	Rainfall (mm)	Relative humidity (%)
Autumn	12/1/2012	20.7	0	NA <sup>b</sup>
Winter	3/4/2012	26.6	0	60
Spring	14/6/2012	17	10.8	94
Summer	11/9/2012	17.8	0	77

<sup>a</sup> Provided by Australian Government - Bureau of Meteorology.

<sup>b</sup> NA: Not available.

**Table 3-2:** Illustrates weather data for Botany Bay area <sup>a</sup>.

Season	(B) Botany - 066037 Sydney Airport AMO NSW			
	Date of sampling	Temperature ( c° )	Rainfall (mm)	Relative humidity (%)
Autumn	1/12/2011	18.8	9.8	NA <sup>b</sup>
Winter	4/4/2012	27.3	0	58
Spring	13/6/2012	15.3	12.2	81
Summer	12/9/2012	22.9	0	62

<sup>a</sup> Provided by Australian Government - Bureau of Meteorology.

<sup>b</sup> NA: Not available.

### 3.4 Laboratory-scale set-ups

Two different laboratory-scale systems were used in this thesis work. They include a cross-flow NF/RO filtration system and a dead-end filtration system. It is notable that a hybrid membrane system was not used in this research because we wanted to investigate each system for removal organic/inorganic contaminants separately to reach in the end the best system for treating contaminated surface and groundwater. Consequently, the most effective solutions for treating surface and groundwater issues at Russell Vale and Botany Bay, respectively, can be recommended.

### **3.4.1 Pressure driven membrane filtration system**

A laboratory-scale, cross-flow membrane filtration system with a stainless steel cross-flow cell was constructed for this study (Figure 3-6). The cell had an effective membrane area of 40 cm<sup>2</sup> (4 cm x 10 cm) and a channel height of 2 mm. The system was equipped with a Hydra-Cell pump (Wanner Engineering Inc., Minneapolis, MN). The temperature of the test solution was kept stable using a Neslab RTE 7 chiller/heater equipped with a stainless steel heat exchanger coil that was submerged directly into a stainless steel reservoir. The permeate flow was measured by a digital flow meter (Optiflow 1000, Agilent Technologies, Palo Alto, CA) connected to a personal computer, and the cross-flow rate was monitored using a rotameter. This apparatus was provided by Dr Long Nghiem (Faculty of Engineering, University of Wollongong).

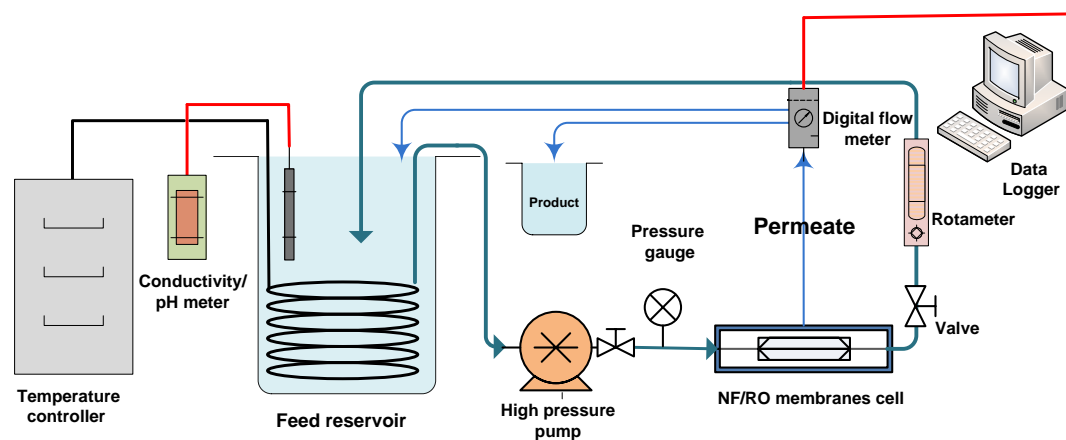


**Figure 3-6:** Schematic diagram and photograph of the laboratory-scale pressure driven membrane filtration system.

### 3.4.2 Dead-end filtration cell setup

The ability of buckypapers to remove organic and inorganic contaminants from aqueous solution was investigated by using buckypapers held within a cross-flow cell constructed by staff of the Faculty of Science workshop, University of Wollongong. The cell had an effective membrane area of  $4.68 \text{ cm}^2$  ( $1.8 \text{ cm} \times 2.6 \text{ cm}$ ) which was

set up in a dead-end filtration system, along with equipment provided by Dr Long Nghiem (Faculty of Engineering; University of Wollongong; Figure 3-7). Compressed air, controlled via an air pressure gauge, was used to force water from the steel reservoir through the cross-flow cell and over the surface of the buckypaper. The flux across the buckypaper was measured by recording the mass of water that passed through the membrane as a function of time using a computer-controlled balance (Mettler-Toledo AB2 with Balancelink software).

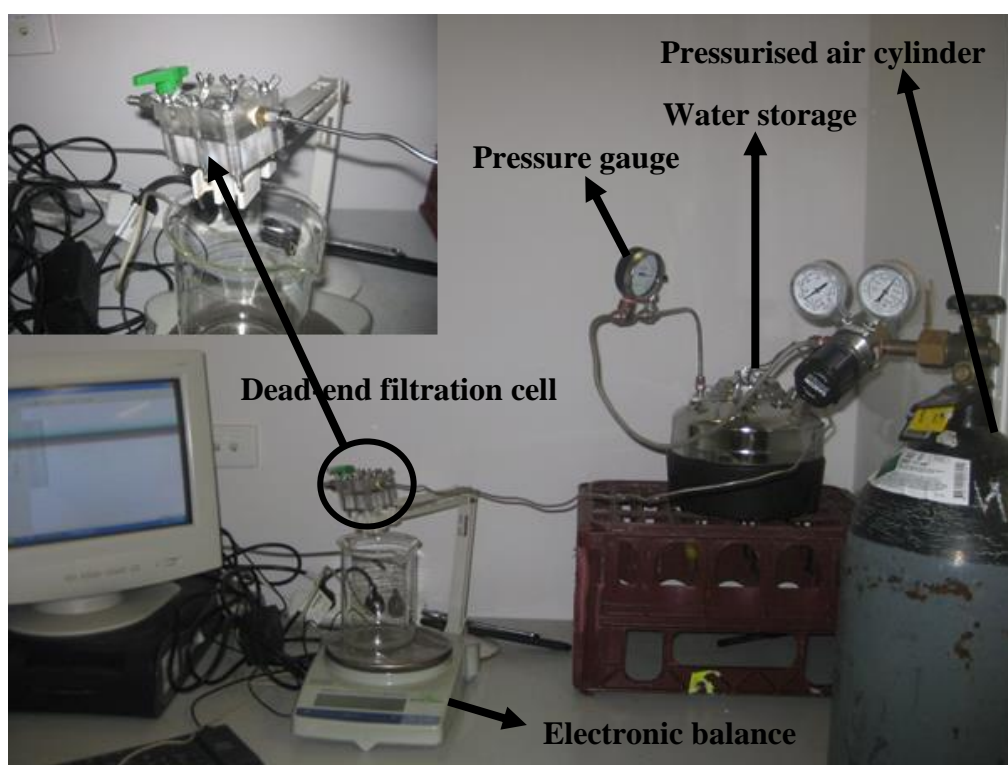
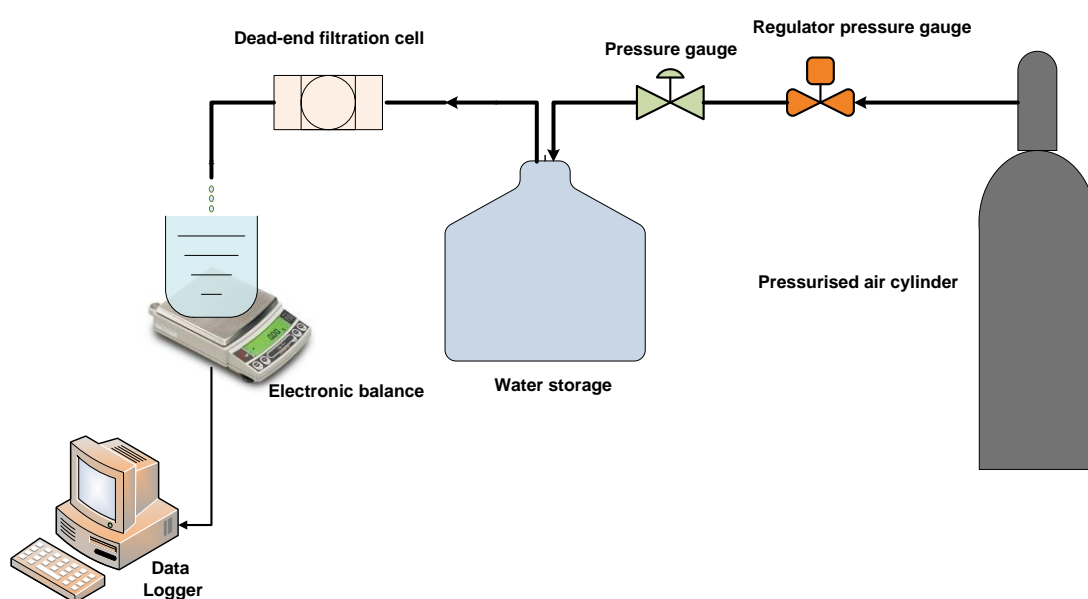


**Figure 3-7:** Schematic diagram and photograph of the laboratory-scale dead end filtration cell setup.

### 3.5 Membranes and membrane modules

#### 3.5.1 Nanofiltration and reverse osmosis (NF/RO) membranes

A NF membrane (namely NF-90) and a RO membrane (namely ESPA2) were used in this project. NF-90 was obtained from Dow Film Tec (Minneapolis, MN, USA) whereas the ESPA2 was obtained from Nitto Denko (Oceanside, CA, USA). These membranes were received as flat sheet samples and stored dry. All membranes used in this study are made of a thin aromatic (or semiaromatic) polyamide active layer and thicker more porous supporting layer. Physicochemical characteristics of these membranes are illustrated in Table 3-3. Based on their estimated pore size, the NF-90 membrane could be classified as a tight nanofiltration membrane whereas ESPA2 can be assumed to have no obviously defined pore structure.

**Table 3-3:** Properties of the selected NF/RO membranes.

Membrane	Average pore Diameter <sup>a</sup> (nm)	Na <sup>+</sup> rejection <sup>b</sup> (%)	Molecular weight cut-off <sup>c</sup> (g/mol)	Contact angle <sup>d</sup> (°)	Surface Roughness <sup>d</sup> (nm)
NF-90	0.68	85.0	~200	42.5	63.9
ESPA2	Not applicable	96.5	~100	60.6	30.0

<sup>a</sup> (Nghiem et al., 2004b).

<sup>b</sup> Feed solution contains 20 mM NaCl and 1 mM CaCl<sub>2</sub> (pH 8).

<sup>c</sup> Provided by the manufacturers.

<sup>d</sup> (Alturki et al., 2010).

#### 3.5.2 Carbon nanotube (CNT) membrane

The CNTs used in this investigation were mainly multi-walled thin nanotubes, with 95% C purity, supplied by Nanocyl (Nanocyl-3100). Triton X-100 (T9284; Dolar et al., 2012a) was supplied by Sigma Aldrich. Dispersion was prepared using Milli-Q water (18 MΩ cm). A hydrophilic 0.22 μm cellulose nitrate (Loncnar et al., 2010) membrane filter was provided by Millipore. Only one type of membrane was used as



the support material for the preparation of the buckypapers in this project. Small, circular buckypapers were made using polytetrafluoroethylene (PTFE) membranes of  $\sim 4.5$  cm diameter (with  $0.22\text{ }\mu\text{m}$  pores).

#### 3.5.2.1 Dispersion preparation

The dispersant used in the preparation of buckypapers was 1% (w/w) Triton X-100. The structure of Triton X-100 can be seen in Figure 3-8.

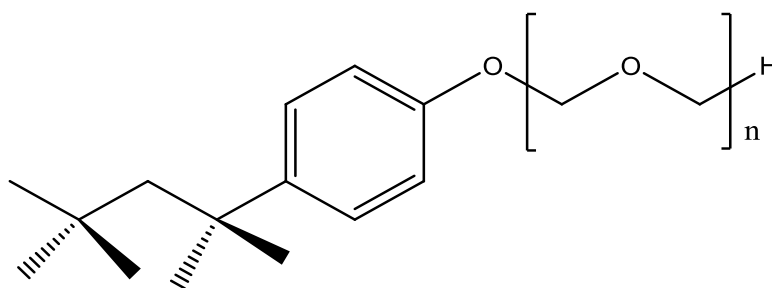


**Figure 3-8:** Structure of surfactant that has been used as CNT dispersant (Triton X-100).

The dispersion in this study was prepared with a multi-walled nanotube (MWNT) concentration of 0.1% in accordance with earlier studies. Basically, 15 mg of MWNTs were dispersed in 15 mL of dispersant solution using a Branson 450 (400 W, Ultrasonics Corp.) digital sonicator horn with a probe diameter of 10 mm (Figure 3-9). A power setting of 30% (120 W) and pulses of 0.5 sec ‘on’ and 0.5 sec ‘off’ were used. The total amount of sonication ‘on’ time (i.e. the amount of time that the horn is energised) was obtained from a series of UV-vis NIR experiments conducted using Triton X-100 dispersions. During sonication, the sample vials containing the MWNTs and dispersant were placed inside an ice water bath to minimise changes in temperature that may happen from the heat generated.

The dispersion (1% in Triton X-100) was prepared and added to 50 mL of dispersant solution before being bath sonicated for 3 minutes. The resulting 80 mL dispersion solution containing 30 mg of MWNTs was then diluted to its ultimate volume using Milli-Q water, and was inverted to facilitate complete mixing.



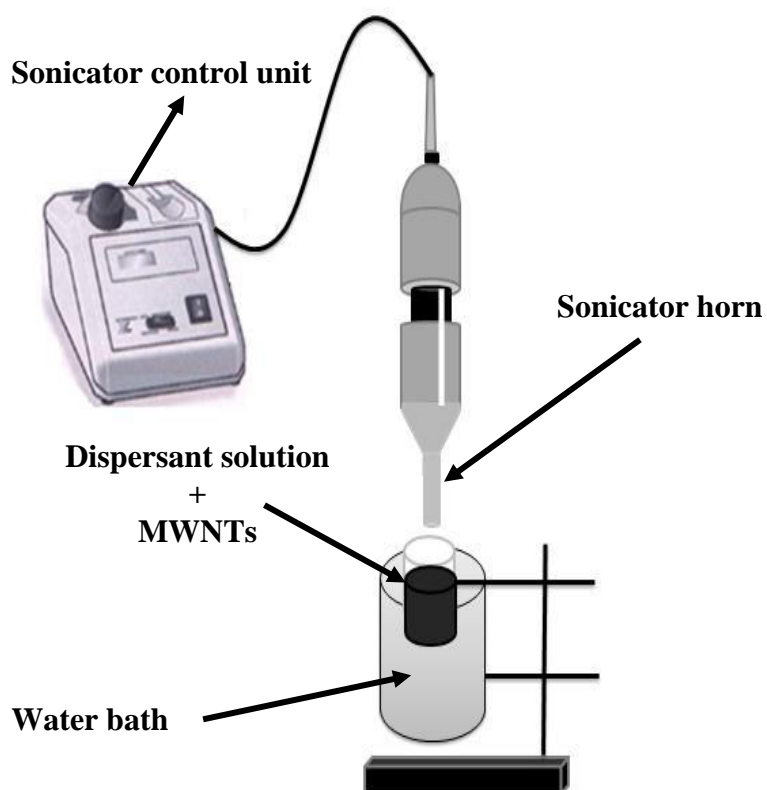


**Figure 3-9:** Schematic illustration of the experimental set-up used to disperse MWNTs. Adapted from (Branson, 2013).

#### 3.5.2.2 Buckypaper preparation

To produce a regular size of buckypapers, circular buckypapers measuring approximately 35 mm in diameter were prepared by using Aldrich glass filtration units (Figure 3-10).

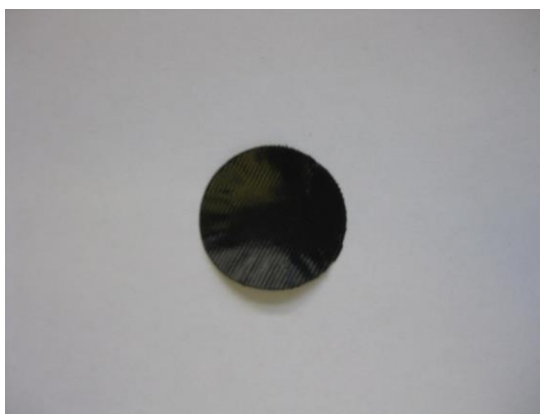


**Figure 3-10:** Photograph of MWNT buckypaper.

The dispersion was drawn through a membrane filter (0.22  $\mu\text{m}$  pore size; Millipore) under vacuum, produced via a Vacuubrand CVC2 pump, operating between 50 and 100 mbar. The upper part of the filtration unit was covered with plastic film to prevent evaporative losses during the filtration process, which typically took roughly one day. After completion of the filtration process for dispersion, the resulting buckypapers were rinsed with 250 mL of Milli-Q water followed by 10 mL of methanol (99.8%, Merck) while still in the filtration unit. After being rinsed, the damp buckypaper was placed between absorbent paper sheets and allowed to dry for 24 hours. In the final step, the dry buckypaper was then carefully peeled away from the filtration membrane. Figure 3-11 demonstrates the vacuum filtration unit which was used to produce MWNT buckypapers.



**Figure 3-11:** Photograph of the vacuum filtration unit used to produce MWNT buckypapers.

### **3.6 Membrane characterization technique**

#### **3.6.1 Membrane characterization techniques for NF/RO membranes**

Significant characterization work has been conducted to examine NF/RO membranes. Electron microscopic investigations, contact angle analysis and zeta potential analysis were examined.

##### **3.6.1.1 Zeta potential measurement**

The surface streaming potential of the membrane was measured using a SurPASS Electrokinetic Analyzer (Anton Paar GmbH, Graz, Austria) in a 1 mM KCl background solution. To calculate the zeta potential from the measured streaming potential the Fairbrother–Mastin method was used, which was performed at 500 mbar and at room temperature ( $25 \pm 1$  °C). The zeta potential of each membrane sample was measured four times, by repeatedly reversing the direction of electrolyte flow at each pH value. Apparatus error counted for less than 0.5 mV of the measurement at any given pH value. Analytical grade potassium hydroxide and hydrochloric acid were used to regulate the pH via automatic titration.

#### 3.6.1.2 Contact angle measurement

According to (Alturki et al., 2010) the contact angle can be measured with a Rame-Hart Goniometer (Model 250, Rame-Hart, Netcong, NJ) by means of the standard sessile drop method. Milli-Q water is used as the reference solvent. The membranes are air dried before the measurement. No less than 5 droplets are applied onto duplicate membrane samples and contact angle is measured on both sides of the droplet.

#### 3.6.1.3 SEM-EDS and AFM analysis

The surface morphology and distribution of calcium, potassium and magnesium deposited on the membrane surface were investigated by field-emission scanning electron microscopy (SEM; Appendix C) using a JEOL JSM-7500FA - (BRUKER-QUANTAX 400), with additional semi-quantitative energy dispersive spectrometer (EDS) analysis. Prior to SEM analysis, the membrane samples were air dried and then coated with an ultra-thin layer of carbon. Significant care was taken when preparing the fouled and scaled membrane samples to ensure that the fouling and scaling layer stayed intact. The surface topography for membranes was examined by means of atomic force microscopy (AFM).  $2\ \mu\text{m} \times 2\ \mu\text{m}$  surface areas in triplicate were needed to investigate surface roughness of membranes using AFM image analysis (Alturki et al., 2010; Vogel et al., 2010).

### 3.6.2 Membrane characterization techniques for CNT membrane

Significant work has been conducted to examine the characterization of MWNT buckypapers. Optimisation of the sonication time, electron microscopic investigation, contact angle analysis, electrical properties measurements, mechanical properties testing, and surface area analysis were examined.

### 3.6.2.1 UV-vis-NIR Spectroscopy

An important step that should be considered before the preparation of a buckypaper is to optimise the sonication time used for preparing the CNT dispersion from which the buckypaper will be made. The reason for that is the energy input during the sonication process could lead to shorter CNTs and subsequently will unfavourably impact the mechanical and electrical properties of the resulting buckypaper. Therefore, UV-vis-NIR spectra of the dispersion (Triton-X) was acquired between 1000 and 300 nm using a Cary 500 UV-vis-NIR spectrophotometer. The dispersion (Triton-X) was diluted in quartz cuvettes by adding 2.4 mL of Milli-Q water to a 0.1 mL sample of dispersion and then mixed by inversion to ensure the absorbances were within the optimal range of the instrument.

### 3.6.2.2 SEM-EDS and AFM analysis

The surface morphology and cross section of buckypapers was examined using a JEOL JSM-7500FA field-emission scanning electron microscope (SEM). Images were analysed using Image Pro Plus software to ascertain quantitative information concerning the size of surface pores. Energy dispersive spectrometer (EDS) analysis was performed in conjunction with imaging using the SEM to provide information on the identity of elements present on the surface of buckypaper samples. The surface topography of membranes was examined by means of atomic force microscopy (AFM). Both SEM and AFM were operated by Mr Tony Romeo in the Electron Microscopy Centre, University of Wollongong, which is where the instrument was located.

### 3.6.2.3 Contact angle measurement

The contact angles of MWNT buckypapers were measured using the sessile drop technique on a custom device developed by R. Taylor (University of Wollongong) utilising a Dinolite am-211 digital microscope. The contact angles of 2  $\mu$ L Milli-Q water droplets on the surfaces of the buckypapers were computed utilizing the

accompanying Data Physics software (SCA20.1). The mean contact angle was computed using measurements performed on at least five water droplets.

#### 3.6.2.4 Electrical properties measurements

The electrical conductivity of buckypaper samples was examined according to a standard two-point probe technique (Blighe et al., 2007). Rectangular strips roughly 3 mm wide and 3–5 cm long were used to test resistance measurements of buckypaper as a function of length. A strip of buckypaper 3 mm wide was connected to pieces of copper tape (3M) on a glass microscope slide using high purity silver paint (SPI). Another glass microscope slide was clamped onto the initial glass slide containing the buckypaper strip using bulldog clips to ensure the sample was protected and a constant force was applied. The I-V characteristics between -0.05 V and 0.05 V were determined using an Agilent waveform generator (33220A) and multi-meter (34410A) connected to the copper tape contacts through a simple circuit. The resistance was computed from the slope of the line in the I-V plot. The strip was shortened and then reconnected to pieces of copper tape on the microscope slide using silver paint before the resistance was measured again. At least 5 lengths were measured for each strip of buckypaper.

#### 3.6.2.5 Mechanical properties testing

The mechanical properties of buckypapers were measured by using a Shimadzu EZ-S universal testing device and buckypaper samples cut into small rectangular strips measuring 15 mm by 3 mm and attached into a small paper frame. Five different strips were used to determine the tensile strength of buckypapers. The distance between the top and bottom of buckypaper strips was kept constant at 10 mm. The paper frame was cut between the clamps prior to testing, and the attached samples were then stretched by means of a 10 N load cell, at a strain rate of  $1 \text{ mm min}^{-1}$  until failure. The tensile strength of every single sample was determined as the maximum stress measured. The ductility was determined by taking the percentage elongation (% EL) of the sample at break, and is defined by Equation (1):

$$Ductility = \frac{l-l_0}{l_0} \times 100 \quad (3-1)$$

Where  $l$  is the length at break and  $l_0$  is the starting length. The Young's modulus of each buckypaper strip was calculated as the slope of the linear part of the stress-strain diagram using the equation (2):

$$E = \frac{\sigma}{\varepsilon} \quad (3-2)$$

Where  $E$  is the Young's modulus (MPa),  $\sigma$  is the stress (MPa) and  $\varepsilon$  is the strain. The toughness of a sample is described as the area under its stress-strain curve up to the point of fracture (Callister and Rethwisch, 2010). The toughness of each buckypaper was linked to its mass and expressed in units of J/g by dividing the toughness (in J/m<sup>3</sup>) by the density of the buckypaper (in g/m<sup>3</sup>).

#### 3.6.2.6 Surface area analysis

Triton-X-100 buckypapers subjected to BET (Brunauer, Emmett, Teller) analysis externally at the King Abdullaziz City for Science & Technology (KACST), Riyadh-Saudi Arabia to evaluate the surface area of the buckypapers. The samples were annealed underneath argon to burn off the surfactant and cut into small pieces, before being tested using a Micrometric ASAP2010 and a Micrometric ASAP2400.

### 3.7 Water permeability experiments of CNT

The permeability of buckypapers towards water was performed using a custom-made dead-end filtration cell setup as described in part 3.4.2. Initially, a pressure of 0.15 bar was applied to induce water transport across the buckypaper and then the

pressure was increased gradually. Permeate was received in a beaker on top of a computer-controlled balance (Mettler Toledo AB2 with Balancelink 1.0 software). MWNT buckypapers were examined by means of five or six different flow rates. At each flow rate, the mass of permeate was recorded every second for 5 minutes. The period of each test was kept to a minimum to avoid fouling of the membrane. The flux of water through the buckypaper was then calculated using following Equation:

$$J = \frac{Q}{A \cdot \Delta t} \quad (3-3)$$

Where  $J$  is the permeation flux ( $L/m^2 \cdot h$ ),  $Q$  is the permeation volume (L) of the testing solution,  $A$  is the effective area of the tested substrate ( $m^2$ ), and  $\Delta t$  is the sampling time (h).

### **3.8 Model contaminated water**

Contaminated surface and groundwater were collected from Russell Vale Golf Course in the Illawarra area and Botany Bay in the Sydney area. 50 litres were collected from each site, two containers were used to collect these amount (25 L the capacity each container). After each sampling, all samples were stored in a cold room at 4 °C until used. Before use these samples were filtered using a Stericup Durapore™ 0.45 µm (Millipore) for separation of colloidal and suspended materials (Figure 3-12). 8 and 2 litres filtered water were used as feed solution for each experiment using the NF/RO filtration system and the dead-end filtration system, respectively.



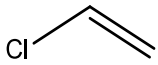
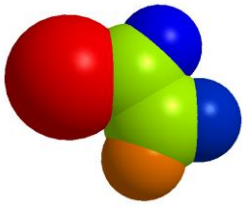
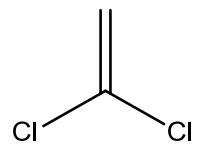
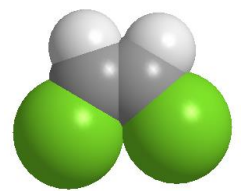
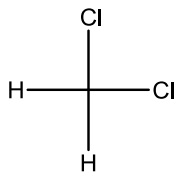
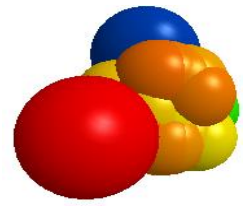
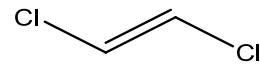
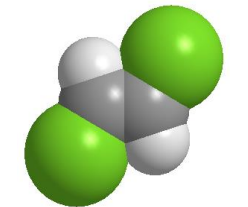


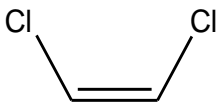
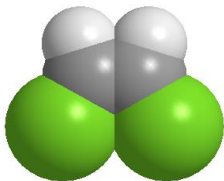
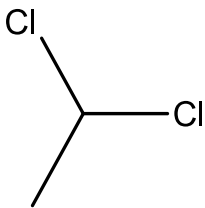
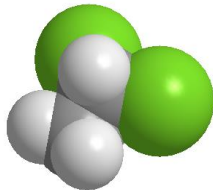
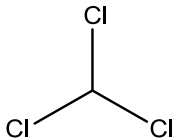
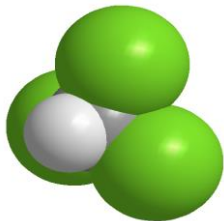
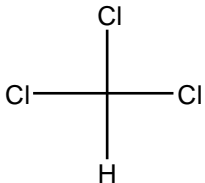
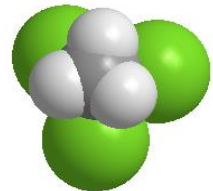
**Figure 3-12:** Photograph of the filter (Stericup Durapore™ 0.45  $\mu\text{m}$ ) used for separation of colloidal and suspended materials.

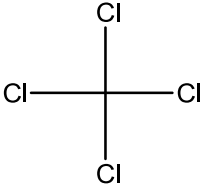
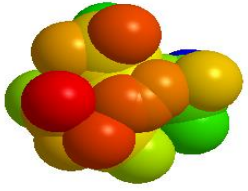
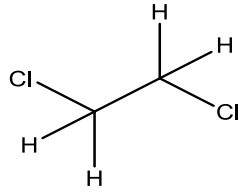
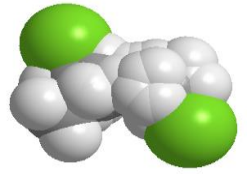
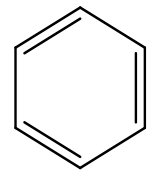
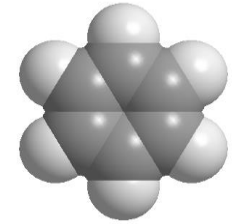
### 3.9 Model organic and inorganic contaminants

A set of twenty six compounds were examined in this study and these represent two main contaminant groups of concern in aquatic resources – namely organic contaminants (chlorinated hydrocarbons) and inorganic contaminants (cations and anions). Selection of these compounds was due to their widespread occurrence in surface and groundwater and their diverse physiochemical properties (e.g. hydrophobicity and molecular size). The physical-chemical properties and structure of the chlorinated solvents which were detected in water samples are demonstrated in Table 3-3. They had molecular weights between 78.11 g/mol (benzene) and 260.76 g/mol (hexachlorobutadiene). The intrinsic hydrophobicity of these compounds varied significantly, as was reflected by the values of their octanol-water partitioning coefficient ( $\log K_{ow}$ ) or  $\log K_{ow}$  at a specific pH (Wells, 2006). As can be seen in Table 3-4 most compounds are hydrophobic with  $\log D$  at pH 7 and 8 of 1.40 and 4.91 respectively. Also it can be seen from the selected organic compounds (VOCs) properties that some compounds are hydrophilic ( $\log D > 2.5$ ) or hydrophobic ( $\log D < 2.5$ ; Wells, 2006).

**Table 3-4:** Summary of relevant physiochemical properties of selected chlorinated solvents.

Compound	CAS no.	MW (g/mol)	Log $K_{ow}$ <sup>a</sup>	Log $D$ <sup>a</sup> at pH 7	Log $D$ <sup>a</sup> at pH 8	Formula	Structure	3D model <sup>a</sup>
Vinyl chloride (Chloroethene)	75-01-4	62.50	1.69	1.69	1.69	C <sub>2</sub> H <sub>3</sub> Cl		
1,1-Dichloroethene	57-53-4	96.94	2.05	2.05	2.05	C <sub>2</sub> H <sub>2</sub> Cl <sub>2</sub>		
DCM: Dichloromethane	75-09-2	84.93	1.40	1.40	1.40	CH <sub>2</sub> Cl <sub>2</sub>		
trans-1,2-Dichloroethene	156-59-2	96.94	2.14	2.14	2.14	C <sub>2</sub> H <sub>2</sub> Cl <sub>2</sub>		

cis-1,2-Dichloroethene	156-59-2	96.94	2.14	2.14	2.14	$C_2H_2Cl_2$		
1,1-Dichloroethane	75-34-3	98.96	1.76	1.76	1.76	$C_2H_4Cl_2$		
Chloroform	67-66-3	119.38	1.94	1.94	1.94	$CHCl_3$		
1,1,1-Trichloroethane	71-55-6	133.40	2.35	2.35	2.35	$C_2H_3Cl_3$		

CTC: Tetrachloromethane (Carbon Tetrachloride).	56-23-5	153.82	2.92	2.92	2.92	$\text{CCl}_4$	 
1,2-Dichloroethane	107-06-2	98.96	1.65	1.65	1.65	$\text{C}_2\text{H}_4\text{Cl}_2$	 
Benzene	71-43-2	78.11	2.18	2.18	2.18	$\text{C}_6\text{H}_6$	 

TCE: Trichloroethylene  
(Trichloroethene)

79-01-6

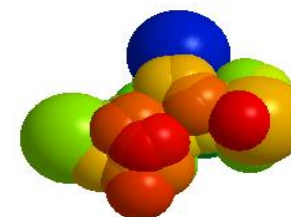
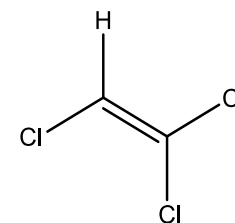
131.39

2.57

2.57

2.57

$C_2HCl_3$



Toluene

108-88-3

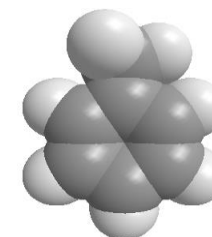
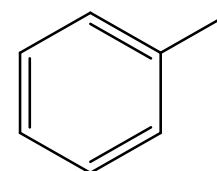
92.14

2.72

2.72

2.72

$C_7H_8$



1,1,2-Trichloroethane

79-00-5

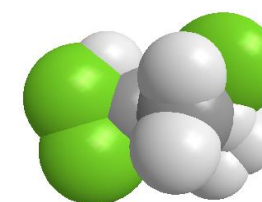
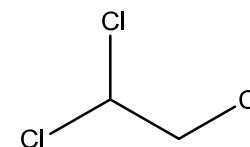
133.40

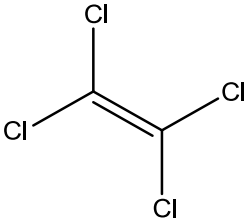
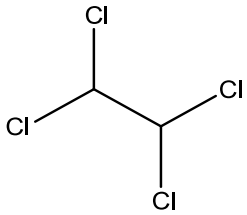
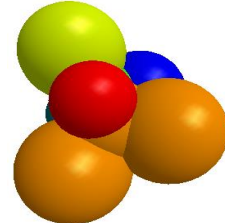
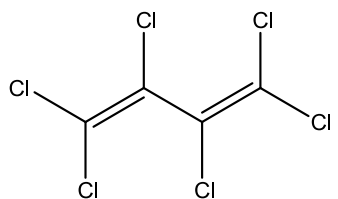
1.92

1.92

1.92

$C_2H_3Cl_3$



PCE: Tetrachloroethylene (Tetrachloroethene or Perchloroethene)	127-18-4	165.83	3.07	3.07	3.07	$C_2Cl_4$	 
1,1,2,2-Tetrachloroethane	79-34-5	167.85	2.33	2.33	2.33	$C_2H_2Cl_4$	 
Hexachlorobutadiene	87-68-3	260.76	4.91	4.91	4.91	$C_4Cl_6$	 

<sup>a</sup> Reference source: SciFinder Scholar, data calculated using Advanced Chemistry Development (ACD/Labs) Software V8.14 for Solaris (1994–2007 ACD/Labs).

On the other hand, ionic characteristics such as ionic radius, hydrated radius and hydration free energy are significant for understanding the ability of ions to transfer through the membrane under transmembrane pressure and molecular weight cut off (MWCO) of the membrane (Tansel, 2012). In particular, ionic radii are a useful tool for predicting and visualising crystal structures and can be obtained from the values of ionic radii according to experimental crystal structure determinations, supplemented by empirical relationships, and theoretical calculations (Haynes et al., 2013). Molecular weight, ionic and hydrated radii for relevant cations and anions which were detected in water samples are demonstrated in Table 3-5. They had molecular weights between 22.99 g/mol ( $\text{Na}^+$ ) and 96.06 g/mol ( $\text{SO}_4^{2-}$ ). Also, as can be seen in Table 3-5, ionic radii for module foulants ranged between 0.065 nm ( $\text{Mg}^{2+}$ ) and 0.264 nm ( $\text{NO}_3^-$ ), while hydrated radii ranged between 0.300 nm ( $\text{SO}_4^{2-}$ ) and 0.428 nm ( $\text{Mg}^{2+}$ ).

**Table 3-5:** Molecular weight, ionic and hydrated radii for relevant cations and anions.

Ion	Molecular weight (g/mol)	Ionic radius (nm)	Hydrated radius (nm)	Ref.
$\text{Na}^+$	22.99	0.095	0.358	(Nightingale.E.R, 1959)
$\text{Ca}^{2+}$	40.08	0.100	0.412	(Volkov et al., 1997)
$\text{K}^+$	39.10	0.133	0.331	(Nightingale.E.R, 1959)
$\text{Mg}^{2+}$	24.31	0.065	0.428	(Nightingale.E.R, 1959)
$\text{Hg}^+$	200.59	0.119	NA <sup>a</sup>	(Haynes et al., 2013)
$\text{SO}_4^{2-}$	96.06	0.215	0.300	(Kiriukhin and Collins, 2002)
$\text{PO}_4^{3-}$	95.0	0.223	0.339	(Kiriukhin and Collins, 2002)
$\text{NO}_3^-$	62.00	0.264	0.335	(Nightingale.E.R, 1959)
$\text{Cl}^-$	35.45	0.181	0.332	(Nightingale.E.R, 1959)
$\text{Br}^-$	79.90	0.195	0.330	(Nightingale.E.R, 1959)

<sup>a</sup> NA: Not available.

### **3.10 Analytical techniques**

#### **3.10.1 Analysis of basic water parameters**

The temperature, turbidity, dissolved oxygen (DO), electrical conductivity (EC), total dissolved solids (TDS), salinity, density, (SG) and redox (water quality parameters) were measured using Water Quality Analyser-MODEL 516 (Figure 3-13) during sampling for all four seasons and are presented in Table 3-6 and Table 3-7. On the other hand, the temperature, conductivity and pH were measured using an Orion 4-Star Plus pH/conductivity meter in all experiments. The measurements were applied at 0 time, one hour and at 8 hours for each experiment.



**Table 3-6:** Water quality parameters for samples which were collected from Leachate pond-Russell Vale Golf Course <sup>a</sup>.

Season	Depth (m)	Turbidity (ntu)	Dissolved Oxygen (mg/l)	Electrical conductivity (µS/cm)	Total Dissolved Solids (g/l)	pH	Temperature (°C)	Salinity (ppt)	Density (mg/cm <sup>3</sup> )	SG (t/m <sup>3</sup> )	Redox (mV)	Description
Spring	0.33	99	3.43	3442	2.129	8.55	15.01	1.72	1000	1.000	+389	Yellow, slightly turbid, no odor.
Summer	0.42	66.5	10.8	2761	1.66	8.23	21.76	1.45	998	0.999	+51	Yellow, slightly turbid, no odor.
Autumn	0.49	178	7.40	2475	1.67	8.27	20.90	1.46	998	0.999	+500	Yellow, slightly turbid, no odor
Winter	0.50	105.1	7.75	1971	1.104	7.99	14.61	0.87	1000	1.000	+387	Yellow, slightly turbid, no odor.

<sup>a</sup> All data were obtained using Water Quality Analyser (MODEL 516).

**Table 3-7:** Water quality parameters for samples which were collected from WGB32 located near the tennis courts outside the fenceline-Orica <sup>a</sup>.

Season	Depth (m)	Turbidity (ntu)	Dissolved Oxygen (mg/l)	Electrical conductivity (µS/cm)	Total Dissolved Solids (g/l)	pH	Temperature (°C)	Salinity (ppt)	Density (mg/cm <sup>3</sup> )	SG (t/m <sup>3</sup> )	Redox (mV)	Description
Spring	5.75	2.1	2.41	8000	5.84	10.5	19.35	4.97	1001	1.002	+540	Brown, slightly turbid, no odour.
Summer	5.80	2.6	1.47	7250	5.79	10.5	21.4	4.91	1000	1.001	- 44	Brown, slightly turbid, no odour.
Autumn	5.75	2.5	1.42	7667	5.34	11	21.86	4.89	1001	1.002	- 43	Brown, slightly turbid, no odour.
Winter	5.38	1.8	0.80	8000	5.58	10.5	19.45	4.77	1001	1.002	+533	Brown, slightly turbid, no odour.

<sup>a</sup> All data were obtained using Water Quality Analyser (MODEL 516).

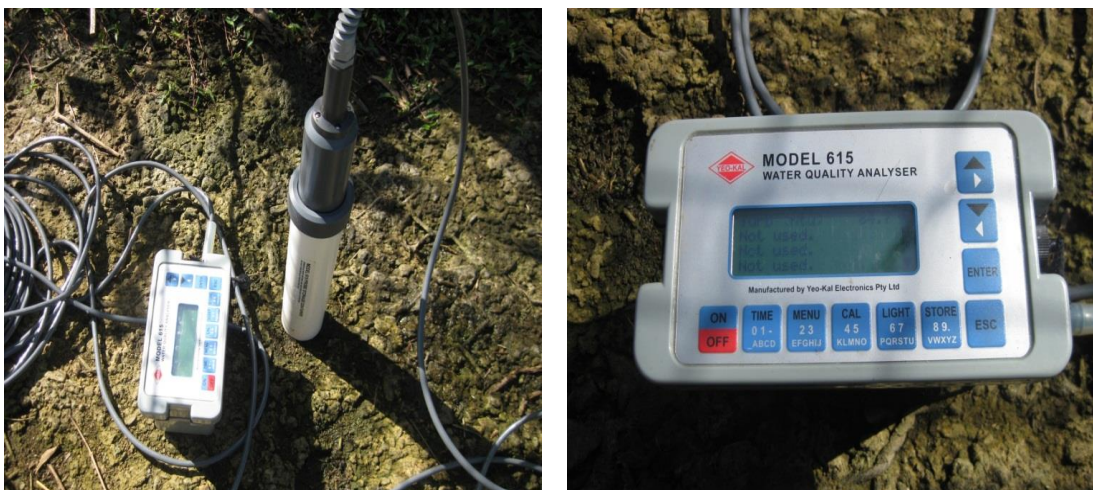


**Figure 3-13:** Photograph of Water Quality Analyser (MODEL 516).

### 3.10.2 Organic and inorganic component analysis

All samples collected before and after filtration using both the NF/RO filtration system and the dead-end filtration system were analysed at ORICA Botany Environmental Laboratories. Cations, anions, mercury and volatile organic compounds (VOC) were analysed by using ICP-OES, IC, FIMS and GC-MS, ICP, respectively.

Cations were digested with aqua regia at 95 °C for 2 hours and then analysed with a Perkin Elmer Optima 7000DV ICP-OES (inductively coupled plasma optical emission spectrometry; Figure 3-14) based on the US EPA Method 200.7. According to this technique, samples are nebulised and the consequent aerosol is transferred to the plasma torch. Production of specific emission spectra for any element is obtained by radio-frequency inductively coupled plasma. The spectra are distributed by a grating spectrometer, and the intensities of the line spectra are checked at definite wavelengths by a photosensitive device. Photocurrents from the photosensitive device are processed and managed by a computer system. A background correction technique is essential to compensate for mutable background participation to the determination of the analysis. Background has to be measured adjacent to the analysed wavelength during analysis and several interferences must be taken into consideration (US Method.200.7, 1994).

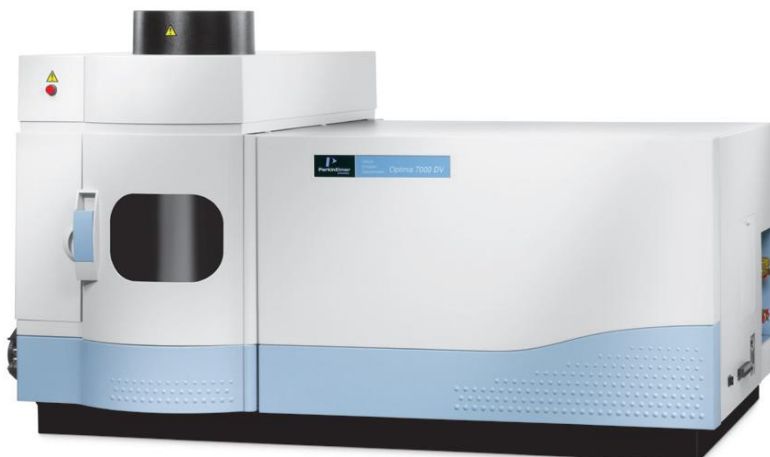


**Figure 3-14:** Perkin Elmer Optima 7000 DV ICP-OES (from PerkinElmer, 2013 ).

Anions were analysed using Metrohm 881 Compact IC Pro Suppression Ion Chromatography (Figure 3-15) based on "Standard methods for the examination of water and wastewater" (American Public Health Association, 2005, American Water Works Association, 2005 and Water Environment Federation, 2005, Method 4110.B). This method is appropriate, after a filtration process to eliminate solid particles using a 0.2 $\mu$ m pore diameter membrane filter. By this method the common anions such as bromide, chloride, fluoride, nitrate, nitrite, phosphate, and sulfate can be determined. Basically, this method uses a prewashed syringe of 1 to 10 mL capacity equipped with a male luer suitable injecting sample or standard. Inject sufficient sample to flush the sample loop many times: for a 0.1 mL sample loop inject at least 1 mL. Shift the ion chromatograph from load to inject mode and record peak heights and retention times on a strip chart recorder. After the last peak (SO<sub>4</sub><sup>2-</sup>) has performed and the conductivity signal has returned to the base line, another sample can be injected. Compute the concentration of each anion, in milligrams per litre, by referring to the appropriate calibration curve. Otherwise, when the response is shown to be linear, use the following equation:

$$C = H \times F \times D \quad (3-4)$$

Where  $C$  = mg anion/L,  $H$  = peak height or area,  $F$  = response factor = concentration of standard/height (or area) of standard, and  $D$  = dilution factor for those samples requiring dilution (Eaton, 2005)



**Figure 3-15:** Metrohm 881 Compact IC Pro Suppression Ion Chromatography (from Metrohm, 2013).

Mercury was digested with aqua regia at 95 °C for 2 hours, and then analysed using a Perkin Elmer FIMS 400 (Flow injection mercury system) according to Method 7470 (Figure 3-16). Method 7470 is a cold-vapor atomic absorption process accepted for determining the concentration of mercury in mobility-procedure extracts, aqueous wastes and groundwaters. This vapor atomic absorption technique is based mainly on the absorption of radiation at 253.7-nm by mercury vapor. The mercury is reduced to the elemental status and ventilated from solution in a sealed system. In the next step, the mercury vapor passes through a cell located in the light path of an atomic

absorption spectrophotometer. Absorbance (peak height) is measured as a function of mercury concentration (Metod.7470A, 1994).

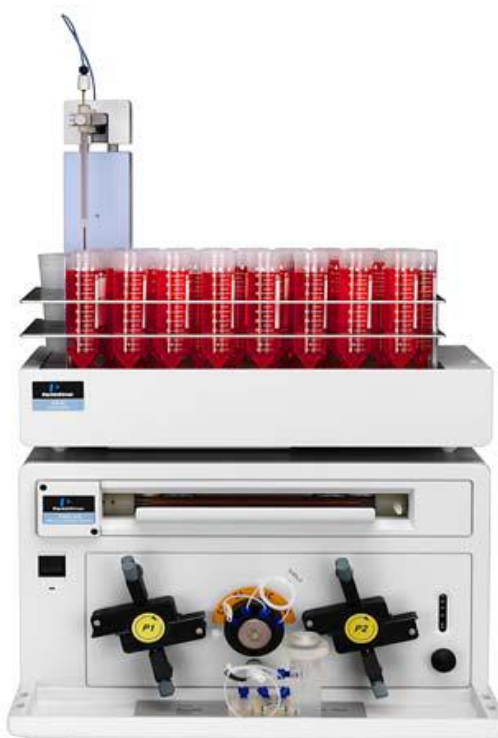


**Figure 3-16:** PerkinElmer FIMS 400 (Flow injection mercury system; from PerkinElmer, 2013).

VOC was analysed using a Shimadzu purge and trap/Gas Chromatography/Mass Spectrometer Detector based on USEPA Methods 5030 and 8260 (Figure 3-17). Method 5030 can be utilised for most volatile organic compounds that have boiling points below 200 °C and are insoluble or somewhat soluble in water. This method can include volatile water-soluble compounds; nevertheless, quantification limits (by GC or GC/MS) are roughly ten times higher due to poor purging efficiency (Method.5030B, 1996). On the other hand, Method 8260 is utilised to determine volatile organic compounds in a range of solid waste matrices. This method is appropriate to nearly all types of samples, irrespective of water content, containing numerous air sampling trapping media, ground and surface water, aqueous sludges, caustic liquors, acid liquors, waste solvents, oily wastes, mousses, tars, fibrous wastes, polymeric emulsions, filter cakes, spent carbons, spent catalysts, soils and sediments (Method.8260B, 1996). This method has an inert gas bubbled through a portion of the aqueous sample at room temperature, and the volatile components are

efficiently conveyed from the aqueous phase to the vapor phase. In the subsequent step, the vapor is swept through a sorbent column where the volatile components are adsorbed. After purging is finished, the sorbent column is heated and back flushed with inert gas to desorb the components onto a gas chromatographic column (Method.5030B, 1996).



**Figure 3-17:** Shimadzu purge and trap/Gas Chromatography/Mass Spectrometer Detector (from Shimadzu, 2013).

### **3.11 Experimental protocols**

#### **3.11.1 Pressure driven membrane filtration experimental protocol**

Prior to each pressure driven filtration experiment, the membrane was compacted using Milli-Q water (8 L) for approximately 1 hour until a stable baseline flux was obtained. The compacting pressures were 12 and 18 bars for the NF and RO membranes, respectively. The Milli-Q water used for membrane compaction was replaced with 8 L of a solution containing contaminated surface or groundwater after filtration using a Stericup Durapore™ 0.45 µm Millipore. The cross-flow velocity flux was adjusted to 30.4 cm/s. The feed reservoir temperature was kept constant at  $20 \pm 0.1$  °C throughout the experiment. Both permeate and concentrate were recirculated back to the feed reservoir (Figure 3-6, part 3.4.1). Permeate and feed

samples of 250 and 100 mL (two duplicates) were collected after 1 hour and at 8 hours of filtration to analyse cations and anions respectively. In case of samples containing volatile organic compounds, the system was completely sealed and the feed reservoir temperature was kept constant at  $4 \pm 0.1$  °C throughout the experiment using an exceptional chiller device to avoid evaporation of these compounds. Permeate and feed samples of 40 mL (two duplicates) were collected after 1 hour and at 8 hours of filtration to analyse for volatile organic compounds. All samples collected both feed and permeate were sent immediately to ORICA Botany Environmental Laboratories for analysis. The rejection rate is defined by Equation:

$$R = \left(1 - \frac{C_p}{C_f}\right) \times 100\% \quad (3-5)$$

where  $C_p$  and  $C_f$  are the permeate and the feed concentrations, respectively.

### **3.11.2 The dead-end filtration experimental protocol**

Typically, the dead end filtration system is similar to the RO/NF filtration unit. The difference here is that high pressure was not needed and the appropriate pressure for this type of membrane is often less than 1 Kpa. Moreover, this membrane needs a support layer made from stainless to support this membrane. Furthermore, the cross-flow cell used in this study has an effective membrane area of 6 cm<sup>2</sup> (2 cm × 3 cm) with a channel height of 2 mm. Only 2 L of a solution containing contaminated surface or groundwater was used as feed solution after filtration using a Stericup Durapore™ 0.45 µm Millipore filtration to investigate the removal organic and inorganic contaminants. Both permeate and concentrate were not recirculated back to the feed reservoir as in case of NF/RO filtration system (Figure 3-7, part 3.4.2).



## **CHAPTER 4: THE REMOVAL OF ORGANIC CONTAMINANTS BY USING NF/RO FILTRATION SYSTEM**

### **4.1 Introduction**

The occurrence and fate of volatile organic compounds (VOCs) in surface and groundwater has been identified as a significant environmental health concern (Nikolaou et al., 2002; Rivett et al., 2011). It would be fair to say that there is full agreement between the scientific community and water authorities to minimise volatile organic compounds, however, the majority of these contaminants in the environment are still poorly understood, and are a topic of growing interest from both research and regulatory perspectives. Reclaimed wastewater, in particular, has some significant benefits, including high reliability of supply, a known quality and frequently, a centralized source near urban demand centres.

In the last decade, nanofiltration (NF) and reverse osmosis (RO) have been proposed as attractive technologies for removal of organic trace contaminants including volatile organic compounds from the aquatic environment instead of conventional wastewater treatment (Van der Bruggen and Vandecasteele, 2003; Nghiem et al., 2004a; Agenson and Urase, 2007; Fujioka et al., 2014; Luo et al., 2014). It can be recognised that conventional treatment processes, such as chemical precipitation, ion exchange and electrochemical removal, are insufficient to remove and minimize organic contaminants to acceptable regulatory standards. Several previous studies have demonstrated the excellent capability of NF/RO to remove a wide range of volatile organic compounds including trihalomethanes, organochloric compounds, petroleum hydrocarbons and other low molecular weight compounds such as toluene and trichloroethylene (Agenson et al., 2003; Agenson and Urase, 2007). These studies have also revealed a substantial degree of complexity associated with the separation processes involved. As a result, various parameters such as membrane properties, solution chemistry and physicochemical properties of the volatile organic compounds can significantly affect the removal efficiency of these components by NF/RO membranes (Agenson et al., 2003; Agenson and Urase, 2007).

A sieving mechanism, integrating molecular width and molecular length as the size parameters, and an interaction component with a logarithmic octanol-water partitioning coefficient ( $\text{Log } K_{ow}$ ) gave the best expectation for the retention of volatile organic compounds and semi-volatile organic compounds (SVOCs) by membranes. Solutes with larger widths, larger lengths and higher  $\text{Log } K_{ow}$  will have higher retentions for most of the membranes used (Agenson et al., 2003). Thus the separation of volatile organic compounds by NF/RO processes is based predominantly on size exclusion (Agenson and Urase, 2007). In the case of charged trace organic compounds, electrostatic interactions between the charged solute and the negatively charged membrane surface can also play a key role (Bellona et al., 2004). Additionally, it has been demonstrated that hydrophobic compounds can adsorb onto membrane surfaces and subsequently may diffuse through RO and especially NF membranes, resulting in lower rejections than would be expected based only on size exclusion mechanisms. In this case hydrophobicity is considered an important factor affecting rejection (Nghiem et al., 2004b).

One of the objectives of this study was to examine the removal of volatile organic compounds by using a NF/RO filtration system. Experiments were conducted using a laboratory-scale and two commercially available NF/RO membranes, namely NF-90 and ESPA2, respectively. Twenty one volatile organic compounds with molecular weights between 78.11 g/mol (benzene) and 260.76 g/mol (hexachlorobutadiene) were selected as model organic contaminants due to their widespread occurrence in surface and groundwater. Removal efficiency by NF/RO filtration was linked to the physicochemical properties of these compounds to focus on the ability and effectiveness of this kind of treatment. Substantial characterisation work has been conducted to investigate the NF/RO membranes.

## **4.2 Materials and methods**

Detailed descriptions of the NF/RO set-up, operation protocol and analytical techniques have been provided in chapter 3. Volatile organic compounds were collected from EWB10D and EWB13D located at Southlands in Botany Bay. The NF/RO filtration system was completely sealed and the feed reservoir temperature was kept constant at  $4 \pm 0.1$  °C throughout the experiment using an exceptional chiller device to avoid evaporation of these compounds. Each experiment used 8 L from the samples as feed solution. In the subsequent step, the NF/RO filtration system was operated for 8 hours in each experiment to collect an adequate amount of permeate (40 mL - two duplicates) which were analysed to determine the removal efficiency of this system. In this chapter, the obtained data is systematically analysed to assess the overall performance of the NF/RO system.

### **4.2.1 Model organic contaminants**

Sixteen compounds were chosen for this study to represent the major organic groups considered contaminants in groundwater samples – namely volatile organic compounds (e.g. dichloromethane, trichloroethylene, tetrachloroethylene, toluene and benzene). The selection of these compounds was also based on their widespread occurrence in surface and groundwater and their diverse physicochemical properties (e.g. hydrophobicity and molecular size). Key physicochemical properties of these organic contaminants are shown in chapter 3 (Table 3-4). The selected volatile organic compounds had molecular weights between 78.11 g/mol (benzene) and 260.76 g/mol (hexachlorobutadiene). The intrinsic hydrophobicity of these compounds varied significantly, as was reflected by the values of their octanol-water partitioning coefficient ( $\text{Log } K_{ow}$ ) or  $\text{Log } K_{ow}$  at specific pH ( $\text{Log } D$ ). As can be seen in Table 3-4, the properties of the selected volatile organic compounds demonstrated that some compounds are hydrophilic ( $\text{Log } D > 2.5$ ) while others are hydrophobic ( $\text{Log } D < 2.5$ ) and ranged between 1.40 and 4.91 ( $\text{log } D$  at pH 7 and 8).

However, most volatile organic compounds which were examined in this study are hydrophobic ( $\log D < 2.5$ ).

### **4.3 Results and discussion**

#### **4.3.1 Characterization of NF-90 and ESPA2 membranes**

##### **4.3.1.1 Membrane surface zeta potential**

NF-90 and ESPA2 membranes consisted of a thin aromatic (or semi-aromatic) polyamide active layer, therefore the active skin of these membranes contains both carboxylic and amine functional groups that can ionise in an aqueous solution (Childress and Elimelech, 1996). The membrane surface zeta potential can vary as a function of the solution chemistry, such as pH and ionic strength. A more negative membrane zeta potential could result in a higher salt rejection because of an improved electrostatic interaction between the negatively charged membrane surface and charged solutes (Schäfer et al., 2004). Both membranes used in this study have negative charge in the examined pH range (Figure 4-1). Moreover, with the increase of pH value, the membrane surface charge density tends to decrease from positive to negative value, irrespective of the ionic strength or any kind of impurities existing in the solution (Tay et al., 2002). This phenomenon proposes that electrostatic interaction can be a significant rejection mechanism of charged solutes, particularly for the NF membrane.

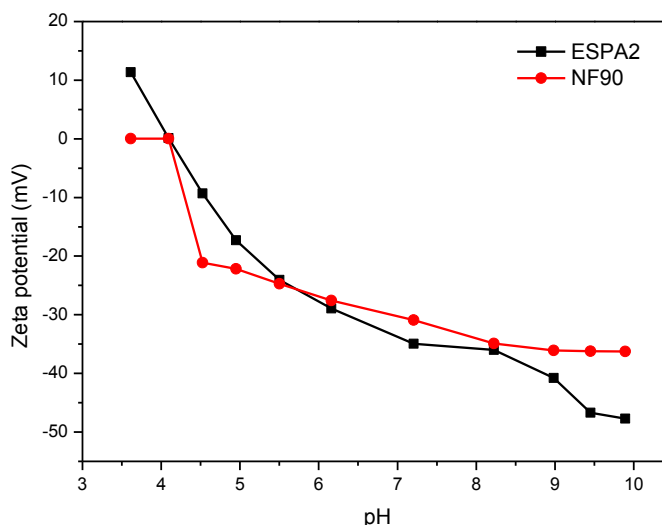


**Figure 4-1:** Zeta potential of the selected membranes (measured at 25 °C, in a background electrolyte solution containing NaCl, CaCl<sub>2</sub> and NaHCO<sub>3</sub> at concentrations of 10 mM, 1 mM, and 1 mM, respectively; pH was adjusted using HCl or KOH solutions).

#### 4.3.1.2 Contact angle data

The contact angle data which reflect the hydrophobicity of the virgin NF-90 and ESPA2 membranes are demonstrated in Table 3-3 (chapter 3). As shown in Table 3-3 the contact angle for the NF-90 differs from the ESPA2 and was 42.5 ° and 60.6 °, respectively; however both membranes seemed to be more hydrophilic than hydrophobic. Higher hydrophobicity could lead to the NF-90 and ESPA2 membranes becoming susceptible to fouling due to hydrophobic interaction between the membrane surface and hydrophobic foulants.

#### 4.3.1.3 SEM-EDS and AFM analysis

The surface topography for NF/RO membranes was investigated by means of atomic force microscopy (AFM). On the other hand, the surface morphology and distribution of organic and inorganic compounds deposited on the membrane surface were examined using field-emission scanning electron microscopy (SEM) on a JEOL JSM-7500FA - (BRUKER-QUANTAX 400), with additional semi-quantitative

energy dispersive spectrometer (EDS) analysis. An atomic force microscope (AFM) is currently considered to be one type of scanning probe microscope, which is utilised mainly to image surface topography and to measure surface forces. Basically, the AFM measures the forces acting between a sharp tip which is attached to the free end of a cantilever and the surface of the sample. The resulting interactions between the tip and the surface will lead to a positive or negative bending of the cantilever. The bending is detected by a laser beam, which is reflected from the back side of the cantilever. The image is then rebuilt by computer software connected with the AFM.

The AFM images of the ESPA2 and NF-90 membranes are described in Figures 4-2 to 4-5 reveal different extents and occurrences of surface roughness. Surface topography of ESPA2, as seen in Figures 4-2 and 4-3, shows a typical nodular (hills and valleys) morphology. This characteristic includes most RO membranes as reported in other studies (Vrijenhoek et al., 2001; Freger et al., 2002). The same applies to the NF-90 membranes used in this study (Figures 4-4 and 4-5) with the hill to hill distance being much smaller, which associates completely with the much lower thickness of the active layer (15–40 nm for NF compared to 200–300 nm for RO). This morphology seems to be affected by means of the underlying supporting layer, and could be viewed as a fingerprint of the thin-film composite (TFC) polyamide (PA) membrane (Freger et al., 2002). Since these “valleys” are likely to be of irregular shape, such as the surface topography of the NF-90 membrane (Figures 4-4 and 4-5), a lodged particle may not fully “plug” the “pore-like” valley, however it may considerably restrict flow through the opening. Thus, the valleys quickly become “clogged,” resulting in remarkable loss of permeate flux. In the case of the ESPA2 membrane (Figures 4-2 and 4-3), the “valleys” are likely to have a slightly more regular shape and there will be less “valley clogging.” Even though the same number of particles are placed on the membrane, they would likely be more equally spaced leading to less overall flux decline (or fouling; Vrijenhoek et al., 2001).

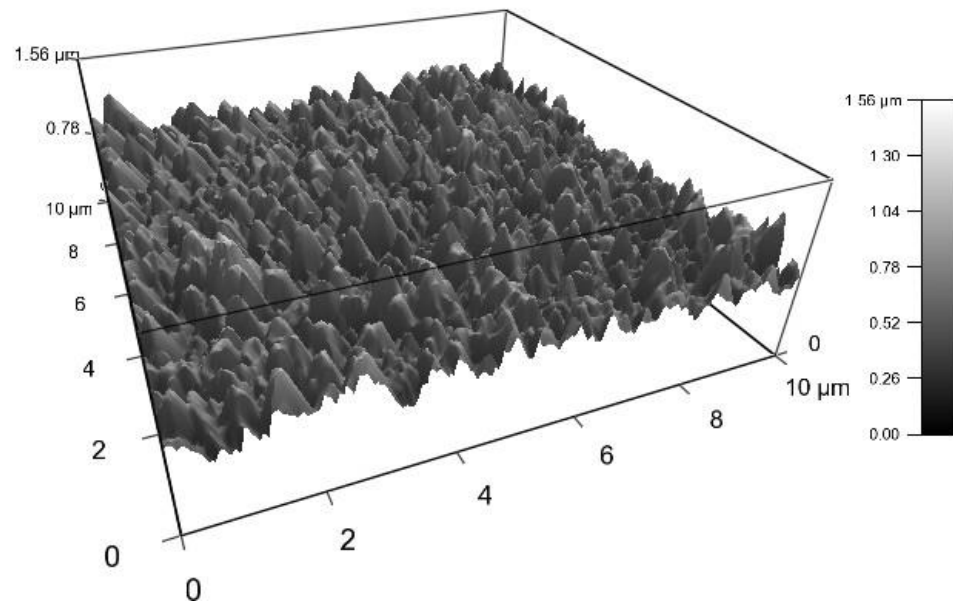


**Figure 4-2:** Surface topography image of ESPA2 membrane.

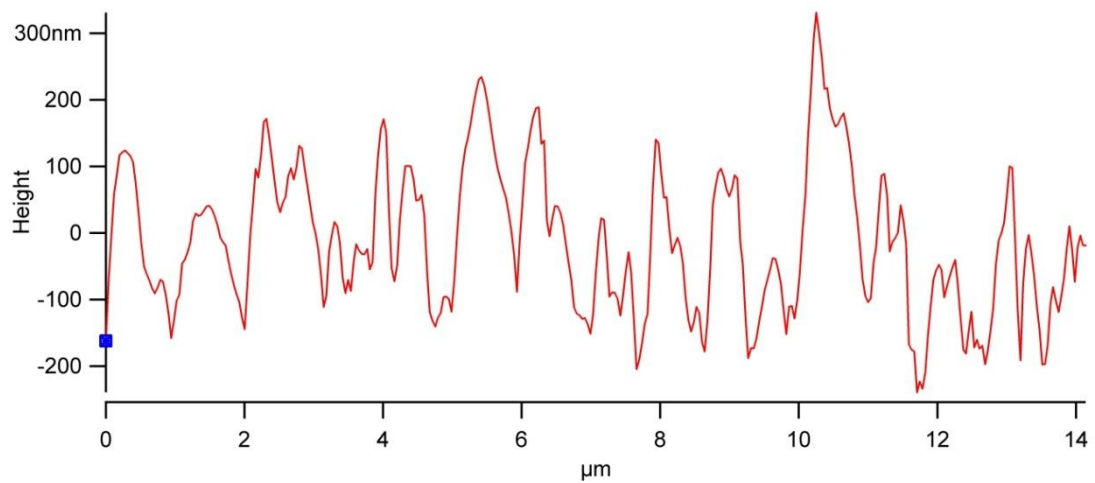


**Figure 4-3:** Section graph of ESPA2 membrane.

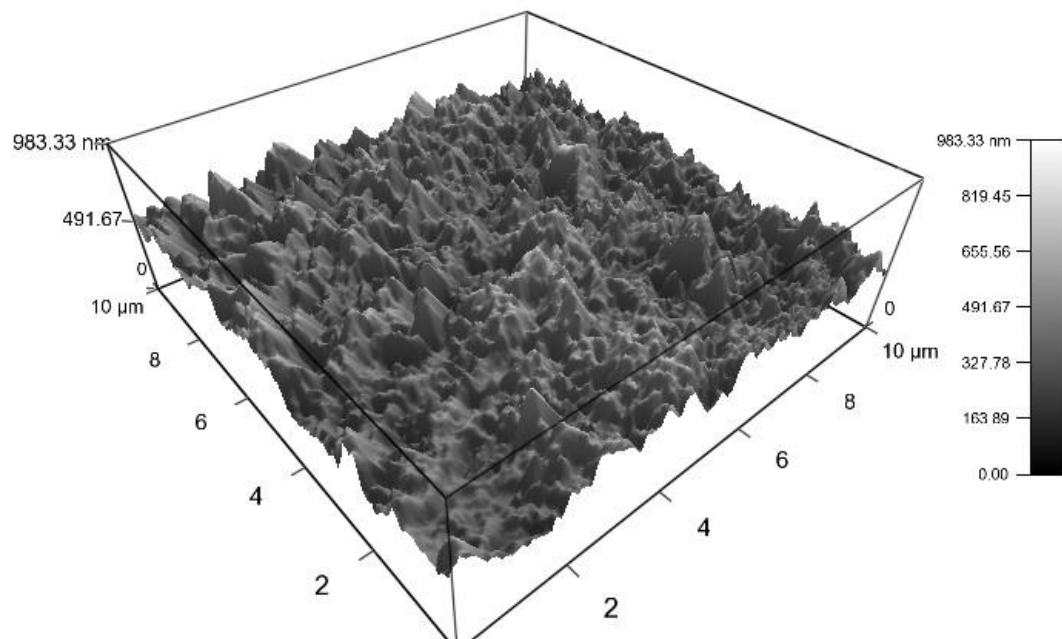


**Figure 4-4:** Surface topography image of NF-90 membrane.

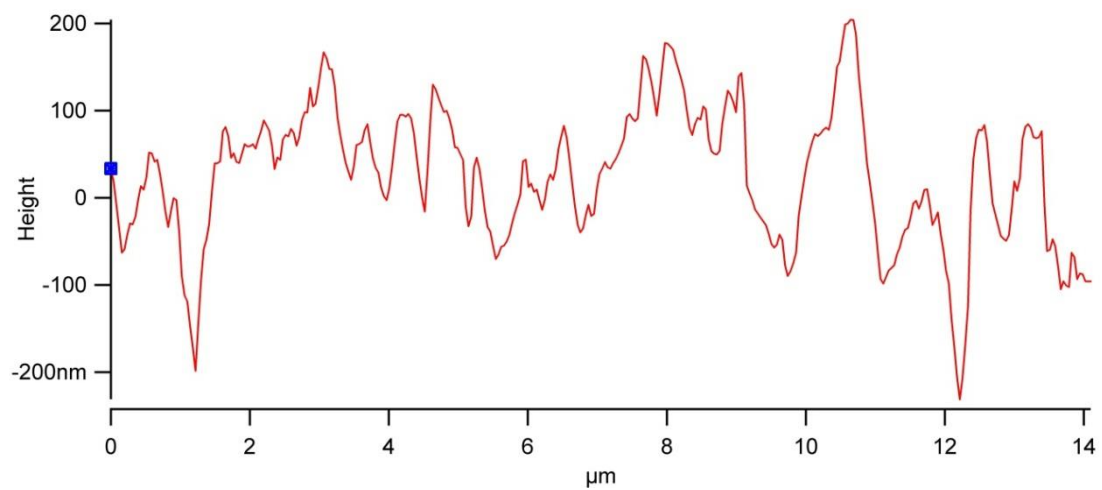


**Figure 4-5:** Section graph of NF-90 membrane.



Statistical analysis displays that the average roughness of the NF-90 membrane (a few nanometres, see Figure 4-6) somewhat increases with modification. In contrast, the average roughness of the ESPA2 membrane (tens of nanometres, see Figure 4-7) is much larger than in the case for the NF-90 membrane. Consequently, it can be concluded that the membranes used in this study were unable to resist colloidal fouling. This was noticed clearly when a NF/RO membrane was used to examine the removal of organic contaminants (volatile organic compounds) from the groundwater samples collected from EWB10D and EWB13D at Southlands Botany Bay. In particular when the NF-90 membrane was used the flux declined because of fouling. On the other hand, the flux showed only slight decline when the ESPA2 membrane was used to investigate the removal of organic contaminants (volatile organic compounds) which were collected from the same sites at Southlands Botany Bay (Freger et al., 2002).

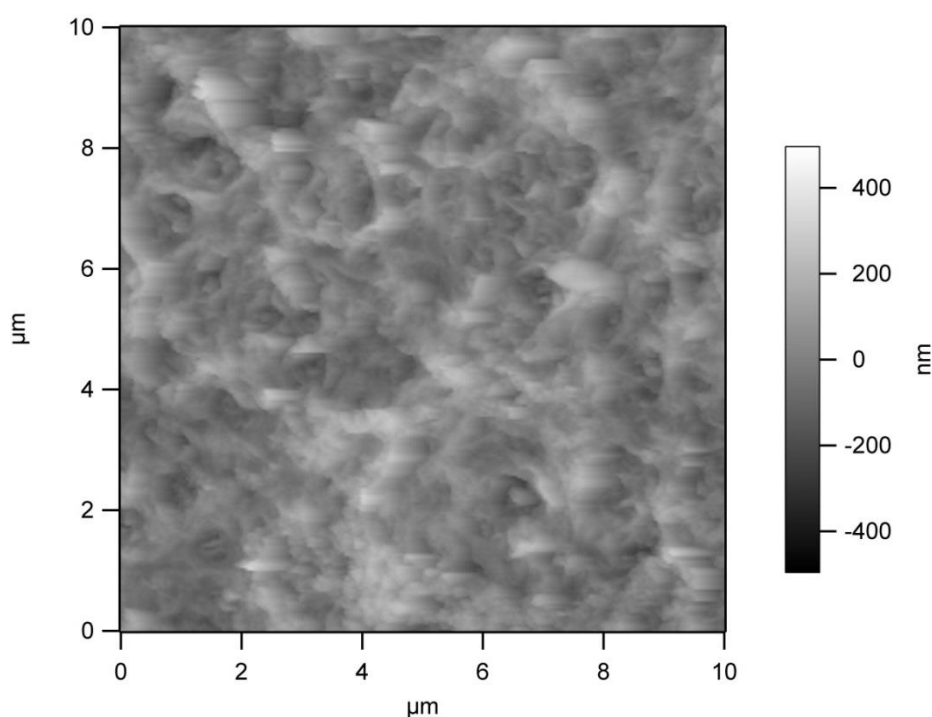


**Figure 4-6:** Plan view images of SIM membrane surfaces reconstructed from AFM roughness statistics for a NF-90 membrane.

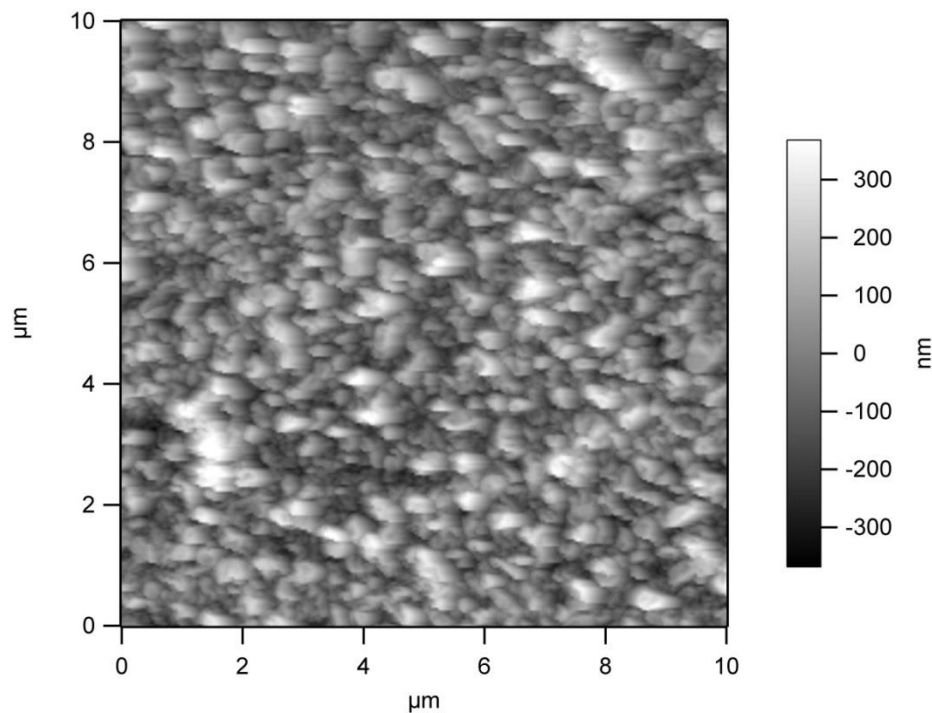


**Figure 4-7:** Plan view images of SIM membrane surfaces reconstructed from AFM roughness statistics for an ESPA2 membrane.

Comparison among the surface of virgin and fouled membrane samples is demonstrated in Figures 4-8 and 4-9. SEM images clearly display the remarkable differences between the surface morphologies of the two membrane samples. While the foulant layer on the fouled membrane surfaces consisted of particulate matter embedded in an apparently amorphous matrix (Figures 4-8B, 4-8C, 4-9B and 4-9C), the virgin membrane appeared clean with a quite smooth surface (Figures 4-8A and 4-9A). Due to the roughness of NF and RO membranes, the colloids are located mainly in the valleys on the surface after filtration; i.e. “valley clogging” has taken place (Vrijenhoek et al., 2001; Hoek et al., 2003). Nevertheless, the colloids are distributed over the entire membrane surface and formed a dense and uniform cake layer on the membrane surface due to hydrophobic interactions between the foulants and membrane surfaces (Jonathan and C., 2002; Boussu et al., 2007).

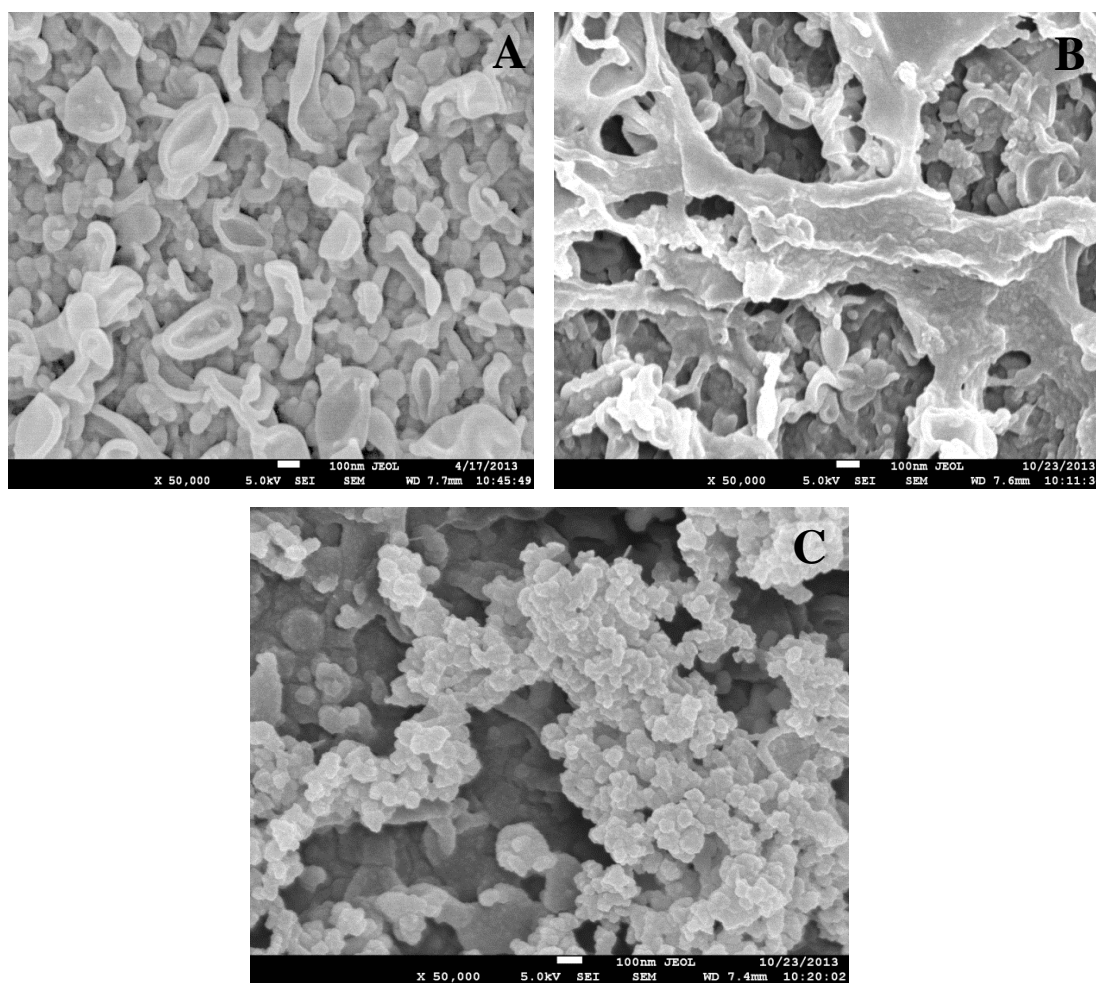


**Figure 4-8:** SEM images of the (A) virgin ESPA2 membrane, (B) ESPA2 membrane surface fouled by EWB10D and (C) ESPA2 membrane surface fouled by EWB13D at Southlands-Botany Bay.

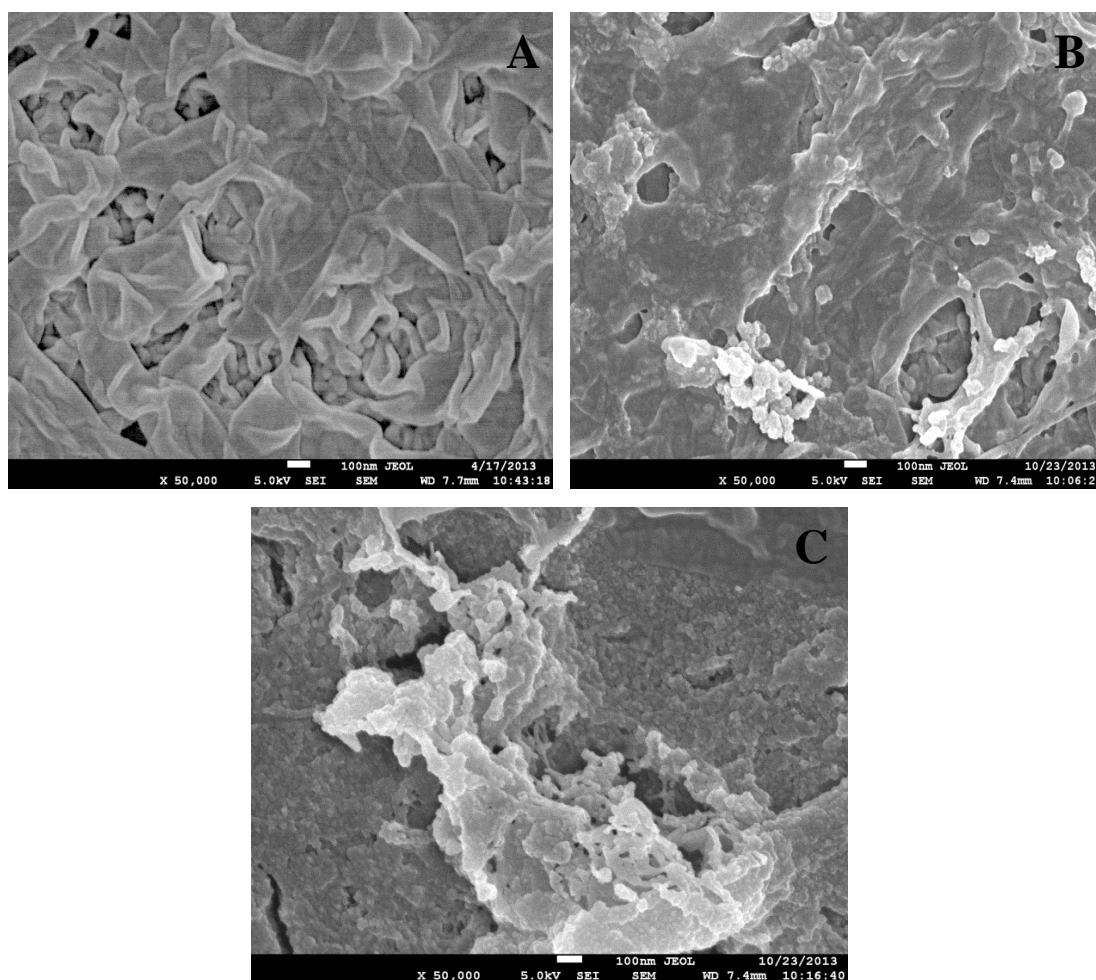


**Figure 4-9:** SEM images of the (A) virgin NF-90 membrane, (B) NF-90 membrane surface fouled by EWB10D and (C) NF-90 membrane surface by fouled EWB13D at Southlands-Botany Bay.

Distribution of elements deposited on the membrane surface which formed the fouling layer was obtained from SEM with additional semi-quantitative energy dispersive spectrometer (EDS) analysis. It was noticed that carbon, oxygen and sulphur were detected in all samples including the virgin membrane because they were parts of the membrane polymeric composition. Noteworthy, platinum existed in all samples, including the virgin membrane as a result of membrane coating. Specifically, a sulphur peak was observed with wastewater samples which were collected from both EWB10D and EWB13D at Southlands-Botany Bay indicating the participation of sulphate scale in fouling (see Figures 4-10B, 4-10C, 4-11B and 4-11C). Small aluminium peaks were noticed on fouled ESPA2 and NF-90 membrane surfaces (Figures 4-10C, 4-11B and 4-11C) and silicon as well (Figure 4-11B)

indicating their high scaling tendency even when present in a small amounts. Furthermore, a small level of sodium was found in the alginate fouling layer (Figures 4-10B and 4-11B) as well as chlorine (Figure 4-11B). The reasons for the deposition of foulants (Si, Al, Na and Cl) on the membranes are caused by the increase in membrane selectivity due to biofouling (Melián-Martel et al., 2012).

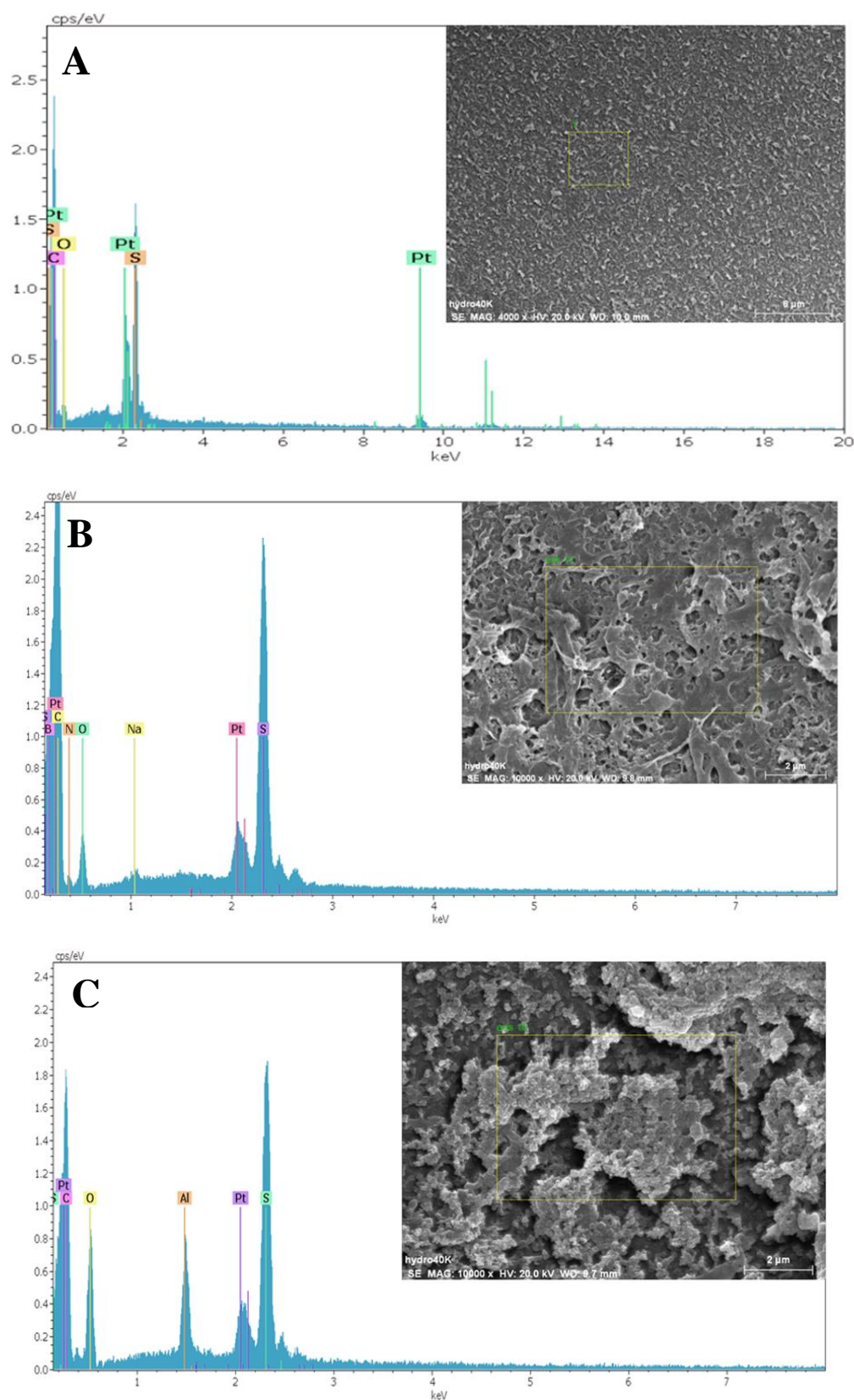


**Figure 4-10:** EDS data of the virgin ESPA2 membrane (A), ESPA2 membrane fouled by EWB10D (B) and ESPA2 membrane fouled by EWB13D (C) at Southlands-Botany Bay.

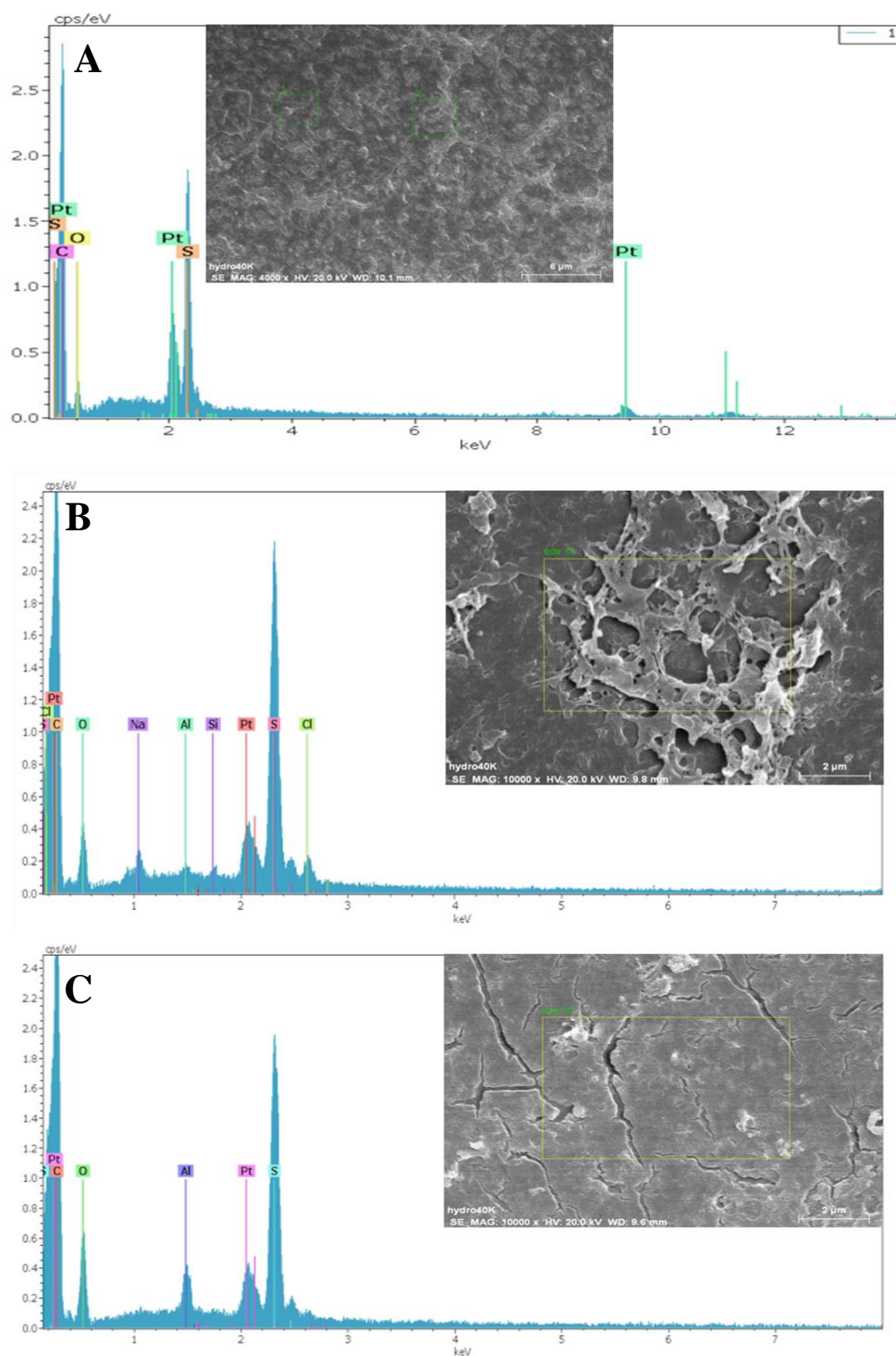


**Figure 4-11:** EDS data of the virgin NF-90 membrane (A), NF-90 membrane fouled by EWB10D (B) and NF-90 membrane fouled by EWB13D (C) at Southlands-Botany Bay.



#### **4.4 Removal of organic contaminants (volatile organic compounds) by the NF/RO system**

To investigate the ability of the NF/RO membranes to remove volatile organic compounds from contaminated groundwater, several experiments were conducted for samples collected from EWB10D and EWB13D at Southlands-Botany Bay.

##### **4.4.1.1 EWB10D at Southlands-Botany Bay**

An overall comparison of NF-90 and ESPA2 membrane performances in terms of removal efficiency is presented in Table 4-1 and Figure 4-12. The results in Table 4-1 and Figure 4-12 exhibited that the performance of the NF-90 and ESPA2 membranes after one hour was better than after 8 hours. Moreover, it was observed that the ESPA2 membrane has a higher ability than the NF-90 membrane for rejecting volatile organic compounds. Additionally, it was notable that the performance of the NF-90 and ESPA2 membranes in rejecting hydrophilic compounds [(Log  $D$  >2.5), carbon tetrachloride, trichloroethylene and tetrachloroethylene] was higher than that for its hydrophobic compounds rejection [(Log  $D$  <2.5), other volatile organic compounds which are demonstrated in Table 4-1]. As stated by Nghiem et al. (2004b) the removal of some hydrophobic compounds can be actually lower than that expected based only on a steric hindrance transport model. It can be elucidated that hydrophobic compounds can adsorb to NF/RO membranes and then diffuse through the dense polymeric matrix, resulting in significant transport of these compounds across the ultra-thin active skin layer. On the other hand, because hydrophilic compounds do not adsorb to the membrane polymeric matrix, hydrophilic volatile organic compounds can be effectively rejected by NF/RO membranes using steric hindrance or size exclusion mechanisms. These results also support the findings which are reported in other previous studies (Agenson and Urase, 2007).

It is noteworthy that the highest rejection achieved by NF-90 and ESPA2 for tetrachloroethylene reached 98.4 % for NF-90 and 100 % for ESPA2 while the



lowest rejection achieved by NF-90 and ESPA2 was for dichloromethane and amounted to 27.6 % and 43.4 %, respectively. According to Wells (2006) tetrachloroethylene has the highest Log  $D$  of the model foulants (3.07) and therefore it is considered to be a hydrophilic compound and it can be effectively rejected by NF/RO membranes using steric hindrance or size exclusion mechanisms, whereas dichloromethane has the lowest Log  $D$  of the model foulants (1.40) and it is classified hydrophobic compound and it can adsorb to NF/RO membranes and then diffuse through the dense polymeric matrix, resulting in the lower removal for this compound compared to tetrachloroethylene (Nghiem et al., 2004b).

Complete rejection of carbon tetrachloride, trichloroethylene, tetrachloroethylene and 1,1,2,2-tetrachloroethane by ESPA2 could be attributed to the sieving (or size exclusion) as result of the molecular weights of these compounds, (which are 153.82 g/mol, 131.39 g/mol, 165.83 g/mol and 167.85 g/mol respectively) higher than the molecular weight cut-off (MWCO) for NF-90 and ESPA (~100 Da). In other words, the sieving of large molecules (carbon tetrachloride, trichloroethylene, tetrachloroethylene and 1,1,2,2-tetrachloroethane) occurs because of the small size of the membrane pores and this phenomenon is named a steric hindrance effect that operates principally for neutral solutes (Agenson and Urase, 2007; Minhas et al., 2013).

**Table 4-1:** Overall removal efficiency of the volatile organic compounds which were detected in EWB10D at Southlands-Botany Bay.

Compound Name	Rejection @ 1hr-NF-90 (%)	Rejection @ 8hrs-NF-90 (%)	Rejection @ 1hr-ESPA2 (%)	Rejection @ 8hrs-ESPA2 (%)
Vinyl Chloride	69.0	60.0	97.7	82.4
1,1-Dichloroethene	86.0	66.7	98.0	94.1
Dichloromethane	47.0	27.6	88.1	43.4
trans-1,2-Dichloroethene	80.0	58.1	99.3	88.0
1,1-Dichloroethane	82.0	72.7	98.2	95.7
cis-1,2-Dichloroethene	80.0	41.2	97.6	68.2
Chloroform	82.6	47.9	98.6	89.1
1,1,1-Trichloroethane	50.0	41.2	50.0	44.4
Carbon tetrachloride	96.3	98.0	100.0	100.0
1,2-Dichloroethane	71.5	20.0	76.2	70.5
Benzene	90.0	66.7	92.9	83.3
Trichloroethylene	97.3	65.3	100.0	98.3
1,1,2-Trichloroethane	80.0	71.4	98.0	92.3
Tetrachloroethylene	98.4	88.0	100.0	99.9
Chlorobenzene	88.9	50.0	88.9	75.0
1,1,2,2-Tetrachloroethane	90.6	88.6	98.8	97.8

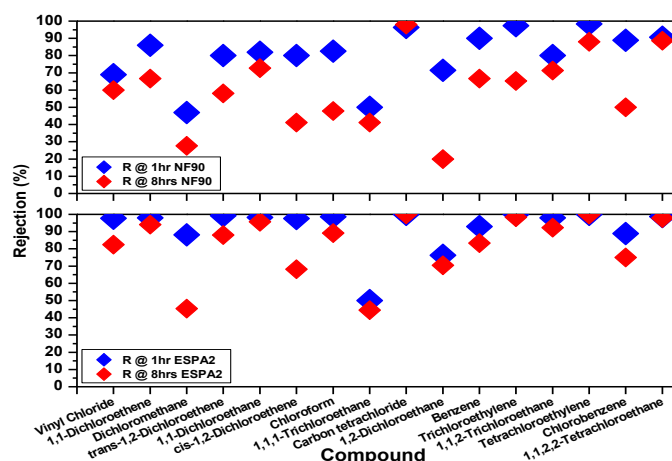


**Figure 4-12:** Overall removal efficiency of the volatile organic compounds which were detected in the contaminated groundwater EWB10D. The NF/RO membrane filtration experiment was conducted at an initial permeate flux of 41 L/m<sup>2</sup>h and temperature of 4 °C, with a cross-flow velocity of 30.4 cm/s. Samples were collected after 1 and 8 hours of filtration.

#### 4.4.1.2 EWB13D at Southlands-Botany Bay

The removal efficiency for both NF-90 and ESPA2 are reported in Table 4-2 and Figure 4-13. The findings shown in Table 4-2 and Figure 4-13 confirm the results concluded above for EWB10D (part 4.3.2.1); however there are some differences between them based on the difference in concentrations of model foulants at this site compared to the previous site (EWB10D). Also, only 11 volatile organic compounds were detected at this site, whereas in EWB10D site, 16 volatile organic compounds were detected. Table 4-2 and Figure 4-13 display that the performance of the NF-90 and ESPA2 membranes after one hour was better than after 8 hours. Furthermore, it was observed that the ESPA2 membrane has a higher ability than the NF-90 membrane for rejecting volatile organic compounds. Moreover, it was noteworthy that the performance of the NF-90 and ESPA2 membranes in rejecting hydrophilic compounds [(Log  $D$  >2.5), trichloroethylene and tetrachloroethylene] was higher than that of its hydrophobic compounds rejection [(Log  $D$  <2.5), other VOCs which are shown in Table 4-1]. The reason for this phenomenon has been explained above in part 4.3.2.1 for the reasons given by Nghiem et al. (2004b).

It is remarkable that the highest rejection achieved by NF-90 and ESPA2 for tetrachloroethylene and has reached 95.7 % for NF-90 and 96.2 % for ESPA2 while the lowest rejection achieved by NF-90 and ESPA2 was for 1,1-dichloroethane and has amounted of 41.2 % and 44.4 %, respectively. According to Wells (2006) the Log  $D$  of tetrachloroethylene is 3.07 and therefore it is considered to be a hydrophilic compound and it can be successfully rejected by NF/RO membranes using steric hindrance or size exclusion mechanisms, whereas the Log  $D$  of 1,1-dichloroethane is 2.05 and thus it is classified as a hydrophobic compound and it can adsorb onto NF/RO membranes and then diffuse through the dense polymeric matrix, resulting in the lower removal for this compound compared to tetrachloroethylene (cf. Nghiem et al., 2004b).

**Table 4-2:** Overall removal efficiency of the volatile organic compounds which were detected in EWB13D at Southlands-Botany Bay.

Compound Name	Rejection @ 1hr-NF-90 (%)	Rejection @ 8hrs-NF-90 (%)	Rejection @ 1hr-ESPA2 (%)	Rejection @ 8hrs-ESPA2 (%)
Vinyl Chloride	73.7	50.0	75.0	66.7
1,1-Dichloroethane	50.0	41.2	54.5	44.4
cis-1,2-Dichloroethene	72.7	66.7	75.0	75.0
Chloroform	68.2	50.0	75.0	75.0
Carbon tetrachloride	85.7	60.0	87.5	61.5
1,2-Dichloroethane	81.0	55.6	82.0	78.2
Benzene	50.0	45.0	75.0	50.0
Trichloroethylene	95.5	94.4	95.7	87.5
1,1,2-Trichloroethane	87.5	75.0	83.3	80.0
Tetrachloroethylene	95.7	95.0	96.2	95.0
1,1,2,2-Tetrachloroethane	90.0	85.7	90.9	85.7

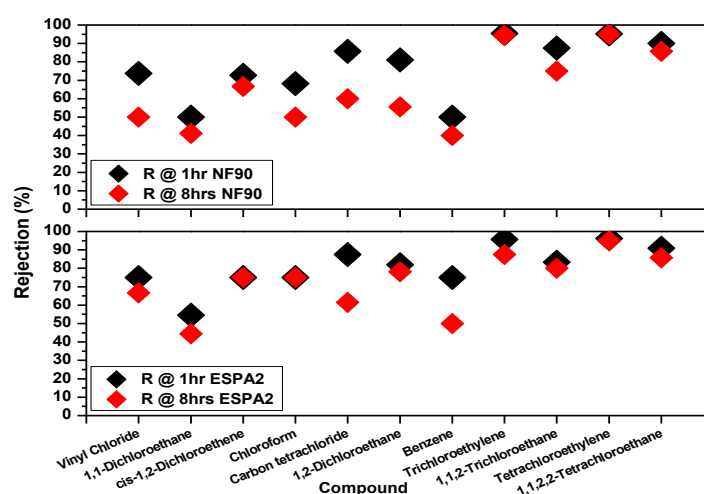


**Figure 4-13:** Overall removal efficiency of the selected volatile organic compounds which were detected in the contaminated groundwater EWB13D. The NF/RO membrane filtration experiment was conducted at an initial permeate flux of 41 L/m<sup>2</sup>h and temperature of 4 °C, with a cross-flow velocity of 30.4 cm/s. Samples were collected after 1 and 8 hours of filtration.

#### **4.4.2 Performance of the NF/RO membranes**

To examine performance of the NF/RO membranes regarding rejecting volatile organic compounds, it is essential to study the membrane permeate flux as a function of filtration time for samples that were collected from different sites (EW10D and EW13D at Southlands-Botany Bay).

##### **4.3.3.1 EWB10D at Southlands-Botany Bay**

Figure 4-14 shows the evolution of the membrane permeate flux as a function of filtration time. Significant permeate flux decline could be observed with the NF-90 membrane exhibiting a permeate flux decline of 34.2 % over 8 hours. In contrast, indiscernible flux decline could be observed with the ESPA2 membrane that only exhibited a permeate flux decline of 1.7 % over 8 hours (Figure 4-14); this can be attributed to membrane surface roughness. Indeed, there is a correlation between fouling tendency and the membrane surface roughness and this totally agrees with previous studies (e.g. Vrijenhoek et al., 2001; Boussu et al., 2007; Xu et al., 2010). As presented in chapter 3 (Table 3-3) the NF-90 has a significant surface roughness of 63.9 nm whereas the ESPA2 has a slightly smoother membrane surface with a corresponding surface roughness (30.0 nm). In fact, the ESPA2 did not show any measurable flux decline over roughly 8 hours of filtration time. On the other hand, there was a noticeable permeate flux decline by the NF-90 membrane and this is consistent with several previous studies (e.g. Alturki et al., 2010). Clogging of membrane pores by organic molecules principally accounts for the flux decline observed in the fouled membranes. A reasonable explanation is that the membrane pores became narrower due to organic molecules being adsorbed onto the membrane polymer, especially chlorinated hydrocarbons in the contaminated water samples. Consequently, the smaller pore sizes of contaminated membranes would theoretically permit only molecules smaller than them to pass (Agenson and Urase, 2007). This would suggest that the membrane should become more effective at rejecting large

contaminants as it becomes contaminated however this negatively affected the flux performance for the membrane.

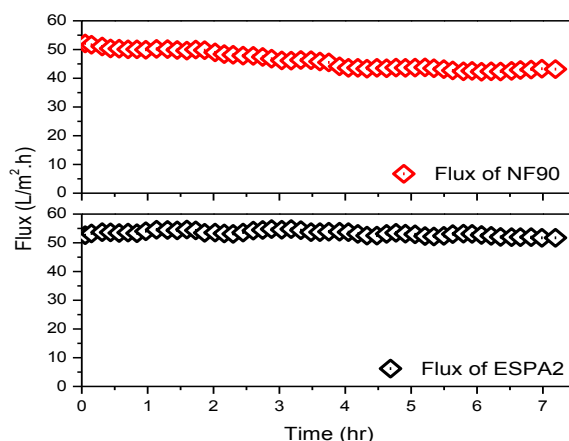


**Figure 4-14:** Permeate flux of the NF-90 and ESPA2 as a function of filtration time. Experiments were conducted at an initial permeate flux of 41 L/m<sup>2</sup>h and temperature of 4 °C, with a cross-flow velocity of 30.4 cm/s. Samples were collected after 1 and 8 hours of filtration. Samples were collected from EWB10D-Botany Bay.

Comparison between feed and permeate samples which were collected before and after passing through NF-90/ESPA2 membranes is displayed in Table 4-3. In this Table, conductivity values, flux, pH, pressure and temperature were measured after 1 hour and 8 hours of the filtration experiments. The ESPA2 membrane, which is classified as a non-porous membrane, has a high efficiency for the removal of target contaminants (Figure 4-12). Correspondingly, the NF-90 membrane, which is classified as a tight nanofiltration membrane exhibited a good efficiency for removal of organic contaminants however it was less efficient than of the ESPA2 membrane (Figure 4-12). This is confirmed by the great difference in conductivity before and after using the NF-90 and ESPA2 membranes, however as shown in Table 4-3 the difference in conductivity before and after using the ESPA2 membrane is greater than the difference in conductivity before and after using the NF-90 membrane. Accordingly, conductivity seems to be a good indicator to assess the removal efficiency of organic contaminants by the tight NF and RO membranes.

**Table 4-3:** Conductivity, flux, pH, pressure and temperature values measured after 1 hour and 8 hours of filtration for samples which were collected from EWB10D located at Southlands-Orica.

Membrane	Time (h)	Flux <sup>a</sup> (L/m <sup>2</sup> .h)	PH		Conductivity (μS/cm)		Pressure (bar)	Temperature (°C)	
			Feed	Permeate	Feed	Permeate		Feed	Permeate
NF-90	1 hr	3.3	4.6	4.2	5750	484	14	4	4
	8 hrs	2.7	4.7	3.9	5630	397	14	4	4
ESPA2	1 hr	3.6	4.6	4	5820	203	22	4	4
	8 hrs	3.4	4.6	3.9	5560	171	22	4	4

<sup>a</sup> Flux at 0 time allows start with 3.6 ml/min for each experiment.

Flux reported in Table 4-3 is considerably low for NF-90 and ESPA2 (2.7 L/m<sup>2</sup> .h and 3.4 L/m<sup>2</sup> .h ESPA2 respectively) after 8 hours of operation. A reasonable explanation is that the membrane pores became narrower due to organic molecules being adsorbed onto the membrane polymer, especially chlorinated hydrocarbons in the contaminated water samples. Consequently, the smaller pore sizes of contaminated membranes would theoretically permit only molecules smaller than them to pass and thus reduce the flux.

#### 4.3.3.2 EWB13D at Southlands-Botany Bay

Figure 4-15 displays the evolution of the membrane permeate flux as a function of filtration time. The same pattern was observed in performance of the NF/RO membranes when they were used to examine the rejection of volatile organic compounds for samples were collected from EWB13D. As seen in Figure 4-15, a noteworthy permeate flux decline was observed with the NF-90 membrane due to fouling and it exhibited a permeate flux decline of 49.2 % over 8 hours. In contrast, a slightly flux decline could be observed with the ESPA2 membrane and it displayed a permeate flux decline of only 15.5 % over 8 hours which can be attributed to the surface roughness of the membrane. Obviously as reported in many studies, there is a strong relationship between fouling tendency and the membrane surface roughness (e.g. Vrijenhoek et al., 2001; Boussu et al., 2007; Xu et al., 2010). The NF-90 membrane has a significant surface roughness 63.9 nm whereas the ESPA2 membrane has slight smoother membrane surface with the corresponding surface

roughness 30.0 nm as shown in Table 3-3 (chapter 3). Therefore the ESPA2 membrane exhibited a slight flux decline over 8 hours of filtration time. Another explanation for flux decline NF-90 membrane is due to physicochemical properties of the membrane particularly pore size. Membranes having a larger pore size (e.g. NF-90) could be more affected with fouling compared to membranes having smaller pore size (e.g. ESPA2 which is classified as nonporous; Nghiem and Hawkes, 2009). This study revealed that permeate flux decline due to membrane fouling would be more severe with membranes having a larger pore size.

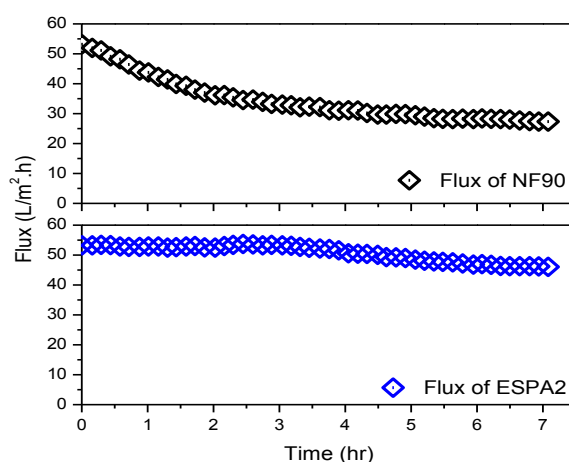


**Figure 4-15:** Permeate flux of the NF-90/ESPA2 membranes as a function of filtration time. Experiments were conducted at an initial permeate flux of 41 L/m<sup>2</sup>h and temperature of 4 °C, with a cross-flow velocity of 30.4 cm/s. Samples were collected after 1 and 8 hours of filtration. Samples were collected from EWB13D-Botany Bay.

Study the relationship between feed and permeate samples which were collected before and after utilizing NF-90/ESPA2 membranes is presented in Table 4-4. This table shows conductivity values, flux, pH, pressure and temperature measured after 1 hour and 8 hours of the filtration experiments. The ESPA2 membrane, which is considered a non-porous membrane, has a high efficiency for the removal of model foulants (Figure 4-13). Similarly, the NF-90 membrane, which is classified as a tight nanofiltration membrane displayed a good efficiency for removal of model foulants but was less efficient than the ESPA2 membrane (Figure 4-13). This is confirmed by the great difference in conductivity before and after using the NF-90 and ESPA2 membranes, however as shown in Table 4-4 the difference in conductivity before and



after using the ESPA2 membrane greater than the difference in conductivity before and after using the NF-90 membrane. Hence, conductivity appears to be a good indicator to evaluate the removal efficiency of organic contaminants by the tight NF and RO membranes.

**Table 4-4:** Conductivity, flux, pH, pressure and temperature values measured after 1 hour and 8 hours of filtration for samples which were collected from EWB13D located at Southlands-Orica.

Membrane	Time (h)	Flux <sup>a</sup> (L/m <sup>2</sup> .h)	PH		Conductivity (μS/cm)		Pressure (bar)	Temperature (°C)	
			Feed	Permeate	Feed	Permeate		Feed	Permeate
NF-90	1 hr	3.3	4.3	3.8	1553	112	14	4	4
	8 hrs	2	4.4	3.8	1457	100	14	4	4
ESPA2	1 hr	3.6	4.4	4	1462	171	22	4	4
	8 hrs	3.2	4.5	4	1435	145	22	4	4

<sup>a</sup> Flux at 0 time allows start with 3.6 ml/min for each experiment.

## 4.5 Conclusion

Results reported in this study indicate that NF/RO membrane filtration can achieve enhanced removal efficiency over the wide range of volatile organic compounds which were detected in groundwater collected from EW10D and EW13D, respectively. Findings of this study revealed that the performance of the NF-90 and ESPA2 membranes after one hour was better than after 8 hours when using these membranes to examine the removal of volatile organic compounds at the two sites (EW10D and EW13D). The performance of the NF-90 and ESPA2 membranes in rejecting hydrophilic compounds (e.g. trichloroethylene and tetrachloroethylene) was higher than that of its hydrophobic compounds (e.g. dichloromethane and vinyl chloride). Since hydrophilic compounds can be effectively rejected by NF/RO membranes using steric hindrance or size exclusion mechanisms, whereas hydrophobic compounds can be adsorb at onto NF/RO membranes and then diffuse through the dense polymeric matrix, resulting in the lower removal for these compounds compared to hydrophilic compounds. Also findings of this study indicate that membrane fouling significantly affects the rejection of volatile organic compounds by NF-90 membranes, however is less significant for thin film composite

ESPA2 membrane. Flux decline through the NF-90 and ESPA2 membranes in this study could be attributed to physicochemical properties of the membranes in particular surface roughness and pore size.

## **CHAPTER 5: THE REMOVAL OF ORGANIC CONTAMINANTS BY USING MWNT BUCKYPAPER MEMBRANE**

### **5.1 Introduction**

Membrane-based water purifications are well known as a useful technology for a wide range of water and wastewater treatment processes. This is due to their low cost and environmentally acceptable process compared to conventional technologies such as distillation and evaporation which usually suffer from disadvantages such as high cost and their requirement for the use of chemicals that need special handling (Goh et al., 2013). Even though these are remarkable features, there is still a need to test a new generation of membranes that may offer more effective solutions to the problems associated with fouling, short service lifetimes and low chemical selectivity (Mulder, 1996). One such material is carbon nanotubes (CNTs), which have exhibited a combination of exceptional mechanical, thermal and electrical properties (Thostenson et al., 2001). Carbon nanotube buckypapers have unique properties such as natural hydrophobicity, high porosity and very high specific surface area, making them promising candidates for separation applications (Dumée et al., 2011).

The separation process of components through a membrane is governed by one or more mechanisms, including adsorption and size exclusion (Bellona et al., 2004; Díaz et al., 2007; Shih and Li, 2008). Adsorption is a dominant mechanism to retain organic contaminants utilizing CNTs. This mechanism is often governed by the relative hydrophilicity or hydrophobicity of the membrane surface, and hydrogen bonding as well as other interactions between solutes and the membrane (Liu et al., 2013b). It has been found that CNTs are superior adsorbents for removing many kinds of organic contaminants, for instance volatile organic compounds (Díaz et al., 2007; Shih and Li, 2008), trihalomethanes (Lu et al., 2005; Lu et al., 2006), organic dyes (Yu et al., 2014), xylene (Es'haghi et al., 2011), natural organic matter (Liu et al., 2013a), phenols (Yu et al., 2014), trace polycyclic aromatic hydrocarbons (Kueseng et al., 2010) and pesticides (Pyrzynska, 2011). On the other hand, electrostatic repulsion and size exclusion mechanisms govern the rejection of positively charged organic contaminants. The size exclusion mechanism occurs when

the solutes size is larger than the pore size of the membrane; as a result contaminants are removed effectively by a sieving mechanism (Chen et al., 2004; Verliefde et al., 2008). In the electrostatic repulsion mechanism, the separation results from the electrostatic interactions between ions and the negatively charged MWNT membrane (Vatanpour et al., 2011).

The aim of this study was to investigate the removal of VOCs by using a dead-end filtration cell setup. Experiments were conducted using a buckypaper (BP) created using MWNT-Trix 1% (w/v) dispersion. Twenty one VOCs had molecular weights between 78.11 g/mol (benzene) and 260.76 g/mol (hexachlorobutadiene) were designated as model organic contaminants because of their widespread occurrence in surface and groundwater. Removal efficiency by the dead-end filtration cell setup was linked to the physicochemical properties of these compounds and focused on the ability and effectiveness of this kind of treatment. Substantial characterization work has been conducted to investigate MWNT buckypaper membranes.

## **5.2 Materials and methods**

Comprehensive descriptions of the dead-end filtration system, operation protocol, and analytical techniques have been provided in chapter 3. Volatile organic compounds (VOCs) were collected from EWB10D and EWB13D located at Southlands in Botany Bay. The dead end filtration cell setup was completely sealed throughout the experiment to avoid evaporation of these compounds. Each experiment used 2 L of sample as the feed solution. Following setup, the dead-end filtration system operated for 8 hours in each experiment to collect an adequate amount of permeate (40 mL - two duplicates) which was analysed to determine the removal efficiency of this system. In this chapter, the obtained data are systematically analysed to assess the overall performance of the dead-end filtration system.

### **5.2.1 Model organic contaminants**

Twenty one compounds were selected for this study to represent key organic groups of concern in groundwater samples – namely volatile organic compounds (e.g. dichloromethane, trichloroethylene, tetrachloroethylene, toluene and benzene). The selection of these compounds was also based on their widespread occurrence in surface and groundwater and their varied physicochemical properties (e.g. hydrophobicity and molecular size). Significant physicochemical properties of these organic contaminants are shown in chapter 3 (Table 3-4). The designated VOCs had molecular weights between 78.11 g/mol (benzene) and 260.76 g/mol (hexachlorobutadiene). The intrinsic hydrophobicity of these compounds differed significantly, as was reflected by the values of their octanol-water partitioning coefficients ( $\log K_{ow}$ ) or  $\log K_{ow}$  at a specific pH ( $\log D$ ). Table 3-4 demonstrated that most VOCs used in this study are hydrophobic with  $\log D$  at pH 7 and 8 of between 1.40 and 4.91, respectively. Also it can be seen from the selected organic compounds (chlorinated hydrocarbons) properties that some compounds are hydrophilic ( $\log D > 2.5$ ) or hydrophobic ( $\log D < 2.5$ ).

## **5.3 Results and discussion**

### **5.3.1 Optimisation of sonication time**

Optimisation of the sonication time to disperse MWNTs in Triton X-100 solutions was conducted using UV-vis-NIR spectrophotometry and samples containing 0.1% (w/v) MWNT and 1% (w/v) Triton X-100 which was used as a surfactant. Spectra were obtained after different periods of sonication and are presented in Figure 5-1. It is clearly observed that absorbance increases at all wavelengths consistent with increasing sonication time, indicating an increase in the quantity of MWNTs dispersed in the aqueous solution [Figure 5-1(a)].

Figure 5-1(b) displays that extremely dispersed MWNT/Triton X solutions were achieved after very short sonication times were used. Nonetheless, after 6 min the

increase in absorbance became more gradual. After 24 min sonication the absorbance became more stable and there was no notable change to the absorbance at 660 nm. This means that after 24 min sonication, additional dispersion of MWNTs into solution is negligible. Additionally, sonication of samples for longer periods of time could expose the nanotubes to increased amounts of energy, which may cause further degradation of the nanotubes and be accompanied by a decrease in the physical properties of the resulting dispersion. Thus, it can be concluded that 24 min is the optimum sonication time to disperse MWNTs in Triton X-100 solutions.

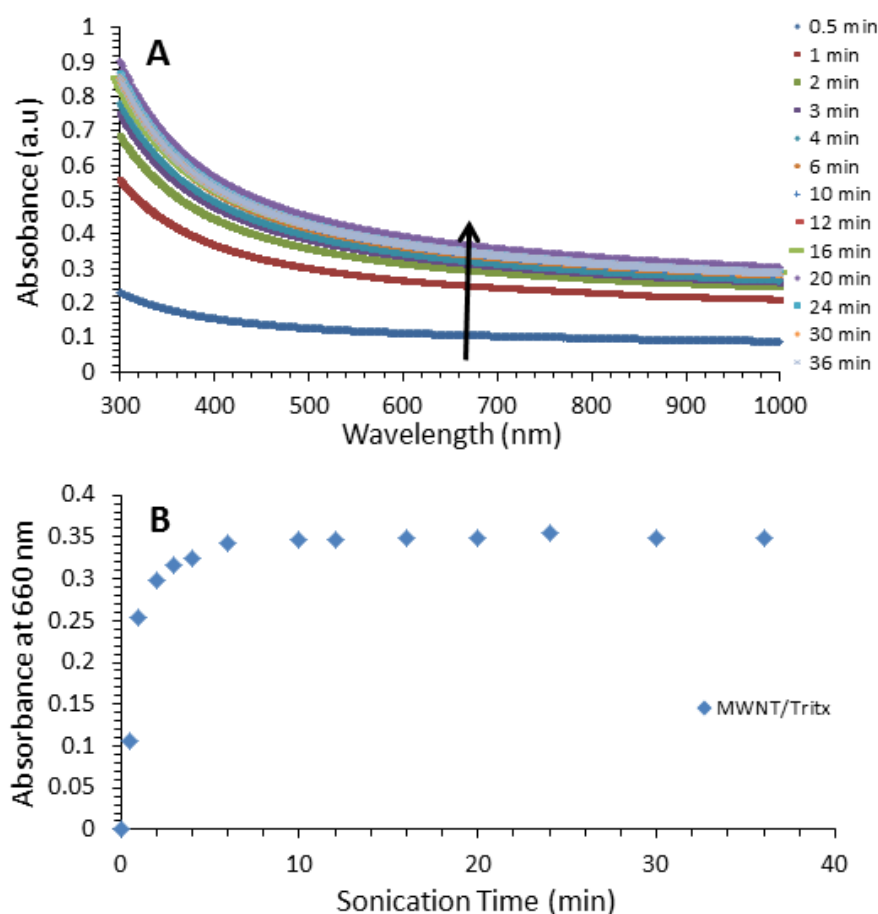


**Figure 5-1:** (a) Absorption spectra of a 0.1% (w/v) MWNT/1% (w/v) Triton-X dispersion taken at different sonication times. (b) Effect of increasing sonication time on the absorbance at 660 nm of the MWNT/Triton X-100 dispersion.

### 5.3.2 AFM, SEM-EDS and BET analysis

#### 5.3.2.1 AFM and SEM-EDS analysis

Average roughness was studied by 3D topographic analysis (see Figures 5-2 and 5-3). The AFM image (Figure 5-2) of the carbon nanofibrous films shows that the vertically aligned CNTs have an average diameter of ~294 nm and length of 10  $\mu\text{m}$ . In this image, the brightest area presents the highest point of the membrane surface and the dark regions indicate valleys and this can be seen clearly in Figure 5-4 (Ahmed et al., 2007). The amount of MWNTs in the composite membrane is an important factor affecting the morphology, so the image in Figure 5-2 indicates that the roughness of the membrane was somewhat smoothed by adding 0.1 wt % MWNT to the composite membrane. This result supports the conclusion reached in a previous study (Vatanpour et al., 2011). In this later study the roughness of the MWNT membrane was reduced by adding 0.04 wt % MWNT to the polymer matrix. Following that, the roughness increased significantly after adding 0.2 wt % and once again reduced by adding 0.4 wt %.

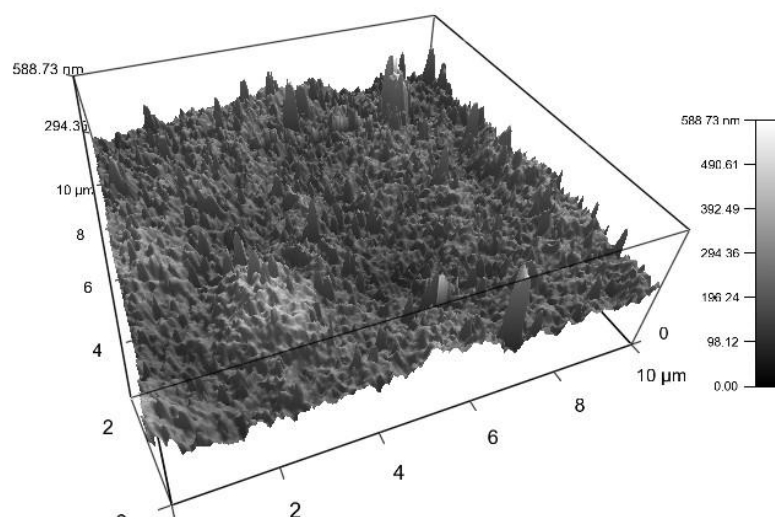


**Figure 5-2:** Surface topography image of MWNT/Triton X-100 buckypaper.

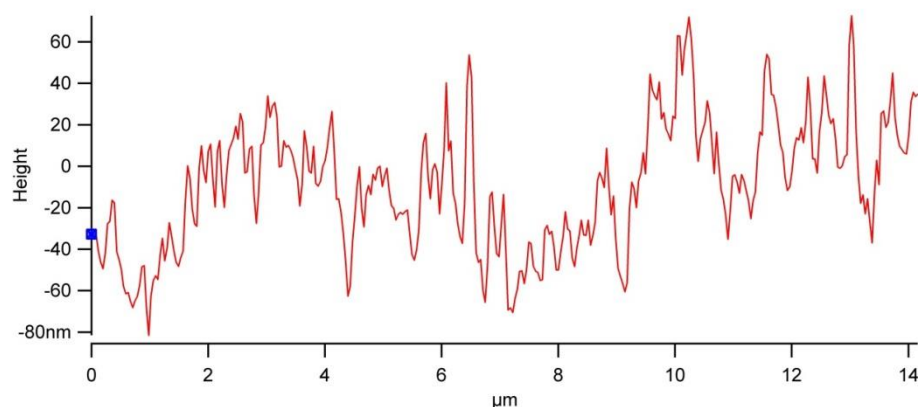


**Figure 5-3:** Section graph of MWNT/Triton X-100 buckypaper.

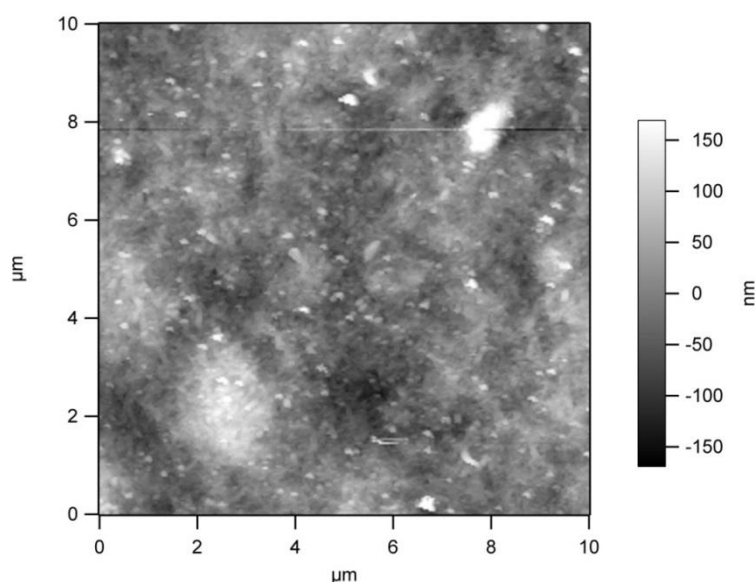


**Figure 5-4:** Plan view image of SIM membrane surfaces reconstructed from AFM roughness statistics for MWNT/Triton X-100 buckypaper.

The surface morphology and cross section of MWNT buckypapers was studied using a JEOL JSM-7500FA field-emission scanning electron microscopy (SEM). Figure 5-5 shows SEM images of MWNT buckypapers prepared using Triton X-100 before (virgin) and after use (fouled) membrane. The surface morphology of the MWNT buckypaper seems to be small bundles of tubes and an abundance of small pores (Figure 5-5A) and this agrees well with the results of a study conducted by Cottinet



et al. (2012). Also from Figure 5-5A, it can be seen that the buckypapers are composed of randomly dispersed MWNTs, which tangle through the van der Waals force and form a uniform porous structure. On the other hand, it was observed that some flattening of the MWNT bundles occurred in Figures 5-5B and 5-5C due to adsorption of contaminants.

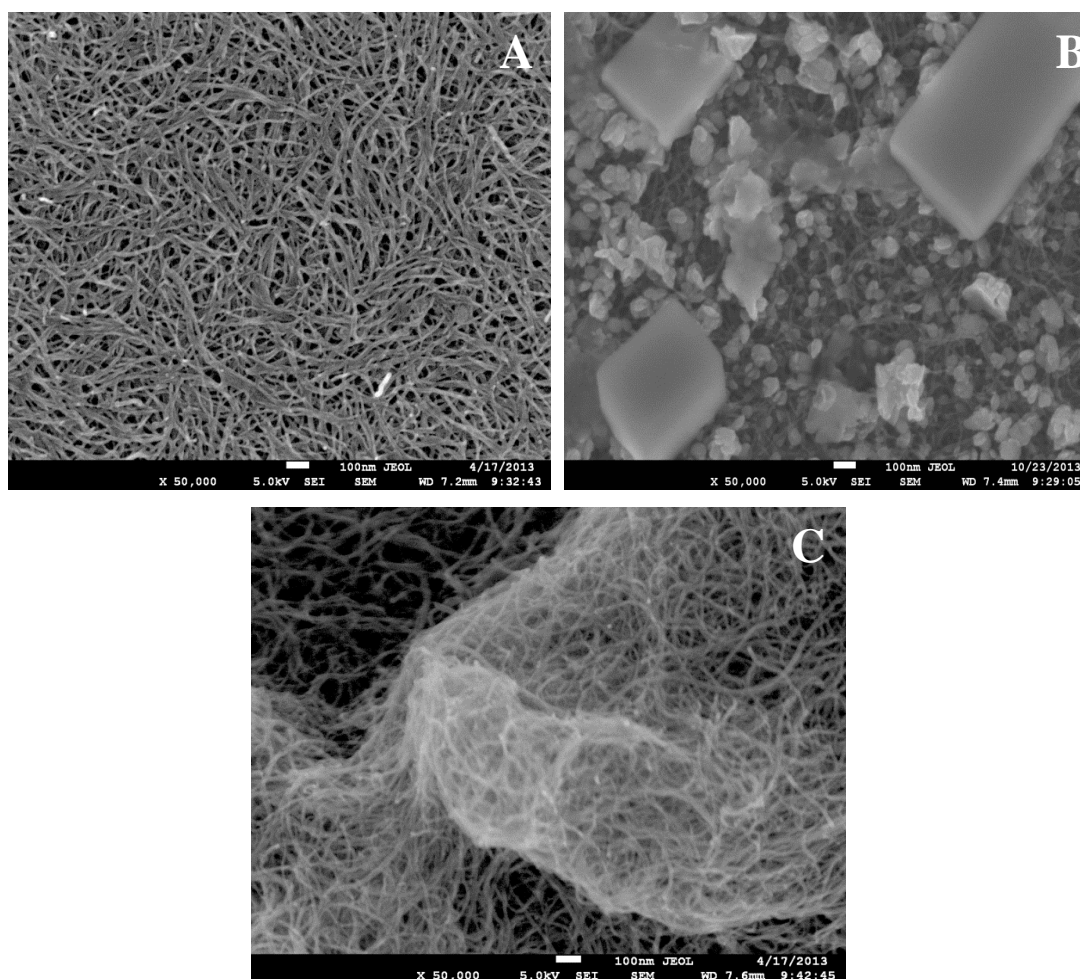


**Figure 5-5:** SEM images of the (A) virgin MWNT buckypaper; (B) MWNT buckypaper membrane fouled by EWB10D and (C) MWNT buckypaper membrane fouled by EWB13D at Sutherland Botany Bay.

Furthermore, the cross-sectional images of MWNT buckypapers show clearly what has been seen above, where Figures 5-6A, 5-6B and 5-6C show the structure and size of the tubes and pores in MWNT membrane as well. As seen Figure 5-6A, MWNT buckypapers appear to consist of small bundles of tubes and an abundance of small pores. In contrast, the MWNT bundles were flattened after the MWNT buckypaper

membranes were used due to adsorption of pollutants (Figures 5-6B and 5-6C). Moreover, from Figure 5-5A it is clear that the MWNT buckypaper membrane possesses a large number of regularly sized pores, with software image analysis (see section 3.6.2.2 for details) revealing an average surface pore diameter of  $65.6 \pm 2$  nm which is similar to that obtained previously for comparable buckypapers produced using MWNTs (Dumée et al., 2010; Sweetman, 2012).

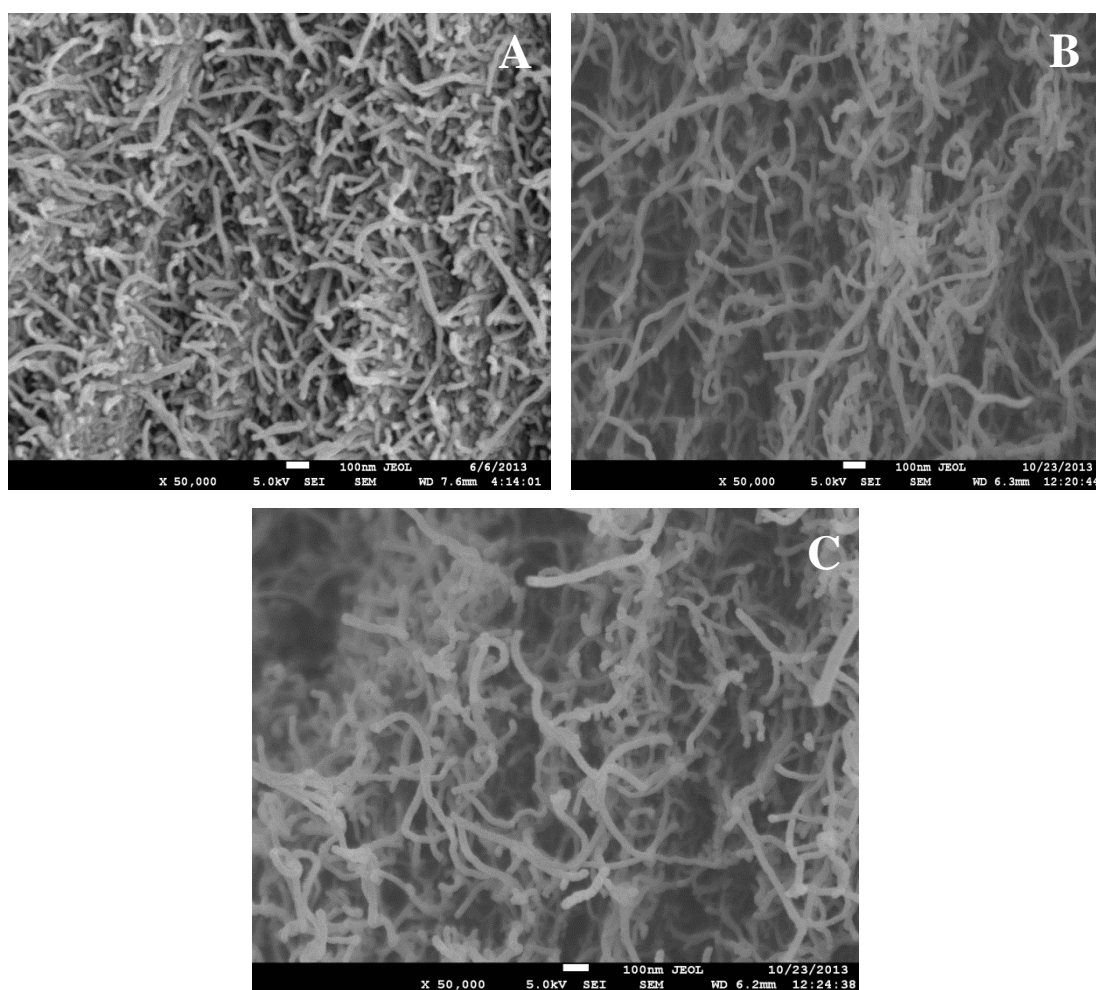


**Figure 5-6:** SEM images cross-section (A) virgin MWNT buckypaper; (B) MWNT buckypaper membrane fouled by EWB10D and (C) MWNT buckypaper membrane fouled by EWB13D at Sutherland Botany Bay.

To investigate the distribution of elements deposited on the membrane surface, MWNT buckypapers were also analysed using SEM with additional semi-quantitative energy dispersive spectrometer (EDS). SEM-EDS images obtained for MWNT buckypapers virgin and fouled membranes are shown in Figures 5-7, 5-8 and

5-9. The EDS spectrum of MWNT buckypapers (Figure 5-7) shows peaks corresponding to titanium and aluminum in addition to the high amount of carbon and a reasonable amount of oxygen as parts of the membrane composition which therefore were detected in all samples (virgin and fouled). The presence of aluminum and titanium is not surprising as these elements are used during the synthesis of MWNTs via the Nanocyl process. Also the presence of iron (Figure 5-9) is not surprising as iron catalysts are used during synthesis of MWNTs via the Nanocyl process. The amount of chlorine found was high in MWNT membrane fouled by EWB10D and somewhat higher in MWNT membrane fouled by EWB13D and this can be attributed to the rejection process for this compound by size exclusion mechanism (see Figures 5-8 and 5-9). A small level of calcium was found in the fouled membrane (Figure 5-8) due to the ability of calcium to complex with carboxyl groups which are very common at the surface of MWNTs. A considerable amount of sodium and sulphate was found in the fouled membranes (Figures 5-8 and 5-9) and this can be attributed to the rejection process for these cations via size exclusion mechanism and consequent diffusion in the membrane surface (Van der Bruggen et al., 2004).

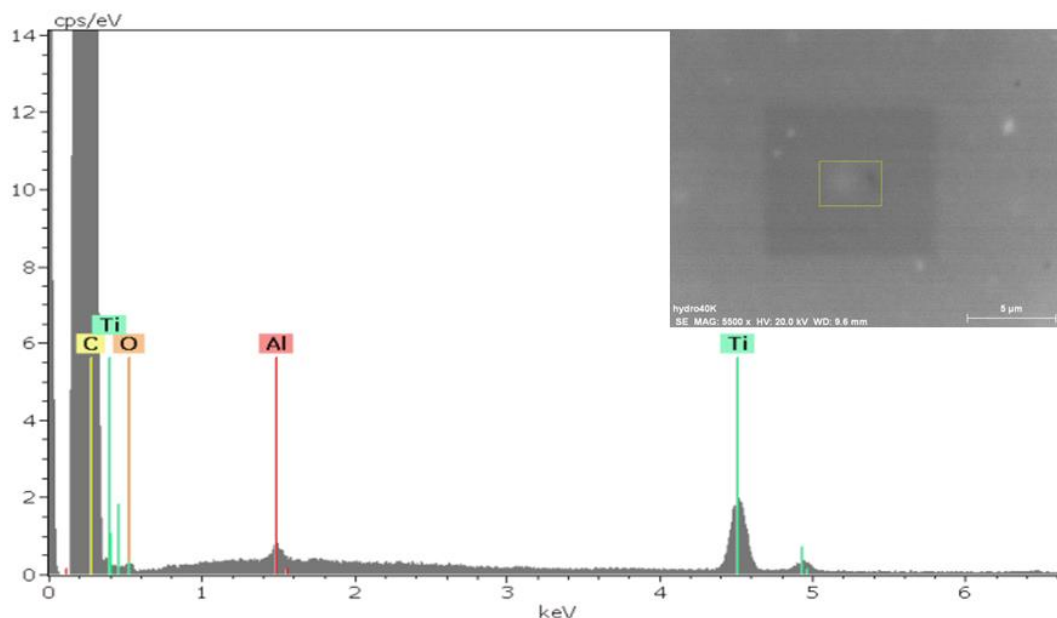


**Figure 5-7:** EDS data of the virgin MWNT/Triton X-100 buckypaper membrane.

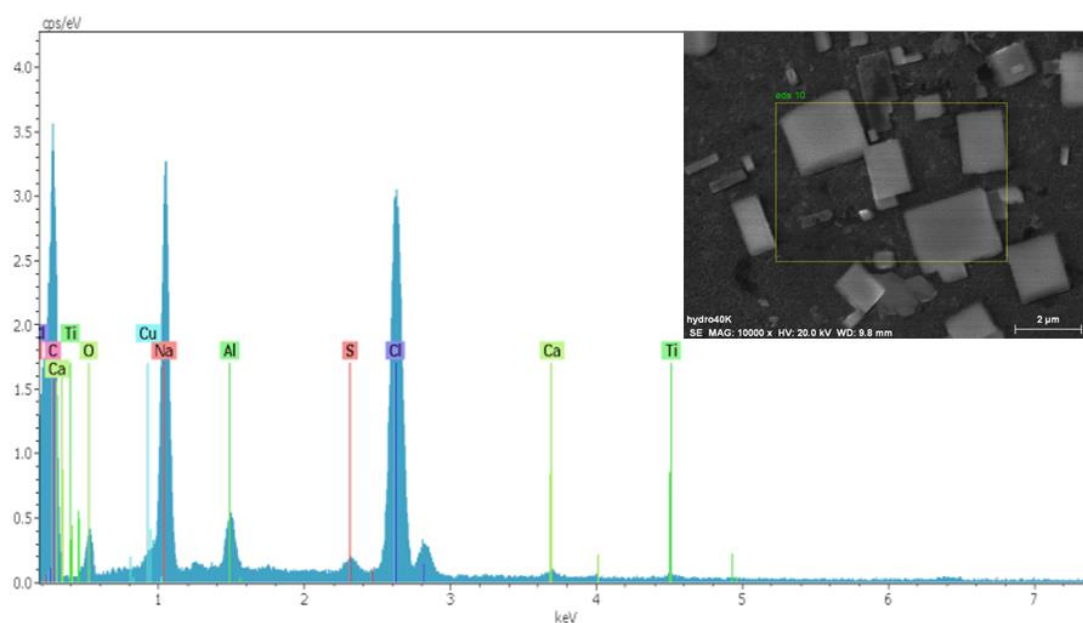


**Figure 5-8:** EDS data of the MWNT/Triton X-100 buckypaper membrane fouled by EWB10D.

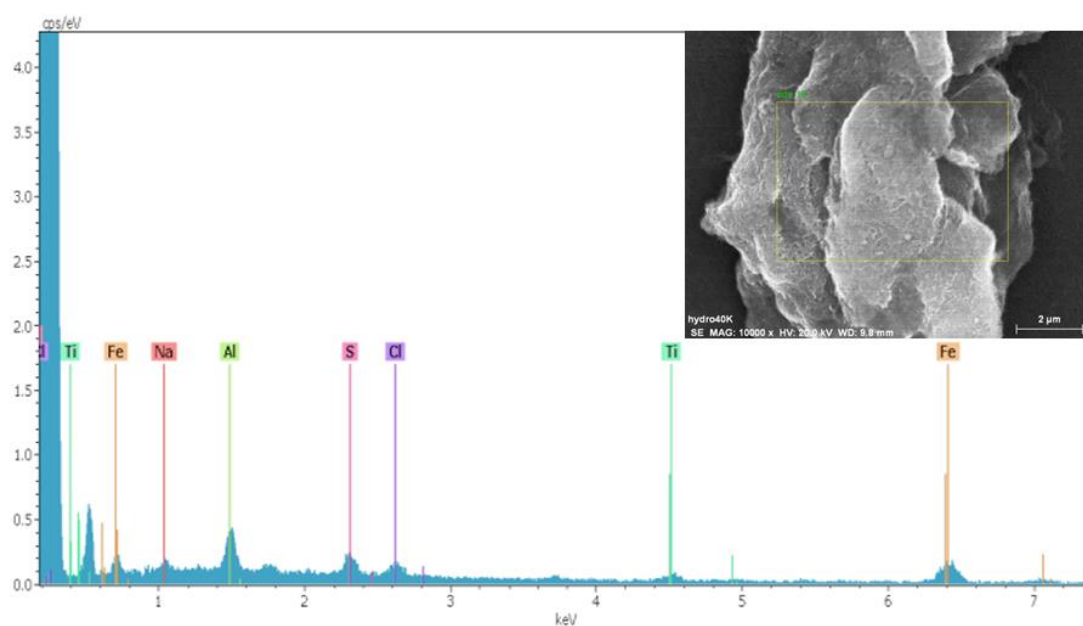


**Figure 5-9:** EDS data of the MWNT/Triton X-100 buckypaper membrane fouled by EWB13D.

### 5.3.2.2 BET analysis

More information about the surface area and average internal pore morphology of the MWNT buckypapers was obtained through analysis of the isotherms derived from nitrogen adsorption/ desorption measurements for all MWNT buckypapers and this is demonstrated in Figure 5-10. The isotherms obtained for the MWNT/Trix buckypapers (Figures 5-10) exhibit that nitrogen adsorption and desorption occur predominantly at  $P/P_o > 0.8$ . The isotherm for the MWNT/Triton-X buckypaper in this study is very comparable to those reported previously for other buckypapers prepared using identical conditions (Rashid et al., 2014). In contrast, the isotherms obtained for the SWNT buckypapers in another study displayed that nitrogen adsorption and desorption occurred at relative pressures ( $P/P_o$ ) below 0.1 can be attributed to the presence of micropores with diameters  $<2$  nm (Sweetman, 2012).

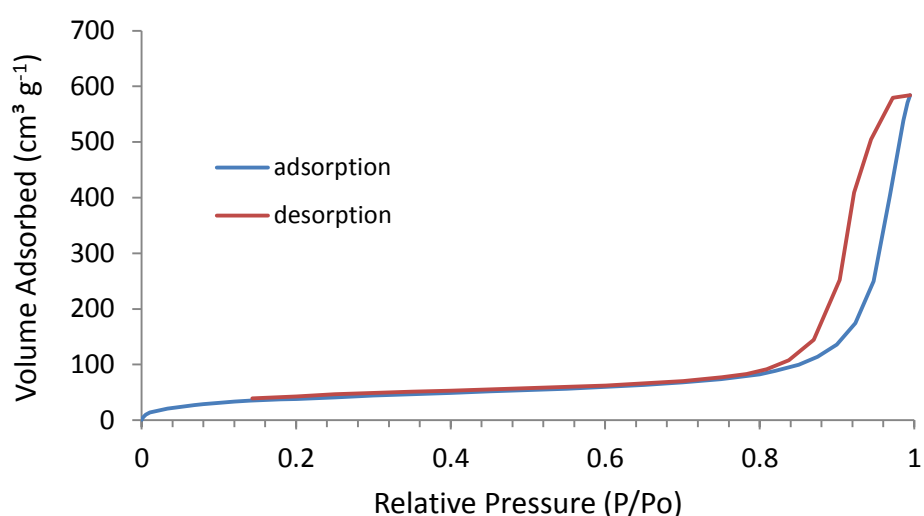


**Figure 5-10:** Nitrogen adsorption (blue)/desorption (red) isotherms for MWNT/Triton X-100.

To investigate the pore structure and surface morphology of MWNT buckypapers, Brunnauer, Emmett and Teller (BET) analysed the results of nitrogen adsorption/desorption measurements. This allowed determination of the specific surface area of the buckypapers and the average pore diameter as well which exists

throughout the samples. Table 5-1 shows surface pore diameter, buckypaper surface area, average internal pore diameter and average nanotube bundle of MWNT buckypapers. If it is assumed that the surface area is related to the outer surface of large CNT bundles, then the bundle diameter ( $D_{bun}$ ) can be calculated using following equation:

$$A_s = \frac{4}{\rho_{CNT} D_{bun}} \quad (5-1)$$

where  $A_s$ ,  $D_{bun}$  and  $\rho_{CNT}$  are the BET surface area, CNT bundle diameter, and nanotube bundle density (estimated as  $1500 \text{ kg/m}^3$ ), respectively (Frizzell et al., 2005).

The Brunnauer, Emmett and Teller (BET) results presented in Table 5-1 display large differences in surface area ( $A_{BET}$ ) and small differences in average internal pore diameter ( $D_{BET}$ ) to those obtained previously for MWNT buckypaper prepared using Triton X-100, which exhibited a surface area of  $300 \text{ m}^2/\text{g}$  and average pore diameter of  $24 \pm 1 \text{ nm}$  (Sweetman et al., 2013). On the other hand, the results obtained for a MWNT/Triton-X buckypaper in this study display a notable difference to those obtained previously for a SWNT/Triton-X buckypaper, which showed a surface area of  $794 \text{ m}^2/\text{g}$  and average internal pore diameter of  $4.0 \pm 0.4 \text{ nm}$  (Sweetman, 2012). The interbundle pore volumes determined for the MWNT buckypaper (86 %) is slightly less than what was measured previously for the corresponding membrane composed of MWNT (prepared under the same conditions) and was (91 %; Sweetman et al., 2013). In contrast, the interbundle pore volumes of SWNT buckypaper studied previously was slightly greater than that found in the current study (85 %; Sweetman, 2012).

**Table 5-1:** <sup>a</sup> $D_{SEM}$  surface pore diameter derived by Image Analysis of SEM micrographs. All other parameters determined through analysis of results obtained from nitrogen adsorption/desorption isotherms, and compared to findings obtained by Sweetman et al. (2013) for the same type.

Buckypaper	$D_{SEM}$ (nm) <sup>a</sup>	$A_{BET}$ (m <sup>2</sup> /g)	$D_{BET}$ (nm)	$D_{bun}$ (nm)	Interbundle pore volume (%)
MWNT/Trix-100	65.6 ± 80	141 ± 2	27.7 ± 2	19 ± 2	86.4 ± 2
MWNT/Trix-100 (Sweetman's findings)	80 ± 20	300 ± 1	24 ± 1	8.8 ± 0.2	91 ± 5

To determine the volume of pores with diameters smaller and larger than 3 nm, MWNT buckypapers were subjected to analysis using the Barrett, Joyner and Halendar (BJH) and Horvath-Kawazoe (HK) methods (Barrett et al., 1951; Horvath and Kawazoe, 1983). Analysis by the HK method gave information on the distribution of small pores (<2 nm) within each of the membranes, whereas the BJH method permitted estimation of the larger pores. Combining the two sets of results produced the pore size distribution profiles shown in Figure 5-11.

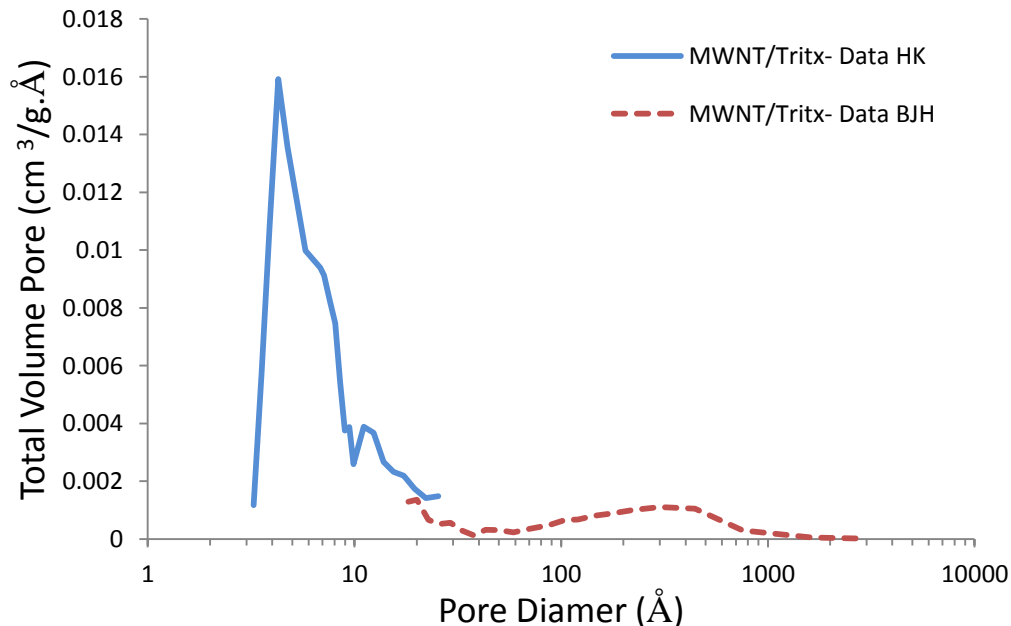


**Figure 5-11:** Pore size distributions for MWNT buckypaper derived by applying the HK method (blue line) and BJH method (brown line) to data obtained from nitrogen adsorption/desorption isotherms.

As seen in Figure 5-11, the large peak ranged between 5 and 10 Å consistent with the channels between CNTs within CNT bundles. In contrast, the second peak was nearly 277 Å consistent with the pores formed between CNT bundles. These results agree well with the average pore diameter calculated using BET and shown in Table 5-1. Numerical combination of curves shown in Figure 5-11 was performed to calculate the average internal pore diameter of the membranes, in addition to the percentage contribution of the interbundle pores to the total free volume. The results of this analysis, along with those obtained by use of the BET method are presented in Table 5-1 (Frizzell et al., 2005).

Numerical integration displays that intertube pores contribute ~14% of the total free volume of the buckypaper. Nevertheless, the pores with a diameter larger than 10 Å are linked to the spaces between bundles. The distribution shows peaks at roughly 2 nm and a small tail out to 1000 nm. As they contribute ~86% of the total free volume, the existence of these pores will have a significant impact on the physical properties of the paper as a whole. These results agree well with the results of a similar study which was conducted by Sweetman et al. (2013) who reported that intertube pores contribute ~12% of the total free volume of the MWNT Triton X-100 buckypaper, whereas interbundle pores contribute ~88% of the total free volume of the buckypaper.

### **5.3.3 Physical properties of MWNT buckypapers**

Physical properties of MWNT buckypapers include the examination of the electrical properties of MWNT buckypapers (e.g. electrical conductivity and resistant of MWNT) and mechanical properties of MWNT buckypapers (e.g. the tensile strength, Young's modulus and ductility).

#### **5.3.3.1 Electrical properties of MWNT buckypapers**

The electrical properties of MWNT buckypapers are important for separation applications through providing an additional means to exhibit selectivity towards



solutes when exposed to an electrochemical potential (Vecitis et al., 2011). The electrical properties are extremely influenced by the filler concentration, the filler morphology (such as particle size and structure) besides filler-filler and filler-matrix interactions which determine the state of dispersion (Bokobza, 2007). The 2-point probe technique explained in section 3.6.2.3 was employed to measure the conductivity of the MWNT buckypapers prepared in this study. The I-V plots obtained for a MWNT buckypaper prepared using Triton X-100 as the dispersant are presented in Figure 5-12. As seen in this figure, the slope of the plots decreased as the length of the strip increased.

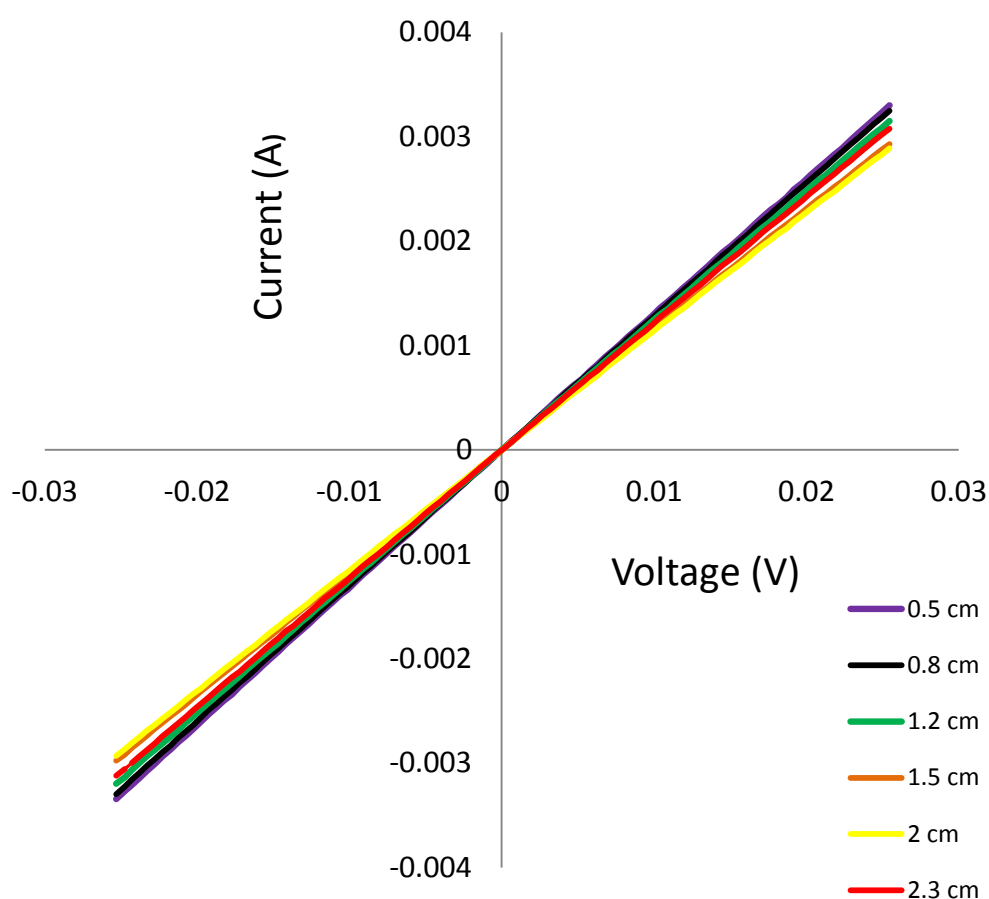


**Figure 5-12:** Current-voltage plots obtained using five different lengths of a strip of gellan gum. The buckypaper was prepared from an 80 mL dispersion using 24 minutes sonication time and filtration through a 0.45  $\mu$ m nylon membrane.

As the inverse of the slope is equal to the resistance, the resistance was found to increase linearly with strip length. This relationship between the resistance and strip

length is presented graphically in Figure 5-13. The resistance in the circuit is described through following equation:

$$R_T = \frac{1}{\sigma A} l + R_C \quad (5-2)$$

Where  $R_T$  is the total resistance ( $\Omega$ ),  $\sigma$  is the bulk conductivity (S/cm),  $A$  is the strip cross-sectional area ( $\text{cm}^2$ ),  $l$  is the length of the strip (cm) and  $R_C$  is the contact resistance ( $\Omega$ ).

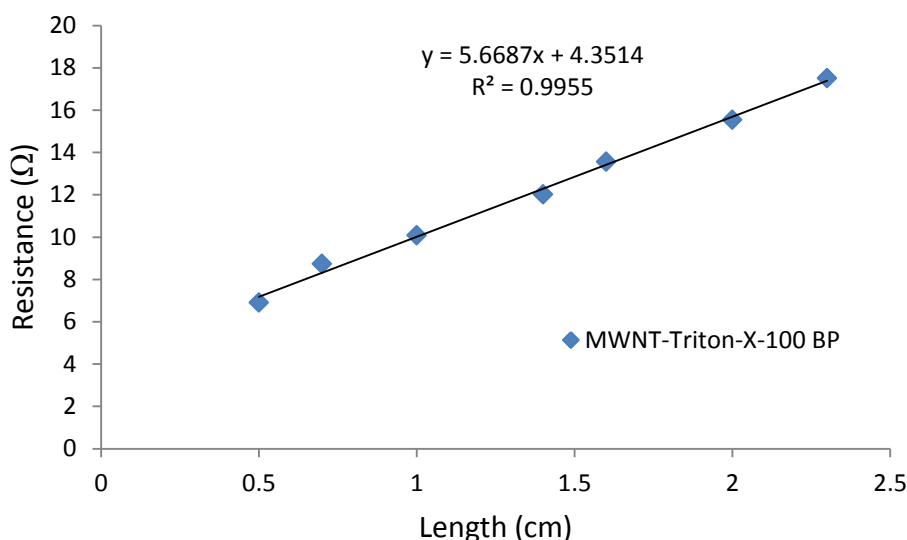


**Figure 5-13:** Effect of length on the resistance of buckypapers prepared from a dispersion containing 0.1% (w/v) MWNT and 1% (w/v) Triton X-100.

Electrical conductivity and resistance of MWNT buckypapers prepared using Triton X-100 are presented in Table 5-2. As shown in Table 5-2, electrical conductivity varies significantly (~56 S/cm) from the reported by Sweetman et al. (2013) for MWNT buckypapers prepared using the same dispersant and prepared using the same conditions to those used here. In fact the average of MWNT/Triton-X buckypapers reported here was approximately double the average conductivity of MWNT/Triton-X buckypapers which were mentioned in Sweetman et al.'s study.

### 5.3.3.2 Mechanical properties of MWNT buckypapers

Mechanical strength is an important property of buckypaper membranes for separation applications because the membrane must be able to survive the application using a wide range of pressures and flow rates (He and Ulbricht, 2006). An examination of the mechanical properties of the MWNT buckypapers was therefore carried out using the tensile test method described in section 3.6.2.4 and these include the tensile strength, Young's modulus and ductility. These properties were determined for MWNT buckypapers prepared using Triton-x-100 dispersant and are shown in Table 5-2.

The values displayed in Table 5-2 vary significantly from those obtained for MWNT buckypapers prepared under the same conditions (Sweetman et al., 2013). For example, the tensile strength, Young's modulus and ductility of a MWNT/Triton X-100 buckypaper prepared in the previous study were  $6 \pm 3$  MPa,  $0.6 \pm 0.3$  GPa and  $1.3 \pm 0.2$  %, respectively.

**Table 5-2:** Physical properties of buckypapers. Values shown are the average of at least 3 samples, with the errors reported determined from the standard deviation obtained from all measurements.

Membrane	Tensile strength (MPa)	Young's modulus (GPa)	Ductility (%)	Thickness ( $\mu\text{m}$ )	Electrical conductivity (S/cm)	Resistant ( $\Omega$ )	Contact angle ( $^\circ$ )
MWNT/Triton X-100	$3.4 \pm 0.8$	$0.4 \pm 0.2$	$2.4 \pm 0.2$	$48 \pm 2$	$56 \pm 3$	$5.4 \pm 0.3$	$50.7 \pm 4$

An elongation and toughness of a MWNT/Triton X-100 buckypaper prepared in this study was  $2.4 \pm 0.2\%$  and  $0.05 \pm 0.01$  MJ/m<sup>3</sup>, respectively. On the other hand, an elongation and toughness of a MWNT/Triton X-100 buckypaper prepared in another previous study were  $8.89 \pm 0.94\%$  and  $0.69 \pm 0.12$  MJ/m<sup>3</sup>, respectively (Han et al., 2014).

### 5.3.4 Hydrophobicity of MWNT buckypapers

To measure the hydrophobicity of material, commonly the contact angle of a water droplet on its surface is used. A data physics SCA goniometer fitted with a digital camera, combined with the data physics software package SCA20.a was used to determine the contact angle of 2  $\mu\text{L}$  water (Milli-Q, Millipore) droplets on the surface of the buckypapers. In the case of measurements performed using water droplets, small contact angles ( $< 90^\circ$ ) indicate that the surface of the material is hydrophilic, whereas large angles ( $> 90^\circ$ ) show that the material is hydrophobic in nature. The contact angles for all MWNTs buckypapers examined in this study were measured using 2  $\mu\text{L}$  water droplets delivered via a syringe, as shown in Figure 5-14.

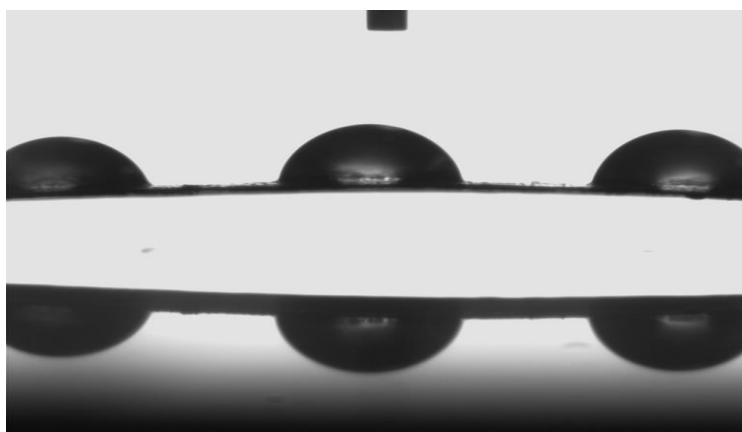


**Figure 5-14:** Images of 2  $\mu\text{L}$  water droplets added to the surface of Buckypaper MWNT/Triton X-100 0.6% w/v, Sonicator time 24min final volume 500 ml.

The mean contact angle of water on MWNT buckypapers calculated based on measurements performed using 5 water droplets is  $51^\circ$ , indicating that their surfaces are in general hydrophilic in nature (Table 5-2). This agrees well with the results of a similar study by Alcock (2010) who reported a water contact angle of  $55^\circ$  for MWNT buckypapers produced from dispersions containing the surfactant Triton-X (Sweetman et al., 2013).

### 5.3.5 Water permeability experiments of MWNT buckypapers

One of the main considerations that should be taken into account when evaluating a potential filtration membrane is its permeability, particularly towards water. Consequently the first objective of this stage of this study was to quantify the permeability of MWNT buckypapers made with Triton-x-100. The second objective was to compare the measured permeability in this study with previous studies which were conducted by (Alcock, 2010; Wise, 2011). To achieving this, small buckypapers were examined as described in section 3.5.2.2. Each buckypaper studied became permeable to water after around 14 kPa of positive pressure was applied. The flux of water across all buckypapers usually looks like that shown in Figure 5-15 with a linear correlation between the mass of permeate and time being observed.

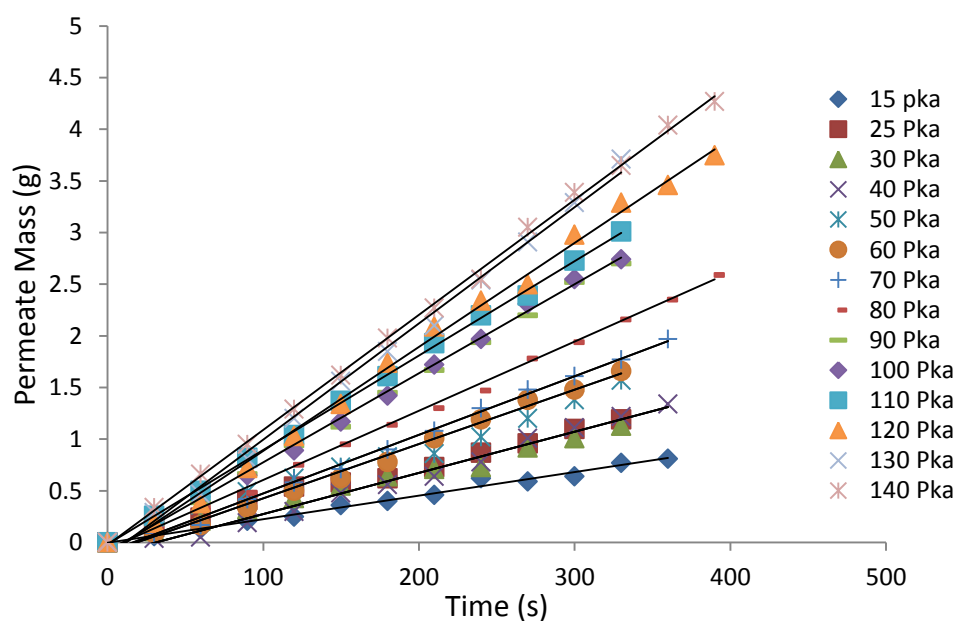


**Figure 5-15:** Effect of pressure on the mass of water permeating across a MWNT/Triton X-100 buckypaper. The slopes of the individual plots give the permeation flux. Data for only selected pressures are shown.

The permeate flux was noticed to increase for all buckypapers as a function of applied pressure until membrane rupture occurred. The slopes of the lines shown in Figure 5-15 were then plotted as a function of the applied pressure to provide the

graph shown in Figure 5-16. From the resulting linear plot the membrane flux was calculated from the slope, after correcting for the actual filtration area. This yielded a flux of  $23 \text{ L m}^{-2} \text{ h}^{-1} \text{ bar}^{-1}$  for MWNT/Triton-x-100 buckypaper. The membrane flux of the MWNT buckypaper prepared in this study is presented in Table 5-3, along with the membrane fluxes obtained Alcock (2010) and Wise (2011) for the same type of buckypaper for comparison.

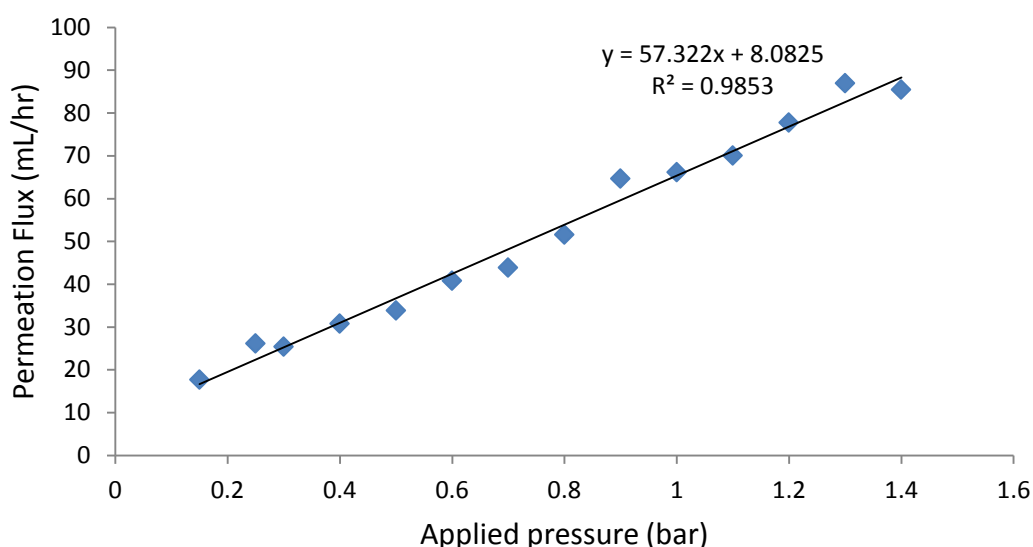


**Figure 5-16:** Effect of applied pressure on the permeation flux of a MWNT/Triton-X buckypaper.

**Table 5-3:** Average membrane fluxes determined for MWNT/Triton X-100 compared to the average membrane fluxes obtained by Alcock (2010) and Wise (2011) for the same type.

Buckypaper	Average flux ( $\text{L m}^{-2} \text{ h}^{-1} \text{ bar}^{-1}$ )	Alcock's average flux ( $\text{L m}^{-2} \text{ h}^{-1} \text{ bar}^{-1}$ )	Anthony's average flux ( $\text{L m}^{-2} \text{ h}^{-1} \text{ bar}^{-1}$ )
MWNT-Triton-x-100	$22.9 \pm 0.14$	$22.4 \pm 6.3$	$22 \pm 6$

### 5.3.6 Removal of organic contaminants by MWNT buckypaper membrane

The results from in the previous section (5.3.6) prove a significant degree of permeability towards water for buckypapers prepared using MWNTs. To investigate

the potential of these materials for filtration applications, it is essential to determine whether they exhibit any selectivity in their permeability towards dissolved solutes. It is noteworthy that only a few studies performed previously have used buckypapers prepared from MWNTs. Thus, as a first step towards remedying this situation, many experiments were conducted for samples collected from EWB10D and EWB13D at Southlands Botany Bay to assess the ability of MWNT/Triton X-100 buckypapers to remove VOCs from contaminated groundwater. Permeate and feed samples of 40 mL were collected before and after 8 hours of filtration to analyse for VOCs.

#### 5.3.6.1 EWB10D at Southlands Botany Bay

The removal efficiency of MWNT buckypaper membrane for EWB10D is reported in Table 5-4 and Figure 5-17. Because of strong van der Waals interactions, MWNT adhere to each other and form bundles, and the space between the bundles can be considered as pores, which provided more adsorption sites. Consequently, MWNT exhibited higher adsorption efficiency for VOCs to some extent, however it still less than the efficiency of NF-90 and ESPA2 membranes in rejecting VOCs (see chapter 4). It was remarkable that the performance of MWNT buckypaper membranes in rejecting hydrophilic compounds [(Log  $D$  >2.5), carbon tetrachloride, trichloroethylene and tetrachloroethylene] was higher than hydrophobic compounds [(Log  $D$  <2.5), other VOCs which are demonstrated in Table 5-4]. According to Nghiem et al. (2004b) the removal of some hydrophobic compounds can be really lower than that predicted based only on a steric hindrance transport model. It can be explained that hydrophobic compounds can adsorb on a MWNT membrane and then diffuse through the bundles, resulting in significant transport of these compounds across the bundles and the space between the bundles which can be considered as pores. On the other hand, because hydrophilic compounds do not absorb to the MWNT membrane, hydrophilic VOCs can be effectively rejected by MWNT membranes using size exclusion mechanism or through the non-electrostatic interactions which include hydrophobic interactions and hydrogen bonding. These results also support the findings from other previous studies (Moreno-Castilla, 2004; Agenson and Urase, 2007).

It is notable that the highest rejection achieved by a MWNT buckypaper membrane was for tetrachloroethylene and it reached 88.5 % whereas the lowest rejection achieved by MWNT buckypaper membrane was for 1,1,2-trichloroethane and has amounted to 27.6 %. According to (Wells, 2006) tetrachloroethylene has the highest Log *D* of the model foulants (3.07) and consequently it is considered to be a hydrophilic compound and it can be effectively rejected by a MWNT buckypaper membrane using steric hindrance or size exclusion mechanisms, while the Log *D* of 1,1,2-trichloroethane was (1.92) and it is classified hydrophobic compound and it can adsorb onto a MWNT buckypaper membrane and then diffuse through the bundles, resulting in the lower removal for this compound compared to tetrachloroethylene.

**Table 5-4:** Overall removal efficiency of the selected volatile organic compounds (VOCs) which were detected in EWB10D at Sutherland-Botany Bay.

Compound Name	Rejection @ 8hr-MWNT (%)
Vinyl Chloride	69.2
1,1-Dichloroethene	75.0
Dichloromethane	62.5
trans-1,2-Dichloroethene	82.4
1,1-Dichloroethane	66.0
cis-1,2-Dichloroethene	67.4
Chloroform	61.1
1,1,1-Trichloroethane	40.0
Carbon tetrachloride	87.8
1,2-Dichloroethane	45.5
Benzene	70.0
Trichloroethylene	82.6
1,1,2-Trichloroethane	39.1
Tetrachloroethylene	88.5
Chlorobenzene	60.0
1,1,2,2-Tetrachloroethane	45.0
Hexachlorobutadiene	50.0



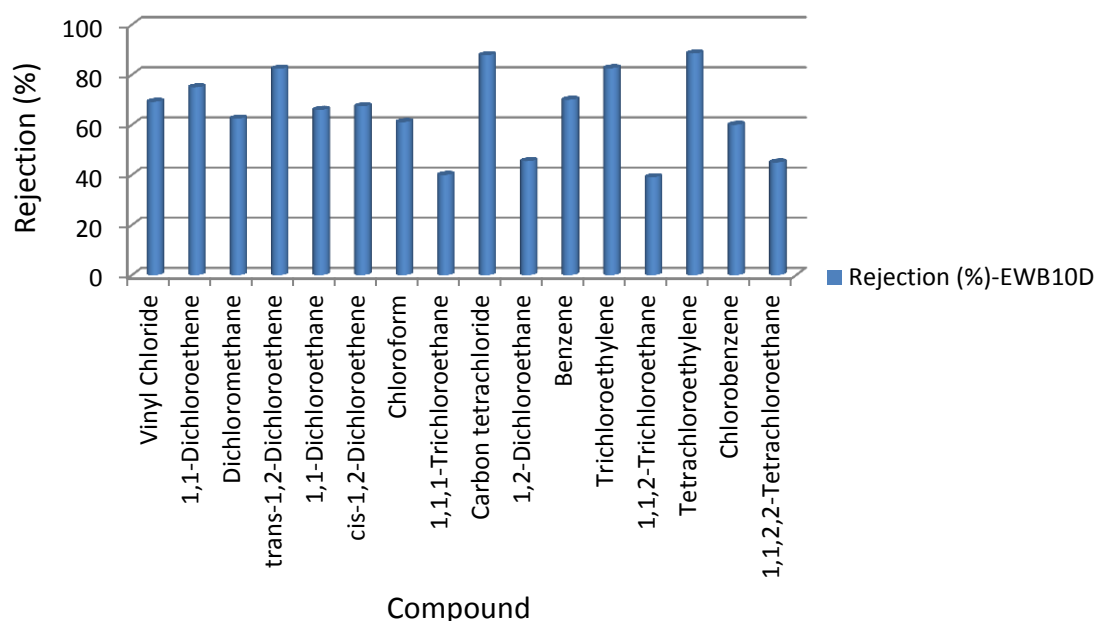


**Figure 5-17:** Overall removal efficiency of the selected VOCs which were detected in contaminated groundwater at EWB10D. MWNT/Triton X-100 buckypaper membrane filtration experiment was conducted at 140 Kpa. Samples were collected after 8 hours of filtration.

#### 5.3.6.2 EWB13D at Southlands Botany Bay

The removal efficiency of the MWNT buckypaper membrane for EWB13D is reported in Table 5-5 and Figure 5-18. It is clear that the removal efficiency of MWNT here is less than its efficiency when used to retain the VOCs detected in EWB10D site. The results presented in Table 5-5 and Figure 5-18 confirm the results given 5.3.3.1; nevertheless there are some differences between them based on the difference in concentrations of model foulants at this site from the previous site (EWB10D). It was noteworthy that the performance of the MWNT buckypaper membrane in rejecting hydrophilic compounds (tetrachloroethylene, carbon tetrachloride, trichloroethylene and trichloroethylene) was higher than hydrophobic compounds (other VOCs which are shown in Table 5-5). The reason for this phenomenon has been explained above in part 5.3.3.1 (Nghiem et al., 2004b).

The highest rejection achieved by a MWNT buckypaper membrane was for tetrachloroethylene and has reached 77.3 % whereas the lowest rejection achieved by MWNT buckypaper membrane was for 1,2-dichloroethane and has reached 33.1 %. It can be elucidated that tetrachloroethylene has the highest Log  $D$  of the model foulants (3.07) and thus it is classified as a hydrophilic compound and it can be effectively rejected by a MWNT buckypaper membrane using size exclusion mechanisms or through the non-electrostatic interactions which include hydrophobic interactions and hydrogen bonding, while the Log  $D$  of 1,2-Dichloroethane was only (1.65) and it is considered to be a hydrophobic compound and it can adsorb onto the MWNT buckypaper membrane and then diffuse through the bundles, resulting in the lower removal for this compound compared to tetrachloroethylene (Wells, 2006).

Lastly, it is observed that the rejection for VOCs at both sites EWB10D and EWB13D doesn't reach as high a value after using a MWNT membrane compared to NF-90 and ESPA2 membranes (chapter 4, sections 4.3.2.1 and 4.3.2.2). This can be attributed to the pore diameter of MWNT ( $24 \pm 1$ ) which is large and consequently allows some contaminants to pass through the MWNT membrane. Remarkably, the small and precise diameter size of CNTs is demonstrated to reject most ions because of the energy barrier present at the channel entries and therefore only water molecules are allowed to pass through the nanotube hollows (Corry, 2008; Das et al., 2014).

**Table 5-5:** Overall removal efficiency of the selected organic compounds (VOCs) which were detected in EWB13D at Sutherland Botany Bay.

Compound Name	Rejection @ 8hr-MWNT (%)
Vinyl Chloride	66.7
1,1-Dichloroethane	50.0
cis-1,2-Dichloroethene	57.1
Chloroform	45.8
Carbon tetrachloride	75.0
1,2-Dichloroethane	33.1
Benzene	50.0
Trichloroethylene	74.2
1,1,2-Trichloroethane	40.0
Tetrachloroethylene	77.3
1,1,2,2-Tetrachloroethane	33.3

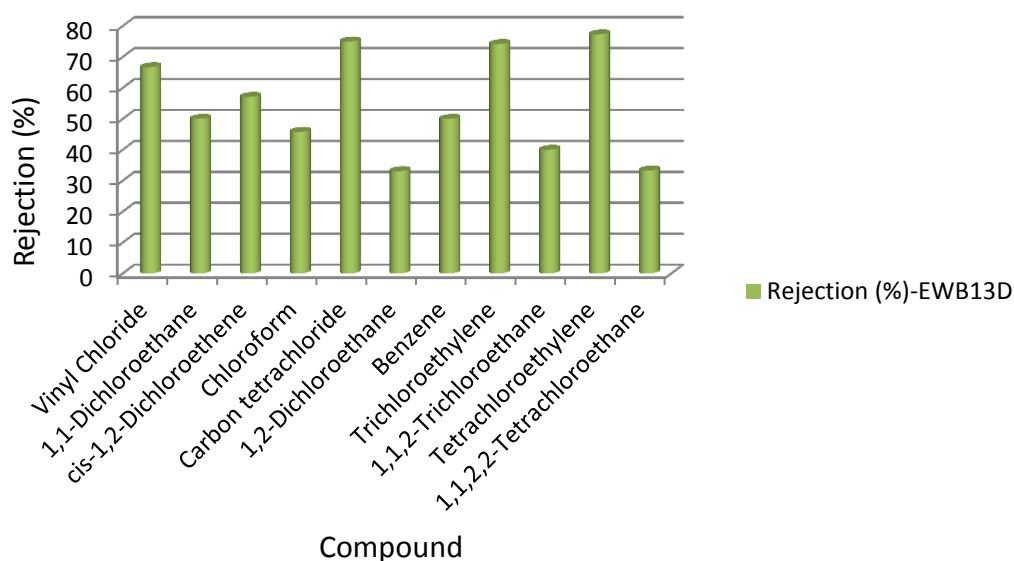


**Figure 5-18:** Overall removal efficiency of the selected VOCs which were detected in contaminated groundwater at EWB13D. MWNT-Triton-X-100 buckypaper membrane filtration experiment was conducted at 140 Kpa. Samples were collected after 8 hours of filtration.

### **5.3.7 Performance of MWNT buckypaper membrane**

To examine the performance of MWNT buckypaper membranes, it is essential to study the membranes permeate flux as a function of filtration time for samples that were collected from two different sites (EWB10D and EWB13D) at Southlands Botany Bay and presented contaminated groundwater.

#### **5.3.7.1 EWB10D at Southlands-Botany Bay**

Figure 5-19 displays the evolution of the membrane permeate flux as a function of filtration time. As seen in this figure, it is observed that flux was excellent during use of a MWNT buckypaper and this is illustrated clearly by the continued linear and constant flux throughout the duration of the experiment. It can be explained that samples at this site were collected from wells and this means that the colloidal and suspended substances existing in these waters were few and as a result gave a high efficiency for this membrane. Another reason for explaining this phenomenon is the critical pore diameter of CNTs. Many previous studies indicate that there is a critical pore diameter of  $\sim 7 \text{ \AA}$  (0.7 nm), above which ions and water will pass but below which they will not (Beckstein et al., 2003; Anishkin and Sukharev, 2004; Beckstein and Sansom, 2004; Corry, 2006). Particularly, the pore diameter of MWNT in this study was above  $7 \text{ \AA}$  ( $\sim 28 \text{ nm}$ ) and that means the MWNT passed water and some contaminants according to this theory. Furthermore, the results in Figure 5-19 revealed that the value of flux was high, linear and stable when a MWNT buckypaper was used as a membrane and ranged between  $\sim 115\text{-}118 \text{ L.m}^2\text{.h}$ . Compared to NF-90 and ESPA2 membranes, the flux was roughly half the flux of MWNT membrane and ranged between  $\sim 35\text{-}52.6 \text{ L.m}^2\text{.h}$  (in case of NF-90 membrane) and  $\sim 51.7\text{-}52.6 \text{ L.m}^2\text{.h}$  (in case of ESPA2 membrane). It can be explained by the porosity of MWNT membrane ( $\sim 28 \text{ nm}$ ) being greater than the porosity of the NF-90 and ESPA2 membranes (0.68 nm and non-porous respectively) and this also confirms what has been inferred above.

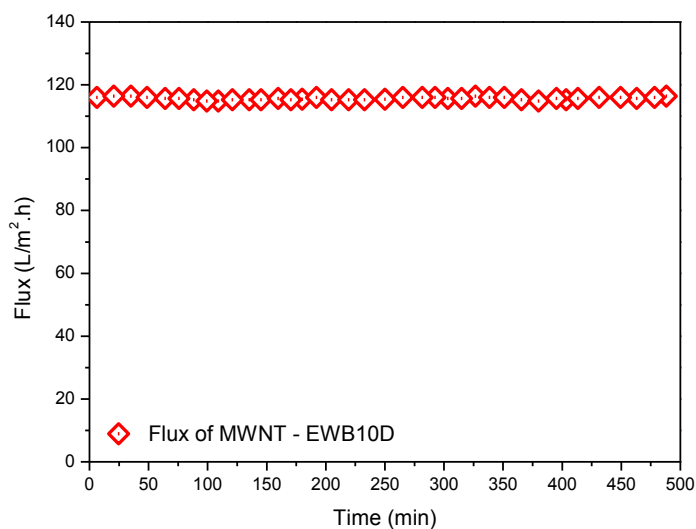


**Figure 5-19:** Permeate flux of MWNT buckypaper membrane as a function of filtration time. Experiment was conducted at 140 Kpa. Samples were collected after 8 hours of filtration.

#### 5.3.7.2 EWB13D at Southlands-Botany Bay

Figure 5-20 shows the evolution of the membrane permeate flux as a function of filtration time for EWB13D. The findings shown in Figure 5-20 confirm the results concluded above (part 5.3.7.1). Also here it is observed that the flux was exceptional during the use of the MWNT buckypaper and this is demonstrated clearly by the continued linear and constant flux during filtration time and this has been explained in detail in the previous section. Additionally, the results in Figure 5-20 revealed that the flux was high, linear and stable when we used MWNT buckypaper as a membrane and ranged between  $\sim 116$ - $119 \text{ L.m}^2.\text{h}$ . In contrast, the flux was somewhat lower and not stable when NF-90 and ESPA2 were used as membranes to separate VOCs from contaminated samples and ranged between  $\sim 27$ - $52.6 \text{ L.m}^2.\text{h}$  and  $\sim 45$ - $52.6 \text{ L.m}^2.\text{h}$ , respectively (chapter 4, parts 4.3.3.1 and 4.3.3.2). This can be attributed to the fact that the porosity of MWNT membrane was high (28 nm) compared to the porosities of the NF-90 and ESPA2 membranes which were low (0.68 nm and non-porous respectively). This is fully consistent with many previous studies, which sees pore size of the membrane playing a significant role in determining the membrane

performance, in particular the flux (Košutić et al., 2000; Corry, 2008; Goh et al., 2013).

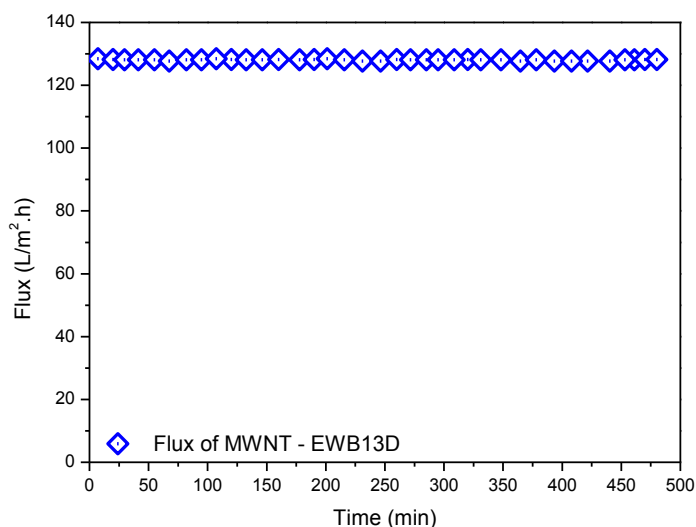


**Figure 5-20:** Permeate flux of MWNT buckypaper membrane as a function of filtration time. Experiment was conducted at 140 Kpa. Samples were collected after 8 hours of filtration.

## 5.4 Conclusion

In this study, the morphological, electrical and mechanical properties of MWNT buckypapers were determined and the feasibility of using these buckypapers as possible filtration membrane materials was evaluated. Results reported in this study indicate that MWNT exhibited higher adsorption efficiency for VOCs to some extent, nevertheless it still less than the efficiency of NF-90 and ESPA2 membranes in rejecting VOCs. It was noteworthy that the performance of MWNT buckypaper membranes in rejecting hydrophilic compounds (carbon tetrachloride, trichloroethylene and tetrachloroethylene) was higher than hydrophobic compounds (other VOCs which are examined in this study). This is because hydrophobic compounds can adsorb onto MWNT membranes and then diffuse through the bundles, causing significant transport of these compounds across the bundles and the space between the bundles which can be considered as pores. Conversely, because hydrophilic compounds do not absorb to the MWNT membrane, hydrophilic VOCs

can be effectively rejected by a MWNT membrane using size the exclusion mechanisms or through the non-electrostatic interactions which include hydrophobic interactions and hydrogen bonding. The results in this study revealed that the highest value of rejection was for tetrachloroethylene and has reached 88.5 % while the lowest rejection achieved by MWNT buckypaper membrane was for 1,1,2-trichloroethane and has amounted 27.6 % and these values depend on the hydrophobicity and hydrophilicity of the compounds.

## **CHAPTER 6: THE REMOVAL OF INORGANIC CONTAMINANTS BY USING NF/RO FILTRATION SYSTEM**

### **6.1 Introduction**

In recent years, the occurrence and fate of inorganic contaminants in the aquatic environment has been recognized as a significant issue of concern (Ortega et al., 2008; Richards et al., 2011). Although there is full agreement between the scientific community and the water authorities to minimize inorganic contaminants, there is also an urgent need to make further efforts to protect water sources from these contaminants using optimized removal during water treatment processes. Recent trends towards reuse of reclaimed surface and groundwater for many purposes, in particular for agricultural and industrial sectors, encourages use of effective treatment to remove inorganic contaminants from contaminated water. During the last decades, numerous technologies have presented innovative solutions to the surface and groundwater contamination issue. For example, inorganic effluent can be removed by conventional treatment processes such as chemical precipitation, ion exchange and electrochemical removal (Barakat, 2010). However, it is well known that these technologies are inadequate to remove and reduce all the inorganic contaminants to acceptable regulatory standards. Hence, there has been a growing interest during the last decade, for effective treatments such as membrane filtration (reverse osmosis [RO], nanofiltration [NF], ultrafiltration [UF] and microfiltration [MF]; Ortega et al., 2008).

Nowadays, RO and NF membranes have become the leading technologies to treat numerous surface, well, brackish, urban and sea waters to produce fresh water (Nicolaisen, 2003; Bottino et al., 2009; Norton-Brandão et al., 2013). NF/RO is able to remove several inorganic contaminants (such as arsenic, calcium, chloride, copper, fluoride, magnesium, manganese, nickel, nitrate, potassium, selenium, sodium, strontium, sulphate and zinc), which can be undesirable when above guideline standards for both health and aesthetic reasons (Sungyun et al., 2008; Richards et al., 2011; Alzahrani et al., 2013a).



Several studies have revealed that the separation of inorganic contaminants is affected by the compound's physicochemical properties and the membrane properties, as well as the solution chemistry (Nghiem and Coleman, 2008; Watson et al., 2012). The separation of salts and inorganic contaminants is mostly attributed to size exclusion as well as Donnan exclusion (charge repulsion mechanism; Yaroshchuk, 2001; Teixeira et al., 2005; Verliefde et al., 2008; Bolong et al., 2009). However, ionic permeation studies show that ionic size alone does not explain the rejection characteristics of ions during membrane filtration processes (Tansel et al., 2009). In the electrostatic repulsion mechanism, the rejection depends on relative charge interaction and not only on molecule size. Thus, electrostatic interactions between charged solutes and the charged membrane surface can also play a role in the rejection (Richards et al., 2011). Moreover, it has been established that hydrophobic solutes can adsorb onto membrane surfaces and subsequently may diffuse through RO and particularly NF membranes, causing lower rejections than would be expected based solely on size exclusion mechanisms (Nghiem and Schäfer, 2002; Braeken et al., 2005). On the other hand, ion transport is considerably affected by hydrated radii and hydration strength because size variations can determine which ions are capable of passing through the membrane pores by means of convection or diffusion. Ions with comparatively smaller ionic radii (i.e.,  $\text{Mg}^{2+}$  and  $\text{Ca}^{2+}$ ) have higher charge, higher hydration numbers, larger hydrated radii, and hold hydration shells more strongly. In contrast, ions with larger ionic radii (i.e.,  $\text{K}^{+}$  and  $\text{Na}^{+}$ ) have weaker hydration shells and smaller hydrated radii, and hence may be capable of separating from their hydration layer when passing through the membrane (Tansel et al., 2006).

The aim of this study was to examine the removal of inorganic contaminants by using NF/RO filtration system. Experiments were conducted using a laboratory-scale experiment with two commercially available NF/RO membranes. Ten inorganic compounds with molecular weights of less than 100 g/mol and a wide range of ionic and hydrated radii were selected as model inorganic contaminants due to their widespread occurrence in surface and groundwater. Removal efficiency by NF/RO filtration was linked to the physicochemical properties of these compounds to focus

on the ability and effectiveness of this kind of treatment. Significant characterization work has been conducted to investigate the NF/RO membranes.

## **6.2 Materials and methods**

Detailed descriptions of the NF/RO set-up, operation protocol, and analytical techniques have been provided in chapter 3. Before use, contaminated surface and groundwater samples were collected from a leachate pond at Russell Vale and WGB32 at Botany Bay. They were filtered using Stericup Durapore™ 0.45 µm (Millipore) for separation of colloidal and suspended materials. Subsequent steps used 8 L of filtered samples as a feed solution for each experiment. The NF/RO filtration system was operated for 8 hours in each experiment to collect an adequate amount of permeate which was analysed to determine the removal efficiency of this system. In this chapter, the obtained data is systematically analysed to assess the overall performance of the NF/RO system.

### **6.2.1 Model inorganic contaminants**

Ten compounds were chosen for this study to represent two major inorganic groups of concern in surface and groundwater samples – namely cations (e.g. mercury, sodium and calcium) and anions (e.g. chloride, nitrate and sulphate). The selection of these model inorganic compounds was also based on their widespread occurrence in aquatic resources and their diverse physicochemical properties (e.g. molecular weight, ionic hydrated radii and hydrophobicity). The main physicochemical properties of these inorganic constituents are shown in chapter 3 (Table 3-4). The selected inorganic contaminants include compounds with molecular weights in the range between 22.99 g/mol (paracetamol) and 96.06 g/mol. The retention of these compounds correlated with both charge and hydrated size. Therefore, multivalent ions with large hydrated radii (i.e.  $\text{Ca}^{2+}$ , and  $\text{SO}_4^{2-}$ ) were retained more than monovalent ions with smaller hydrated radii (i.e.  $\text{Cl}^-$ ,  $\text{K}^+$  and  $\text{Na}^+$ ; Richards et al., 2011). Additionally, the quantity of charge on the surface of the membrane impacts

the degree of electrostatic repulsion and removal of negatively charged solutes (Xu et al., 2005).

## **6.3 Results and discussion**

### **6.3.1 Characterization of NF-90 and ESPA2 membranes**

Surface roughness morphology, contact angle analysis and zeta potential analysis were examined and presented in chapter 4. The following part will be focused on SEM-EDS analysis for the NF-90 and ESPA2 membranes before and after being used to investigate the removal of inorganic contaminants from samples collected from a leachate pond at Russell Vale and WGB32 at Botany Bay.

#### **6.3.1.1 SEM-EDS analysis**

The clean and fouled membranes were visually characterised with scanning electron microscopy (SEM) using a JEOL JSM-7500FA - (BRUKER-QUANTAX 400). On the other hand, the elemental analysis was determined using an integrated energy-dispersive spectrometer (EDS). To visualize the fouling effects, SEM images of the membrane surfaces were taken before and after fouling, as demonstrated in Figures 6-1 and 6-2 for the ESPA2 and NF-90 membranes respectively. Due to the roughness of NF and RO membranes, after filtration the colloids are located principally in the valleys on the surface; i.e. “valley clogging” has taken place (Vrijenhoek et al., 2001; Hoek et al., 2003). However, the colloids are also distributed over the entire membrane surface and formed a dense and uniform cake layer on the membrane surface as a result of hydrophobic interactions between the foulants and the membrane surfaces (Brant and Childress, 2002; Boussu et al., 2007).

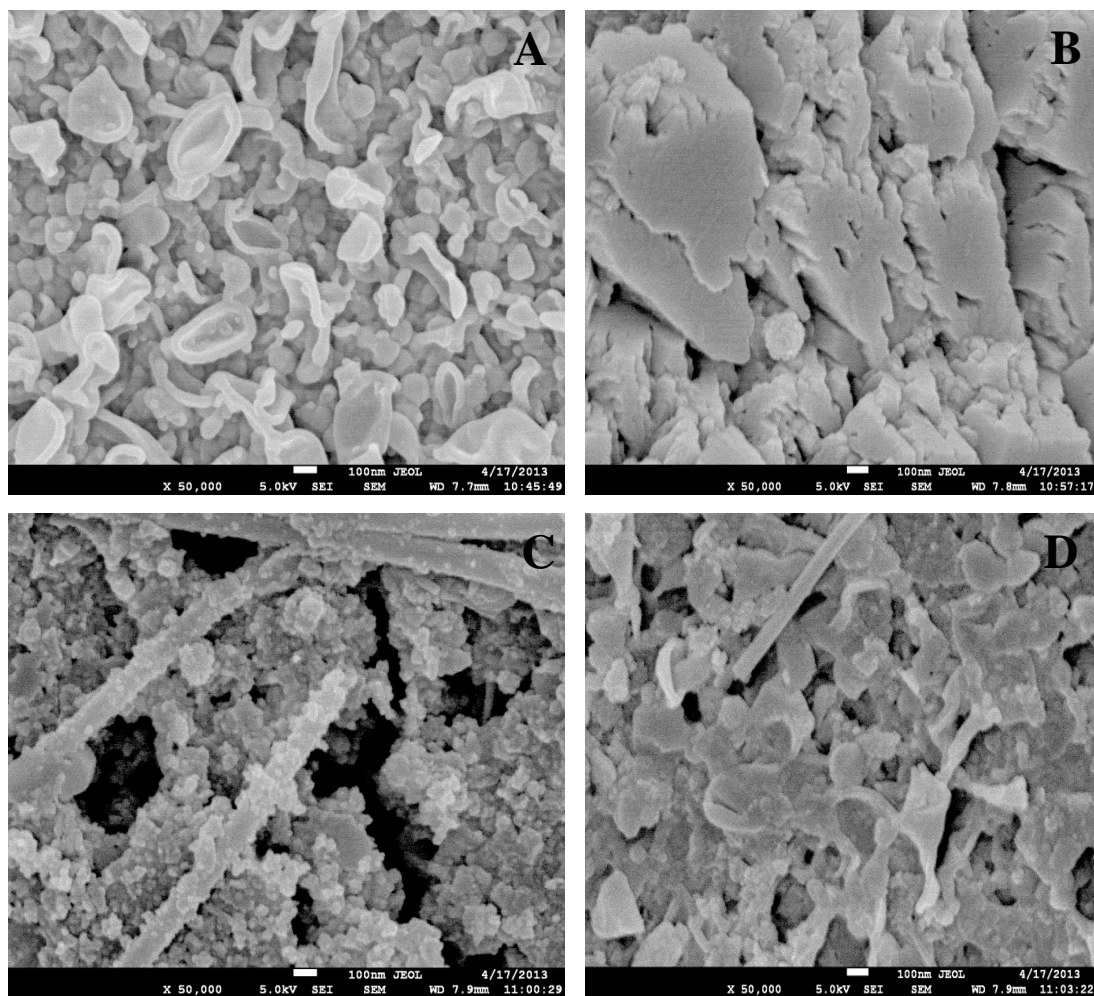


**Figure 6-1:** SEM images of the (A) virgin ESPA2 membrane, (B) ESPA2 membrane surface fouled by leachate pond-autumn, (C) ESPA2 membrane surface fouled by WGB32-spring and (D) ESPA2 membrane surface fouled by WGB32-winter.

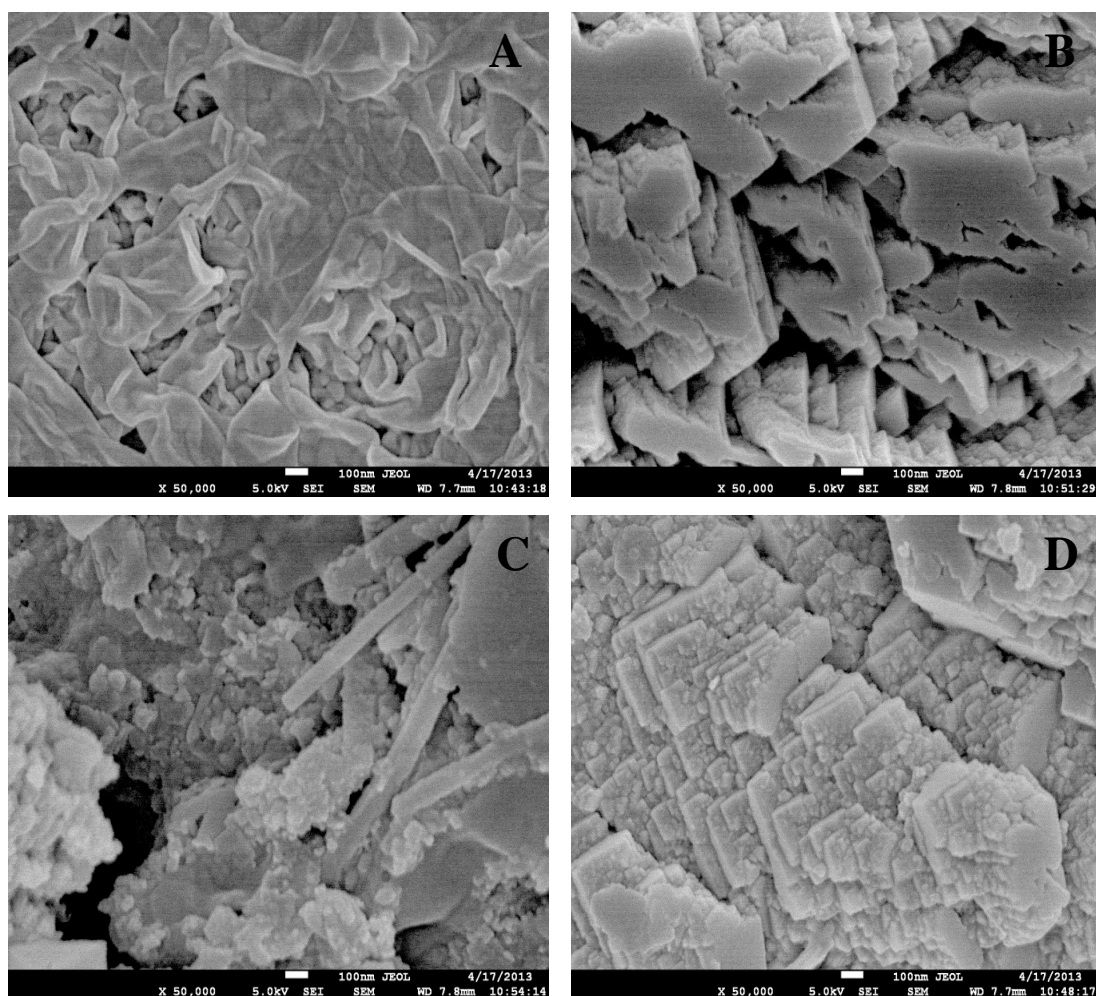


**Figure 6-2:** SEM images of the (A) virgin NF-90 membrane, (B) NF-90 membrane surface fouled by leachate pond-autumn, (C) NF-90 membrane surface fouled by WGB32-spring and (D) NF-90 membrane surface fouled by leachate pond-summer.

Distribution of elements deposited in the fouling layer on the membrane surface was obtained from SEM with additional semi-quantitative energy dispersive spectrometer (EDS) analysis. An example of SEM-EDS images obtained for the ESPA and NF-90 virgin and fouled membranes is shown in Figures 6-3 and 6-4. In addition to the model foulants, carbon, oxygen and sulphur from parts of the membrane polymeric composition and therefore were detected in all samples, including the virgin membrane. Noteworthy, platinum existed in all samples, including the virgin membrane as a result of membrane coating. A high level of calcium was found in the alginate fouling layer (Figures 6-3B-2, 6-3B-3, 6-4B-2 and 6-4B-3) due to the ability of calcium to complex with carboxyl groups which are very common in

organic foulants in addition to the surface of NF/RO membranes (Mo et al., 2011). This result is consistent with previous studies that calcium could make cross-links with alginate molecules and accumulate in the alginate fouling layer (Lee et al., 2006; Li et al., 2007; Antony et al., 2012). Specifically, a sulphur peak was observed with contaminated samples which were collected from WGB32 at Botany Bay indicating the participation of sulphate scale in fouling (see Figures 6-4B-2 and 6-4B-3). Small silicon and aluminium peaks were noticed with membrane surfaces fouled by WGB32-Spring (Figure 6-4B-3) indicating their high scaling tendency even when present in a small amount. Additionally, a small level of sodium and chlorine was found in the alginate fouling layer (Figures 6-4B2 and 6-4B-3). It can be explained by the deposition of foulants (Si, Al, Na and Cl) on the membranes caused by the increase in membrane selectivity due to biofouling (Melián-Martel et al., 2012).

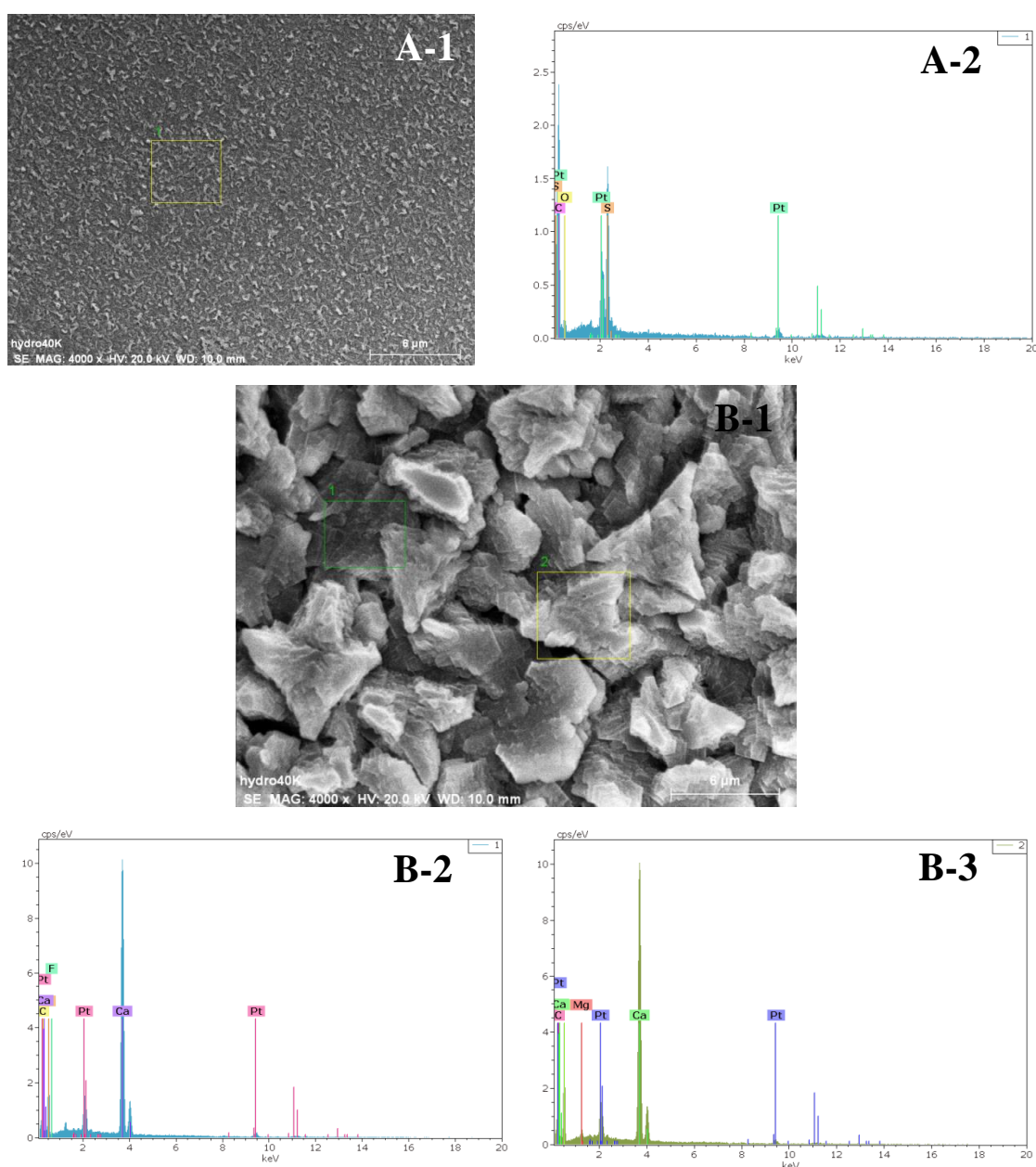


**Figure 6-3:** EDS data of the virgin ESPA2 membrane (A-1 and A-2) and ESPA2 membrane fouled by leachate pond at Russell Vale-autumn (B-1, B-2 and B-3).

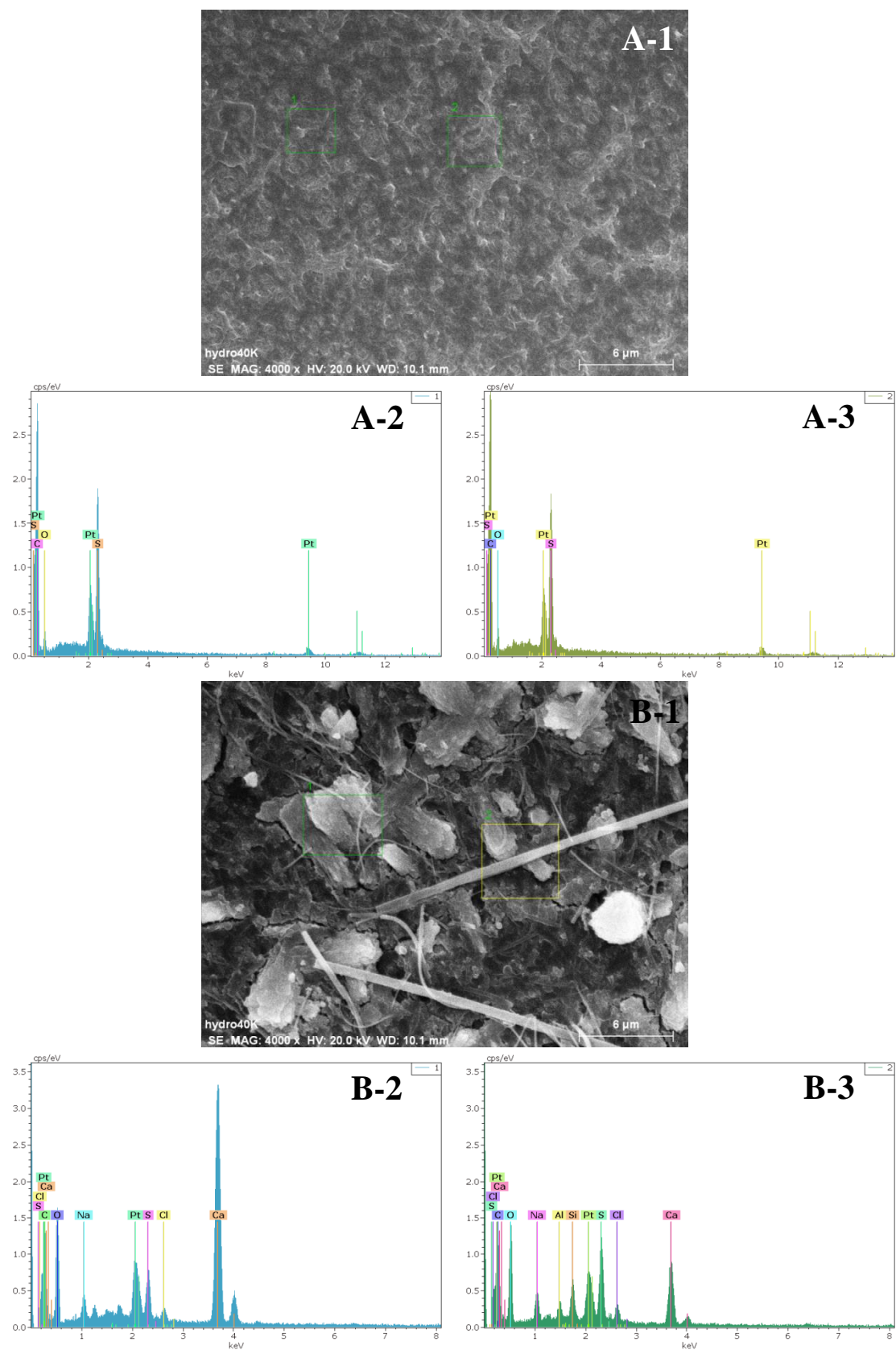


**Figure 6-4:** EDS data of virgin NF-90 membrane (A-1, A-2 and A-3) and NF-90 membrane fouled by WGB32 at Botany Bay-spring (B-1, B-2 and B-3).



### **6.3.2 Removal of inorganic contaminants by the NF/RO system**

To examine the ability of the NF/RO membranes to remove inorganic contaminants from contaminated surface and groundwater, many experiments were conducted at difference seasons for samples collected from a leachate pond at Russell Vale Golf Course and WGB32 at Botany Bay.

#### **6.3.2.1 Leachate pond at Russell Vale Golf Course**

Contaminated surface water is represented by samples collected from a leachate pond at Russell Vale Golf Course during 2012 for four seasons. The removal efficiency for both NF-90 and ESPA2 membranes are reported in Figure 6-5. The findings in Figure 6-5 showed that the performance of the NF-90 and ESPA2 membranes after 8 hours was better than after one hour. Further, it was observed that the ESPA2 membrane has a higher capability than the NF-90 membrane for rejecting cations and anions. Moreover, it was notable that the performance of the NF-90 and ESPA2 membranes in rejecting divalent ions was higher than that of its monovalent ion rejection and this is consistent with the findings from previous studies (Liikanen et al., 2003; Alzahrani et al., 2013a; Antony et al., 2012). This phenomenon can be explained since multivalent ions with large hydrated radii (e.g.  $Mg^{2+}$ ,  $Ca^{2+}$  and  $SO_4^{2-}$ ) were retained more than monovalent ions with smaller hydrated radii (e.g.  $K^+$  and  $Na^+$ ; Richards et al., 2011). The removal efficiency of the NF-90 membrane ranged between 85.9 and 98.3 % for cations, compared with anions, which showed a slightly lower rejection ranging from 71.4 to 99.2 %. In contrast, the removal efficiency of the ESPA2 membrane ranged between 94.1 and 98.4 % for cations while anion rejection ranged between 89.5 and 99.7 %. It is noteworthy that the highest rejection achieved by both NF-90 and ESPA2 was for sulphate that reached 99.7% while the lowest rejection achieved by both NF-90 and ESPA2 was for bromide which amounted to 71.4 %. Also, as seen in Figure 6-5 the performance of the NF-90 and ESPA2 membranes in rejecting the model foulants was high in all seasons except for the summer season in particular when the NF-90 was fouled by algal suspensions.

This can be explained since the higher temperature during summer season participates significantly in the growth of algae booms (Babel et al., 2002). Algae can release extracellular organic matter (EOM). This extracellular, mucilaginous slime material can raise resistance to filtration (Kwon et al., 2005). It has been observed that characteristics of EOM could significantly influence the specific cake resistance developed in membrane filtration (Babel et al., 2002).

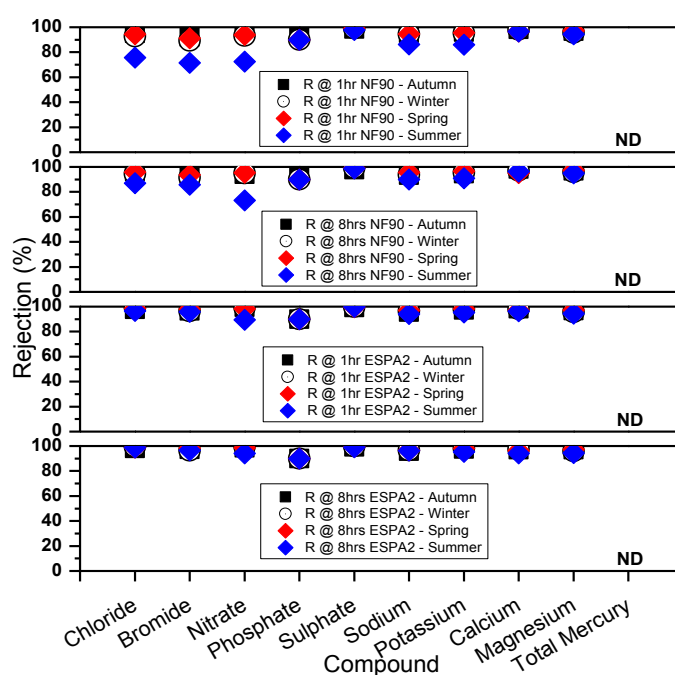


**Figure 6-5:** Overall removal efficiency of the selected inorganic compounds which were detected in contaminated surface water at Russell Vale. NF/RO membrane filtration experiment was conducted at an initial permeate flux of 41 L/m<sup>2</sup>h at a temperature of 20 °C and a cross-flow velocity of 30.4 cm/s. Samples were collected after 1 and 8 hours of filtration.

### 6.3.2.2 WGB32 at Botany Bay

Contaminated groundwater is represented by samples collected from Orica (Botany Bay) in the Sydney area during 2012 for four seasons. An overall comparison of NF-90 and ESPA2 membrane performances in terms of removal efficiency is presented in Figure 6-6. The results from Figure 6-6 exhibited that the performance of the NF-90 and ESPA2 membranes after 8 hours was better than after one hour. Moreover, it

was noteworthy that the performance of the NF-90 and ESPA2 membranes in rejecting multivalent ions was higher than that of its monovalent ion rejection in particular for sulphate. This is consistent with both the results reported above and previous studies (e.g. Alzahrani et al., 2013a).

The removal efficiency of the NF-90 membrane ranged between 60 and 100 % for cations while anion rejection ranged between 64.8 and 99.5 %. On the other hand, the removal efficiency of the ESPA2 membrane ranged between 76 and 100 % for cations while anion rejection ranged from 76 to 99.7 %. It is remarkable that the highest rejection achieved by both NF-90 and ESPA2 was for total mercury and this compound was almost completely rejected, while the lowest rejection achieved by both NF-90 and ESPA2 was for calcium which amounted to 60%. Complete rejection of total mercury could be attributed to sieving (or size exclusion) as the molecular weight of mercury is 200.59 g/mol which is higher than the molecular weight cut-off (MWCO) of NF-90 and ESPA (~200 Da and ~100 Da). In other words, the sieving of large molecules occurs through the small membrane pores and this phenomenon is called the steric hindrance effect that operates principally for neutral solutes (Minhas et al., 2013).

Furthermore, as shown in Figure 6-6 the performance of the NF-90 and ESPA2 membranes in rejecting the model foulants was high in all seasons except winter and spring in the case of NF-90 that was somewhat low. This result is consistent with the findings concluded in previous studies (Reznik et al., 2011). Reznik et al. (2011) concluded that both loose (NF-270) and tight (NF-90) NF membranes, exhibited a high dependency on the water matrix and season for rejection of carbamazepine, where the rejection of this component was higher in summer ( $84 \pm 5\%$  average and up to 92%) than in winter ( $54 \pm 10$  average and down to 50%). Changes in the effluent organic matter seasonally produced during the biological stage could explain this phenomenon.

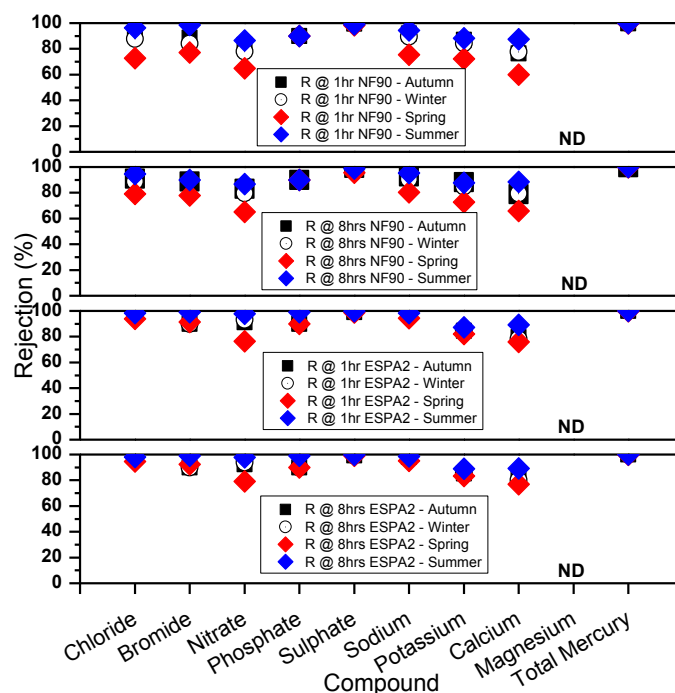


**Figure 6-6:** Overall removal efficiency of the selected inorganic compounds which were detected in contaminated groundwater at Orica (Botany Bay). NF/RO membrane filtration experiment was conducted at an initial permeate flux of 41 L/m<sup>2</sup>h at a temperature of 20 °C and a cross-flow velocity of 30.4 cm/s. Samples were collected after 1 and 8 hours of filtration.

### 6.3.3 Performance of the NF/RO membranes

To investigate the performance of NF/RO membranes, it is essential to study the membrane permeate flux as a function of filtration time for samples that were collected in different seasons and from different sites (leachate pond at Russell Vale and WGB32 at Botany Bay).

#### 6.3.3.1 Leachate pond at Russell Vale Golf Course

Figure 6-7 shows the evolution of the membrane permeate flux as a function of filtration time. Substantial permeate flux decline was observed with both the NF-90 and ESPA2 membranes in particular for samples that were collected in autumn and summer seasons from the leachate pond due to fouling of the membranes (Table 6-

1). Fouling due to living cells, such as algae, is quite complex since these cells change their sizes, morphology, and have extracellular organic matter (EOM) attached to their cells. High temperatures and light intensity as well as nutrient availability in these two seasons inhibit the growth and photosynthesis process and result in high release of EOM. Consequently, the existence of EOM in the reservoir frequently clogs the pores of the membranes, leading to permeate flux decline (Babel et al., 2002). Furthermore, as seen in Figure 6-7 the permeate flux for the ESPA2 membrane (Figure 6-7B) was better than the permeate flux for the NF-90 membrane (Figure 6-7A) specifically in winter and spring seasons. There is a correlation between fouling tendency and the membrane surface roughness, and this strongly agrees with previous studies (e.g. Vrijenhoek et al., 2001; Boussu et al., 2007). NF-90 has a significant surface roughness (63.9 nm) whereas ESPA2 has a rather smooth membrane surface with a corresponding surface roughness of 30.0 nm (Table 3-3 chapter 3). Indeed, with the exception of the autumn and summer seasons, where there was a significant decline of flux caused by fouling, the ESPA2 membranes (Figure 6-7B) did not show any measurable flux decline over approximately 8 hours of filtration time in other seasons (winter and spring). In contrast, there was permeate flux decline for the NF-90 membrane in autumn and summer seasons and slight flux decline for winter and spring seasons (Figure 6-7A). Also physiochemical properties of membranes, in particular pore size, could play a significant role in the extent of organic fouling. Permeate flux decline because of membrane fouling could be more severe with membranes having a larger pore size (NF-90) compared to ESPA2 (which is classified as nonporous). This conclusion is consistent with previous literature (Nghiem and Hawkes, 2009) which revealed that permeate flux decline is governed by the pore size of membrane.

**Table 6-1:** Comparison between permeate flux decline (%) of the NF-90 and ESPA2 membranes for samples collected from the leachate pond at Russell Vale after 8 hours of filtration.

Season	Permeate Flux Decline of NF-90 (%) <sup>a</sup>	Permeate Flux Decline of ESPA2 (%) <sup>b</sup>
Autumn	45	69.7
Winter	47	19
Spring	27.3	14.4
Summer	85	83.4

<sup>a/b</sup> Data calculated using following Equation:  $Flux\ Decline\ (\%) = \left(1 - \frac{J}{J_0}\right) \times 100$

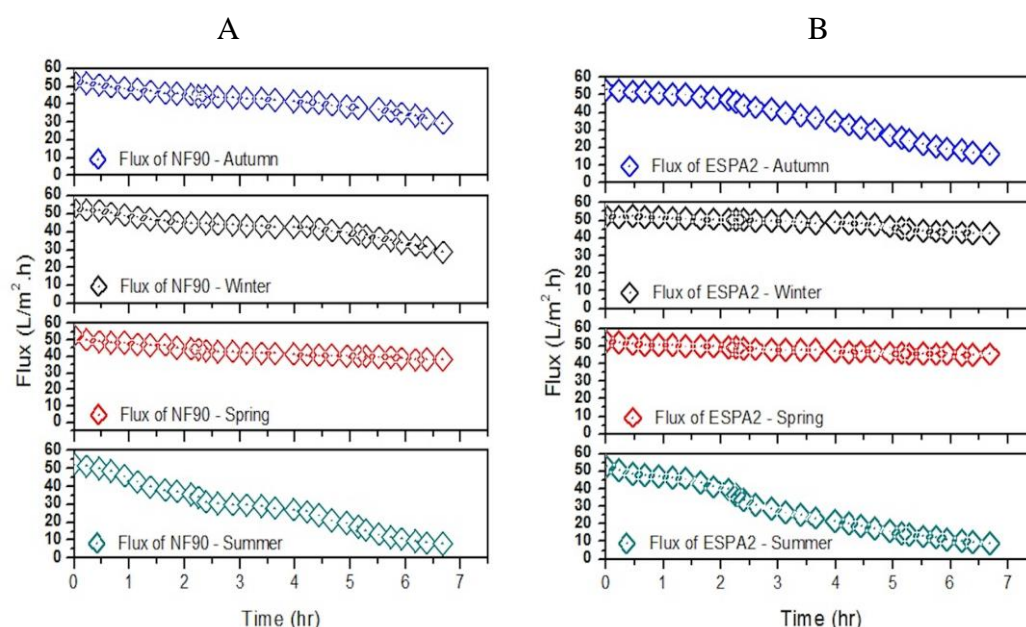


**Figure 6-7:** Permeate flux of (A) the NF-90 and (B) the ESPA2 membranes as a function of filtration time. Experiments were conducted at an initial permeate flux of 41 L/m<sup>2</sup>h, temperature of 20 °C and cross-flow velocity of 30.4 cm/s. Permeate were collected after 8 hours of filtration. Data for samples collected from the leachate pond at Russell Vale.

Comparison between water samples which were collected from the leachate pond at Russell Vale before and after the use of NF-90/ESPA2 membranes (feed and permeate) is displayed in Figure 6-8. Also, conductivity values measured after 1 hour and 8 hours of filtration are shown in Table 6-2 as well as the flux, pH, pressure and temperature values measured after 1 hour and 8 hours of the filtration experiments. The ESPA2 membrane, which is classified as a non-pours membrane, has a high efficiency for the removal of target contaminants in all seasons (Figure 6-5).

Similarly, the NF-90 membrane, which is classified as a tight nano-filtration membrane showed a good efficiency for removal of inorganic contaminants, nevertheless is less efficient than the ESPA2 membrane (Figure 6-5). This is confirmed by the great difference in conductivity before and after using the NF-90 and ESPA2 membranes, however as shown in Table 6-2 the difference in conductivity before and after using the ESPA2 membrane is larger than the difference in conductivity before and after using the NF-90 membrane. Consequently, conductivity appears to be a good indicator to assess the removal efficiency of inorganic contaminants by the tight NF and RO membranes.

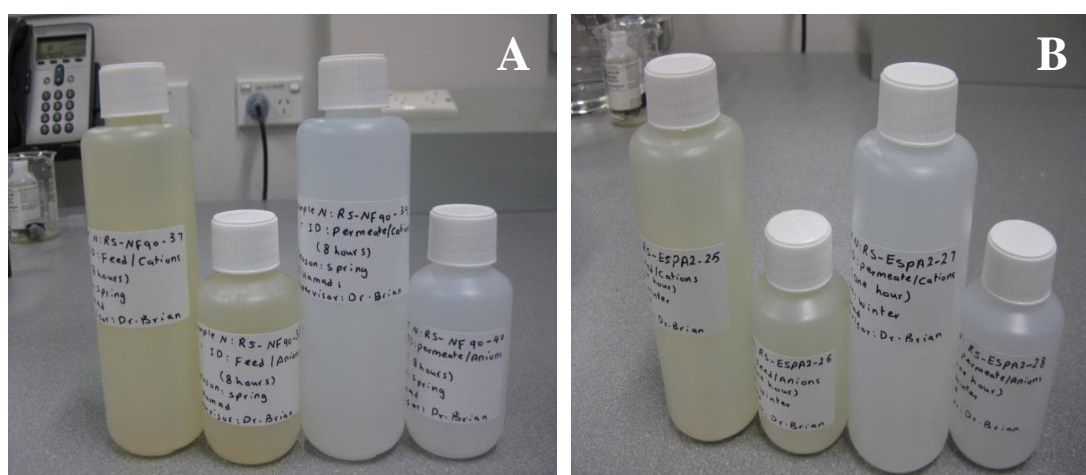


**Figure 6-8:** Images demonstrating water samples collected from the leachate pond at Russell Vale before and after using NF-90 (a) and ESPA2 (b) membranes.

**Table 6-2:** Conductivity, flux, pH, pressure and temperature values measured after 1 hour and 8 hours of filtration for samples collected from the leachate pond at Russell Vale.

Season	Membrane	Time (h)	Flux <sup>a</sup> (ml/min)	pH		Conductivity (μS/cm)		Pressure (bar)	Temperature (°C)	
				Feed	Permeate	Feed	Permeate		Feed	Permeate
Spring	NF-90	1 hr	2.8	8.4	8.6	3170	142	8.5	20	22
		8 hrs	2.4	8.5	8.9	3340	127	8.5	20	21
	ESPA2	1 hr	3.2	8.3	8.7	3260	74	14.5	20	21
		8 hrs	2.9	8.4	8.9	3420	73	14.5	20	22
Summer	NF-90	1hr	1.2	8.3	7.4	1820	220	10	20	21
		8 hrs	0.5	8.3	7.7	1979	212	10	20	21
	ESPA2	1 hr	1.3	8.2	7	1804	55	24	20	22
		8 hrs	0.6	8.3	7.4	1888	50	24	20	21
Autumn	NF-90	1 hr	3.3	8.1	8.6	2522	102	8	20	21
		8 hrs	1.1	8.4	8.9	2585	156	8	20	22
	ESPA2	1 hr	3.4	8.2	8.8	2665	77	14	20	21
		8 hrs	1.2	8.4	8.8	2716	79	14	20	21
Winter	NF-90	1 hr	2.8	8.2	8.3	1772	98	8	20	21
		8 hrs	2.2	8.3	8.4	1794	87	8	20	22
	ESPA2	1 hr	3.4	8.2	8.7	1757	36	14	20	21
		8hrs	2.7	8.2	8.7	1808	35	14	20	21

<sup>a</sup> Flux at 0 time starts with 3.6 ml/min for each experiment.



### 6.3.3.2 WGB32 at Botany Bay

Figure 6-9 displays the evolution of the membrane permeate flux as a function of filtration time for WGB32. Significant permeate flux decline could be observed with the NF-90 membrane (Table 6-3 and Figure 6-9A). A small, but however discernible, flux decline could also be observed with the ESPA2 membrane (Table 6-3 and Figure 6-9B).

Obviously there is a correlation between fouling propensity and the membrane surface roughness and this completely agrees with previous studies (e.g. Vrijenhoek et al., 2001; Boussu et al., 2007). As shown in (Table 3-3 chapter 3), the NF-90 has a significant surface roughness of 63.9 nm, while the ESPA2 has somewhat smooth membrane surface with the corresponding surface roughness of 30.0 nm. In fact, the ESPA2 membrane did not show any measurable flux decline over approximately 8 hours of filtration time. In contrast, there was slight permeate flux decline when using the NF-90 membrane in all seasons and this is consistent with several previous studies (e.g. Alturki et al., 2010).

**Table 6-3:** Comparison between permeate flux decline (%) of the NF-90 and ESPA2 membranes for samples collected from WGB32 at Botany Bay after 8 hours of filtration.

Season	Permeate Flux Decline of NF-90 (%)	Permeate Flux Decline of ESPA2 (%)
Autumn	11.5	4.7
Winter	12.7	4
Spring	16	8.7
Summer	20	8.8

<sup>a/b</sup> Data calculated using following Equation:  $Flux\ Decline\ (\%) = \left(1 - \frac{J}{J_0}\right) \times 100$

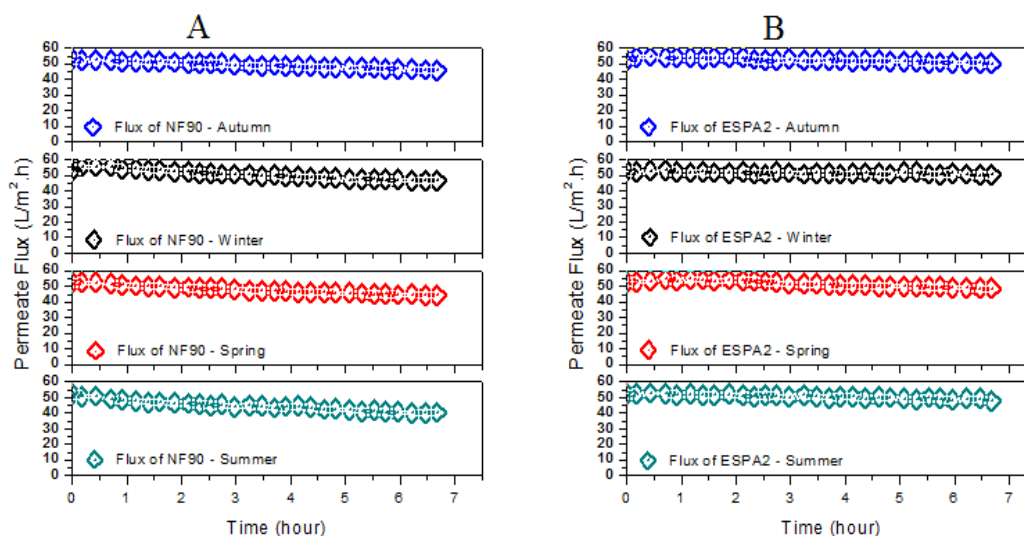


**Figure 6-9:** Permeate flux of (A) the NF-90 and (B) the ESPA2 membranes as a function of filtration time. Experiments were conducted at an initial permeate flux of 41 L/m<sup>2</sup>h, temperature of 20 °C and cross-flow velocity of 30.4 cm/s. Permeate were collected after 8 hours of filtration. Data for samples were collected from WGB32 at Botany Bay.

Comparison between of water samples which were collected from WGB32 at Botany Bay before and after the use of a NF-90 membrane (feed and permeate) is shown in Figure 6-10. Also, conductivity values measured after 1 hour and 8 hours of filtration are displayed in Table 6-4 in addition to flux, pH, pressure and temperature values measured after 1 hour and 8 hours of the filtration experiments. The ESPA2 membrane has a high efficiency for the removal of model foulants in all seasons except for the spring season that was marginally lower (Figure 6-6). In the same way, the NF-90 membrane showed a good efficiency for removal of target contaminants, but was less efficient than the ESPA2 membrane, especially in the spring season (Figure 6-6). This is confirmed by the great difference in conductivity before and after using the NF-90 and ESPA2 membranes, nevertheless as shown in Table 6-4 the difference in conductivity before and after using the ESPA2 membrane was larger than the difference in conductivity before and after using the NF-90 membrane. Thus, conductivity appears to be a good indicator to assess the removal efficiency of inorganic contaminants by the tight NF and RO membranes.



**Figure 6-10:** Image demonstrates a water sample, which was collected from WGB32at Botany Bay, before and after using a NF-90 membrane.

**Table 6-4:** Conductivity, flux, pH, pressure and temperature values measured after 1 hour and 8 hours of filtration for samples collected from WGB32 located near the tennis courts outside the Botany Industrial Park (BIP) fenceline at Orica.

Season	Membrane	Time (h)	Flux <sup>a</sup> (ml/min)	pH		Conductivity (μS/cm)		Pressure (bar)	Temperature (°C)	
				Feed	Permeate	Feed	Permeate		Feed	Permeate
Spring	NF-90	1 hr	3.3	10.4	10.1	8690	2300	17	20	21
		8 hrs	2.9	10.3	10	9560	2140	17	20	22
	ESPA2	1 hr	3.5	10.4	9.7	9110	578	22	20	21
		8 hrs	3.2	10.3	9.2	10210	594	22	20	21
Summer	NF-90	1hr	3.1	10.3	9.8	6470	462	10	20	21
		8 hrs	2.8	10.3	9.7	6800	389	10	20	22
	ESPA2	1 hr	3.4	10.3	9.6	6570	124	14	20	21
		8 hrs	3.3	10.3	8.9	6980	117	14	20	21
Autumn	NF-90	1 hr	3.4	10.1	9.9	8150	778	10	20	21
		8 hrs	3.1	10	9.4	8890	803	10	20	21
	ESPA2	1 hr	3.5	10.2	9.4	8090	198	15	20	21
		8 hrs	3.4	10.1	9.7	8800	201	15	20	21
Winter	NF-90	1 hr	3.4	10.2	9.7	8440	1116	10	20	21
		8 hrs	3.2	10.1	9.6	9050	1065	10	20	22
	ESPA2	1 hr	3.5	10.2	9.1	8330	171	15	20	21
		8hrs	3.4	10.1	9.5	9170	181	15	20	22

<sup>a</sup> Flux at 0 time starts with 3.6 ml/min for each experiment.

#### **6.4 Conclusion**

Results reported in this study indicate that NF/RO membrane filtration can achieve enhanced removal efficiency for a wide range of inorganic contaminants detected in surface and groundwater collected from the leachate pond and WGB32, respectively. The findings of this study exhibited that the performance of the NF-90 and ESPA2 membranes after 8 hours was better than after one hour for the removal of model foulants in two sites (leachate pond and WGB32). Since the NF-90 has a significant surface roughness, the flux through this membrane declined significantly in autumn and summer and declined slightly for winter and spring for samples collected from the leachate pond. However the flux declined slightly in all seasons in case of samples collected from WGB32. In contrast, the ESPA2 has a somewhat smoother membrane surface and therefore it did not show any measurable flux decline over approximately 8 hours of filtration time for samples collected from WGB32. Nevertheless there was a significant decline in flux in autumn and summer for samples collected from the leachate pond. Considerable permeate flux decline was observed with the NF-90 and ESPA2 membranes for samples collected from the leachate pond specifically in summer season due to the fouling. High temperatures and light intensity as well as nutrient availability in this season favour the growth and photosynthesis process and result in high release of extracellular organic matter (EOM) from algae (e.g. *Microcystis aeruginosa*). Accordingly, the presence of EOM in feed reservoir frequently clogs the pores of membranes, leading to permeate flux decline. The performance of the NF-90 membrane in rejecting the model foulants was high in all seasons except winter and spring in the case of samples collected from WGB32 and could be explained by differences in the effluent organic matter seasonally produced during the biological stage.

## **CHAPTER 7: THE REMOVAL OF INORGANIC CONTAMINANTS BY USING MWNT BUCKYPAPER MEMBRANE**

### **7.1 Introduction**

The rapid growth in nanotechnology has encouraged significant use of this technology in the environmental applications particularly to produce clean water and protect the environment in a sustainable manner. CNTs have principally attracted significant growing attention because of their ability to exhibit superior durability and separation characteristics (Goh et al., 2013). Their remarkable mechanical, electrical and thermal properties allow fluid flow through their interior (Dumée et al., 2010). In particular, carbon nanotube buckypapers have exceptional properties such as natural hydrophobicity, high porosity and very high specific surface area, making them promising candidates for separation applications (Dumée et al., 2011).

The separation of inorganic contaminants is typically attributed to size exclusion in addition to Donnan exclusion (a charge repulsion mechanism; Yaroshchuk, 2001; Teixeira et al., 2005; Verliefde et al., 2008; Bolong et al., 2009). The size exclusion mechanism occurs when the solute size is greater than the pore size of the membrane. Accordingly, contaminants are removed effectively by a sieving mechanism (Chen et al., 2004; Verliefde et al., 2008). The electrostatic repulsion mechanism is another key factor affecting the ability of a CNT membrane to separate charged solutes present in a mixture. According to this mechanism, the ion separation results from the electrostatic interactions between ions and the negatively charged MWNT membrane (Vatanpour et al., 2011). On the other hand, adsorption is considered a dominant mechanism to retain some inorganic contaminants and it is a simple and efficient method for the removal of such contaminants from contaminated water (Liu et al., 2013b). This mechanism is often governed by the relative hydrophilicity or hydrophobicity of the membrane surface, and hydrogen bonding as well as other interactions between solutes and the membrane (Li et al., 2003; Liu et al., 2013b).

The objective of this study was to examine the ability of MWNT membranes (buckypapers) to remove inorganic contaminants from contaminated surface and groundwater. Experiments were conducted using laboratory-scale and synthesized

MWNT buckypapers. Ten inorganic compounds with molecular weights of less than 100 g/mol and a wide range of ionic and hydrated radii were selected as model inorganic contaminants due to their widespread occurrence in surface and groundwater. Removal efficiency for MWNT buckypapers was correlated to the physicochemical properties of these compounds to focus on the ability and effectiveness of this kind of treatment. Significant characterization work has been conducted to investigate MWNT buckypaper membranes.

## **7.2 Materials and methods**

Detailed descriptions of the dead-end filtration system, its operation protocol and analytical techniques have been provided in chapter 3. Before use, contaminated surface and groundwater samples were collected from a leachate pond at Russell Vale and WGB32 at Botany Bay. They were filtered using a Stericup Durapore<sup>TM</sup> 0.45  $\mu\text{m}$  (Millipore) filter for separation of colloidal and suspended materials. Following that, 2 L of each filtered sample was used as feed solution for each experiment. In the next step, the dead-end filtration system was operated for at least 24 hours in each experiment to collect an adequate amount of permeate, which was then analysed to determine the removal efficiency of this system. In this chapter, the obtained data is systematically analysed to assess the overall performance of the dead-end filtration system.

## **7.3 Results and discussion**

### **7.3.1 Characterization of MWNT buckypapers**

Optimisation of the sonication time, electron microscopic investigation, contact angle analysis, electrical properties measurements, mechanical properties testing and surface area analysis were investigated and presented in chapter 5. The following part will focus on the SEM-EDS analysis of the MWNT buckypaper membrane before and after being used to examine the removal of inorganic contaminants from samples collected from a leachate pond at Russell Vale and WGB32 at Botany Bay.

#### 7.3.1.1 SEM-EDS analysis

The surface morphology of MWNT buckypapers was examined using field-emission scanning electron microscopy (SEM) on a JEOL JSM-7500FA - (BRUKER-QUANTAX 400), and cross-sections were viewed as well. Figure 7-1 shows SEM images of MWNT buckypapers prepared using Triton X-100 before (virgin) and after use (fouled) as a membrane. The surface morphology of the MWNT buckypaper appears to consist of small bundles of tubes and an abundance of small pores (Figure 7-1A) which agrees well with the results of a study conducted by (Cottinet et al., 2012). In contrast, it was observed that some flattening of the MWNT bundles in Figure 7-1B occurred due to adsorption of contaminants.

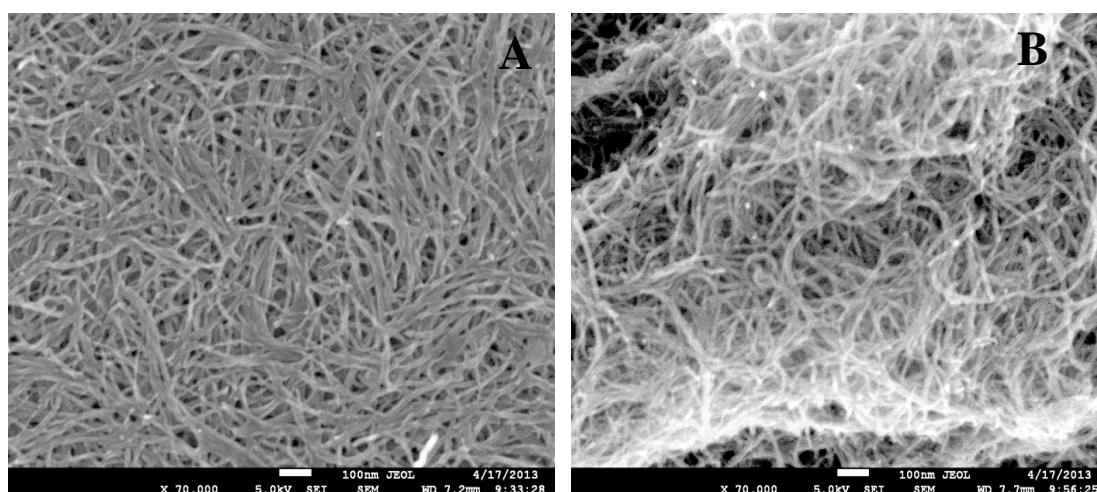


**Figure 7-1:** SEM images of the (A) virgin MWNT buckypaper and (B) MWNT buckypaper fouled by leachate pond-winter.

Also, the cross-sectional images of MWNT buckypapers display clearly what has been seen above, where the Figures 7-2A and 7-2B show the structure and size of the tubes and pores in the MWNT membrane. As seen in Figure 7-2A, the MWNT buckypaper seem to contain small bundles of tubes and an abundance of small pores. On the other hand, the MWNT buckypaper bundles were flattened after use as a membrane because of adsorption of pollutants (Figure 7-2B).

Moreover, it is clear from Figure 7-2A that the MWNT buckypaper membrane possesses a large number of regularly sized pores, with software image analysis (see



section 3.6.2.2, chapter 3, for details) revealing an average surface pore diameter of  $65.6 \pm 8$  nm (Table 5-1) which is similar to that obtained previously for comparable buckypapers produced using MWNTs (Dumée et al., 2010; Sweetman, 2012).

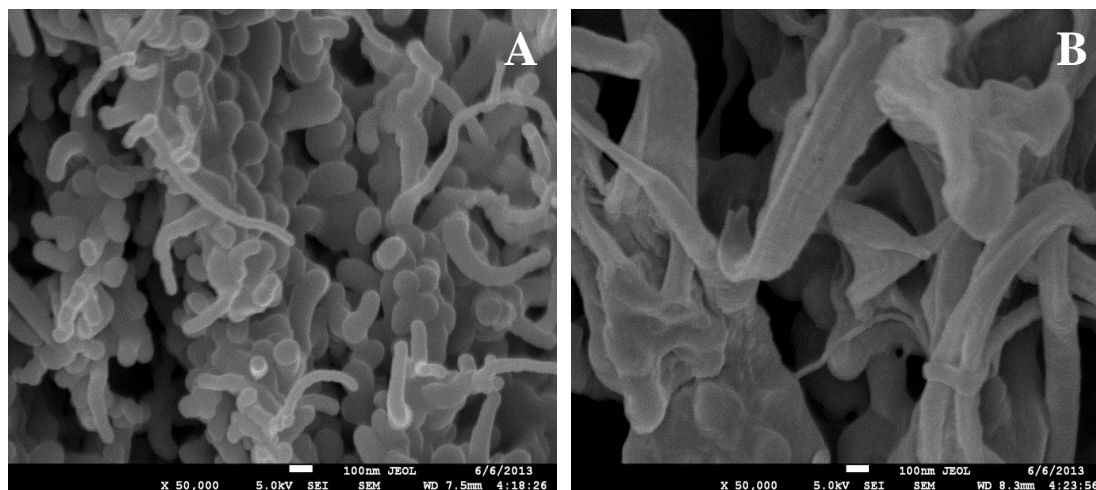


**Figure 7-2:** SEM images of the (A) virgin MWNT buckypaper and (B) MWNT buckypaper fouled by leachate pond-winter.

To investigate the distribution of elements deposited on the membrane surface, MWNT buckypapers were also analysed using SEM with an additional semi-quantitative energy dispersive spectrometer (EDS). An example of SEM-EDS images obtained for virgin and fouled MWNT buckypapers membranes is shown in (Figures 7-3 and 7-4). The EDS spectrum of MWNT buckypapers (Figure 7-3B) shows peaks corresponding to titanium and aluminum in addition to a large amount of carbon and a reasonable amount of oxygen as part of the membrane composition and, therefore, the elements were detected in all samples (virgin and fouled). The presence of aluminum and titanium is not surprising as these elements are used during synthesis of MWNTs via the Nanocyl process. On the other hand, as observed in the corresponding Figures 7-3B and 7-4B, the oxygen content is somewhat significant. These results suggest that a considerable number of carboxyl groups have been introduced onto the surface of the buckypaper during synthesis of the MWNTs. A high level of calcium was found in the fouled membrane (Figure 7-4B) due to the ability of calcium to complex with carboxyl groups which are very common at the surface of CNTs. Also, a low level of magnesium was found in the fouled membrane

(Figure 7-4B) and this can be attributed to the rejection process for this cation via the size exclusion mechanism and consequent diffusion into the membrane surface (Van der Bruggen et al., 2004).

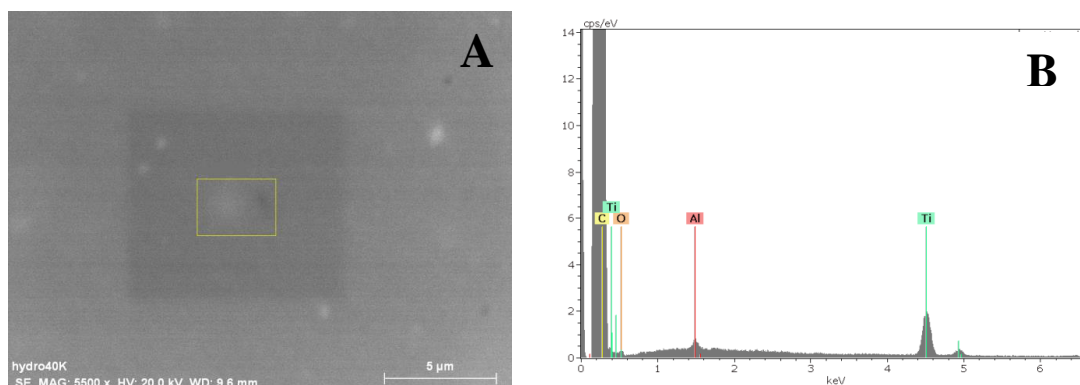


**Figure 7-3:** EDS data of the virgin MWNT-Triton X-100 membrane (A and B).

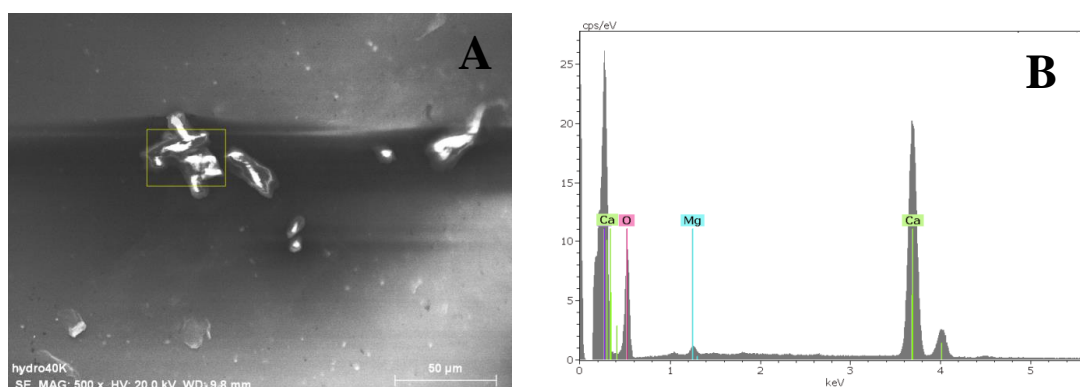


**Figure 7-4:** EDS data of the MWNT-Triton X-100 membrane fouled by leachate from the pond at Russell Vale in spring (A and B).

### **7.3.2 Removal of inorganic contaminants by MWNT buckypaper membrane**

To investigate the potential of these MWNT materials for filtration applications, it is essential to determine whether they exhibit any selectivity in their permeability towards dissolved solutes. It is noteworthy that only a few studies have been performed previously using buckypapers prepared from MWNTs. Thus, as a first step towards remedying this situation, many experiments were conducted on samples collected in different seasons from the leachate pond at Russell Vale and WGB32 at

Botany Bay to evaluate the ability of MWNT-Triton-X-100 buckypapers to remove inorganic contaminants from contaminated surface and groundwater. Permeate and feed samples of 250 mL and 100 mL were collected before and after 24 hours of filtration to analyse for cations and anions, respectively.

#### 7.3.2.1 Leachate pond at Russell Vale Golf Course

Contaminated surface water is represented by samples collected from the leachate pond at Russell Vale Golf Course in the Illawarra area during 2012 for four seasons. The removal efficiency for MWNT buckypapers are reported in Table 7-1 and Figure 7-5. In general, the performance of the MWNT membrane in rejecting the model foulants was low in all seasons compared to the performance of the NF-90 and ESPA2 membranes in rejecting the same model foulants. This was due to the high porosity of the MWNT buckypaper membrane (see chapter 6). The results from Figure 7-5 showed that the performance of the MWNT buckypaper membranes in rejecting anions was higher than that of its cations rejection. This phenomenon can be explained by the Donnan exclusion mechanism (charge repulsion mechanism); the anion separation resulting from the electrostatic interactions between the negative charge of the anions and the negative charge on the MWNT membrane (Vatanpour et al., 2011). Except for mercury, which was not detected in contaminated surface water samples at Russell Vale, the molecular weight of the anions is greater than the cations and ranged between 35.45 g/mol ( $\text{Cl}^-$ ) and 96.06 g/mol ( $\text{SO}_4^{2-}$ ), whereas the molecular weight of the cations ranged between 22.99 g/mol ( $\text{Na}^+$ ) and 40.08 g/mol ( $\text{Ca}^{2+}$ ; see Table 3-5, chapter 3). This may give an added reason for the higher rejection of anions than cations.

Also as seen in Figure 7-5, it was notable that the rejection of calcium was high compared to other cations and is attributed to the fact that it has a large molecular weight (40.08 g/mol), while other cations for example sodium and magnesium have smaller molecular weights (22.99 g/mol and 24.31 g/mol respectively). Consequently, calcium was rejected by size exclusion mechanism and according this mechanism size variation can determine which ions are able to pass through the

membrane pores by diffusion (Van der Bruggen et al., 2004). Furthermore, the results in Figure 7-5 revealed that calcium recorded the highest value of rejection reaching 51%, followed by phosphate 47.8%, then magnesium 19.4%, while the lowest value of rejection was for potassium where no rejection occurred (0%). This can be explained by divalent and multivalent ions with large hydrated radii (i.e.  $Mg^{2+}$ ,  $Ca^{2+}$  and  $PO_4^{3-}$ ) were retained more than monovalent ions with smaller hydrated radii (i.e.  $K^+$ ; Richards et al., 2011). Lastly, it is observed that there was no relationship between seasonal effects when using MWNT buckypaper membranes, as found in the cases of the NF-90 and ESPA2 membranes. It is quite clear from Figure 7-5, that the rejection rate of the model foulants was close in all seasons.

**Table 7-1:** Overall removal efficiency of the selected inorganic compounds which were detected in contaminated surface water from the leachate pond in Russell Vale.

Compound	Rejection (%)			
	Summer	Autumn	Winter	Spring
Chloride	8.7	4.8	7.7	20.7
Bromide	3.8	4.8	7.1	5.7
Nitrate	16.7	11	5.3	4.7
Phosphate	47.8	50	45	30
Sulphate	5.7	1.6	4.6	8.3
Sodium	6	5.1	3.7	3.2
Potassium	0	0	0	0
Magnesium	16.1	19.4	14.3	11.8
Calcium	14.3	35.9	22.4	51
Total Mercury <sup>a</sup>	ND	ND	ND	ND

<sup>a</sup> ND: Not detected.

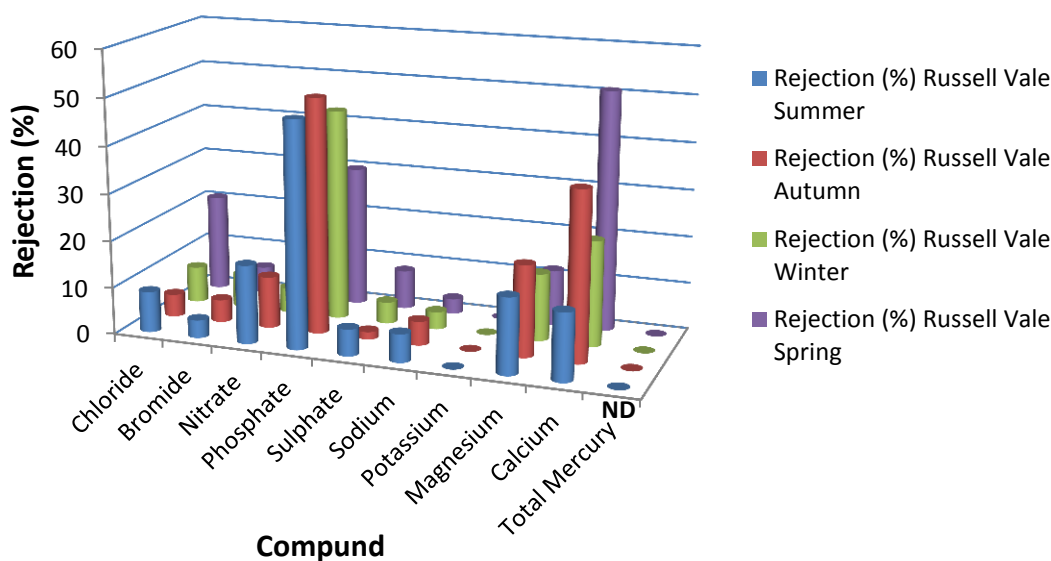


**Figure 7-5:** Overall removal efficiency of the selected inorganic compounds which were detected in contaminated surface water at Russell Vale. MWNT-Triton-X-100 buckypaper membrane filtration experiment was conducted at 140 Kpa and temperature of 20 °C. Samples were collected after 24 hours of filtration.

### 7.3.2.2 WGB32 at Botany Bay

The performance of MWNT membranes in rejecting the model foulants in samples WGB32 are reported in Table 7-2 and Figure 7-6. The situation is not much different to the surface water when contaminated groundwater samples collected from WGB32 site at Botany Bay were used to investigate the efficiency of MWNT buckypaper membranes to reject inorganic contaminants. A comparison between the NF-90 and ESPA2 membranes and MWNT membrane, in terms of the removal efficiency of inorganic contaminants, shows that the MWNT membrane is much less efficient than the NF-90 and ESPA2 membranes and this is due to the high porosity of the MWNT buckypaper membrane (see chapter 6). The findings from Figure 7-6 displays that the performance of MWNT buckypaper membranes in rejecting anions was better than that of its cation rejection. This phenomenon can be attributed to the Donnan exclusion mechanism (charge repulsion mechanism); the anions separation

resulting from the electrostatic interactions between negative charges on the anions and the MWNT membrane (Vatanpour et al., 2011). Furthermore, the results in Figure 7-6 revealed that phosphate recorded the highest rejection value reaching 69.2%, whereas the lowest rejection value was for potassium where no rejection occurred (0%). The reason for this is that the molecular weight of phosphate (95.0 g/mol) is greater than the molecular weight of potassium (39.10 g/mol).

Also, as shown in Figure 7-6, it was noteworthy that the rejection of phosphate was high compared to other anions followed by sulphate, nitrate then chloride. This can be explained by multivalent ions with large hydrated radii (i.e.  $\text{PO}_4^{3-}$ ) were retained more than monovalent ions with smaller hydrated radii (i.e.  $\text{Cl}^-$ ; Richards et al., 2011). In case of cations, the highest value of rejection was for magnesium that reached 15%, followed by mercury 13.7% then calcium 7.4% and after that sodium 4.3%, while the lowest value of rejection was for potassium where no rejection occurred (0%). This can be explained since ions with large hydrated radii (i.e.  $\text{Mg}^{2+}$ ,  $\text{Hg}^+$  and  $\text{Ca}^{2+}$ ) were retained more than ions with smaller hydrated radii (i.e.  $\text{Na}^+$ ; Richards et al., 2011). Finally, it is observed that there is no relationship between seasonal effects using MWNT buckypaper membranes as found in the case of the NF-90 and ESPA2 membranes. This is quite clear from Figure 7-6, where the rejection of the model foulants was similar in all seasons.

**Table 7-2:** Overall removal efficiency of the selected inorganic compounds which were detected in contaminated groundwater water from WGB32 in Botany Bay.

Compound	Rejection (%)			
	Summer	Autumn	Winter	Spring
Chloride	15	12.5	13.6	16.4
Bromide <sup>a</sup>	ND	ND	ND	ND
Nitrate	17.5	13.3	16.7	12.7
Phosphate	69.2	48.5	20	32
Sulphate	22.5	5	6.5	7.2
Sodium	4.2	2.8	4.3	1.3
Potassium	0	0	0	0
Magnesium	15	12.5	15	12.5
Calcium	2.9	3.6	7.4	3.8
Total Mercury	13.7	17.1	6.9	13.6

<sup>a</sup> ND: Not detected.

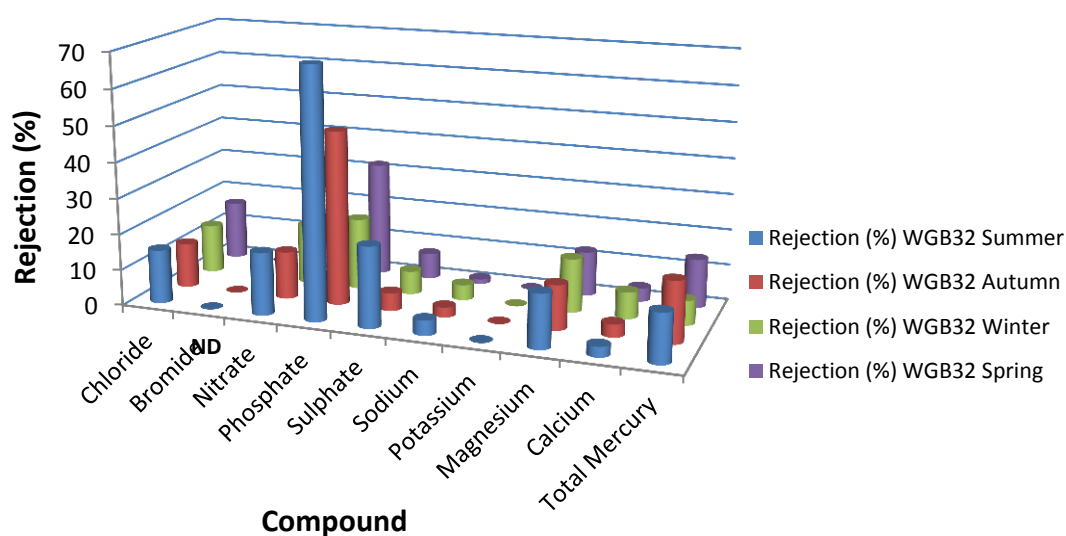


**Figure 7-6:** Overall removal efficiency of the selected inorganic compounds which were detected in contaminated groundwater water in WGB32 at Botany Bay. Experiments were conducted at 140 Kpa and temperature of 20 °C. Samples were collected after 24 hours of filtration.

### **7.3.3 Performance of The MWNT buckypaper membrane**

To investigate the performance of MWNT buckypaper membranes, it is important to study the membrane permeate flux as a function of filtration time for samples collected in different seasons and from different sites (i.e. leachate pond at Russell Vale Golf Course and WGB32 at Botany Bay).

#### **7.3.3.1 Leachate pond at Russell Vale Golf Course**

Figure 7-7 shows the evolution of the membrane permeate flux as a function of filtration time. As shown in Figure 7-7, it is observed that the flux was better for samples which were collected in winter and spring seasons compared to samples collected in autumn and summer seasons. In particular, the flux was the lowest for samples which were collected in the summer season and this can be attributed to existing living cells such as extracellular organic matter (EOM) that is released from algae. In the summer season, higher temperatures participate significantly in the growth of algal blooms and the chance to release this substance becomes more probable. This extracellular, mucilaginous slime material can elevate resistance to filtration (Kwon et al., 2005). It has been found that characteristics of EOM can impact the specific resistance developed in membrane filtration in particular when it is present in the feed reservoir (Babel et al., 2002).

The results in Figure 7-7 revealed that the highest value of flux was in the winter and ranged between  $\sim 48\text{-}50 \text{ L.m}^2.\text{h}$  followed by spring ( $\sim 46\text{-}48 \text{ L.m}^2.\text{h}$ ) after that autumn ( $\sim 38\text{-}40 \text{ L.m}^2.\text{h}$ ) and the lowest value found in summer season and ranged between  $\sim 20\text{-}25 \text{ L.m}^2.\text{h}$ . Also, it is remarkable that after using MWNT buckypaper as a membrane in this study flux was linear and stable in all studied seasons. In contrast, flux was not linear and stable in all studied seasons in case of using the NF-90 and ESPA2 as membranes in particular for samples which were collected in autumn and summer seasons (see part 6.3.3.1 chapter 6). This can be explained by the porosity of MWNT the membrane ( $\sim 28 \text{ nm}$ ) being higher than the porosity of the NF-90 and ESPA2 membranes ( $0.68 \text{ nm}$  and non-porous respectively).



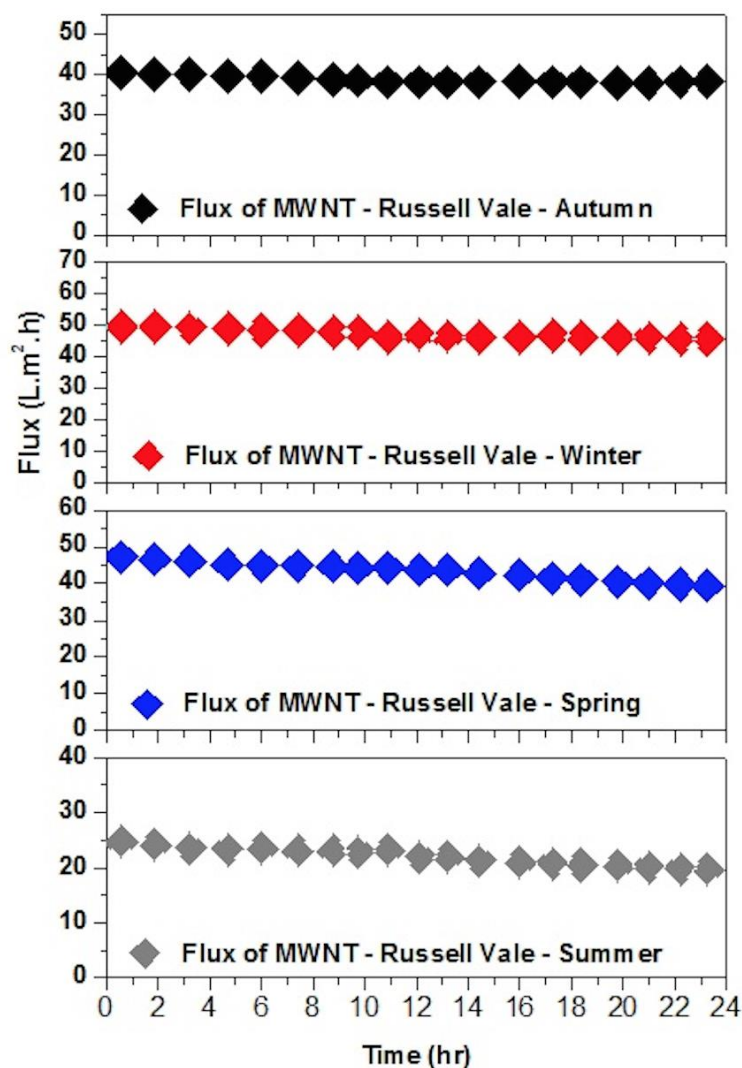


**Figure 7-7:** Permeate flux of The MWNT buckypaper membrane as a function of filtration time. Experiment was conducted at 140 Kpa and temperature of 20 °C. Samples used in this experiment were collected from the leachate pond at Russell Vale.

### 7.3.3.2 WGB32 at Botany Bay

Samples collected from WGB32 represent contaminated groundwater. Figure 7-8 displays the progress of the membrane permeate flux as a function of filtration time. The situation here is not much different when contaminated groundwater samples collected from this site compared to contaminated surface water samples collected from the leachate pond at Russell Vale. Results in Figure 7-8 indicate that flux was good for samples collected in all seasons, even those collected during the summer

season. It can be explained that higher temperatures and light intensity, in addition to nutrient availability, in summer did not play any role here, because these samples were collected from a well and therefore there was no favourable opportunity for the growth and photosynthesis process and subsequent high release of EOM (Babel et al., 2002). If EOM is available, mucilaginous slime material can increase resistance to filtration (Kwon et al., 2005). It has been found that the characteristics of EOM can influence the specific resistance developed in membrane filtration, in particular when it is present in the feed reservoir (Babel et al., 2002).

The results in Figure 7-8 show that the highest value of flux was in the winter and ranged between ~53-56 L.m<sup>2</sup>.h, followed by spring (~49-51 L.m<sup>2</sup>.h) after that autumn (~41-47 L.m<sup>2</sup>.h) and the lowest value found in summer season and ranged between ~29-37 L.m<sup>2</sup>.h. Furthermore, it is noteworthy that the flux through the MWNT buckypaper membrane in this study was linear and stable in all seasons. In the same way, flux also was linear and stable in all seasons in the case of the NF-90 and ESPA2 membranes. However, the flux after using these membranes was somewhat better than the flux after using the MWNT membrane in all seasons (see part 6.3.3.2, chapter 6). It can be concluded that since samples from this site were collected from a well the colloidal and suspended substances in these waters was slightly less compared to the contaminated surface water samples collected from the leachate pond at Russell Vale. Consequently, the flux after using both the MWNT membrane and the NF-90/ESPA2 membranes was much better compared to the flux after their use to investigate the removal of the inorganic contaminants detected in samples collected from the leachate pond at Russell Vale due to lack of fouling effects.

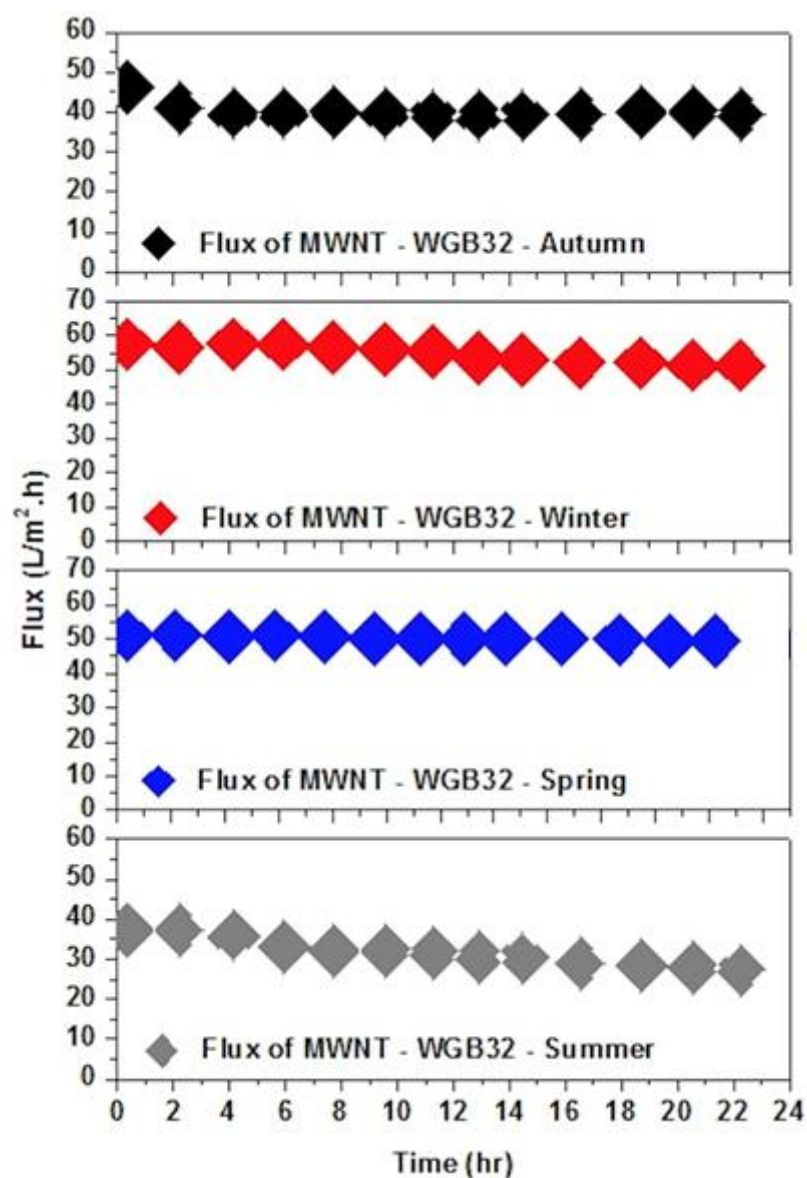


**Figure 7-8:** Permeate flux of The MWNT buckypaper membrane as a function of filtration time. Experiment was conducted at 140 Kpa and temperature of 20 °C. Samples were collected from WGB32 at Botany Bay.

#### 7.4 Flux decline

Comparison between permeate flux decline through MWNT membranes for samples collected from the leachate pond at Russell Vale and WGB32 at Botany Bay is shown in Table 7-3. Considerable permeate flux decline was observed with the MWNT membranes for samples which were collected in summer season from both

the leachate pond and WGB32 due to fouling of the membranes. However, flux decline values for the MWNT membranes demonstrated in Table 7-3 are considerably smaller than the flux decline values for the NF-90 and ESPA2 membranes especially for samples collected in autumn and summer seasons from the leachate pond (see parts 6.3.3.1 and 6.3.3.2 chapter 6). This can be explained since the porosity of the MWNT membrane (~28 nm) is higher than the porosity of the NF-90 and ESPA2 membranes (0.68 nm and non-porous, respectively) and thus the possibility of fouling of the NF-90 and ESPA2 membranes is much greater than the fouling of the MWNT membranes due to retention of contaminants. Moreover, the CNT membrane has antifouling, self-cleaning and reusable functions (Das et al., 2014) and this means a lack of likelihood of fouling for the MWNT membranes.

**Table 7-3:** Comparison between permeate flux decline of MWNT membranes for samples collected from the leachate pond at Russell Vale and WGB32 at Botany Bay.

Season	Permeate Flux Decline for MWNT-Leachate pond (%) <sup>a</sup>	Permeate Flux Decline for MWNT-WGB32 (%) <sup>b</sup>
Autumn	5	4.7
Winter	4	5.3
Spring	4.2	3.9
Summer	20 <sup>c</sup>	21.6 <sup>d</sup>

<sup>a/b</sup> Data calculated using following Equation:  $Flux\ Decline\ (\%) = \left(1 - \frac{J}{J_0}\right) \times 100$ .

<sup>c</sup> Caused by EOM.

<sup>d</sup> It could be attributed to the changes in the effluent organic matter seasonally produced during the biological stage.

## 7.5 Conclusion

Results reported in this study indicate that the performance of the MWNT membrane in rejecting inorganic contaminants detected in samples collected from the leachate pond and WGB32 was low in all seasons compared to the performance of the NF-90 and ESPA2 membranes in rejecting the same model foulants. This was due to the high porosity of the MWNT buckypaper membrane. It is observed that the performance of MWNT buckypaper membranes in rejecting anions was greater than that for its cations rejection. This can be explained that by the Donnan exclusion

mechanism; the anions separation resulted from the electrostatic interactions between the negative charge of anions and the negative charge of the MWNT membrane. The results in this study revealed that the highest value of rejection was for multivalent and divalent ions ( $\text{PO}_4^{3-}$ ,  $\text{Ca}^{2+}$ ) while the lowest value of rejection was for monovalent ( $\text{K}^+$ ). This can be elucidated since multivalent and divalent ions with large hydrated radii (i.e.  $\text{PO}_4^{3-}$ ,  $\text{Ca}^{2+}$ ) were retained more than monovalent ions with smaller hydrated radii (i.e.  $\text{K}^+$ ). Furthermore, it is remarkable that the MWNT buckypaper membrane gave a linear and stable flux in all studied seasons. However, the flux was not linear and stable in all studied seasons when the NF-90 and ESPA2 were used; especially for contaminated surface water samples collected from the leachate pond at Russell Vale in the autumn and summer seasons. It can be deduced that this phenomenon is related to the higher porosity of the MWNT membrane (~28 nm) than the porosity of the NF-90 and ESPA2 membranes (0.68 nm and non-porous, respectively).

## **CHAPTER 8: FURTHER DISCUSSION: THE CRITICAL AND FUNDAMENTAL FINDINGS**

### **8.1 Introduction**

Water scarcity is a significant global issue and is being further exacerbated due to increasing population growth, industrialization and contamination of available fresh water sources. Water scarcity is in most cases a climate-bound regional problem and currently exists all over the world, including Australia. Water in Australia, like other countries, is centred around four types: freshwater, brackish water, saline water and contaminated water. Natural fresh water resources such as lakes, rivers and groundwater are overused or misused; consequently, these resources are either declining or becoming saline (Greenlee et al., 2009). A good example of this situation is Australia's increasing use of groundwater that has been augmented critically over recent decades. From 1983 to 1996 Australian national dependence on groundwater rose by approximately 90% and future usage of groundwater is expected to increase, particularly as surface water resources may become less available because of climate change and prolonged droughts (Geoscience Australia, 2014).

Brackish water sources are mostly groundwaters; these groundwaters can be naturally saline aquifers or groundwater that has become brackish because of brine water intrusion or anthropogenic effects (e.g., overuse and irrigation). Surface brackish waters are not epidemic but can be found naturally or through anthropogenic activities (Greenlee et al., 2009). Saline water usually represents sea and ocean waters, which basically contain 30,000–45,000 mg/L total dissolved solids (TDS; Greenlee et al., 2009). This kind of the water can be tapped to get fresh water through desalination; however this costs a lot of money and consumes energy. Contaminated water is the water which is unfit for use due to contamination, whether the source of this contamination is anthropogenic, natural or biogenic in origin. The most common contaminants associated with contaminated water include the following: synthetic organic contaminants exemplified by pesticides, herbicides, industrial solvents and chemicals (e.g. volatile organic compounds); inorganic

contaminants such as nitrate, arsenic and toxic metals (e.g. heavy metals), cations and anions (e.g. mercury, chloride); natural organic matter (NOM) such as taste and odor causing compounds, plus disinfection by-product (DBP) precursors both measured as total organic carbon (TOC); and microorganisms such as protozoa, bacteria and viruses (Ravindran et al., 2009). As a result, in many locations across Australia, water limitations were imposed, and projects for water reuse, wastewater recycling and seawater desalination were planned and/or applied (Hurlimann and Dolnicar, 2012).

## **8.2 The efficiency of membrane technology to treat different kinds of water**

Recent advances in materials science and process engineering have allowed membrane technology to play a crucial role in the treatment of non-traditional water sources for further use including indirect potable reuse applications (Wintgens et al., 2005; Bellona and Drewes, 2007). Nowadays, membrane technology is extensively used in various aspects of life. Specifically, high pressure membrane filtration processes such as nanofiltration (NF) and reverse osmosis (RO), and carbon nanotubes (CNTs) have been used to treat many types of water, whether brackish water, saline water or contaminated water. Mohsen et al. (2003) have conducted a study to examine desalination of brackish water by nanofiltration and reverse osmosis and they concluded that both processes are effective, as they extensively reduce the organic and inorganic contents existing in the raw waters. Also, Walha et al. (2007) reported that RO was highly efficient since it significantly reduced the content of inorganic matter existing in raw waters. On the other hand, many previous studies concluded that CNT membranes can be used for desalination of brackish water (Ahn et al., 2012; Das et al., 2014).

Membrane technology is used widely to treat saline water or seawater (Khawaji et al., 2008; Greenlee et al., 2009; Das et al., 2014; Goh et al., 2013). Many studies have revealed that NF, as a single process, cannot reduce seawater salinity to drinking water standards; however NF has been used successfully to treat mildly

brackish feed water (Lhassani et al., 2001; M'nif et al., 2007). Both RO and NF can be used to treat seawater (Hamed, 2005; Hassan et al., 1998; Hilal et al., 2005). Nowadays, seawater RO membranes have salt rejections greater than 99% (Reverter et al., 2001; Bartels et al., 2009). Goh et al. (2013) concluded that CNT materials will also play a significant role in the world of desalination technology to provide a comprehensive system to address the critical water issues.

Many studies have shown that membrane technology (NF, RO and CNT membranes) is an effective technology to remove organic and inorganic contaminants from contaminated water (Nghiem and Schäfer, 2004; Yoon and Lueptow, 2005; Nghiem and Coleman, 2008; Yuan et al., 2008; Tofighy and Mohammadi, 2011; Yüksel et al., 2013). Recent studies demonstrated that membrane technology is a very effective technology to remove trace contaminants from aqueous solutions. Nghiem et al. (2005) reported that carbamazepine was rejected at approximately 85% by NF-270 and approximately 96% by NF-90 membranes at pH 8. Also Yangali-Quintanilla et al. (2009) concluded that a clean NF-90 membrane rejected almost all of the hydrophobic neutral compounds (95-98%). High rejection was also achieved by using a RO membrane (>99% for macrolides, pharmaceuticals, cholesterol and BPA, 95% for diclofenac and >93% removal of sulphonamides; Sahar et al., 2011). Furthermore, RO membranes show high rejection (always higher than 99%) for pharmaceutical compounds which existed in municipal wastewater at a coastal wastewater treatment plant (Castell-Platja d'Aro, Spain; Dolar et al., 2012a). Numerous previous studies have demonstrated the remarkable ability of NF/RO to remove a wide range of volatile organic compounds include the trihalomethanes, organochloric compounds, petroleum hydrocarbons and other low molecular weight compounds such as toluene and trichloroethylene (Agenson et al., 2003; Agenson and Urase, 2007). Rashid et al. (2014) concluded that the removal of bisphenol A (BPA) using multi-walled carbon nanotube (MWNT) buckypapers remained constant at roughly 90% throughout the experiment. Joseph et al. (2011b) examined the adsorption of endocrine distributed compounds (EDC) from artificial seawater, brackish water, or a mixture of them using CNTs and stated a higher removal efficiency for 17 $\alpha$ -ethinyl estradiol (EE2; 95–98%).



On the other hand, many researches have demonstrated that membrane technology is a reliable process and effective technology for the removal of toxic and heavy metals from contaminated water (Sudilovskiy et al., 2008; Cséfalvay et al., 2009; Kosa et al., 2012). Murthy and Chaudhari (2009) conducted many research studies for the removal of heavy metal ions using NF membranes. One of these research investigations examined the binary heavy metal (cadmium and nickel) separation capability of a commercial NF membrane from aqueous solutions. They concluded that solute rejection of nickel and cadmium ions is 98.94% and 82.69%, respectively, for an initial feed concentration of 5 mg/L. Hong et al. (2009) reported that the NF-90 exhibited 99% rejection of phosphate and 79% rejection of chloride. High rejection was achieved for  $\text{Cu}^{2+}$  and  $\text{Ni}^{2+}$  ions after using the RO membrane and the rejection efficiency of the two ions increased up to 99.5% by using  $\text{Na}_2\text{EDTA}$  (Mohsen-Nia et al., 2007). Removal of phosphates was investigated by Dolar et al. (2011a) and they reported a high rejection (>97%) of phosphate by the RO-XLE membrane. Hilal et al. (2004) stated that the removal of nitrate was high (94%) after using a RO membrane. Pillaya et al. (2009) concluded that the functionalised MWCNTs demonstrated the greatest adsorption capability with up to 98% of a 100 ppb Cr (VI) solution being adsorbed. Chen et al. (2011) reported that CNTs also exhibited excellent adsorption efficiency for lead.

Results that have been concluded in this study emphasize the principle that the membrane technology is a promising and effective technology to remove contaminants found in water, whether these contaminants are organic or inorganic. What has been inferred in this study obviously expresses the possibility of using membrane technology to treat all kinds of water which have been reviewed above and all contaminants existing in water through focusing on the two main types of contaminants (organic and inorganic). In fact, organic and inorganic contaminants represent all potential contaminants which may exist in water whether these contaminants are trace contaminants or normal contaminants. This study revealed that high rejection of tetrachloroethylene was achieved by using NF-90 (98.4 %) and ESPA2 (100 %) for samples collected from EWB10D at Southlands-Botany Bay. Samples collected from EWB13D at Southlands-Botany Bay also recorded high

rejection for tetrachloroethylene achieved by NF-90 and ESPA2 that reached 95.7 % and 96.2 %, respectively. On the other hand, this study also demonstrated a high adsorption capability with up to 88.5 % achieved by using a MWNT buckypaper membrane for tetrachloroethylene for samples collected from EWB10D and 77.3 % for samples collected from EWB13D at Southlands-Botany Bay.

This trend represents the investigation of the removal of volatile organic compounds present in groundwater at Botany Bay. In contrast, the investigation of the removal of inorganic compounds (cations and anions) present in a leachate pond at Russell Vale and WGB32 at Botany Bay showed the following:

- Samples collected from the leachate pond at Russell Vale: the removal efficiency of the NF-90 membrane ranged between 85.9 and 98.3 % for cations, compared with anions, which showed a slightly lower rejection ranging from 71.4 to 99.2 %. Furthermore, the removal efficiency of the ESPA2 membrane ranged between 94.1 and 98.4 % for cations whereas anion rejection ranged between 89.5 and 99.7 %. The highest rejection achieved by both NF-90 and ESPA2 was for sulphate that reached 99.7%.
- Samples collected from WGB32 at Botany: the removal efficiency of the NF-90 membrane ranged between 60 and 100 % for cations whereas anion rejection ranged between 64.8 and 99.5 %. On the other hand, the removal efficiency of the ESPA2 membrane ranged between 76 and 100 % for cations whereas anion rejection ranged from 76 to 99.7 %. The highest rejection achieved by both NF-90 and ESPA2 was for total mercury and this compound was almost totally was rejected.
- The highest rejection achieved by using a MWNT buckypaper membrane was for calcium which reached 51% for samples collected from the leachate pond at Russell Vale (according to size exclusion mechanism). In contrast, samples collected from WGB32 at Botany showed that the highest rejection achieved by a MWNT buckypaper membrane was for phosphate which reached 69.2% (according to charge repulsion mechanism).

Moreover, the results from this study revealed that the performance of NF and RO membranes in rejecting hydrophilic organic compounds was higher than that for hydrophobic organic compounds and the highest rejection achieved by using NF and RO membranes amounted 98.4 % and 100 %, respectively. Hydrophilic compounds can be effectively rejected by NF/RO membranes using steric hindrance or size exclusion mechanisms. This result totally agrees with previous studies (e.g. Yangali-Quintanilla et al., 2009). In this study, the rejection of hydrophilic neutral compounds by a clean NF-90 membrane was in the range of 62–96% and steric hindrance was the predominant rejection mechanism by this membrane. The same trend was found for a RO membrane (Kimura et al., 2003). High rejection of hydrophilic neutral solutes by NF-90 was also stated in other study (Xu et al., 2006). The role of steric hindrance (size exclusion) in the separation of trace organic contaminants was dramatically shown in a study by Nghiem et al. (2010) and confirms what we found in this study.

The results from this study revealed that the performance of NF and RO membranes in rejecting hydrophobic compounds was lower than that for hydrophilic compounds since they can be adsorbed onto NF/RO membranes and then diffuse through the dense polymeric matrix, resulting in the lower removal for these compounds compared to hydrophilic compounds. This finding in this research is consistent with previous studies (Nghiem et al., 2006). Since ibuprofen is a highly hydrophobic compound, as reflected by its high  $\log K_{ow}$  value (3.5) at pH 4, it adsorbed onto the NF membrane. This observed adsorption can probably be attributed to hydrophobic interactions between ibuprofen and hydrophobic domains within the membrane polymer matrix.

The same trend was seen in the performance of MWNT buckypaper membranes in rejecting hydrophilic organic compounds. It was higher than for hydrophobic organic compounds and the highest rejection reached 88.5 %, however it remains less efficient than the NF and RO membranes in rejecting VOCs. It can be elucidated that hydrophobic compounds can adsorb onto the MWNT membrane and then diffuse

through the bundles, causing significant transport of these compounds across the bundles and the spaces between the bundles, which can be considered as pores. This completely agrees with previous studies (Shih and Li, 2008). This study concluded that the adsorption of VOCs (hydrophobic compounds), such as trichloroethylene, *n*-hexane, and benzene onto MWCNTs seem to decrease marginally with a decreasing trend of their molecular weight, suggesting that van der Waals interactions control the sorption process between these hydrophobic compounds and surface of MWCNTs. On the other hand, because hydrophilic compounds do not absorb onto the MWNT membrane, hydrophilic compounds can be effectively rejected by the MWNT buckypaper membrane through the non-electrostatic interactions, which include hydrophobic interactions and hydrogen bonding. This can be illustrated by what has been inferred in another study by Moreno-Castilla (2004). This study stated that compounds consisting of large molecules were reported to enter the inner pores of CNTs with diameters of 3-5 nm. It can be interpreted that the organic molecules are too large to fit into the inner pores of CNTs. Accordingly, the availability of sites for organic chemical adsorption on CNTs is greatly dependent on CNT properties as well as their aggregation. In contrast, Qu et al. (2013) concluded that CNTs have much higher adsorption capacity for some large organic molecules since their larger pores occur in bundles with more available sorption sites. In other words, CNT aggregates have interstitial spaces and grooves, which are considered high adsorption sites for organic molecules (Pan and Xing, 2008).

### **8.3 Separation mechanisms**

The separation of volatile organic compounds by high-pressure membranes is mainly attributed to the size exclusion mechanism (steric hindrance mechanism) created between the solutes and the membrane's polymeric matrix (Agenson and Urase, 2007; Verliefde et al., 2007b). Organic contaminants larger than the membrane pore size are usually efficiently removed as a consequence of a sieving effect, whereas smaller contaminants can pass through the membrane (Van der Bruggen et al., 1999; Van der Bruggen and Vandecasteele, 2002; Chen et al., 2004). Hydrophobic

interactions between hydrophobic compounds and membranes could play a role in retention of organic compounds. These compounds may adsorb onto membrane surfaces and subsequently may diffuse through RO and particularly NF membranes, resulting in lower rejections than would be expected based only on size exclusion mechanisms (Nghiem and Schäfer, 2002; Nghiem et al., 2004b; Braeken et al., 2005). Since most NF/RO membranes are negatively charged at neutral pH, electrostatic interactions between charged organic compounds and the charged membrane surface can also play a role in the rejection of trace organic contaminants. Many studies that have focused on electrostatic interactions, showed an increase in rejection of negatively charged organic compounds because of electrostatic repulsion between the negatively charged membrane and the negatively charged organic compound (Nghiem et al., 2006; Verliefde et al., 2007b; Verliefde et al., 2008).

Results reported in this study are fully compatible with the previous studies mentioned above with regard to the rejection mechanism of volatile organic compounds which were detected in groundwater collected from EW10D and EW13D. Results in this study revealed that the performance of the NF-90 and ESPA2 membranes in rejecting hydrophilic compounds (e.g. trichloroethylene and tetrachloroethylene) was higher than that of its hydrophobic compounds (e.g. dichloromethane and vinyl chloride). Whereas hydrophilic compounds can be effectively rejected by NF/RO membranes using steric hindrance or size exclusion mechanisms, hydrophobic compounds can be adsorbed onto NF/RO membranes and then diffuse through the dense polymeric matrix, resulting in lower rejections for hydrophobic compounds than may be expected purely based on size exclusion effects.

The separation of inorganic contaminants through NF/RO membranes is mostly attributed to size exclusion along with Donnan exclusion (charge repulsion mechanism; Yaroshchuk, 2001; Teixeira et al., 2005; Verliefde et al., 2008; Bolong et al., 2009). Nevertheless, ionic permeation studies show that ionic size alone does not explain the rejection characteristics of ions during membrane filtration processes (Tansel et al., 2009). In the electrostatic repulsion mechanism (Donnan exclusion),

the rejection is subject to relative charge interaction and not only on molecule size. Accordingly, electrostatic interactions between charged solutes and the charged membrane surface can also play a role in the rejection (Richards et al., 2011). The results obtained from this study demonstrate that the separation of inorganic contaminants (cations and anions) through NF/RO membranes was basically controlled by size exclusion and the electrostatic repulsion mechanism (Donnan exclusion) and this finding is consistent with many previous studies (Yaroshchuk, 2001; Teixeira et al., 2005; Verliefde et al., 2008; Bolong et al., 2009).

On the other hand, the separation process of volatile organic compounds through a MWNT membrane is governed by one or more mechanisms, including adsorption and size exclusion (Bellona et al., 2004; Díaz et al., 2007; Shih and Li, 2008). Adsorption is a dominant mechanism to retain organic contaminants utilizing MWNTs. The prediction of adsorption of organics onto MWNTs is a complex process; however numerous possible interactions between organic molecules and MWNTs have been suggested. Hydrophobic interactions,  $\pi$ - $\pi$  stacking interactions, van der Waals forces, electrostatic interactions, and hydrogen bonding interactions might act individually or simultaneously (Yu et al., 2014). The findings in this research confirm what has been reached in previous studies that reported some of the rejection mechanisms of volatile organic compounds using a MWNT membrane. It was observed that the performance of MWNT buckypaper membranes in rejecting hydrophilic compounds (carbon tetrachloride, trichloroethylene and tetrachloroethylene) was higher than hydrophobic compounds (other VOCs which were examined in this study). This is because hydrophobic compounds can adsorb onto MWNT membranes and then diffuse through the bundles, causing substantial transport of these compounds through the bundles and the space between the bundles which can be considered as pores. Van der Waals interactions control the sorption process between these hydrophobic compounds and surface of MWNTs. On the other hand, since hydrophilic compounds do not absorb onto the MWNT membrane, hydrophilic VOCs can be effectively rejected by a MWNT membrane using size the exclusion mechanisms or through the non-electrostatic interactions which include hydrophobic interactions and hydrogen bonding.

The separation of inorganic contaminants by MWNT membranes is fundamentally attributed to size exclusion as well as Donnan exclusion (charge repulsion mechanism; Yaroshchuk, 2001; Teixeira et al., 2005; Verliefde et al., 2008; Bolong et al., 2009). Size exclusion occurs when the solutes size is larger than the pore size of the MWNT membrane. Therefore, contaminants are removed effectively by a sieving mechanism (Chen et al., 2004; Verliefde et al., 2008). The electrostatic repulsion mechanism is another significant factor affecting the ability of a MWNT membrane to separate charged solutes existing in a mixture. According to this mechanism, the ion separation results from the electrostatic interactions between ions and the negatively charged MWCNT membrane (Vatanpour et al., 2011). In contrast, adsorption also is considered a key mechanism to retain some inorganic contaminants and it is an efficient technique for the removal of such contaminants from contaminated water (Liu et al., 2013b). The adsorption mechanism is commonly governed by the relative hydrophilicity or hydrophobicity of the membrane surface, and hydrogen bonding in addition to other interactions between solutes and the membrane (Li et al., 2003; Liu et al., 2013b). Results reveal that the separation of inorganic contaminants (cations and anions) through MWNT membranes was attributed to size exclusion and the electrostatic repulsion mechanism (Donnan exclusion) and this finding supports what has been inferred in previous studies (Ahn et al., 2012; Das et al., 2014).

#### **8.4 Flux decline and roughness**

Significant permeate flux decline was observed with the NF-90 and ESPA2 membranes, especially for samples which were collected in the summer season from the leachate pond and amounted to 85% and 83.4%, respectively. On the other hand, substantial permeate flux decline could be observed with the NF-90 membrane that exhibited a permeate flux decline of 49.2% and 34.2 % over 8 hours for samples collected from EWB13D and EWB10D, respectively. In contrast, indiscernible flux decline could be observed with the ESPA2 membrane that only exhibited a permeate flux decline of 15.5 % and 1.7 % for samples were collected from EWB13D and EWB10D, respectively; this can be attributed to membrane surface roughness. In

fact, there is a strong correlation between fouling tendency and the membrane surface roughness and this totally agrees with many previous studies (e.g. Vrijenhoek et al., 2001; Boussu et al., 2007; Xu et al., 2010). As stated in Table 3-3 (chapter 3), the NF-90 has a substantial surface roughness of 63.9 nm, whereas the ESPA2 has a slightly smoother membrane surface with a corresponding surface roughness of 30.0 nm. Additionally, it is notable that after using MWNT buckypaper as a membrane in this study the flux was linear. However, flux was not linear and stable in cases when NF-90 and ESPA2 were used as membranes, particularly for contaminated surface water samples collected from the leachate pond at Russell Vale, specifically for those samples that were collected in autumn and summer seasons. This phenomenon can be explained by the porosity of the MWNT membrane (~28 nm) being higher than the porosity of the NF-90 and ESPA2 membranes (0.68 nm and non-porous respectively).

The AFM images of the ESPA2 and NF-90 membranes which were obtained in this study confirmed existing different extents and occurrences of surface roughness. Surface topography of ESPA2 showed a typical nodular (hills and valleys) morphology. This feature can be found in most RO membranes as stated in previous studies (Vrijenhoek et al., 2001; Freger et al., 2002). The same thing applies to the NF-90 membrane used in this study with the hill to hill distance being much smaller, which associates totally with the much lower thickness of the active layer (15–40 nm for NF compared to 200–300 nm for RO). This morphology seems to be influenced by the underlying supporting layer, and could be observed as a fingerprint of the thin-film composite (TFC) polyamide (PA) membrane (Freger et al., 2002). Because these “valleys” are expected to be of irregular shape, such as the surface topography of the NF-90 membrane, a lodged particle may not fully “plug” the “pore-like” valley; nevertheless it may significantly restrict flow through the opening. Consequently, the valleys quickly become “clogged,” resulting in notable loss of permeate flux. In the case of the ESPA2 membrane, the AFM images revealed the “valleys” are expected to have a slightly more regular shape and there will be less “valley clogging.” Although the same number of particles are placed on the membrane, they would likely be more equally spaced leading to less overall flux



decline (or fouling; Vrijenhoek et al., 2001). The results obtained in this study indicate that the colloids are located mainly in the valleys on the surface after filtration; i.e. “valley clogging” has taken place (e.g. Vrijenhoek et al., 2001; Hoek et al., 2003). This happened as a result of the roughness of the NF and RO membranes. However, the colloids are distributed over the entire membrane surface and created a dense and uniform cake layer on the membrane surface because of hydrophobic interactions between the contaminants and membrane surfaces (Jonathan and C., 2002; Boussu et al., 2007).

On the other hand, the AFM image of the carbon nanofibrous films exhibited that the vertically aligned CNTs have an average diameter of ~294 nm and length of 10 µm. The amount of MWNTs in the composite membrane is an important factor affecting the morphology, therefore the AFM images (in chapter 5) indicate that the roughness of the membrane was somewhat smoothed by adding 0.1 wt % MWNT to the composite membrane. This result is consistent with what has been reached in previous studies (Vatanpour et al., 2011). In this study the roughness of the MWNT membrane was reduced by adding 0.04 wt % MWNT to the polymer matrix. Subsequently, the roughness increased considerably after adding 0.2 wt % and once again reduced by adding 0.4 wt %.

## **8.5 SEM-EDS analysis**

Distribution of elements deposited on NF/RO membranes was obtained from SEM with additional semi-quantitative energy dispersive spectrometer (EDS) analysis. SEM-EDS images obtained for virgin NF/RO membranes and membranes fouled by EWB10D, EWB13D, WGB32 (all these three sites are located at Botany Bay) and the leachate pond (this site is located at Russell Vale) showed that carbon, oxygen and sulphur were detected in all samples including the virgin membrane because they were parts of the membrane polymeric composition. Notably, platinum existed in all samples, including the virgin membrane, as a result of membrane coating. Specifically, a sulphur peak was found clearly in NF-90 and ESPA2 membranes fouled by EWB10D and EWB13D indicating the participation of sulphate scale in

fouling. Additionally, a small level of silicon, aluminium, sodium and chlorine were found in the alginate fouling layer of NF-90 membranes fouled by WGB32 and EWB13D. It can be explained by the deposition of contaminants (Si, Al, Na and Cl) on the membranes caused by the increase in membrane selectivity due to biofouling (Melián-Martel et al., 2012). A high level of calcium existed in the alginate fouling layer of NF-90 and ESPA2 membranes fouled by leachate pond and WGB32 samples due to the ability of calcium to complex with carboxyl groups which are very common in organic foulants, as well as the surface of NF/RO membranes (Mo et al., 2011). This finding is totally consistent with previous studies that calcium could make cross-links with alginate molecules and accumulate in the alginate fouling layer (Lee et al., 2006; Li et al., 2007; Antony et al., 2012).

Also the distribution of elements deposited on MWNT membranes was analysed using SEM with an additional semi-quantitative energy dispersive spectrometer (EDS). The EDS spectrum of virgin MWNT buckypaper membranes and membranes fouled by EWB10D, EWB13D, WGB32 and the leachate pond displayed peaks corresponding to titanium and aluminum as well as a large amount of carbon and a considerable amount of oxygen as part of the membrane composition, and consequently, the elements were detected in all samples (virgin and fouled). A high level of calcium was found in the MWNT membrane fouled by the leachate pond due to the ability of calcium to complex with carboxyl groups which are very common at the surface of CNTs. The large amount of chlorine found in the MWNT membrane fouled by EWB10D and the lower amounts in the MWNT membrane fouled by EWB13D can be attributed to the rejection process for this compound by the size exclusion mechanism. A low level of magnesium was found in the MWNT membrane fouled by the leachate pond whereas a considerable amount of sodium and sulphate was found in a MWNT membranes fouled by EWB10D and EWB13D, respectively. This can be attributed to the rejection process for these compounds through the size exclusion mechanism and resulting diffusion into the membrane surface (Van der Bruggen et al., 2004).

## 8.6 Mitigation of flux decline effects

Flux decline is considered a significant issue caused by fouling and adversely affects membrane performance due to declining permeate flux, increased operational cost, and shortened membrane life. So that we can propose solutions to address the fouling we must understand the process of fouling which can be simplified through Figure 8-1.

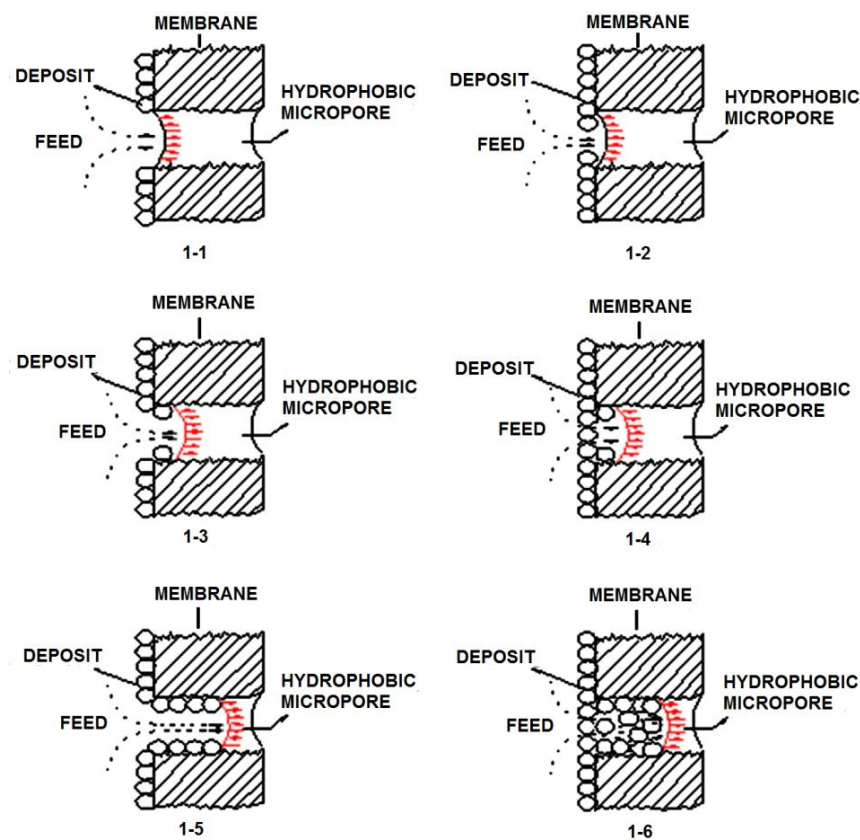


**Figure 8-1:** Process of membrane fouling (adapted from Wang et al., 2014)

To alleviate this problem, two approaches are commonly used. The first method involves reducing the fouling by employing sufficient feed pretreatment.

### **8.6.1 Pretreatment**

Pretreatment is one of the key factors determining the success or failure of a filtration process. To control and decrease fouling occurrences in pressure driven processes, pretreatment is typically used prior to the filtration, aiming to reduce the content of particles and macromolecules which are able to be gathered on the membrane surface. In fact, many performance problems can be traced back to insufficient pretreatment of the feedwater followed by fouling or scaling of the membrane surface. Several approaches of pretreatment for filtration process have been recommended by many researchers. Conventional pretreatment depends on mechanical treatment (media filters, cartridge filters) supported by extensive chemical treatment (Sikora et al., 1989). Previously, conventional pretreatment (i.e., coagulation, flocculation, acid treatment, pH adjustment, addition of anti-sealant and media-filtration) were commonly used (Sikora et al., 1989). The key issue in using traditional pretreatment is corrosion and corrosion products (Hilal et al., 2004). Furthermore, this pretreatment is considered complex, labour intensive and space consuming (Van Hoof et al., 2001).

The most effective techniques widely used as pretreatment in filtration processes are microfiltration (MF) and ultrafiltration (UF). MF can eliminate suspended solids and lower the silt density index (SDI), whereas UF not only retains suspended solids and large bacteria, but also retains (dissolved) macromolecules, colloids and small bacteria (Hilal et al., 2004). A great feature of using MF or UF pretreatment is that these systems can remove particles and colloids as small as 0.2  $\mu\text{m}$  for MF and 0.02  $\mu\text{m}$  for UF, and have more than 4 log scale removals of bacteria. Log removal is usually calculated as follows (Equation 8-1):

$$\text{Log Removal} = -\log_{10} (100 - x) + 2 \quad (8-1)$$

where  $x$  is the percentage removal of bacteria from feedwater. Larger log removal values correspond to a greater proportion of bacteria removed from feedwater. This

leads to consistently high treated water quality, with SDI consistently less than 3 (Gray et al., 2011). Several studies have been conducted to examine the potential of using MF and UF membranes as pretreatment for filtration processes and they concluded that MF and UF systems were identified as promising techniques and a good alternative to replace conventional pretreatment (Redondo, 2001; Van Hoof et al., 2001; Barredo-Damas et al., 2006; Li et al., 2012; Domingues et al., 2014).

In this study a MF membrane (0.45  $\mu\text{m}$ ) was used for separation of colloidal and suspended materials which are present in contaminated surface and groundwater samples collected from the leachate pond at Russell Vale and WGB32 at Botany Bay. This technique is a feasible and effective way to remove colloidal and suspended solids and subsequently delayed fouling occurrences in the pressure driven processes. However, this technique was insufficient when used as pretreatment for samples collected from a leachate pond at Russell Vale in the summer season due to continued fouling. High temperatures and light intensity, as well as nutrient availability, in this season favour the growth and photosynthetic processes and result in high release of extracellular organic matter (EOM). Because the molecular weight of EOM is smaller than pore size of the MF membrane, the rejection of this material will be low and later will exist in feed reservoir of the NF/RO filtration system. Consequently, it caused harmful effects on the filtration system represented by high fouling. Results that have been concluded in this study regarding inefficiency of MF to remove EOM are consistent with previous studies. Zhang et al. (2013) conducted a study to examine the influence of pretreatment of algal organic matter (AOM) on the fouling of a ceramic MF membrane by comparing the flux decline and reversible fouling for 0.45  $\mu\text{m}$ , 1  $\mu\text{m}$  and 5  $\mu\text{m}$  pretreatment of water containing AOM and non-pretreatment for AOM. They concluded that the 0.45  $\mu\text{m}$  and 1  $\mu\text{m}$  pretreatment AOM caused more rapid flux decline compared with the 5  $\mu\text{m}$  pretreatment for AOM. It can be interpreted that the flux decline was fundamentally caused by the gel/cake layer formed mostly because of the deposition of large AOM molecules on the surface of the ceramic MF membrane. According to the size exclusion mechanism, these large AOM molecules can pass through the 5

$\mu\text{m}$  pretreatment more readily than 0.45  $\mu\text{m}$  and 1  $\mu\text{m}$  pre-treatments thus it shows less flux decline.

### **8.6.2 Membrane modification**

The second method includes membrane treatment and membrane modification which is carried out to restore membrane flux efficiency. To modify the surface of membranes many methods can be used. However the most effective surface modification methods are surface adsorption, surface coating, plasma treatment and chemical reactions. Many efforts are made by scientists to modify the surface properties of water filtration membranes (Xie et al., 2007). Zou et al. (2011) conducted a study to investigate surface hydrophilic modification of RO membranes by plasma polymerization for low organic fouling. They concluded that the modified membranes achieved an exceptional maintenance of flux compared to the untreated membranes. After 210 min of filtration, no flux decline was found for the modified membranes, whereas a 27% reduction of the initial flux was noticed for the untreated membrane. Also, Zhou et al. (2009) examined the modification of a polyamide RO membrane by electrostatic self-assembly of polyethyleneimine (PEI) on the membrane surface. They concluded that the charge reversal on the membrane surface due to using the PEI layer was shown to increase the fouling resistance to cationic foulants because of the enhanced electrostatic repulsion and increased surface hydrophilicity as well.

Since surface coating is a simple method and easily applied, it has attracted the attention of many researchers and membrane manufacturers to modify the surface of membranes. Kim and Lee (2006) conducted a study to examine RO and NF membranes with decreased surface charge and surface roughness that were used to treat dyeing process wastewater. These membranes after being coated with polyvinyl alcohol (PVA) showed a significant reduction in fouling. Louie et al. (2006) in another study used a physical coating to investigate polyamide RO membranes with polyether–polyamide block copolymer (sold commercially under the trade name

PEBAX), which was a very hydrophilic block copolymer of nylon-6 and poly (ethylene glycol). The coating significantly reduced surface roughness without notable change in contact angle. Also, Hernadi et al. (2003) conducted a study aimed to know the effect of coating on composite MWNT. This study concluded that an effective interfacial bonding between the carbon nanotube surface and forerunners offers a constant reinforcement composite fiber, which provides a favourable wettability for dispersion in either polymer or metal matrices.

Surface modification using plasma treatment is considered one of the most significant technologies of polymer materials to enhance the surface properties. The significant advantage of plasma modification is that the surface properties and biocompatibility can be improved selectively whereas the bulk attributes of the membrane remain unchanged (Xu et al., 2009). Zou et al. (2011) reported that surface hydrophilic modification of RO membranes by plasma polymerisation has displayed a perfect improvement in membrane anti-fouling performance. Reid et al. (2014) conducted a study to examine biofouling control by hydrophilic surface modification of polypropylene feed spacers by plasma polymerisation. These authors concluded that plasma treatment of conventional feed spacers has the potential to decrease affinity for bacterial attachment, and can offer a viable and complementary method to direct membrane surface modification for biofouling control. Kim et al. (2011), after they conducted many experiments, concluded that the membrane surface hydrophilicity was improved after using the plasma treatment.

### **8.6.3 Membrane cleaning**

Chemical treatment of membranes is the dominant means for chemically modified reactions and is essential to recover the permeate flux. To ensure effective chemical treatment without damaging the membrane, it is essential to take into account the ideal use of chemicals, their concentrations, the time of exposure, temperature, flow and pressure (Simon et al., 2012). The choice of chemical cleaning of fouled membranes is dependent on the type of fouling to be removed. For chemical cleaning

of fouled membranes, five groups of cleaning agents are usually used: alkalies, acids, metal chelating agents, surfactants and enzymes. These chemicals can be used separately or in combination. Liikanen et al. (2002) reported that alkaline and chelating cleaning agents, such as ethylene diamine tetra acetic acid (EDTA), increased membrane flux. The acidic cleaning is considered an effective method for removal of precipitated salts (scaling) from the surface of the membrane and from the pore (Schäfer et al., 2005).

There are many common acidic cleaners used effectively for cleaning scale compounds and metal oxides through solubilisation and chelating, such as nitric acid, hydrochloric acid and phosphoric acid. For example, Alzahrani et al. (2013c) conducted a study aimed to identify foulants, fouling mechanisms and cleaning efficiency for NF and RO treatment of produced water and concluded that cleaning with sodium dodecyl sulfate (SDS) for up to 5 min resulted in up to 85.7% recovery of flux in NF membranes, whereas cleaning for 15 min resulted in almost 100% flux recovery. In case of RO membranes, SDS was more effective at breaking the fouling layer and totally restored permeability when applied for 5 min and gave better results than when applied for 15 min. Al-Amoudi et al. (2008) concluded an increase in NaCl rejection by NF membranes (NF-DK and NF-DL) occurred after immersion of the membranes overnight in a caustic cleaning solution.

Cleaning using enzymes has the benefits of operating in mild conditions, reduced chemical usage, lower energy costs because of lower cleaning temperatures, and biodegradable effluents (Mulder, 1996). Muñoz-Aguado et al. (1996) stated that  $\alpha$ -chymotrypsin (bovine pancreas) enzyme could clean a polysulfone membrane fouled by whey with up to 99% of flux recovery. Also, Argüello et al. (2003) concluded that high cleaning efficiency was achieved (close to 100%) in short operating times (20 min) after using enzymatic cleaning for membranes.

Surfactants are amphiphilic compounds with hydrophobic and hydrophilic segments. They can displace foulants from surfaces by strong adsorption characteristics and prevent redeposition. Chen et al. (1992) noted that surfactant coatings can provide



resistance to protein fouling over short periods. Also Wilbert et al. (1998) concluded that using non-ionic surfactant [such as, octylphenol-poly ethylene oxide (PEO) with nine PEO repeat units, Triton X-100] as pretreatment for RO and NF membranes has the potential to decrease the cost of producing drinking water.

### **8.7 Characterisation of MWNT buckypaper membranes**

The electrical, mechanical and morphological properties of MWNT buckypaper membranes have been characterised and are compared to those of the corresponding buckypaper membranes containing the same surfactant Triton X-100. Results stated in this study revealed that electrical conductivity varies significantly from those reported for MWNT buckypapers prepared using the same dispersant. The average electrical conductivity of MWNT/Triton-X buckypapers reported here ( $\sim 56$  S/cm) was roughly double the average conductivity of MWNT/Triton-X buckypapers which were mentioned in a previous study ( $\sim 24$  S/cm; Sweetman et al., 2013). Mechanical property measurements in this research displayed significant variation from those obtained for MWNT buckypapers prepared under the same conditions (Sweetman et al., 2013). For example, the tensile strength, Young's modulus and ductility of a MWNT/Triton X-100 buckypaper prepared in this study was  $3.4 \pm 0.8$  MPa,  $0.4 \pm 0.2$  GPa and  $2.4 \pm 0.2\%$  respectively. In contrast, the tensile strength, Young's modulus and ductility of a MWNT/Triton X-100 buckypaper prepared in a previous study were  $6 \pm 3$  MPa,  $0.6 \pm 0.3$  GPa and  $1.3 \pm 0.2\%$ , respectively (Sweetman et al., 2013). Also, other mechanical properties such as an elongation and toughness in this research exhibited substantial variation from those obtained for MWNT buckypapers prepared under the same conditions (Han et al., 2014). The elongation and toughness of a MWNT/Triton X-100 buckypaper prepared in this study was  $2.4 \pm 0.2\%$  and  $0.05 \pm 0.01$  MJ/m<sup>3</sup>, respectively. In contrast, the elongation and toughness of a MWNT/Triton X-100 buckypaper prepared in previous study were  $8.89 \pm 0.94\%$  and  $0.69 \pm 0.12$  MJ/m<sup>3</sup>, respectively (Han et al., 2014).

Analysis of scanning electron microscopic images of the surfaces of MWNT/Triton X-100 buckypapers which prepared in this study revealed that the diameter of their surface pores ( $65.6 \pm 2$  nm) was marginally smaller than that of the corresponding materials prepared using MWNTs ( $80 \pm 2$  nm; Sweetman et al., 2013). Also, the average internal pore diameter of MWNT buckypapers prepared in this study ( $27.7 \pm 2$  nm) was found to be slightly higher than that of their MWNT counterparts ( $24 \pm 1$  nm; Sweetman et al., 2013), after analysis of binding isotherms derived from nitrogen adsorption/desorption measurements performed on the materials. On the other hand, another study (Han et al., 2014) revealed that the diameter of their surface pores (61.5 nm) was slightly smaller than that of our finding ( $65.6 \pm 2$  nm) for MWNT buckypapers prepared using the same dispersant (Triton X-100). In contrast, the average internal pore diameter (29.4 nm) of MWNT buckypapers in the study conducted by Han et al. (2014) was found to be slightly higher than that concluded in this thesis ( $27.7 \pm 2$  nm), based on analysis of binding isotherms derived from nitrogen adsorption/desorption measurements performed on the materials. The impregnation quality of the composite samples can be assessed by analysing the specific surface area (ABET). The ABET of the buckypapers in this study was  $141 \pm 2$  m<sup>2</sup>/g, which is comparable with those reported by Han et al. (2014;  $\sim 178$  m<sup>2</sup>/g) and considerably smaller than those reported by Sweetman et al. (2013;  $300 \pm 1$  m<sup>2</sup>/g).

To determine the volume of pores with diameters smaller and larger than 3 nm, MWNT buckypapers were subjected to analysis using the Barrett, Joyner and Halendar (BJH) and Horvath-Kawazoe (HK) methods (Barrett et al., 1951; Horvath and Kawazoe, 1983). Numerical integration in our study shows that intertube pores contribute  $\sim 14\%$  of the total free volume of the buckypaper, while interbundle pores contribute  $\sim 86\%$  of the total free volume. These results completely agree with the results of a similar study which was conducted by Sweetman et al. (2013) who reported that intertube pores contribute  $\sim 12\%$  of the total free volume of the MWNT Triton X-100 buckypaper, whereas interbundle pores contribute  $\sim 88\%$  of the total free volume of the buckypaper. Comparison of morphological and mechanical properties of MWNT buckypaper prepared in this study to those of corresponding

buckypaper membranes containing the same surfactant Triton X-100 are presented in Table 8-1.

**Table 8-1:** Comparison of morphological and mechanical properties of MWNT buckypaper prepared in this study to those of corresponding buckypaper membranes containing same surfactant Triton X-100.

Buckypaper	$A_{\text{BET}}$ ( $\text{m}^2/\text{g}$ )	$D_{\text{BET}}$ (nm)	Interbundle pore volume (%)	Tensile strength (MPa)	Young's modulus (GPa)	Toughness (J/g)
MWNT/Trix-100 <sup>a</sup>	$141 \pm 2$	$27.7 \pm 2$	$86.4 \pm 2$	$3.4 \pm 0.8$	$0.4 \pm 0.2$	$0.05 \pm 0.01$
MWNT/Trix-100 (Sweetman et al., 2013)	$300 \pm 1$	$24 \pm 1$	$91 \pm 5$	$6 \pm 3$	$0.6 \pm 0.3$	$0.10 \pm 0.06$
MWNT/Trix-100 (Han et al., 2014)	$\sim 178$	$29.4$	$61.5$	$\sim 1.37$	NA <sup>b</sup>	$0.69 \pm 0.12$
SWNT/Trix-100 (Sweetman, 2012)	$790 \pm 4$	$4.0 \pm 0.4$	$84 \pm 5$	$20 \pm 10$	$1.7 \pm 0.3$	$0.3 \pm 0.2$

<sup>a</sup> Findings of this study.

<sup>b</sup> Not available.

From the above, it can be said that there are significant variations in the values of mechanical, electrical and morphological properties of MWNT buckypaper membranes reported in this study compared with MWNT buckypaper membranes being which were mentioned in previous studies despite these membranes prepared under the same conditions. This can be attributed to conditions associated with the manufacturing process of buckypapers, such as the purity and provider of the carbon nanotubes.

## 8.8 The relationship between seasonal effects using membrane technology

The relationship between seasonal effects using membrane technology was also examined in this study. Results indicate that flux was good for samples which were collected from contaminated surface and groundwater in all seasons, except for samples which were collected from the leachate pond at Russell Vale specifically in the summer season due to fouling. High temperatures and light intensity as well as nutrient availability in this season favour the growth of algae blooms. Adverse

effects of cyanobacterial species in the algal blooming (e.g. *Microcystis aeruginosa*) can create lethal toxins and soluble extracellular organic matter (EOMs) into water during cell growth and lysis (Codd, 2000; Henderson et al., 2008; Ma et al., 2012). Aqueous EOM resulting from algae metabolites entering downstream water treatment systems can lead to water treatment operational issues such as an increasing coagulant demand and membrane fouling (Fang et al., 2010; Henderson et al., 2010; Zhou et al., 2014). Chiou et al. (2010) stated that algae with more EOM caused faster flux decline. Accordingly, the presence of EOM in the reservoir frequently clogs the pores of membranes, leading to permeate flux decline. Findings revealed that the highest flux decline was 85% and 83.4% for NF-90 and ESPA2, respectively due to fouling as a result of high temperatures in the summer season specifically for samples collected from the leachate pond at Russell Vale.

There is a strong relationship between resistance and deposition of extracellular organic materials (EOM) on the membrane as reported in previous studies. For example, Babel et al. (2002) concluded that the resistance increased linearly with the amount of EOM. Microscopic investigation of the deposited cells on the membrane showed that when algae do not release EOM, cells are dispersed as they are negatively charged resulting in void space between cells and thus higher flux. On the other hand, when cells release EOM, these void spaces are filled by EOM causing reduced flux and higher resistance (Babel et al., 2002). Extracellular materials can lead to linkages between the cells and encourage a more compact deposit ultimately causing less flux. Figure 8-2 can explain a possible mechanism depicting filtration when algae release EOM in matrix. During the filtration process, cells are enclosed with a soft polymer shell (EOM) which is compressible. Water flows through the matrix of extracellular polymer, whereas the polymers are being compressed by higher pressure (Babel and Takizawa, 2010).

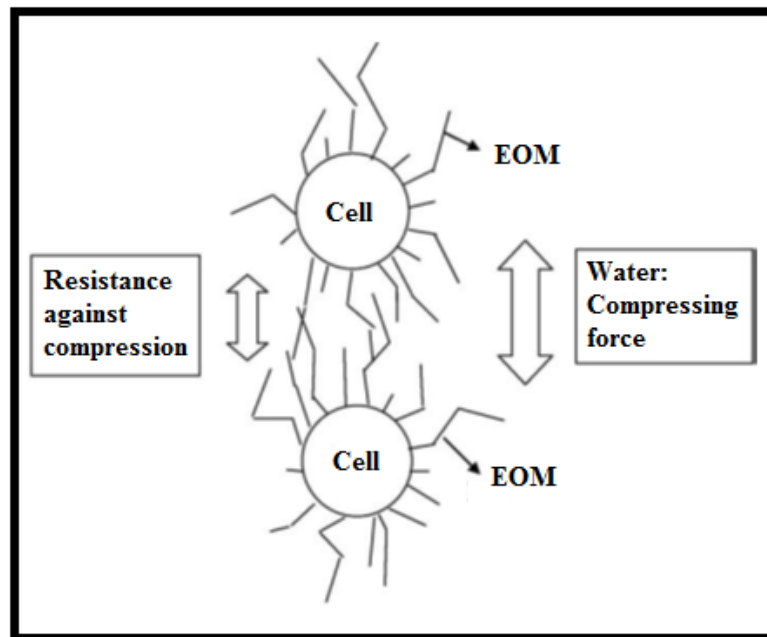


**Figure 8-2:** Explanation a possible mechanism when *Chlorella* release EOM in matrix during filtration process (Babel and Takizawa, 2010).

### 8.9 Comparison of common NF/RO membranes widely used in purification

In this study we used two commercial membranes (namely NF-90 and ESPA2); however beside these membranes there is another two membranes (namely NF270 and BW30) are used commonly in water treatment. Based on the estimation of pore size, the NF270 membrane could be classified as a loose nanofiltration membrane whereas the NF-90 could be classified as a tight nano-filtration membrane and consequently it can retain the contaminants more than NF270. On the other hand, the two reverse osmosis membranes (BW30 and ESPA2) can be assumed to have no clearly defined pore structure. In fact, as can be seen in Table 8-2, sodium rejection was in the order of the classified pore diameter: NF-270<NF-90<BW30~ESPA2. Therefore, it can be said that the BW30 and ESPA2 membranes have been used quite extensively for water recycling applications as well as NF-90 membrane.

**Table 8-2:** Comparison of properties for four NF/RO membranes.

Membrane	Average pore Diameter <sup>a</sup> (nm)	Na <sup>+</sup> rejection <sup>b</sup> (%)	Molecular weight cut-off <sup>c</sup> (g/mol)	Contact angle <sup>d</sup> (°)	Surface Roughness <sup>d</sup> (nm)
<b>NF270</b>	0.84	45.0	200-300	24	4.1
<b>NF-90</b>	0.68	85.0	~200	42.5	63.9
<b>ESPA2</b>	Not applicable	96.5	~100	60.6	30.0
<b>BW30</b>	Not applicable	97.7	~100	53.4	62.3

<sup>a</sup> (Nghiem et al., 2004b).

<sup>b</sup> Feed solution contains 20 mM NaCl and 1 mM CaCl<sub>2</sub> (pH 8).

<sup>c</sup> Provided by the manufacturers.

<sup>d</sup> (Alturki et al., 2010).

Finally, through what has been discussed in this chapter recommendations can be presented for treatment of waters collected from Russell Vale and Botany Bay. According to the result obtained from this study, water samples collected from EWB10D and EWB13D do not need pretreatment because these samples collected from wells and colloidal as well as solid materials do not exist in these waters. Also, results reported in this study revealed that permeate flux decline was observed with the NF-90 and ESPA2 membranes when investigated water samples collected from EWB10D and EWB13D. This issue can be solved by using chemical cleaning of fouled membranes using alkalies, acids and metal chelating agents. Usually chemical cleaning [e.g. cleaning with sodium dodecyl sulfate (SDS)] used for 5 minutes to 15 minutes as many scientific researchers have been recommended (Alzahrani et al., 2013c). This leads to improved membrane performance and recovery of flux in membranes. Moreover, results obtained from this study concluded that the preferred filtration system to retain contaminants from water samples collected from EWB10D and EWB13D is RO system are represented by using ESPA2 membrane.

On the other hand, water samples collected from leachate pond and WGB32 need pretreatment using microfiltration because these samples contain colloidal and solid materials. Results reported in this study revealed that a significant flux decline was observed with the NF-90 and ESPA2 membranes when using the examined water samples collected from leachate pond and WGB32. To solve this issue, the same approach which was mentioned above can be used. Furthermore, results reported in this study revealed that the preferred filtration system to retain contaminants from water samples collected from leachate pond and WGB32 is the NF or RO systems, represented by using NF-90 or ESPA2 membranes. Table 8-3 summarised the recommended treatment for waters collected from EWB10D, EWB13D, leachate pond and WGB32.

**Table 8-3:** The recommended treatment for contaminated waters collected from sites at Russell Vale and Botany Bay.

The recommended treatment	Site name			
	EWB10D at Botany Bay	EWB10D at Botany Bay	Leachate pond at Russell Vale	WGB32 at Botany Bay
<b>Pretreatment</b>	No need	No need	Microfiltration	Microfiltration
<b>Preferred filtration method</b>	ESPA2	ESPA2	ESPA2 or NF-90	ESPA2 or NF-90
<b>Membrane cleaning</b>	Chemical treatment	Chemical treatment	Chemical treatment	Chemical treatment

Additionally, results reported in this study revealed that permeate flux decline was not observed with MWNT buckypaper membranes when used to investigate water samples collected from EWB10D, EWB13D, leachate pond and WGB32. On the contrary, after using MWNT buckypaper as a membrane in this study the flux was stable and linear. This is due to the higher porosity of the MWNT membrane (~28 nm) compared with the porosity of the NF-90 and ESPA2 membranes (0.68 nm and non-porous respectively). To increase the ability of the MWNT membrane to become a preferred filtration system, improvement of the hydrophilicity of membrane is essential. Surface coating, plasma treatment, radical grafting and chemical reactions

are considered the most effective methods used to improve the membrane surface of MWNT.

#### **8.10 The comparison among the performance of RO, NF and MWNT membranes for removal of organic and inorganic contaminants**

Results that have been reported in this study emphasize the principle that the membrane technology is a promising and effective technology to remove contaminants found in water, whether these contaminants are organic or inorganic. The results stated in this study indicate that the removal efficiency of RO was better than NF and MWNT in rejecting both organic and inorganic contaminants detected in surface and groundwater. This study revealed that the removal efficiency of organic contaminants using ESPA2 ranged between 43.4 - 100 % and 44.4 - 96.2 % for samples collected from EWB10D and EWB13D, respectively, which are located at Botany Bay. On the other hand, the removal efficiency of ESPA2 in rejecting inorganic contaminants ranged between 89.5 - 99.7 % and 76 - 100 % for samples collected from Leachate pond at Russell Vale and WGB32 at Botany Bay, respectively.

Also this study concluded that the removal efficiency of NF-90 in rejecting organic contaminants ranged between 27.6 - 98.4 % and 41.2 - 95.7 % for samples collected from EWB10D and EWB13D at Botany Bay respectively. In contrast, the removal efficiency of NF-90 in rejecting inorganic contaminants ranged between 71.4 - 99.2 % and 60 - 100 % for samples collected from Leachate pond at Russell Vale and WGB32 at Botany Bay, respectively. It is notable that the removal efficiency of MWNT in rejecting organic and inorganic contaminants was the lowest compared to the removal efficiency of RO and NF. This study demonstrated that the removal efficiency of MWNT in rejecting organic contaminants ranged between 39.1 - 88.5 % and 33.1 - 77.3 % for samples collected from EWB10D and EWB13D at Botany Bay, respectively. On the other hand, the removal efficiency of MWNT in rejecting inorganic contaminants ranged between 1.6 - 50 % and 1.3 - 69.2% for samples collected from Leachate pond at Russell Vale and WGB32 at Botany Bay



respectively. Table 8-4 summarised the comparison among the performance of RO, NF and MWNT membranes for removal of organic and inorganic contaminants.

From the above, it can be concluded that the reverse osmosis system (RO) is considered the most reliable and effective system to remove contaminants from surface and groundwater. Consequently, it can strongly recommend this system is used to solve issues related surface and groundwater at Russell Vale and Botany Bay for Wollongong City Council and Orica.

**Table 8-4:** The comparison among the performance of RO, NF and MWNT membranes for removal of organic/inorganic contaminants.

Membrane	The removal rate of organic contaminants (%)		The removal rate of inorganic contaminants (%)	
	EWB10D at Botany Bay	EWB13D at Botany Bay	Leachate pond at Russell Vale	WGB32 at Botany Bay
<b>ESPA2</b>	Ranged between 43.4 - 100 %.	Ranged between 44.4 - 96.2 %.	Ranged between 89.5 - 99.7 %.	Ranged between 76 - 100 %.
<b>NF-90</b>	Ranged between 27.6 - 98.4 %.	Ranged between 41.2 - 95.7 %.	Ranged between 71.4 to 99.2 %.	Ranged between 60 - 100 %.
<b>MWNT buckypaper</b>	Ranged between 39.1 - 88.5 %.	Ranged between 33.1 - 77.3 %.	Ranged between 1.6 - 50 %.	Ranged between 1.3 - 69.2%.

## 8.11 Summary

This chapter began with a thorough literature review to address water scarcity as a significant global issue facing all countries of the world including Australia and therefore water reuse, wastewater recycling and seawater desalination have to be used to mitigate the effects of this problem. Nowadays, membrane technology has become a promising technology that plays a significant role to solve the shortage of traditional sources of water. In particular, membrane technology received more attention in this research, because this study is based on the use of NF/RO and MWNT membranes to rehabilitate contaminated surface and groundwater. Effectiveness of this technology to remove both organic and inorganic contaminants from contaminated water has been discussed.

The separation mechanisms of organic and inorganic contaminants through NF/RO and MWNT membranes have been explained and should be one of the following mechanisms: the size exclusion mechanism (steric hindrance mechanism), the electrostatic repulsion mechanism (Donnan exclusion) and adsorption. However, the separation of organic and inorganic contaminants by NF/RO processes is based predominantly on size exclusion, whereas the separation of organic and inorganic contaminants through MWNT membranes is mostly attributed to an adsorption mechanism.

Flux decline poses an obstacle to using NF/RO and MWNT membranes due to fouling. By reducing or removing fouling, membrane life is extended and consequently economics of membrane applications can increase significantly. To mitigate this issue, two methods are mostly used. The first method involves reducing the fouling by using sufficient feed pretreatment. The second method includes membrane modification which is applied to reinstate membrane flux efficiency. To modify the surface of membranes many approaches can be used, however the most effective surface modification methods are surface adsorption, surface coating, plasma treatment and chemical reactions.

The electrical, mechanical and morphological properties of MWNT buckypaper membranes have been characterised and are compared to those of the corresponding buckypaper membranes prepared under the same conditions using the same surfactant (Triton X-100) as dispersant. Some results related to the characterisation of MWNT membranes which are reported in this study were consistent completely with previous studies, such as intertube pores and interbundle pores of the buckypapers. In contrast, other results reported in this study varied marginally (e.g. the average surface pore diameter and the average internal pore diameter) or significantly (e.g. the electrical conductivity, the tensile strength, Young's modulus and ductility) from previous studies. This can be attributed to conditions associated with the manufacturing process of buckypapers, such as the purity of the carbon nanotubes.

The relationship between seasonal effects using membrane technology has been discussed in this chapter. Results obtained from this study show that flux was good for samples which were collected from contaminated surface and groundwater in all seasons except samples which were collected from the leachate pond at Russell Vale during summer because of fouling. It can be interpreted that the availability of high temperatures, light intensity and nutrients in this season favour the growth and photosynthesis processes and lead to large releases of extracellular organic matter (EOM). Consequently, the existence of EOM in the reservoir frequently clogs the pores of membranes, causing permeate flux decline.

## **CHAPTER 9: CONCLUSIONS AND RECOMMENDATIONS FOR FUTURE STUDIES**

In this dissertation a comprehensive comparison of the performance of three treatment processes to remove the emerging volatile organic compounds (VOCs), cations and anions from contaminated surface and groundwater has been examined. These organic and inorganic contaminants were exposed to the single physical separation mechanisms (NF, RO and MWNT) to measure their removal efficiency. Numerous major factors affecting the removal of volatile organic compounds, cations and anions by these selected processes have also been investigated. Therefore, the challenge in this case is how to harmonise these systems in order to eliminate the diverse types of organic and inorganic contaminants and their changing physicochemical properties.

The results reported in this study indicate that the RO membrane is the preferred membrane for treatment compared to NF and MWNT membranes, and it will contribute to development of clean water for many purposes, in particular agricultural and industrial sectors. However, the high pressures usually used in RO (14-24 bars) resulted in a considerable energy cost. Consequently, membranes with lower rejections of dissolved components, but with higher water permeability, would be preferable to use in water treatment. NF offers numerous advantages such as low operation pressure (8-14 bars), high flux, high rejection of organic and inorganic contaminants, low operation and maintenance costs and it can be a great choice for separation technology. On the other hand, the MWNT mostly removed the volatile organic compounds, in particular the hydrophilic compounds that were rejected through the MWNT buckypaper membrane using the size exclusion mechanism. There is a limitation in removal of hydrophobic organic compounds, cations and anions in untreated MWNT buckypaper membranes. Thus, further membrane development to achieve a smaller pore size, higher pore density and functionalised MWNT (MWNT-COOH and MWNT-NH<sub>2</sub>) combined with different dispersants such as biopolymer (chitosan) is needed to improve the removal of these small organic and inorganic compounds.

The ability of NF/RO and CNT systems as advanced treatment using two commercially available nanofiltration (NF) or reverse osmosis (RO) and MWNT buckypaper membrane (synthesised by vacuum filtration) to remove volatile organic compounds (VOCs) has been investigated. The results revealed that the performance of NF and RO membranes in rejecting hydrophilic compounds was higher than that for hydrophobic compounds and the highest rejection achieved by NF and RO membranes amounted 98.4 % and 100 %, respectively. Hydrophilic compounds can be effectively rejected by NF/RO membranes using the steric hindrance or size exclusion mechanism, whereas hydrophobic compounds can be adsorbed into NF/RO membranes and then diffuse through the dense polymeric matrix, resulting in the lower removal for these compounds compared to hydrophilic compounds. Also the performance of MWNT buckypaper membranes in rejecting hydrophilic compounds was higher than for hydrophobic compounds and the highest rejection reached was 88.5 %. However, it remains less efficient than NF and RO membranes in rejecting VOCs. It can be elucidated that hydrophobic compounds can adsorb onto MWNT membrane and then diffuse through the bundles, causing significant transport of these compounds across the bundles and the spaces between the bundles, which can be considered as pores. On the other hand, because hydrophilic compounds do not adsorb onto the MWNT membrane, they can be effectively rejected by MWNT buckypaper membrane using the size exclusion mechanism.

The rejection of inorganic contaminants by NF/RO and MWNT membranes was investigated using a set of 10 cations and anions. The findings in this study indicate that the performance of the NF and RO membranes in rejecting divalent ions was higher than that for monovalent ion rejection. This phenomenon can be explained by multivalent ions with large hydrated radii (e.g.  $\text{Mg}^{2+}$ ,  $\text{Ca}^{2+}$  and  $\text{SO}_4^{2-}$ ) were retained more than monovalent ions with smaller hydrated radii (e.g.  $\text{K}^+$  and  $\text{Na}^+$ ). The removal efficiency of the NF membrane ranged from 85.9 to 98.3 % for cations, compared with anions, which showed a lower rejection ranging from 71.4 to 99 %. On the other hand, the removal efficiency of the RO membrane ranged from 94.1 to 98.4 % for cations while anion rejection ranged from 89.5 to 99.7 %. In contrast, the performance of MWNT buckypaper membranes in rejecting cations and anions was

much less compared to NF/RO membranes. Moreover, the performance of MWNT buckypaper membranes in rejecting anions was better than for cation rejection and this can be attributed to a charge repulsion mechanism; the anion separation resulting from the electrostatic interactions between negative charge of anions and negative charge existing in the MWNT composite. Additionally, phosphate recorded the highest value of rejection by MWNT buckypaper membrane compared to other anions and reached 69.2% and this can be attributed to multivalent ions with large hydrated radii (e.g.  $\text{PO}_4^{3-}$ ) being retained more than monovalent ions with smaller hydrated radii (e.g.  $\text{Cl}^-$ ). On the other hand, the rejection of calcium was high compared to other cations and it can be explained since calcium has a larger molecular weight (40.08 g/mol), while sodium and magnesium have smaller molecular weight (22.99 g/mol and 24.31 g/mol, respectively) and therefore calcium was rejected by the size exclusion mechanism.

The electrical, mechanical and morphological properties of MWNT buckypaper membranes have been characterised and are compared to those of the corresponding buckypaper membranes containing the same surfactant Triton X-100. Results stated in this study revealed that electrical conductivity varies significantly from those reported for other MWNT buckypapers prepared using the same dispersant. The average of MWNT/Triton-X buckypapers reported here ( $\sim 56$  S/cm) was roughly double the average conductivity of MWNT/Triton-X buckypapers which were mentioned in a previous study ( $\sim 24$  S/cm; Sweetman et al., 2013). Mechanical properties measurements in this research displayed significant variation from those obtained for MWNT buckypapers prepared under the same conditions (Sweetman et al., 2013). For example, the tensile strength, Young's modulus and ductility of a MWNT/Triton X-100 buckypaper prepared in this study were  $3.4 \pm 0.8$  MPa,  $0.4 \pm 4$  GPa and  $2.4 \pm 0.2\%$ , respectively. In contrast, the tensile strength, Young's modulus and ductility of a MWNT/Triton X-100 buckypaper prepared in a previous study were  $6 \pm 3$  MPa,  $0.6 \pm 0.3$  GPa and  $1.3 \pm 0.2\%$ , respectively (Sweetman et al., 2013). Analysis of scanning electron microscopic images of the surfaces of MWNT/Triton X-100 buckypapers revealed that the diameter of their surface pores ( $65.6 \pm 2$  nm) was marginally smaller than that of the corresponding materials

prepared using MWNTs ( $80 \pm 2$  nm). In contrast, the average internal pore diameter of MWNT buckypapers ( $27.7 \pm 2$  nm) was found to be slightly higher than that of their MWNT counterparts ( $24 \pm 1$  nm), after analysis of binding isotherms derived from nitrogen adsorption/desorption measurements performed on the materials.

The relationship of seasonal effects using membrane technology was also examined in this study. Results indicate that flux was good for samples which were collected from contaminated surface and groundwater in all seasons except for samples which were collected from the leachate pond at Russell Vale in the summer season due to biological fouling. High temperatures and light intensity as well as nutrient availability in this season favour the growth and photosynthesis processes and result in high release of extracellular organic matter (EOM). Accordingly, the presence of EOM in the reservoir frequently clogs the pores of membranes, leading to permeate flux decline. Findings revealed that the highest flux decline (85% and 83.4%, respectively) because of fouling was for NF-90 and ESPA2 in the summer season for samples collected from the leachate pond at Russell Vale.

Finally, through what has been discussed in this thesis it can be concluded that the RO membrane (ESPA2) is the preferred membrane for separation contaminants existing in surface and groundwater which have been investigated in this study in particular EWB10D and EWB13D sites. However, the NF membrane (NF-90) also offered high performance to retain both the organic and inorganic contaminants existing in all sites which have been examined in this study. Another consideration is that NF-90 consumes less energy compared to ESPA2. Consequently, it can be said that we need one system (NF or RO) to be set up for water purification because both of them offered a high performance to removal contaminants existing in the study sites when used individually. Flux decline is considered a significant issue caused by fouling and adversely affects membrane performance. This issue can be solved by using chemical treatment of fouled membranes used: alkalies, acids and metal chelating agents. Typically chemical treatment [e.g. cleaning with sodium dodecyl sulfate (SDS)] used at least for 5 minutes to clean the membranes but does not exceed to 15 minutes as many studies have been recommended (Alzahrani et al., 2013c). This leads to improved membrane performance and recovery of flux in membranes.

Results reported in this thesis have led to various recommendations for further studies in addition to specific recommendations for Wollongong City Council and Orica:

**General recommendation for further studies**

- This study proved that using NF, RO and MWNT processes for removing volatile organic compounds (VOCs), cations and anions from contaminated surface and groundwater is feasible. The efficient, cost-effective treatment of surface and groundwater using these three systems and the fouling potential of the membranes will need to be investigated in a pilot scale experiment over an extended period.
- The RO membrane is considered the preferred membrane for treatment compared to NF and MWNT membranes as results indicated in this study and it will contribute to improvement of water for many purposes in particular agricultural and industrial sectors. However, the NF membrane exhibited high performance in rejecting organic and inorganic contaminants and it could be preferable to use in water treatment since, in particular, it does not consume a much energy compared to a RO system.
- The MWNT mostly removed the volatile organic compounds, especially hydrophilic compounds, which were rejected through MWNT buckypaper membrane using the size exclusion mechanism. There was a limitation in removal of hydrophobic organic compounds, cations and anions in MWNT buckypaper membrane. Therefore, further membrane development is required to remove these smaller organic and inorganic compounds.
- Fouling was a critical issue that adversely affected membrane performance in this research causing declining permeate flux, increased operational cost, and shortened membrane life. Reduction of fouling by employing sufficient feed pretreatment, membrane modification and chemical cleaning of fouled



membrane is needed to improve the efficiency of membrane performance and extend the membrane life.

- This study demonstrated clearly that there is a relationship between seasonal effects when using membrane technology. This is reflected in a negative impact on the permeate flux specifically in the summer season due to fouling. An efficient and effective pretreatment of water samples collected in the summer season will need to be examined in a pilot scale experiment in future researches.

### **Recommendations for Wollongong City Council**

To solve the issues associated with irrigation using leachate water which subsequent cause degradation to the soil structure and devastate turfgrass, we can present following recommendations for Wollongong City Council:

- We recommend NF filtration system to be set up for treatment of leachate water when taking into account NF offers numerous advantages such as low operation pressure (8-14 bars), high flux, high rejection of contaminants, low operation and maintenance costs and it can be the preferred filtration system for removal of contaminants existing in leachate pond.
- To make NF membrane more effective and extend lifetime of this membrane to become eventually a feasibility, pretreatment is required before running this system and chemical cleaning is essential during operation process to control fouling.
- Conduct periodic evaluation of soil and plant (grass) samples before and after use NF filtration system to assess the consequences of use of this system.

### **Recommendations for Orica**

To solve the issues associated with chlorinated hydrocarbons (CHCs) existing in groundwater in Botany Bay which may have risks for the health of humans and adverse effect for other organisms, we can present following recommendations for Orica:

- We recommend RO filtration system to be set up for purification of groundwater from volatile organic compounds existing in EWB10D and EWB13D sites because this system removed almost all these compounds which have been examined in this study.
- We recommend NF filtration system to be set up for purification of groundwater from inorganic compounds (e.g. mercury) existing in WGB32 site because this system showed high ability to remove most of all inorganic contaminates which have been investigated in this study.
- To make NF and RO membranes more effective and serve for a longer period to become eventually feasibility, pretreatment is required before running this system and chemical cleaning is essential during operation process to control fouling.

## REFERENCES

- ACHILLI, A., CATH, T. Y., MARCHAND, E. A. & CHILDRESS, A. E., 2009. The forward osmosis membrane bioreactor: a low fouling alternative to MBR processes. *Desalination*, 239, 10-21.
- ADOLPH, M. A., XAVIER, Y. M., KRIVESHINI, P. & RUI, K., 2012. Phosphine functionalised multiwalled carbon nanotubes: a new adsorbent for the removal of nickel from aqueous solution. *Journal of Environmental Sciences*, 24, 1133-1141.
- AGENSON, K. O., OH, J.-I. & URASE, T., 2003. Retention of a wide variety of organic pollutants by different nanofiltration/reverse osmosis membranes: controlling parameters of process. *Journal of Membrane Science*, 225, 91-103.
- AGENSON, K. O. & URASE, T., 2007. Change in membrane performance due to organic fouling in nanofiltration (NF)/reverse osmosis (RO) applications. *Separation and Purification Technology*, 55, 147-156.
- AGNIHOTRI, S., ROOD, M. J. & ROSTAM-ABADI, M., 2005. Adsorption equilibrium of organic vapors on single-walled carbon nanotubes. *Carbon*, 43, 2379-2388.
- AHMAD, A. L., TAN, L. S. & ABD. SHUKOR, S. R., 2008. The role of pH in nanofiltration of atrazine and dimethoate from aqueous solution. *Journal of Hazardous Materials*, 154, 633-638.
- AHMED, S. F., DAS, S., MITRA, M. K. & CHATTOPADHYAY, K. K., 2007. Effect of temperature on the electron field emission from aligned carbon nanofibers and multiwalled carbon nanotubes. *Applied Surface Science*, 254, 610-615.
- AHN, C. H., BAEK, Y., LEE, C., KIM, S. O., KIM, S., LEE, S., KIM, S.-H., BAE, S. S., PARK, J. & YOON, J., 2012. Carbon nanotube-based membranes: Fabrication and application to desalination. *Journal of Industrial and Engineering Chemistry*, 18, 1551-1559.
- AJO-FRANKLIN, J. B., GELLER, J. T. & HARRIS, J. M., 2006. A survey of the geophysical properties of chlorinated DNAPLs. *Journal of Applied Geophysics*, 59, 177-189.
- AL-AMOUDI, A., WILLIAMS, P., AL-HOBAIB, A. S. & LOVITT, R. W., 2008. Cleaning results of new and fouled nanofiltration membrane characterized by contact angle, updated DSPM, flux and salts rejection. *Applied Surface Science*, 254, 3983-3992.
- AL-AMOUDI, A. S., 2010. Factors affecting natural organic matter (NOM) and scaling fouling in NF membranes: a review. *Desalination*, 259, 1-10.
- AL-AMOUDI, A. S. & FAROOQUE, A. M., 2005. Performance restoration and autopsy of NF membranes used in seawater pretreatment. *Desalination*, 178, 261-271.
- AL-RIFAI, J. H., KHABBAZ, H. & SCHAFER, A. I., 2010. Removal of pharmaceuticals and endocrine disrupting compounds in a water recycling process using reverse osmosis systems. *Separation and Purification Technology*, 77, 60-67.
- AL-SAMMARRAEE, M., CHAN, A., SALIM, S. M. & MAHABALESWAR, U. S., 2009. Large-eddy simulations of particle sedimentation in a longitudinal

- sedimentation basin of a water treatment plant. Part I: particle settling performance. *Chemical Engineering Journal*, 152, 307-314.
- ALCOCK, L., 2010. *Characterization and Transport Study Involving Multi-Walled Carbon Nanotube Membranes*. Bachelor of Nanotechnology with Honours, University of Wollongong.
- ALMASRI, M. N., 2007. Nitrate contamination of groundwater: a conceptual management framework. *Environmental Impact Assessment Review*, 27, 220-242.
- ALTURKI, A. A., TADKAEW, N., MCDONALD, J. A., KHAN, S. J., PRICE, W. E. & NGHIEM, L. D., 2010. Combining MBR and NF/RO membrane filtration for the removal of trace organics in indirect potable water reuse applications. *Journal of Membrane Science*, 365, 206-215.
- ALZAHRANI, S., MOHAMMAD, A. W., HILAL, N., ABDULLAH, P. & JAAFAR, O., 2013a. Comparative study of NF and RO membranes in the treatment of produced water—Part I: assessing water quality. *Desalination*, 315, 18–26.
- ALZAHRANI, S., MOHAMMAD, A. W., HILAL, N., ABDULLAH, P. & JAAFAR, O., 2013b. Comparative study of NF and RO membranes in the treatment of produced water II: toxicity removal efficiency. *Desalination*, 315, 27-32.
- ALZAHRANI, S., MOHAMMAD, A. W., HILAL, N., ABDULLAH, P. & JAAFAR, O., 2013c. Identification of foulants, fouling mechanisms and cleaning efficiency for NF and RO treatment of produced water. *Separation and Purification Technology*, 118, 324-341.
- ANG, W. L., MOHAMMAD, A. W., HILAL, N. & LEO, C. P., 2015. A review on the applicability of integrated/hybrid membrane processes in water treatment and desalination plants. *Desalination*, 363, 2-18.
- ANISHKIN, A. & SUKHAREV, S., 2004. Water dynamics and dewetting transitions in the small mechanosensitive channel *Biophysical Journal*, 86, 2883-2895.
- ANTONY, A., SUBHI, N., HENDERSON, R. K., KHAN, S. J., STUETZ, R. M., CLECH, P. L., CHEN, V. & LESLIE, G., 2012. Comparison of reverse osmosis membrane fouling profiles from Australian water recycling plants. *Journal of Membrane Science* 407–408, 8–16.
- ARGÜELLO, M. A., ÁLVAREZ, S., RIERA, F. A. & ÁLVAREZ, R., 2003. Enzymatic cleaning of inorganic ultrafiltration membranes used for whey protein fractionation. *Journal of Membrane Science*, 216, 121-134.
- ARSUAGA, J. M., LÓPEZ-MUÑOZ, M. J., AGUADO, J. & SOTTO, A., 2008. Temperature, pH and concentration effects on retention and transport of organic pollutants across thin-film composite nanofiltration membranes. *Desalination*, 221, 253-258.
- BA, C. & ECONOMY, J., 2010. Preparation and characterization of a neutrally charged antifouling nanofiltration membrane by coating a layer of sulfonated poly(ether ether ketone) on a positively charged nanofiltration membrane. *Journal of Membrane Science*, 362, 192-201.
- BABEL, S. & TAKIZAWA, S., 2010. Microfiltration membrane fouling and cake behavior during algal filtration. *Desalination*, 261, 46-51.

- BABEL, S., TAKIZAWA, S. & OZAKI, H., 2002. Factors affecting seasonal variation of membrane filtration resistance caused by *Chlorella* algae. *Water Research*, 36, 1193–1202.
- BAKER, R. W., 2012. *Membrane Technology and Applications*. Somerset, NJ, USA: Wiley-Blackwell.
- BALLET, G. T., HAFIANE, A. & DHAHBI, M., 2007. Influence of operating conditions on the retention of phosphate in water by nanofiltration. *Journal of Membrane Science*, 290, 164–172.
- BARAKAT, M. A., 2010. New trends in removing heavy metals from industrial wastewater. *Arabian Journal of Chemistry*, In Press, Corrected Proof.
- BARREDO-DAMAS, S., ALCAINA-MIRANDA, M. I., IBORRA-CLAR, M. I., BES-PIÁ, A., MENDOZA-ROCA, J. A. & IBORRA-CLAR, A., 2006. Study of the UF process as pretreatment of NF membranes for textile wastewater reuse. *Desalination*, 200, 745–747.
- BARRETT, E. P., JOYNER, L. G. & HALENDA, P. P., 1951. The determination of pore volume and area distributions in porous substances. I. Computations from nitrogen isotherms. *Journal of the American Chemical Society*, 73, 373–380.
- BARTELS, C. R., RYBAR, S., ANDES, K. & FRANKS, R., 2009. Optimized Removal of Boron and Other Specific Contaminants by SWRO Membranes. *IDA World Congress-Dubai UAE. IDAWC/DB09-143*.
- BAUGHMAN, R. H., ZAKHIDOV, A. A. & DE HEER, W. A., 2002. Carbon nanotubes--the route toward applications. *Science*, 297, 787–792.
- BECKSTEIN, O., BIGGIN, P. C., BOND, P., BRIGHT, J. N., DOMENE, C., GROTTESI, A., HOLYOAKE, J. & SANSOM, M. S. P., 2003. Ion channel gating: insights via molecular simulations. *FEBS Letters*, 555, 85–90.
- BECKSTEIN, O. & SANSOM, M. S. P., 2004. The influence of geometry, surface character, and flexibility on the permeation of ions and water through biological pores. *Physical Biology*, 1, 42–52.
- BELKACEM, M., BEKHTI, S. & BENSADOK, K., 2007. Groundwater treatment by reverse osmosis. *Desalination*, 206, 100–106.
- BELLONA, C. & DREWES, J. E., 2007. Viability of a low-pressure nanofilter in treating recycled water for water reuse applications: a pilot-scale study. *Water Research*, 41, 3948–3958.
- BELLONA, C., DREWES, J. E., XU, P. & AMY, G., 2004. Factors affecting the rejection of organic solutes during NF/RO treatment—a literature review. *Water Research*, 38, 2795–2809.
- BERKOWITZ, B., ISHAI, D. & BRUNO, Y., 2008. *Contaminant Geochemistry: Interactions and Transport in the Subsurface Environment*, Berlin Springer.
- BIZIUK, M. & PRZYJAZNY, A., 1996. Methods of isolation and determination of volatile organohalogen compounds in natural and treated waters. *Journal of Chromatography A*, 733, 417–448.
- BLIGHE, F. M., HERNANDEZ, Y. R., BLAU, W. J. & COLEMAN, J. N., 2007. Observation of percolation-like scaling-far from the percolation threshold-in high volume fraction, high conductivity polymer-nanotube composite films. *Advanced Materials*, 19, 4443–4447.
- BOKOBZA, L., 2007. Multiwall carbon nanotube elastomeric composites: a review. *Polymer*, 48, 4907–4920.

- BOLONG, N., ISMAIL, A. F., SALIM, M. R. & MATSUURA, T., 2009. A review of the effects of emerging contaminants in wastewater and options for their removal. *Desalination*, 239, 229-246.
- BOTTINO, A., CAPANNELLI, G., COMITE, A., FERRARI, F., FIRPO, R. & VENZANO, S., 2009. Membrane technologies for water treatment and agroindustrial sectors. *Comptes Rendus Chimie*, 12, 882-888.
- BOUSSU, K., BELPAIRE, A., VOLODIN, A., VAN HAESENDONCK, C., VAN DER MEEREN, P., VANDECASTEELE, C. & VAN DER BRUGGEN, B., 2007. Influence of membrane and colloid characteristics on fouling of nanofiltration membranes. *Journal of Membrane Science*, 289, 220-230.
- BRAEKEN, L., RAMAEKERS, R., ZHANG, Y., MAES, G., BRUGGEN, B. V. D. & VANDECASTEELE, C., 2005. Influence of hydrophobicity on retention in nanofiltration of aqueous solutions containing organic compounds. *Journal of Membrane Science*, 252, 195-203.
- BRANSON. 2013. *ultrasonication* [Online]. Available: <https://www.google.com.au/search?q=branson+ultrasonic&tbm=isch&tbo=u&source=univ&sa=X&ei=6kctUrv0IMKKkAW8k4DQAw&ved=0CGEQsAQ&biw=2048&bih=947> [Accessed 9/09/2013].
- BRANT, J. A. & CHILDRESS, A. E., 2002. Membrane-colloid interactions: comparison of extended DLVO predictions with AFM force measurements *Environmental Engineering Science*, 19, 413-427.
- BRODIE, R., SUNDARAM, B., TOTTENHAM, R., HOSTETLER, S. & RANSLEY, T., 2007. An adaptive management framework for connected groundwater-surface water resources in Australia. In: DEPARTMENT OF AGRICULTURE, F. A. F. (ed.). Canberra: Bureau of Rural Sciences.
- CAIRNS, E., THARUMAKULASINGAM, K., ATHAR, M., YOUSAF, M., CHENG, I., HUANG, Y., LU, J. & YAP, D., 2011. Source, concentration, and distribution of elemental mercury in the atmosphere in Toronto, Canada. *Environmental Pollution*, 159, 2003-2008.
- CALLISTER, W. D. & RETHWISCH, D. G., 2010. *Materials science and engineering: an introduction*.
- CARTAGENA, P., EL KADDOURI, M., CASES, V., TRAPOTE, A. & PRATS, D., 2013. Reduction of emerging micropollutants, organic matter, nutrients and salinity from real wastewater by combined MBR-NF/RO treatment. *Separation and Purification Technology*, 110, 132-143.
- CHANG, E. E., LIANG, C.-H., HUANG, C.-P. & CHIANG, P.-C., 2012. A simplified method for elucidating the effect of size exclusion on nanofiltration membranes. *Separation and Purification Technology*, 85, 1-7.
- CHAPMAN WILBERT, M., PELLEGRINO, J. & ZYDNEY, A., 1998. Bench-scale testing of surfactant-modified reverse osmosis/nanofiltration membranes. *Desalination*, 115, 15-32.
- CHARY, N. S. & FERNANDEZ-ALBA, A. R., 2012. Determination of volatile organic compounds in drinking and environmental waters. *Trends in Analytical Chemistry*, 32, 60-75.
- CHEN, G. C., SHAN, X. G., PEI, Z. G., WANG, H., ZHENG, L. R., ZHANG, J. & XIE, Y. N., 2011. Adsorption of diuron and dichlobenil on multiwalled carbon nanotubes as affected by lead. *Journal of Hazardous Materials*, 188, 156-163.

- CHEN, S.-S., TAYLOR, J. S., MULFORD, L. A. & NORRIS, C. D., 2004. Influences of molecular weight, molecular size, flux, and recovery for aromatic pesticide removal by nanofiltration membranes. *Desalination*, 160, 103-111.
- CHEN, V., FANE, A. G. & FELL, C. J. D., 1992. The use of anionic surfactants for reducing fouling of ultrafiltration membranes: their effects and optimization. *Journal of Membrane Science*, 67, 249-261.
- CHILDRESS, A. E. & ELIMELECH, M., 1996. Effect of solution chemistry on the surface charge of polymeric reverse osmosis and nanofiltration membranes. *Journal of Membrane Science*, 119, 253-268.
- CHIOU, Y.-T., HSIEH, M.-L. & YEH, H.-H., 2010. Effect of algal extracellular polymer substances on UF membrane fouling. *Desalination*, 250, 648-652.
- CHOONG, T. S. Y., CHUAH, T. G., ROBIAH, Y., GREGORY KOAY, F. L. & AZNI, I., 2007. Arsenic toxicity, health hazards and removal techniques from water: an overview. *Desalination*, 217, 139-166.
- CHOWDARY, V., RAO, N. & SARMA, P., 2005. Decision support framework for assessment of non-point-source pollution of groundwater in large irrigation projects. *Agricultural Water Management*, 75, 194-225.
- CLARKSON, T. W., 1993. Mercury: major issues in environmental health. *Environmental Health Perspectives*, 100, 31.
- CODD, G. A., 2000. Cyanobacterial toxins, the perception of water quality, and the prioritisation of eutrophication control. *Ecological Engineering*, 16, 51-60.
- COLEMAN, J. N., KHAN, U., BLAU, W. J. & GUN'KO, Y. K., 2006. Small but strong: a review of the mechanical properties of carbon nanotube-polymer composites. *Carbon*, 44, 1624-1652.
- COMERTON, A. M., ANDREWS, R. C. & BAGLEY, D. M., 2009. The influence of natural organic matter and cations on fouled nanofiltration membrane effective molecular weight cut-off. *Journal of Membrane Science*, 327, 155-163.
- COMERTON, A. M., ANDREWS, R. C., BAGLEY, D. M. & HAO, C., 2008. The rejection of endocrine disrupting and pharmaceutically active compounds by NF and RO membranes as a function of compound and water matrix properties. *Journal of Membrane Science*, 313, 323-335.
- COOPER, R., 2005a. Irrigation suitability analysis-leachate pond, Russell Vale Golf Course. Wollongong: Wollongong City Council, 1-10.
- COOPER, R., 2005b. Irrigation suitability analysis-mine waste water, Russell vale Golf Course. Wollongong: Wollongong City Council.
- CORRY, B., 2006. An energy-efficient gating mechanism in the acetylcholine receptor channel suggested by molecular and Brownian dynamics. *Biophysical Journal*, 90, 799-810.
- CORRY, B., 2008. Designing carbon nanotube membranes for efficient water desalination. *Journal of Physical Chemistry*, 112, 1427-1434.
- COTTINET, P. J., SOUDERS, C., TSAI, S. Y., LIANG, R., WANG, B. & ZHANG, C., 2012. Electromechanical actuation of buckypaper actuator: material properties and performance relationships. *Physics Letters A*, 376, 1132-1136.
- CSÉFALVAY, E., PAUER, V. & MIZSEY, P., 2009. Recovery of copper from process waters by nanofiltration and reverse osmosis. *Desalination*, 240, 132-142.

- DALTON, S. K., BRANT, J. A. & WIESNER, M. R., 2005. Chemical interactions between dissolved organic matter and low-molecular weight organic compounds: impacts on membrane separation. *Journal of Membrane Science*, 266, 30-39.
- DAS, R., ALI, M. E., HAMID, S. B. A., RAMAKRISHNA, S. & CHOWDHURY, Z. Z., 2014. Carbon nanotube membranes for water purification: a bright future in water desalination. *Desalination*, 336, 97-109.
- DASTOOR, A. P. & LAROCQUE, Y., 2004. Global circulation of atmospheric mercury: a modelling study. *Atmospheric Environment*, 38, 147-161.
- DENG, J., SHAO, Y., GAO, N., DENG, Y., TAN, C., ZHOU, S. & HU, X., 2012. Multiwalled carbon nanotubes as adsorbents for removal of herbicide diuron from aqueous solution. *Chemical Engineering Journal*, 193-194, 339-347.
- DÍAZ-CRUZ, M. S. & BARCELO, D., 2008. Trace organic chemicals contamination in ground water recharge. *Chemosphere*, 72, 333-342.
- DÍAZ, E., ORDÓÑEZ, S. & VEGA, A., 2007. Adsorption of volatile organic compounds onto carbon nanotubes, carbon nanofibers, and high-surface-area graphites. *Journal of Colloid and Interface Science*, 305, 7-16.
- DOLAR, D., GROS, M., RODRIGUEZ-MOZAZ, S., MORENO, J., COMAS, J., RODRIGUEZ-RODA, I. & BARCELÓ, D., 2012a. Removal of emerging contaminants from municipal wastewater with an integrated membrane system, MBR-RO. *Journal of Hazardous Materials*, 239-240, 64-69.
- DOLAR, D., KOŠUTIĆ, K. & VUČIĆ, B., 2011a. RO/NF treatment of wastewater from fertilizer factory — removal of fluoride and phosphate. *Desalination*, 265, 237-241.
- DOLAR, D., PELKO, S., KOŠUTIĆ, K. & HORVAT, A. J. M., 2012b. Removal of anthelmintic drugs and their photodegradation products from water with RO/NF membranes. *Process Safety and Environmental Protection*, 90, 147-152.
- DOLAR, D., VUKOVIĆ, A., AŠPERGER, D. & KOŠUTIĆ, K., 2011b. Effect of water matrices on removal of veterinary pharmaceuticals by nanofiltration and reverse osmosis membranes. *Journal of Environmental Sciences*, 23, 1299-1307.
- DOMINGUES, R. C. C., RAMOS, A. A., CARDOSO, V. L. & REIS, M. H. M., 2014. Microfiltration of passion fruit juice using hollow fibre membranes and evaluation of fouling mechanisms. *Journal of Food Engineering*, 121, 73-79.
- DUCOM, G. & CABASSUD, C., 1999. Interests and limitations of nanofiltration for the removal of volatile organic compounds in drinking water production. *Desalination*, 124, 115-123.
- DUMÉE, L., GERMAIN, V., SEARS, K., SCHÜTZ, J., FINN, N., DUKE, M., CERNEAUX, S., CORNU, D. S. & GRAY, S., 2011. Enhanced durability and hydrophobicity of carbon nanotube bucky paper membranes in membrane distillation. *Journal of Membrane Science*, 376, 241-246.
- DUMÉE, L. F., SEARS, K., SCHÜTZ, J., FINN, N., HUYNH, C., HAWKINS, S., DUKE, M. & GRAY, S., 2010. Characterization and evaluation of carbon nanotube bucky-paper membranes for direct contact membrane distillation. *Journal of Membrane Science*, 351, 36-43.



- DUNN, S. M., VINTEN, A. J. A., LILLY, A., DEGROOTE, J. & MCGECHAN, M., 2005. Modelling nitrate losses from agricultural activities on a national scale. *Water Science & Technology*, 51, 319-327.
- EATON, A. D., 2005. *Standard Methods for the Examination of Water and Wastewater.*, Washington, American Public Health Association; Water Environment Federation; American Water Works Association.
- ES'HAGHI, Z., EBRAHIMI, M. & HOSSEINI, M.-S., 2011. Optimization of a novel method for determination of benzene, toluene, ethylbenzene, and xylenes in hair and waste water samples by carbon nanotubes reinforced sol-gel based hollow fiber solid phase microextraction and gas chromatography using factorial experimental design. *Journal of Chromatography A*, 1218, 3400-3406.
- FAGAN, S. B., SOUZA FILHO, A., LIMA, J., MENDES FILHO, J., FERREIRA, O., MAZALI, I., ALVES, O. & DRESSELHAUS, M., 2004. 1, 2-dichlorobenzene interacting with carbon nanotubes. *Nano Letters*, 4, 1285-1288.
- FAKHRI' L-RAZI, A., PENDASHTEH, A., ABDULLAH, L. C., BIAK, D. R. A., MADAENI, S. S. & ABIDIN, Z. Z., 2009. Review of technologies for oil and gas produced water treatment. *Journal of Hazardous Materials*, 170, 530-551.
- FANE, A. G., TANG, C. Y. & WANG, R., 2011. Membrane technology for water: microfiltration, ultrafiltration, nanofiltration, and reverse osmosis. In: PETER, W. (ed.) *Treatise on Water Science*. Oxford: Elsevier, 301-335.
- FANG, J., YANG, X., MA, J., SHANG, C. & ZHAO, Q., 2010. Characterization of algal organic matter and formation of DBPs from chlor(am)ination. *Water Research*, 44, 5897-5906.
- FIGOLI, A., CASSANO, A., CRISCUOLI, A., MOZUMDER, M. S. I., UDDIN, M. T., ISLAM, M. A. & DRIOLI, E., 2010. Influence of operating parameters on the arsenic removal by nanofiltration. *Water Research*, 44, 97-104.
- FRANSON, M. A. H., 1998. *Standard Methods for the Examination of Water and Wastewater*, Washington, DC, American Public Health Association
- FREGER, V., GILRON, J. & BELFER, S., 2002. TFC polyamide membranes modified by grafting of hydrophilic polymers: an FT-IR/AFM/TEM study. *Journal of Membrane Science*, 209, 283-292.
- FRIZZELL, C., IN HET PANHUIS, M., COUTINHO, D., BALKUS, K., MINETT, A. & BLAU, W., 2005. Reinforcement of macroscopic carbon nanotube structures by polymer intercalation: the role of polymer molecular weight and chain conformation. *Physical Review B*, 72, 245420,1-8.
- FU, F. & WANG, Q., 2011. Removal of heavy metal ions from wastewaters: a review. *Journal of Environmental Management*, 92, 407-418.
- FUJIOKA, T., KHAN, S. J., MCDONALD, J. A. & NGHIEM, L. D., 2014. Nanofiltration of trace organic chemicals: a comparison between ceramic and polymeric membranes. *Separation and Purification Technology*, 136, 258-264.
- FUJIOKA, T., NGHIEM, L. D., KHAN, S. J., MCDONALD, J. A., POUSSADE, Y. & DREWES, J. E., 2012. Effects of feed solution characteristics on the rejection of N-nitrosamines by reverse osmosis membranes. *Journal of Membrane Science*, 409-410, 66-74.

- GARCIA, N., MORENO, J., CARTMELL, E., RODRIGUEZ-RODA, I. & JUDD, S., 2013. The cost and performance of an MF-RO/NF plant for trace metal removal. *Desalination*, 309, 181-186.
- GAUDEN, P. A., TERZYK, A. P., RYCHLICKI, G., KOWALCZYK, P., LOTA, K., RAYMUNDO-PINERO, E., FRACKOWIAK, E. & BÉGUIN, F., 2006. Thermodynamic properties of benzene adsorbed in activated carbons and multi-walled carbon nanotubes. *Chemical Physics Letters*, 421, 409-414.
- GEOSCIENCE AUSTRALIA. 2014. *Groundwater Use. Australian Government, Geoscience Australia* [Online]. Available: <http://www.ga.gov.au/groundwater/basics/groundwater-use.h>. [Accessed 18/9/2014 2014].
- GERBER, G. B., LÉONARD, A. & HANTSON, P., 2002. Carcinogenicity, mutagenicity and teratogenicity of manganese compounds. *Critical Reviews in Oncology/Hematology*, 42, 25-34.
- GOH, P. S., ISMAIL, A. F. & NG, B. C., 2013. Carbon nanotubes for desalination: performance evaluation and current hurdles. *Desalination*, 308, 2-14.
- GOULA, A. M., KOSTOGLU, M., KARAPANTSIOS, T. D. & ZOUBOULIS, A. I., 2008. A CFD methodology for the design of sedimentation tanks in potable water treatment: case study: the influence of a feed flow control baffle. *Chemical Engineering Journal*, 140, 110-121.
- GRAY, N. F., 2010. *Water Technology: an Introduction for Scientists and Engineers*, Burlington, MA, USA, Butterworth-Heinemann.
- GRAY, S. R., SEMIAT, R., DUKE, M., RAHARDIANTO, A. & COHEN, Y., 2011. Seawater use and desalination technology. In: WATER SCIENCE (ed.). Wilderer, Peter A, ed. Elsevier.
- GREENLEE, L. F., LAWLER, D. F., FREEMAN, B. D., MARROT, B. & MOULIN, P., 2009. Reverse osmosis desalination: Water sources, technology, and today's challenges. *Water Research*, 43, 2317-2348.
- GUPTA, V. K. & ALI, I., 2013. Chapter 4 - Water Treatment by Reverse Osmosis Method. In: GUPTA, V. K. & IMRAN, A. (eds.) *Environmental Water*. Elsevier.
- GUR-REZNIK, S., KOREN-MENASHE, I., HELLER-GROSSMAN, L., RUFEL, O. & DOSORETZ, C. G., 2011. Influence of seasonal and operating conditions on the rejection of pharmaceutical active compounds by RO and NF membranes. *Desalination*, 277, 250-256.
- HACHISUKA, H. & IKEDA, K., 2001. Composite reverse osmosis membrane having a separation layer with polyvinyl alcohol coating and method of reverse osmotic treatment of water using the same. *US Patent 6*, 177,011 B1.
- HAMED, O. A., 2005. Overview of hybrid desalination systems — current status and future prospects. *Desalination*, 186, 207-214.
- HAN, J.-H., ZHANG, H., CHEN, M.-J., WANG, G.-R. & ZHANG, Z., 2014. CNT buckypaper/thermoplastic polyurethane composites with enhanced stiffness, strength and toughness. *Composites Science and Technology*, 103, 63-71.
- HARRISON, C. J., LE GOUELLEC, Y. A., CHENG, R. C. & CHILDRESS, A. E., 2007. Bench-scale testing of nanofiltration for seawater desalination. *Journal of Environmental Engineering-ASCE*, 1004.

- HARTER, T., DAVIS, H., MATHEWS, M. C. & MEYER, R. D., 2002. Shallow groundwater quality on dairy farms with irrigated forage crops. *Journal of Contaminant Hydrology*, 55, 287-315.
- HASSAN, A. M., AL-SOFI, M. A. K., AL-AMOUDI, A. S., JAMALUDDIN, A. T. M., FAROOQUE, A. M., ROWAILI, A., DALVI, A. G. I., KITHER, N. M., MUSTAFA, G. M. & AL-TISAN, I. A. R., 1998. A new approach to membrane and thermal seawater desalination processes using nanofiltration membranes (Part 1). *Desalination*, 118, 35-51.
- HAYNES, W. M., BRUNO, T. J. & LIDE, D. R., 2013. CRC Handbook of Chemistry and Physics. 94th Edition ed.
- HE, D. & ULBRICHT, M., 2006. Surface-selective photo-grafting on porous polymer membranes via a synergist immobilization method. *Journal of Materials Chemistry*, 16, 1860 - 1868.
- HE, J. & BALASUBRAMANIAN, R., 2010. Semi-volatile organic compounds (SVOCs) in ambient air and rainwater in a tropical environment: concentrations and temporal and seasonal trends. *Chemosphere*, 78, 742-751.
- HENDERSON, R. K., BAKER, A., PARSONS, S. A. & JEFFERSON, B., 2008. Characterisation of algogenic organic matter extracted from cyanobacteria, green algae and diatoms. *Water Research*, 42, 3435-3445.
- HENDERSON, R. K., PARSONS, S. A. & JEFFERSON, B., 2010. The impact of differing cell and algogenic organic matter (AOM) characteristics on the coagulation and flotation of algae. *Water Research*, 44, 3617-3624.
- HERNADI, K., LJUBOVIĆ, E., SEO, J. W. & FORRÓ, L., 2003. Synthesis of MWNT-based composite materials with inorganic coating. *Acta Materialia*, 51, 1447-1452.
- HIGGINS, J., WARNKEN, J., SHERMAN, P. P. & TEASDALE, P. R., 2002. Survey of users and providers of recycled water: quality concerns and directions for applied research. *Water Research*, 36, 5045-5056.
- HILAL, N., AL-ZOUBI, H., DARWISH, N. A., MOHAMMA, A. W. & ABU ARABI, M., 2004. A comprehensive review of nanofiltration membranes: treatment, pretreatment, modelling, and atomic force microscopy. *Desalination*, 170, 281-308.
- HILAL, N., AL-ZOUBI, H., MOHAMMAD, A. W. & DARWISH, N. A., 2005. Nanofiltration of highly concentrated salt solutions up to seawater salinity. *Desalination*, 184, 315-326.
- HIROSE, M., ITO, H. & KAMIYAMA, Y., 1996. Effect of skin layer surface structures on the flux behaviour of RO membranes. *Journal of Membrane Science*, 121, 209-215.
- HOEK, M. V., BHATTACHARJEE, S. & ELIMELECH, M., 2003. Effect of membrane surface roughness on colloid-membrane DLVO interactions. *American Chemical Society*, 19, 4836-4847.
- HOLMES, P., JAMES, K. & LEVY, L., 2009. Is low-level environmental mercury exposure of concern to human health? *Science of The Total Environment*, 408, 171-182.
- HONG, C.-E., LEE, J.-H., KALAPPA, P. & ADVANI, S. G., 2007. Effects of oxidative conditions on properties of multi-walled carbon nanotubes in polymer nanocomposites. *Composites Science and Technology*, 67, 1027-1034.

- HONG, S. U., OUYANG, L. & BRUENING, M. L., 2009. Recovery of phosphate using multilayer polyelectrolyte nanofiltration membranes. *Journal of Membrane Science*, 327, 2-5.
- HORVATH, G. & KAWAZOE, K., 1983. Method for the calculation of effective pore size distribution in molecular sieve carbon. *Journal of Chemical Engineering of Japan*, 16, 470 - 475.
- HOUNSLOW, A., 1995. *Water Quality Data: Analysis and Interpretation*, Boca Raton, Lewis Publishers.
- HU, J., TONG, Z., HU, Z., CHEN, G. & CHEN, T., 2012. Adsorption of roxarsone from aqueous solution by multi-walled carbon nanotubes. *Journal of Colloid and Interface Science*.
- HU, J. Y., JIN, X. & ONG, S. L., 2007. Rejection of estrone by nanofiltration: influence of solution chemistry. *Journal of Membrane Science*, 302, 188-196.
- HUANG, H., CHO, H., SCHWAB, K. & JACANGELO, J. G., 2011. Effects of feedwater pretreatment on the removal of organic microconstituents by a low fouling reverse osmosis membrane. *Desalination*, 281, 446-454.
- HUCK, P. & SOZAŃSKI, M., 2011. 3.16 - Chemical basis for water technology. In: PETER, W. (ed.) *Treatise on Water Science*. Oxford: Elsevier.
- HUDAK, P. F., 2000. Sulfate and chloride concentrations in Texas aquifers. *Environment International*, 26, 55-61.
- HURLIMANN, A. & DOLNICAR, S., 2012. Newspaper coverage of water issues in Australia. *Water Research*, 46, 6497-6507.
- IJIMA, S., 1991. Helical microtubules of graphitic carbon. *Nature*, 354, 56-58.
- IKEM, A., 2010. Measurement of volatile organic compounds in bottled and tap waters by purge and trap GC-MS: are drinking water types different? *Journal of Food Composition and Analysis*, 23, 70-77.
- ISMAIL, A. F., GOH, P. S., SANIP, S. M. & AZIZ, M., 2009. Transport and separation properties of carbon nanotube-mixed matrix membrane. *Separation and Purification Technology*, 70, 12-26.
- JAKUBOWSKA, N., ZYGMUNT, B., POLKOWSKA, Ż., ZABIEGAŁA, B. & NAMIEŚNIK, J., 2009. Sample preparation for gas chromatographic determination of halogenated volatile organic compounds in environmental and biological samples. *Journal of Chromatography A*, 1216, 422-441.
- JARUSUTTHIRAK, C., MATTARAJ, S. & JIRARATANANON, R., 2007. Factors affecting nanofiltration performances in natural organic matter rejection and flux decline. *Separation and Purification Technology*, 58, 68-75.
- JONATHAN, A. B. & C., A. E., 2002. Membrane-colloid interactions: comparison of extended DLVO predictions with AFM force measurements. *Environmental Engineering Science*, 19, 413-427.
- JORDAN, C. & SMITH, R., 2005. Methods to predict the agricultural contribution to catchment nitrate loads: designation of nitrate vulnerable zones in Northern Ireland. *Journal of Hydrology*, 304, 316-329.
- JOSEPH, L., HEO, J., PARK, Y.-G., FLORA, J. R. V. & YOON, Y., 2011a. Absorption of bisphenol A and 17 $\alpha$ -ethinyl estradiol on single walled carbon nanotubes from seawater and brackish water. *Desalination*, 281, 68-74.
- JOSEPH, L., ZAIB, Q., KHAN, I. A., BERGE, N. D., PARK, Y.-G., SALEH, N. B. & YOON, Y., 2011b. Removal of bisphenol A and 17 $\alpha$ -ethinyl estradiol from

- landfill leachate using single-walled carbon nanotubes. *Water Research*, 45, 4056-4068.
- JUNG, Y.-J., KISO, Y., RABI ATUL ADAWIH BINTI, O., IKEDA, A., NISHIMURA, K., MIN, K.-S., KUMANO, A. & ARIJI, A., 2005. Rejection properties of aromatic pesticides with a hollow-fiber NF membrane. *Desalination*, 180, 63-71.
- JURADO, A., VÁZQUEZ-SUÑÉ, E., CARRERA, J., LÓPEZ DE ALDA, M., PUJADES, E. & BARCELÓ, D., 2012. Emerging organic contaminants in groundwater in Spain: a review of sources, recent occurrence and fate in a European context. *Science of The Total Environment*, 440, 82-94.
- KAMON, M., ENDO, K. & KATSUMI, T., 2003. Measuring the k-S-p relations on DNAPLs migration. *Engineering Geology*, 70, 351-363.
- KANG, G.-D. & CAO, Y.-M., 2012. Development of antifouling reverse osmosis membranes for water treatment: a review. *Water Research*, 46, 584-600.
- KHAWAJI, A. D., KUTUBKHANAH, I. K. & WIE, J.-M., 2008. Advances in seawater desalination technologies. *Desalination*, 221, 47-69.
- KIM, E.-S., YU, Q. & DENG, B., 2011. Plasma surface modification of nanofiltration (NF) thin-film composite (TFC) membranes to improve anti organic fouling. *Applied Surface Science*, 257, 9863-9871.
- KIM, I.-C. & LEE, K.-H., 2006. Dyeing process wastewater treatment using fouling resistant nanofiltration and reverse osmosis membranes. *Desalination*, 192, 246-251.
- KIM, T.-U., DREWES, J. E., SCOTT SUMMERS, R. & AMY, G. L., 2007. Solute transport model for trace organic neutral and charged compounds through nanofiltration and reverse osmosis membranes. *Water Research*, 41, 3977-3988.
- KIMURA, K., AMY, G., DREWES, J. E., HEBERER, T., KIM, T.U. & WATANABE, Y., 2003. Rejection of organic micropollutants (disinfection by-products, endocrine disrupting compounds, and pharmaceutically active compounds) by NF/RO membranes. *Journal of Membrane Science*, 227, 113-121.
- KIRIUKHIN, M. Y. & COLLINS, K. D., 2002. Dynamic hydration numbers for biologically important ions. *Biophysical Chemistry*, 99, 155-168.
- KISO, Y., KON, T., KITAO, T. & NISHIMURA, K., 2001a. Rejection properties of alkyl phthalates with nanofiltration membranes. *Journal of Membrane Science*, 182, 205-214.
- KISO, Y., SUGIURA, Y., KITAO, T. & NISHIMURA, K., 2001b. Effects of hydrophobicity and molecular size on rejection of aromatic pesticides with nanofiltration membranes. *Journal of Membrane Science*, 192, 1-10.
- KÖHLER, A. R., SOM, C., HELLAND, A. & GOTTSCHALK, F., 2008. Studying the potential release of carbon nanotubes throughout the application life cycle. *Journal of Cleaner Production*, 16, 927-937.
- KOSA, S. A., AL-ZHRANI, G. & ABDEL SALAM, M., 2012. Removal of heavy metals from aqueous solutions by multi-walled carbon nanotubes modified with 8-hydroxyquinoline. *Chemical Engineering Journal*, 181-182, 159-168.
- KOŠUTIĆ, K., DOLAR, D., AŠPERGER, D. & KUNST, B., 2007. Removal of antibiotics from a model wastewater by RO/NF membranes. *Separation and Purification Technology*, 53, 244-249.

- KOŠUTIĆ, K., FURAČ, L., SIPOS, L. & KUNST, B., 2005. Removal of arsenic and pesticides from drinking water by nanofiltration membranes. *Separation and Purification Technology*, 42, 137-144.
- KOŠUTIĆ, K., KAŠTELAN-KUNST, L. & KUNST, B., 2000. Porosity of some commercial reverse osmosis and nanofiltration polyamide thin-film composite membranes. *Journal of Membrane Science*, 168, 101-108.
- KOŠUTIĆ, K. & KUNST, B., 2002. Removal of organics from aqueous solutions by commercial RO and NF membranes of characterized porosities. *Desalination*, 142, 47-56.
- KUESENG, P., THAMMAKHET, C., THAVARUNGKUL, P. & KANATHARANA, P., 2010. Multiwalled carbon nanotubes/cryogel composite, a new sorbent for determination of trace polycyclic aromatic hydrocarbons. *Microchemical Journal*, 96, 317-323.
- KUO, C.-Y., WU, C.-H. & WU, J.-Y., 2008. Adsorption of direct dyes from aqueous solutions by carbon nanotubes: determination of equilibrium, kinetics and thermodynamics parameters. *Journal of Colloid and Interface Science*, 327, 308-315.
- KWON, B., PARK, N. & CHO, J., 2005. Effect of algae on fouling and efficiency of UF membranes. *Desalination*, 179, 203-214.
- LAPWORTH, D. J., BARAN, N., STUART, M. E. & WARD, R. S., 2012. Emerging organic contaminants in groundwater: a review of sources, fate and occurrence. *Environmental Pollution*, 163, 287-303.
- LEE, S., ANG, W. S. & ELIMELECH, M., 2006. Fouling of reverse osmosis membranes by hydrophilic organic matter: implications for water reuse. 187, 313-321.
- LEE, Y.-C., KWON, T.-S., YANG, J.-S. & YANG, J.-W., 2007. Remediation of groundwater contaminated with DNAPLs by biodegradable oil emulsion. *Journal of Hazardous Materials*, 140, 340-345.
- LHASSANI, A., RUMEAU, M., BENJELLOUN, D. & PONTIE, M., 2001. Selective demineralization of water by nanofiltration Application to the defluorination of brackish water. *Water Research*, 35, 3260-3264.
- LI, P., FENG, X. B., QIU, G. L., SHANG, L. H. & LI, Z. G., 2009. Mercury pollution in Asia: a review of the contaminated sites. *Journal of Hazardous Materials*, 168, 591-601.
- LI, Q., XU, Z. & PINNAU, I., 2007. Fouling of reverse osmosis membranes by biopolymers in wastewater secondary effluent: role of membrane surface properties and initial permeate flux. *Journal of Membrane Science*, 229, 173-181.
- LI, S., HEIJMAN, S. G. J., VERBERK, J. Q. J. C., AMY, G. L. & VAN DIJK, J. C., 2012. Seawater ultrafiltration fouling control: backwashing with demineralized water/SWRO permeate. *Separation and Purification Technology*, 98, 327-336.
- LI, S., LI, X. & WANG, D., 2004. Membrane (RO-UF) filtration for antibiotic wastewater treatment and recovery of antibiotics. *Separation and Purification Technology*, 34, 109-114.
- LI, Y.-H., DING, J., LUAN, Z., DI, Z., ZHU, Y., XU, C., WU, D. & WEI, B., 2003. Competitive adsorption of  $Pb^{2+}$ ,  $Cu^{2+}$  and  $Cd^{2+}$  ions from aqueous solutions by multiwalled carbon nanotubes. *Carbon*, 41, 2787-2792.

- LIIKANEN, R., MIETTINEN, I. & LAUKKANEN, R., 2003. Selection of NF membrane to improve quality of chemically treated surface water. *Water Research*, 37, 864-872.
- LIIKANEN, R., YLI-KUIVILA, J. & LAUKKANEN, R., 2002. Efficiency of various chemical cleanings for nanofiltration membrane fouled by conventionally-treated surface water. *Journal of Membrane Science*, 195, 265-276.
- LIN, C.-J., SHIRAZI, S., RAO, P. & AGARWAL, S., 2006. Effects of operational parameters on cake formation of  $\text{CaSO}_4$  in nanofiltration. *Water Research*, 40, 806-816.
- LIN, Y.-L., CHIANG, P.-C. & CHANG, E. E., 2007. Removal of small trihalomethane precursors from aqueous solution by nanofiltration. *Journal of Hazardous Materials*, 146, 20-29.
- LIU, A., MING, J. & ANKUMAH, R. O., 2005. Nitrate contamination in private wells in rural Alabama, United States. *Science of The Total Environment*, 346, 112-120.
- LIU, F.-F., FAN, J.-L., WANG, S.-G. & MA, G.-H., 2013a. Adsorption of natural organic matter analogues by multi-walled carbon nanotubes: comparison with powdered activated carbon. *Chemical Engineering Journal*, 219, 450-458.
- LIU, J., ZHANG, G., QIN, J., ZHANG, W., XING, Y., GUO, D. & SHEN, Z., 2010. Field emission from combined structures of carbon nanotubes and carbon nanofibers. *Physica B: Condensed Matter*, 405, 2551-2555.
- LIU, X., WANG, M., ZHANG, S. & PAN, B., 2013b. Application potential of carbon nanotubes in water treatment: a review. *Journal of Environmental Sciences*, 25, 1263-1280.
- LONCINAR, M., ZUPANCIC, M., BUKOVEC, P. & JUSTIN, M. Z., 2010. Fate of saline ions in a planted landfill site with leachate recirculation. *Waste Management*, 30, 110-118.
- LOUIE, J. S., PINNAU, I., CIOBANU, I., ISHIDA, K. P., NG, A. & REINHARD, M., 2006. Effects of polyether-polyamide block copolymer coating on performance and fouling of reverse osmosis membranes. *Journal of Membrane Science*, 280, 762-770.
- LU, C. & CHIU, H., 2006. Adsorption of zinc (II) from water with purified carbon nanotubes. *Chemical Engineering Science*, 61, 1138-1145.
- LU, C., CHUNG, Y.-L. & CHANG, K.-F., 2005. Adsorption of trihalomethanes from water with carbon nanotubes. *Water Research*, 39, 1183-1189.
- LU, C., CHUNG, Y.-L. & CHANG, K.-F., 2006. Adsorption thermodynamic and kinetic studies of trihalomethanes on multiwalled carbon nanotubes. *Journal of Hazardous Materials*, 138, 304-310.
- LU, C. & SU, F., 2007. Adsorption of natural organic matter by carbon nanotubes. *Separation and Purification Technology*, 58, 113-121.
- LUO, Y., GUO, W., NGO, H. H., NGHIEM, L. D., HAI, F. I., ZHANG, J., LIANG, S. & WANG, X. C., 2014. A review on the occurrence of micropollutants in the aquatic environment and their fate and removal during wastewater treatment. *Science of The Total Environment*, 473-474, 619-641.
- LV, L., WANG, Y., WEI, M. & CHENG, J., 2008. Bromide ion removal from contaminated water by calcined and uncalcined  $\text{MgAl-CO}_3$  layered double hydroxides. *Journal of Hazardous Materials*, 152, 1130-1137.

- M'NIF, A., BOUGUECHA, S., HAMROUNI, B. & DHAHBI, M., 2007. Coupling of membrane processes for brackish water desalination. *Desalination*, 203, 331-336.
- MA, M., LIU, R., LIU, H., QU, J. & JEFFERSON, W., 2012. Effects and mechanisms of pre-chlorination on *Microcystis aeruginosa* removal by alum coagulation: significance of the released intracellular organic matter. *Separation and Purification Technology*, 86, 19-25.
- MACQUARRIE, K. T. B., SUDICKY, E. A. & ROBERTSON, W. D., 2001. Numerical simulation of a fine-grained denitrification layer for removing septic system nitrate from shallow groundwater. *Journal of Contaminant Hydrology*, 52, 29-55.
- MADAENI, S. S., ZINADINI, S. & VATANPOUR, V., 2013. Preparation of superhydrophobic nanofiltration membrane by embedding multiwalled carbon nanotube and polydimethylsiloxane in pores of microfiltration membrane. *Separation and Purification Technology*, 111, 98-107.
- MALAMIS, S., KATSOU, E., TAKOPOULOS, K., DEMETRIOU, P. & LOIZIDOU, M., 2012. Assessment of metal removal, biomass activity and RO concentrate treatment in an MBR–RO system. *Journal of Hazardous Materials*, 209–210, 1-8.
- MÄNTTÄRI, M., PIHLAJAMÄKI, A. & NYSTRÖM, M., 2006. Effect of pH on hydrophilicity and charge and their effect on the filtration efficiency of NF membranes at different pH. *Journal of Membrane Science*, 280, 311-320.
- MATILAINEN, A., VEPSÄLÄINEN, M. & SILLANPÄÄ, M., 2010. Natural organic matter removal by coagulation during drinking water treatment: a review. *Advances in Colloid and Interface Science*, 159, 189-197.
- MELIÁN-MARTEL, N., SADHWANI, J. J., MALAMIS, S. & OCHSENKÜHN-PETROPOULOU, M., 2012. Structural and chemical characterization of long-term reverse osmosis membrane fouling in a full scale desalination plant. *Desalination*, 305, 44-53.
- METHOD.200.7, 1994. Determination of metals and trace elements in water and wastes by inductively coupled plasma atomic emission spectrometry (ICP-AES). Revision 4.4 ed. Ohio: United States Environmental Protection Agency.
- METHOD.5030B, 1996. Purge-and-Trap for Aqueous Samples. Revision 2 ed. Ohio: United States Environmental Protection Agency.
- METHOD.8260B, 1996. Volatile Organic Compounds by Gas Chromatography/Mass Spectrometry (GC/MS). Revision 2 ed. Ohio: United States Environmental Protection Agency.
- METHOD.7470A, 1994. Mercury in liquid waste (manual cold-vapor technique). USEPA.
- METROHM. 2013. *Metrohm 881 Compact IC Pro Suppression Ion chromatography*. [Online]. Available: [http://www.metrohm.com/com/Produkte2/IC/ProfiC\\_Compact.html?identifier=28810030&language=en&name=28810030](http://www.metrohm.com/com/Produkte2/IC/ProfiC_Compact.html?identifier=28810030&language=en&name=28810030) [Accessed 9/3/2013].
- MINHAS, F. T., MEMON, S., BHANGER, M. I., IQBAL, N. & MUJAHID, M., 2013. Solvent resistant thin film composite nanofiltration membrane: characterization and permeation study. *Applied Surface Science*, 282, 887-897.



- MISDAN, N., LAU, W. J. & ISMAIL, A. F., 2012. Seawater Reverse Osmosis (SWRO) desalination by thin-film composite membrane—Current development, challenges and future prospects. *Desalination*, 287, 228-237.
- MO, Y., XIAO, K., SHEN, Y. & HUANG, X., 2011. A new perspective on the effect of complexation between calcium and alginate on fouling during nanofiltration. *Separation and Purification Technology*, 82, 121-127.
- MOHAMMAD, A. W. & ALI, N. A., 2002. Understanding the steric and charge contributions in NF membranes using increasing MWCO polyamide membranes. *Desalination*, 147, 205-212.
- MOHAMMAD, A. W., TEOW, Y. H., ANG, W. L., CHUNG, Y. T., OATLEY-RADCLIFFE, D. L. & HILAL, N., 2015. Nanofiltration membranes review: recent advances and future prospects. *Desalination*, 356, 226-254.
- MOHSEN-NIA, M., MONTAZERI, P. & MODARRESS, H., 2007. Removal of Cu<sup>2+</sup> and Ni<sup>2+</sup> from wastewater with a chelating agent and reverse osmosis processes. *Desalination*, 217, 276-281.
- MOHSEN, M. S., JABER, J. O. & AFONSO, M. D., 2003. Desalination of brackish water by nanofiltration and reverse osmosis. *Desalination*, 157, 167.
- MONDAL, S. & WICKRAMASINGHE, S. R., 2012. Photo-induced graft polymerization of N-isopropyl acrylamide on thin film composite membrane: produced water treatment and antifouling properties. *Separation and Purification Technology*, 90, 231-238.
- MORENO-CASTILLA, C., 2004. Adsorption of organic molecules from aqueous solutions on carbon materials. *Carbon*, 42, 83-94.
- MULDER, M., 1996. *Basic Principles of Membrane Technology*, Boston, Kluwer Academic.
- MUÑOZ-AGUADO, M. J., WILEY, D. E. & FANE, A. G., 1996. Enzymatic and detergent cleaning of a polysulfone ultrafiltration membrane fouled with BSA and whey. *Journal of Membrane Science*, 117, 175-187.
- MURTHY, Z. V. P. & CHAUDHARI, L. B., 2009. Separation of binary heavy metals from aqueous solutions by nanofiltration and characterization of the membrane using Spiegler–Kedem model. *Chemical Engineering Journal*, 150, 181-187.
- MUTTER, J., NAUMANN, J., SADAGHIANI, C., WALACH, H. & DRASCH, G., 2004. Amalgam studies: disregarding basic principles of mercury toxicity. *International Journal of Hygiene and Environmental Health*, 207, 391-397.
- NEALE, P. A., 2009. *Influence of Solute-Solute Interactions on Membrane Filtration*. PhD, University of Edinburgh: Edinburgh.
- NGHIEM, L. D. & COLEMAN, P. J., 2008. NF/RO filtration of the hydrophobic ionogenic compound triclosan: transport mechanisms and the influence of membrane fouling. *Separation and Purification Technology*, 62, 709-716.
- NGHIEM, L. D., COLEMAN, P. J. & ESPENDILLER, C., 2010. Mechanisms underlying the effects of membrane fouling on the nanofiltration of trace organic contaminants. *Desalination*, 250, 682-687.
- NGHIEM, L. D. & HAWKES, S., 2009. Effects of membrane fouling on the nanofiltration of trace organic contaminants. *Desalination*, 236, 273-281.
- NGHIEM, L. D., MANIS, A., SOLDENHOFF, K. & SCHÄFER, A. I., 2004a. Estrogenic hormone removal from wastewater using NF/RO membranes. *Journal of Membrane Science*, 242, 37-45.

- NGHIEM, L. D. & SCHÄFER, A., 2004. Trace Contaminant Removal with Nanofiltration. In: SCHÄFER A.I., W. T. D., FANE A.G. (ed.) *Nanofiltration – Principles and Applications*. Edinburgh: Elsevier, 479-520.
- NGHIEM, L. D. & SCHÄFER, A. I., 2002. Adsorption and transport of trace contaminant estrone in NF/RO membranes. *Environmental Engineering Science*, 19, 441-451.
- NGHIEM, L. D., SCHÄFER, A. I. & ELIMELECH, M., 2004b. Removal of natural hormones by nanofiltration membranes: measurement, modeling, and mechanisms. *Environmental Science & Technology*, 38 1888–1896.
- NGHIEM, L. D., SCHÄFER, A. I. & ELIMELECH, M., 2005. Pharmaceutical retention mechanisms by nanofiltration membranes. *Environmental Science & Technology*, 39, 7698-7705.
- NGHIEM, L. D., SCHÄFER, A. I. & ELIMELECH, M., 2006. Role of electrostatic interactions in the retention of pharmaceutically active contaminants by a loose nanofiltration membrane. *Journal of Membrane Science*, 286, 52-59.
- NI, J.-Q., ROBARGE, W. P., XIAO, C. & HEBER, A. J., 2012. Volatile organic compounds at swine facilities: a critical review. *Chemosphere*, 89, 769-788.
- NICOLAISEN, B., 2003. Developments in membrane technology for water treatment. *Desalination*, 153, 355-360.
- NIEUWENHUIJSEN, M. J., TOLEDANO, M. B., EATON, N. E., FAWELL, J. & ELLIOTT, P., 2000. Chlorination disinfection byproducts in water and their association with adverse reproductive outcomes: a review. *Occupational and Environmental Medicine*, 57, 73–85.
- NIGHTINGALE, E. R., 1959. Phenomenological theory of ion solvation. Effective radii of hydrated ions. *Journal of physical chemistry*, 63, 1381–1387.
- NIKOLAOU, A. D., GOLFINOPOULOS, S. K., KOSTOPOULOU, M. N., KOLOKYTHAS, G. A. & LEKKAS, T. D., 2002. Determination of volatile organic compounds in surface waters and treated wastewater in Greece. *Water Research*, 36, 2883-2890.
- NORTON-BRANDÃO, D., SCHERRENBURG, S. M. & VAN LIER, J. B., 2013. Reclamation of used urban waters for irrigation purposes – a review of treatment technologies. *Journal of Environmental Management*, 122, 85–98.
- OHURA, T., AMAGAI, T. & FUSAYA, M., 2006. Regional assessment of ambient volatile organic compounds in an industrial harbor area, Shizuoka, Japan. *Atmospheric Environment*, 40, 238-248.
- ORICA. 2011. *Orica Botany Transformation Projects* [Online]. Sydney: Orica Ltd. Available: <http://www.oricabotanytransformation.com/index.asp?page=2project=27> [Accessed 11/11/2011].
- ORIŇÁKOVÁ, R. & ORIŇÁK, A., 2011. Recent applications of carbon nanotubes in hydrogen production and storage. *Fuel*, 90, 3123-3140.
- ORON, G., GILLERMAN, L., BICK, A., BURIKOVSKY, N., MANOR, Y., BEN-YITSHAK, E., KATZ, L. & HAGIN, J., 2006. A two stage membrane treatment of secondary effluent for unrestricted reuse and sustainable agricultural production. *Desalination*, 187, 335-345.
- ORON, G., GILLERMAN, L., BICK, A., MANOR, Y., BURIKOVSKY, N. & HAGIN, J., 2007. Advanced low quality waters treatment for unrestricted use purposes: imminent challenges. *Desalination*, 213, 189-198.

- ORTEGA, L. M., LEBRUN, R., BLAIS, J.-F. & HAUSLER, R., 2008. Removal of metal ions from an acidic leachate solution by nanofiltration membranes. *Desalination*, 227, 204-216.
- OZAKI, H. & LI, H., 2002. Rejection of organic compounds by ultra-low pressure reverse osmosis membrane. *Water Research*, 36, 123-130.
- PAN, B., SUN, K. & XING, B., 2010. Adsorption kinetics of 17-ethinyl estradiol and bisphenol A on carbon nanomaterials. II. Concentration-dependence. *Journal of Soils and Sediments*, 10, 845-854.
- PAN, B. & XING, B., 2008. Adsorption mechanisms of organic chemicals on carbon nanotubes. *Environmental Science & Technology*, 42 (24) 9005–9013.
- PAPADOPOULOS, A., FATTA, D., PARPERIS, K., MENTZIS, A., HARALAMBOUS, K. J. & LOIZIDOU, M., 2004. Nickel uptake from a wastewater stream produced in a metal finishing industry by combination of ion-exchange and precipitation methods. *Separation and Purification Technology*, 39, 181-188.
- PARADISE, M. & GOSWAMI, T., 2007. Carbon nanotubes – Production and industrial applications. *Materials & Design*, 28, 1477-1489.
- PENG, X., LI, Y., LUAN, Z., DI, Z., WANG, H., TIAN, B. & JIA, Z., 2003. Adsorption of 1, 2-dichlorobenzene from water to carbon nanotubes. *Chemical Physics Letters*, 376, 154-158.
- PERKINELMER. 2013. *Perkin Elmer FIMS 400 (Flow Injection Mercury System)*. [Online]. Available: <http://mx.nthu.edu.tw/~ycsun/main/instrument/FIMS400.pdf> [Accessed 9/9/2013].
- PERKINELMER. 2013 *Analysis of Trace Metals in Drinking Water with the Optima 7000 DV ICP-OES*. [Online]. Available: [http://www.perkinelmer.com/CMSResources/Images/4474318APP\\_TraceMetalsinDrinkingWaterbyOptima7000.pdf](http://www.perkinelmer.com/CMSResources/Images/4474318APP_TraceMetalsinDrinkingWaterbyOptima7000.pdf) [Accessed 9/9/2013].
- PILLAY, K., CUKROWSKA, E. M. & COVILLE, N. J., 2009. Multi-walled carbon nanotubes as adsorbents for the removal of parts per billion levels of hexavalent chromium from aqueous solution. *Journal of Hazardous Materials*, 166, 1067-1075.
- PIRRONE, N. & WICHMANN-FIEBIG, M., 2003. Some recommendations on mercury measurements and research activities in the European Union. *Atmospheric Environment*, 37, 3-8.
- PLAKAS, K. V. & KARABELAS, A. J., 2012. Removal of pesticides from water by NF and RO membranes — a review. *Desalination*, 287, 255-265.
- POLKOWSKA, Ż., KOZŁOWSKA, K., MAZERSKA, Z., GÓRECKI, T. & NAMIEŚNIK, J., 2003. Relationship between volatile organohalogen compounds in drinking water and human urine in Poland. *Chemosphere*, 53, 899-909.
- POPOV, V. N., 2004. Carbon nanotubes: properties and application. *Materials Science and Engineering: R: Reports*, 43, 61-102.
- PYRZYŃSKA, K., 2011. Carbon nanotubes as sorbents in the analysis of pesticides. *Chemosphere*, 83, 1407-1413.
- QIAN, J., ZHANG, L., CHEN, H., HOU, M., NIU, Y., XU, Z. & LIU, H., 2009. Distribution of mercury pollution and Its source in the soils and vegetables in

- Guilin area, China. *Bulletin of Environmental Contamination and Toxicology*, 83, 920-925.
- QIN, X. S., HUANG, G. H., CHAKMA, A., CHEN, B. & ZENG, G. M., 2007. Simulation-based process optimization for surfactant-enhanced aquifer remediation at heterogeneous DNAPL-contaminated sites. *Science of The Total Environment*, 381, 17-37.
- QU, X., ALVAREZ, P. J. J. & LI, Q., 2013. Applications of nanotechnology in water and wastewater treatment. *Water Research*, 47, 3931-3946.
- RADJENOVIĆ, J., PETROVIĆ, M., VENTURA, F. & BARCELÓ, D., 2008. Rejection of pharmaceuticals in nanofiltration and reverse osmosis membrane drinking water treatment. *Water Research*, 42, 3601-3610.
- RÄISÄNEN, J., NIEMELÄ, R. & ROSENBERG, C., 2001. Tetrachloroethylene emissions and exposure in dry cleaning. *Journal of the Air & Waste Management Association*, 51, 1671-1675.
- RAO, G. P., LU, C. & SU, F., 2007. Sorption of divalent metal ions from aqueous solution by carbon nanotubes: a review. *Separation and Purification Technology*, 58, 224-231.
- RASHID, M. H.-O., PHAM, S. Q. T., SWEETMAN, L. J., ALCOCK, L. J., WISE, A., NGHIEM, L. D., TRIANI, G., PANHUIS, M. I. H. & RALPH, S. F., 2014. Synthesis, properties, water and solute permeability of MWNT buckypapers. *Journal of Membrane Science*, 456, 175-184.
- RAVINDRAN, V., TSAI, H.-H., WILLIAMS, M. D. & PIRBAZARI, M., 2009. Hybrid membrane bioreactor technology for small water treatment utilities: Process evaluation and primordial considerations. *Journal of Membrane Science*, 344, 39-54.
- REDONDO, J. A., 2001. Brackish-, sea- and wastewater desalination. *Desalination*, 138, 29-40.
- REID, K., DIXON, M., PELEKANI, C., JARVIS, K., WILLIS, M. & YU, Y., 2014. Biofouling control by hydrophilic surface modification of polypropylene feed spacers by plasma polymerisation. *Desalination*, 335, 108-118.
- REINHARD, M., GOODMAN, N. L., MCCARTY, P. L. & ARGO, D. G., 1986. Removing trace organics by reverse osmosis using cellulose acetate and polyamide membranes. *Journal of the American Water Works Association*, 78, 163-74.
- REN, X., CHEN, C., NAGATSU, M. & WANG, X., 2011. Carbon nanotubes as adsorbents in environmental pollution management: a review. *Chemical Engineering Journal*, 170, 395-410.
- RENOU, S., GIVAUDAN, J. G., POULAIN, S., DIRASSOUYAN, F. & MOULIN, P., 2008. Landfill leachate treatment: review and opportunity. *Journal of Hazardous Materials*, 150, 468-493.
- REVERTER, J. A., TALO, S. & ALDAY, J., 2001. Las Palmas III — the success story of brine staging. *Desalination*, 138, 207-217.
- REZNIK, S. G., MENASHE, I. K., GROSSMAN, L. H., RUFEL, O. & DOSORETZ, C. G., 2011. Influence of seasonal and operating conditions on the rejection of pharmaceutical active compounds by RO and NF membranes. *Desalination*, 277, 250-256.
- RICHARD, Q. & YANG, R. T., 2001. Carbon nanotubes as superior sorbent for dioxin removal. *Journal of the American Chemical Society*, 123, 2058-2059.

- RICHARDS, L. A., RICHARDS, B. S. & SCHÄFER, A. I., 2011. Renewable energy powered membrane technology: salt and inorganic contaminant removal by nanofiltration/reverse osmosis. *Journal of Membrane Science*, 369, 188-195.
- RIGET, F., DIETZ, R., VORKAMP, K., JOHANSEN, P. & MUIR, D., 2004. Levels and spatial and temporal trends of contaminants in Greenland biota: an updated review. *Science of The Total Environment*, 331, 29-52.
- RITCHIE, S. M. C. & BHATTACHARYYA, D., 2002. Membrane-based hybrid processes for high water recovery and selective inorganic pollutant separation. *Journal of Hazardous Materials*, 92, 21-32.
- RIVETT, M. O., WEALTHALL, G. P., DEARDEN, R. A. & MCALARY, T. A., 2011. Review of unsaturated-zone transport and attenuation of volatile organic compound (VOC) plumes leached from shallow source zones. *Journal of Contaminant Hydrology*, 123, 130-156.
- RUTKIEWICZ, I., KUJAWSKI, W. & NAMIEŚNIK, J., 2010. Pervaporation of volatile organohalogen compounds through polydimethylsiloxane membrane. *Desalination*, 264, 160-164.
- SAHAR, E., DAVID, I., GELMAN, Y., CHIKUREL, H., AHARONI, A., MESSALEM, R. & BRENNER, A., 2011. The use of RO to remove emerging micropollutants following CAS/UF or MBR treatment of municipal wastewater. *Desalination*, 273, 142-147.
- SAITÚA, H., GIANNINI, F. & PADILLA, A. P., 2012. Drinking water obtaining by nanofiltration from waters contaminated with glyphosate formulations: process evaluation by means of toxicity tests and studies on operating parameters. *Journal of Hazardous Materials*, 227-228, 204-210.
- SALVESON, A. T., REQUA, D. A., WHITLEY, R. D. & TCHOBANOGLIOUS, G., 2000. Potable versus reclaimed: water quality, regulatory issues, emerging concerns. *Proceedings of the Water Environment Federation*, 2000, 546-558.
- SAVAGE, N. D., M.S, 2005. Nanomaterials and water purification: opportunities and challenges. *Journal of Nanoparticle Research*, 7, 331-341.
- SCHÄFER, A. I., FANE, A. G. & WAITE, T. D. (eds.), 2005. *Nanofiltration: principles and applications*. : Elsevier.
- SCHÄFER, A. I., NGHIEM, L. D., MEIER, A. & NEALE, P. A., 2010. Impact of organic matrix compounds on the retention of steroid hormone estrone by a 'loose' nanofiltration membrane. *Separation and Purification Technology*, 73, 179-187.
- SCHÄFER, A. I., PIHLAJAMÄKI, A., FANE, A. G., WAITE, T. D. & NYSTRÖM, M., 2004. Natural organic matter removal by nanofiltration: effects of solution chemistry on retention of low molar mass acids versus bulk organic matter. *Journal of Membrane Science*, 242, 73-85.
- SCHÜTH, C., DISSER, S., SCHÜTH, F. & REINHARD, M., 2000. Tailoring catalysts for hydrodechlorinating chlorinated hydrocarbon contaminants in groundwater. *Applied Catalysis B: Environmental*, 28, 147-152.
- SCHÜTH, C., KUMMER, N.-A., WEIDENTHALER, C. & SCHAD, H., 2004. Field application of a tailored catalyst for hydrodechlorinating chlorinated hydrocarbon contaminants in groundwater. *Applied Catalysis B: Environmental*, 52, 197-203.

- SHANNON, M. A., BOHN, P. W., ELIMELECH, M., GEORGIADIS, J. G., MARINAS, B. J. & MAYES, A. M., 2008. Science and technology for water purification in the coming decades. *Nature*, 452, 301-310.
- SHAO, D., CHEN, C. & WANG, X., 2012. Application of polyaniline and multiwalled carbon nanotube magnetic composites for removal of Pb (II). *Chemical Engineering Journal*, 185-186, 144-150.
- SHI, T., SHAO, M., ZHANG, H., YANG, Q. & SHEN, X., 2011. Surface modification of porous poly(tetrafluoroethylene) film via cold plasma treatment. *Applied Surface Science*, 258, 1474-1479.
- SHIH, Y.-H. & LI, M.-S., 2008. Adsorption of selected volatile organic vapors on multiwall carbon nanotubes. *Journal of Hazardous Materials*, 154, 21-28.
- SHIMADZU. 2013. *Shimadzu Purge & Trap/Gas Chromatography/Mass Spectrometer Detector*. [Online]. Available: <http://www.gentechscientific.com/gc-ms-systems/product/10724/agilent-6890-gc-with-5973-mass-spec-and-oi-4660-eclipse-purge-&-trap> [Accessed 9/9/2013].
- SHIRAZI, S., LIN, C.-J. & CHEN, D., 2010. Inorganic fouling of pressure-driven membrane processes — a critical review. *Desalination*, 250, 236-248.
- SHON, H. K., VIGNESWARAN, S., KIM, I. S., CHO, J. & NGO, H. H., 2004. Effect of pretreatment on the fouling of membranes: application in biologically treated sewage effluent. *Journal of Membrane Science*, 234, 111-120.
- SIKORA, J., HANSSON, C.-H. & ERICSSON, B., 1989. Pre-treatment and desalination of mine drainage water in a pilot plant. *Desalination*, 75, 363-378.
- SIMON, A., PRICE, W. E. & NGHIEM, L. D., 2012. Effects of chemical cleaning on the nanofiltration of pharmaceutically active compounds (PhACs). *Separation and Purification Technology*, 88, 208-215.
- STAMATIALIS, D. F., DIAS, C. R. & NORBERTA DE PINHO, M., 1999. Atomic force microscopy of dense and asymmetric cellulose-based membranes. *Journal of Membrane Science*, 160, 235-242.
- STEELE, M. K. & AITKENHEAD-PETERSON, J. A., 2011. Long-term sodium and chloride surface water exports from the Dallas/Fort Worth region. *Science of The Total Environment*, 409, 3021-3032.
- STERN, A. H., 2005. A review of the studies of the cardiovascular health effects of methylmercury with consideration of their suitability for risk assessment. *Environmental Research*, 98, 133-142.
- SUDILOVSKIY, P. S., KAGRAMANOV, G. G. & KOLESNIKOV, V. A., 2008. Use of RO and NF for treatment of copper containing wastewaters in combination with flotation. *Desalination*, 221, 192-201.
- SUN, L., PERDUE, E. M. & MCCARTHY, J. F., 1995. Using reverse osmosis to obtain organic matter from surface and ground waters. *Water Research*, 29, 1471-1477.
- SUNDARAM, B., FEITZ, A., CARITAT, P., PLAZINSKA, A., BRODIE, R., CORAM, J. & RANSLEY, T., 2009. Groundwater Sampling and Analysis – A Field guide. In: DEPARTMENT OF RESOURCES, E. A. T. (ed.). Canberra: Geoscience Australia.

- SUNGYUN, L., EUNKYUNG, L., JINSUNG, R., BYUNGCHAEON, L., SUHAN, K., SEOK, H. C., SANG, D. K. & JAEWEON, C., 2008. Characterization of marine organic matters and heavy metals with respect to desalination with RO and NF membranes. *Desalination*, 221, 244–252.
- SWEETMAN, L., 2012. *Synthesis, Characterisation and Applications of Carbon Nanotube Membrane Containing Macrocycles and Antibiotics*. PhD, University of Wollongong, Wollongong.
- SWEETMAN, L. J., ALCOCK, L. J., MCARTHUR, J. D., STEWART, E. M., TRIANI, G., PANHUIS, M. & RALPH, S. F., 2013. Bacterial filtration using carbon nanotube/antibiotic buckypaper membranes *Journal of Nanomaterials*, 2013, 781212, 1–11.
- TAKHT RAVANCHI, M., KAGHAZCHI, T. & KARGARI, A., 2009. Application of membrane separation processes in petrochemical industry: a review. *Desalination*, 235, 199–244.
- TANSEL, B., 2012. Significance of thermodynamic and physical characteristics on permeation of ions during membrane separation: hydrated radius, hydration free energy and viscous effects. *Separation and Purification Technology*, 86, 119–126.
- TANSEL, B., SAGER, J., GARLAND, J. & XU, S., 2009. Effect of transmembrane pressure on overall membrane resistance during cross-flow filtration of solutions with high-ionic content. *Journal of Membrane Science*, 328, 205–210.
- TANSEL, B., SAGER, J., RECTOR, T., JAY GARLAND, C., STRAYER, R., LEVINE, L., ROBERTS, M., HUMMERICK, M. & BAUER, J., 2006. Significance of hydrated radius and hydration shells on ionic permeability during nanofiltration in dead end and cross flow modes. *Separation and Purification Technology*, 51, 40–47.
- TAY, J.-H., LIU, J. & DELAI SUN, D., 2002. Effect of solution physico-chemistry on the charge property of nanofiltration membranes. *Water Research*, 36, 585–598.
- TEIXEIRA, M. R., ROSA, M. J. & NYSTRÖM, M., 2005. The role of membrane charge on nanofiltration performance. *Journal of Membrane Science*, 265, 160–166.
- THIRUVENKATACHARI, R., VIGNESWARAN, S. & NAIDU, R., 2008. Permeable reactive barrier for groundwater remediation. *Journal of Industrial and Engineering Chemistry*, 14, 145–156.
- THOSTENSON, E. T., REN, Z. & CHOU, T.-W., 2001. Advances in the science and technology of carbon nanotubes and their composites: a review. *Composites Science and Technology*, 61, 1899–1912.
- TOFIGHY, M. A. & MOHAMMADI, T., 2011. Adsorption of divalent heavy metal ions from water using carbon nanotube sheets. *Journal of Hazardous Materials*, 185, 140–147.
- TOZE, S., 2006. Water reuse and health risks--real vs. perceived. *Desalination*, 187, 41–51.
- TU, K. L., CHIVAS, A. R. & NGHIEM, L. D., 2011. Effects of membrane fouling and scaling on boron rejection by nanofiltration and reverse osmosis membranes. *Desalination*, 279, 269–277.

- UPADHYAYULA, V. K. K., DENG, S., MITCHELL, M. C. & SMITH, G. B., 2009. Application of carbon nanotube technology for removal of contaminants in drinking water: a review. *Science of The Total Environment*, 408, 1-13.
- URGUN-DEMIRTAS, M., BENDA, P. L., GILLENWATER, P. S., NEGRI, M. C., XIONG, H. & SNYDER, S. W., 2012. Achieving very low mercury levels in refinery wastewater by membrane filtration. *Journal of Hazardous Materials*, 215-216, 98-107.
- USEPA. 2011. *An Introduction to Indoor Air Quality (IAQ) – Volatile Organic Compounds (VOCs)* [Online]. [Accessed 18/7/2012 2012].
- UYAK, V., KOYUNCU, I., OKTEM, I., CAKMAKCI, M. & TOROZ, I., 2008. Removal of trihalomethanes from drinking water by nanofiltration membranes. *Journal of Hazardous Materials*, 152, 789-794.
- VAN DER BRUGGEN, B., BRAEKEN, L. & VANDECASTEELE, C., 2002. Flux decline in nanofiltration due to adsorption of organic compounds. *Separation and Purification Technology*, 29, 23-31.
- VAN DER BRUGGEN, B., KONINCKX, A. & VANDECASTEELE, C., 2004. Separation of monovalent and divalent ions from aqueous solution by electrodialysis and nanofiltration. *Water Research*, 38, 1347-1353.
- VAN DER BRUGGEN, B., SCHAEPE, J., MAES, W., WILMS, D. & VANDECASTEELE, C., 1998. Nanofiltration as a treatment method for the removal of pesticides from ground waters. *Desalination*, 117, 139-147.
- VAN DER BRUGGEN, B., SCHAEPE, J., WILMS, D. & VANDECASTEELE, C., 1999. Influence of molecular size, polarity and charge on the retention of organic molecules by nanofiltration. *Journal of Membrane Science*, 156, 29-41.
- VAN DER BRUGGEN, B. & VANDECASTEELE, C., 2002. Modelling of the retention of uncharged molecules with nanofiltration. *Water Research*, 36, 1360-1368.
- VAN DER BRUGGEN, B. & VANDECASTEELE, C., 2003. Removal of pollutants from surface water and groundwater by nanofiltration: overview of possible applications in the drinking water industry. *Environmental Pollution*, 122, 435-445.
- VAN HOOFF, S. C. J. M., MINNERY, J. G. & MACK, B., 2001. Dead-end ultrafiltration as alternative pre-treatment to reverse osmosis in seawater desalination: a case study. *Desalination*, 139, 161-168.
- VAN WAGNER, E. M., SAGLE, A. C., SHARMA, M. M., LA, Y.-H. & FREEMAN, B. D., 2011. Surface modification of commercial polyamide desalination membranes using poly(ethylene glycol) diglycidyl ether to enhance membrane fouling resistance. *Journal of Membrane Science*, 367, 273-287.
- VARDON, M., LENZEN, M., PEEVOR, S. & CREASER, M., 2007. Water accounting in Australia. *Ecological Economics*, 61, 650-659.
- VATANPOUR, V., MADAENI, S. S., MORADIAN, R., ZINADINI, S. & ASTINCHAP, B., 2011. Fabrication and characterization of novel antifouling nanofiltration membrane prepared from oxidized multiwalled carbon nanotube/polyethersulfone nanocomposite. *Journal of Membrane Science*, 375, 284-294.



- VECITIS, C. D., SCHNOOR, M. H., RAHAMAN, M. S., SCHIFFMAN, J. D. & ELIMELECH, M., 2011. Electrochemical multiwalled carbon nanotube filter for viral and bacterial removal and inactivation. *Environmental Science and Technology*, 45, 3672 - 3679.
- VERLIEFDE, A., CORNELISSEN, E., AMY, G., VAN DER BRUGGEN, B. & VAN DIJK, H., 2007a. Priority organic micropollutants in water sources in Flanders and the Netherlands and assessment of removal possibilities with nanofiltration. *Environmental Pollution*, 146, 281-289.
- VERLIEFDE, A. R. D., CORNELISSEN, E. R., HEIJMAN, S. G. J., VERBERK, J. Q. J. C., AMY, G. L., VAN DER BRUGGEN, B. & VAN DIJK, J. C., 2008. The role of electrostatic interactions on the rejection of organic solutes in aqueous solutions with nanofiltration. *Journal of Membrane Science*, 322, 52-66.
- VERLIEFDE, A. R. D., HEIJMAN, S. G. J., CORNELISSEN, E. R., AMY, G., VAN DER BRUGGEN, B. & VAN DIJK, J. C., 2007b. Influence of electrostatic interactions on the rejection with NF and assessment of the removal efficiency during NF/GAC treatment of pharmaceutically active compounds in surface water. *Water Research*, 41, 3227-3240.
- VILLANUEVA, C. M., CANTOR, K. P., CORDIER, S., JAAKKOLA, J. J. K., KING, W. D., LYNCH, C. F., PORRU, S. & KOGEVINAS, M., 2004. Disinfection byproducts and bladder cancer: a pooled analysis. *Epidemiology*, 15, 357.
- VOGEL, D., SIMON, A., ALTURKI, A. A., BILITEWSKI, B., PRICE, W. E. & NGHIE, L. D., 2010. Effects of fouling and scaling on the retention of trace organic contaminants by a nanofiltration membrane: the role of cake-enhanced concentration polarisation. *Separation and Purification Technology*, 73, 256-263.
- VOLKOV, A. G., PAULA, S. & DEAMER, D. W., 1997. Two mechanisms of permeation of small neutral molecules and hydrated ions across phospholipid bilayers. *Bioelectrochemistry and Bioenergetics*, 42, 153-160.
- VOORTHUIZEN, E. M., ZWIJNENBURG, A. & WESSLING, M., 2005. Nutrient removal by NF and RO membranes in a decentralized sanitation system. *Water Research*, 39, 3657-3667.
- VRIJENHOEK, E. M., HONG, S. & ELIMELECH, M., 2001. Influence of membrane surface properties on initial rate of colloidal fouling of reverse osmosis and nanofiltration membranes. *Journal of Membrane Science*, 188, 115-128.
- WAKIDA, F. T. & LERNER, D. N., 2005. Non-agricultural sources of groundwater nitrate: a review and case study. *Water Research*, 39, 3-16.
- WALHA, K., AMAR, R. B., FIRDAOUS, L., QUÉMÉNEUR, F. & JAOUEN, P., 2007. Brackish groundwater treatment by nanofiltration, reverse osmosis and electrodialysis in Tunisia: performance and cost comparison. *Desalination*, 207, 95-106.
- WANG, C., SUCH, G. K., WIDJAYA, A., LOMAS, H., STEVENS, G., CARUSO, F. & KENTISH, S. E., 2012a. Click poly(ethylene glycol) multilayers on RO membranes: Fouling reduction and membrane characterization. *Journal of Membrane Science*, 409-410, 9-15.

- WANG, J., FENG, X., ANDERSON, C. W. N., XING, Y. & SHANG, L., 2012b. Remediation of mercury contaminated sites – a review. *Journal of Hazardous Materials*, 221–222, 1-18.
- WANG, L., LI, B., GAO, X., WANG, Q., LU, J., WANG, Y. & WANG, S., 2014. Study of membrane fouling in cross-flow vacuum membrane distillation. *Separation and Purification Technology*, 122, 133-143.
- WANG, Q., KIM, D., DIONYSIOU, D. D., SORIAL, G. A. & TIMBERLAKE, D., 2004. Sources and remediation for mercury contamination in aquatic systems—a literature review. *Environmental Pollution*, 131, 323-336.
- WARD, M. H., 2005. Workgroup report: drinking-water nitrate and health-recent findings and research needs. *Environmental Health Perspectives*, 113, 1607.
- WATSON, K., FARRÉ, M. J. & KNIGHT, N., 2012. Strategies for the removal of halides from drinking water sources, and their applicability in disinfection by-product minimisation: a critical review. *Journal of Environmental Management*, 110, 276-298.
- WEI, X., WANG, Z., ZHANG, Z., WANG, J. & WANG, S., 2010. Surface modification of commercial aromatic polyamide reverse osmosis membranes by graft polymerization of 3-allyl-5,5-dimethylhydantoin. *Journal of Membrane Science*, 351, 222-233.
- WEINER, E. R., 2007. *Application of Environmental Aquatic Chemistry - A Practical Guide*, Boca Raton, Taylor & Francis.
- WELLS, M. J. M., 2006. Log  $D_{ow}$  : key to understanding and regulating wastewater-derived contaminants. *Environmental Chemistry*, 3, 439-449.
- WINTGENS, T., MELIN, T., SCHÄFER, A., KHAN, S., MUSTON, M., BIXIO, D. & THOEYE, C., 2005. The role of membrane processes in municipal wastewater reclamation and reuse. *Desalination*, 178, 1-11.
- WISE, A., 2011. *Carbon Nanotube Membranes for Filtration*. Bachelor of Nanotechnology with Honours, University of Wollongong.
- WOLFE, A. H. & PATZ, J. A., 2002. Reactive nitrogen and human health: acute and long-term implications. *AMBIO: A Journal of the Human Environment*, 31, 120-125.
- WOLLONGONG CITY COUNCIL. 2011. *A Brief History of the Russell Vale Golf Course Site* [Online]. Wollongong city council Available: [http://www.russellvalegolfclub.com.au/history\\_board.html](http://www.russellvalegolfclub.com.au/history_board.html) [Accessed 10/2/2011].
- XIE, M., NGHIEM, L. D., PRICE, W. E. & ELIMELECH, M., 2012. Comparison of the removal of hydrophobic trace organic contaminants by forward osmosis and reverse osmosis. *Water Research*, 46, 2683-2692.
- XIE, Y.-J., YU, H.-Y., WANG, S.-Y. & XU, Z.-K., 2007. Improvement of antifouling characteristics in a bioreactor of polypropylene microporous membrane by the adsorption of Tween 20. *Journal of Environmental Sciences*, 19, 1461-1465.
- XU, G.-R., WANG, J.-N. & LI, C.-J., 2013. Strategies for improving the performance of the polyamide thin film composite (PA-TFC) reverse osmosis (RO) membranes: Surface modifications and nanoparticles incorporations. *Desalination*, 328, 83-100.
- XU, P., BELLONA, C. & DREWES, J. E., 2010. Fouling of nanofiltration and reverse osmosis membranes during municipal wastewater reclamation:

- membrane autopsy results from pilot-scale investigations. *Journal of Membrane Science*, 353, 111-121.
- XU, P., DREWES, J., BELLONA, C., AMY, G., KIM, T. & ADAM, M., 2005. Rejection of emerging organic micropollutants in nanofiltration-reverse osmosis membrane applications. *Water Environment Research*, 77, 40-48.
- XU, P., DREWES, J. E., KIM, T. U., BELLONA, C. & AMY, G., 2006. Effect of membrane fouling on transport of organic contaminants in NF/RO membrane applications. *Journal of Membrane Science*, 279, 165-175.
- XU, Z., HUANG, X. & WAN, L., 2009. *Surface Engineering of Polymer Membranes*, Berlin Springer.
- YAN, H., GONG, A., HE, H., ZHOU, J., WEI, Y. & LV, L., 2006. Adsorption of microcystins by carbon nanotubes. *Chemosphere*, 62, 142-148.
- YAN, X., SHI, B., LU, J., FENG, C., WANG, D. & TANG, H., 2008. Adsorption and desorption of atrazine on carbon nanotubes. *Journal of Colloid and Interface Science*, 321, 30-38.
- YANG, K. & XING, B., 2007. Desorption of polycyclic aromatic hydrocarbons from carbon nanomaterials in water. *Environmental Pollution*, 145, 529-537.
- YANGALI-QUINTANILLA, V., SADMANI, A., MCCONVILLE, M., KENNEDY, M. & AMY, G., 2009. Rejection of pharmaceutically active compounds and endocrine disrupting compounds by clean and fouled nanofiltration membranes. *Water Research*, 43, 2349-2362.
- YAROSHCHUK, A. E., 2001. Non-steric mechanisms of nanofiltration: superposition of Donnan and dielectric exclusion. *Separation and Purification Technology*, 22-23 143-158.
- YOON, Y. & LUEPTOW, R. M., 2005. Removal of organic contaminants by RO and NF membranes. *Journal of Membrane Science*, 261, 76-86.
- YU, J.-G., ZHAO, X.-H., YANG, H., CHEN, X.-H., YANG, Q., YU, L.-Y., JIANG, J.-H. & CHEN, X.-Q., 2014. Aqueous adsorption and removal of organic contaminants by carbon nanotubes. *Science of The Total Environment*, 482-483, 241-251.
- YU, J.-J. & CHOU, S.-Y., 2000. Contaminated site remedial investigation and feasibility removal of chlorinated volatile organic compounds from groundwater by activated carbon fiber adsorption. *Chemosphere*, 41, 371-378.
- YUAN, W., JIANG, G., CHE, J., QI, X., XU, R., CHANG, M. W., CHEN, Y., LIM, S. Y., DAI, J. & CHAN-PARK, M. B., 2008. Deposition of silver nanoparticles on multiwalled carbon nanotubes grafted with hyperbranched poly (amidoamine) and their antimicrobial effects. *The Journal of Physical Chemistry*, 112, 18754-18759.
- YÜKSEL, S., KABAY, N. & YÜKSEL, M., 2013. Removal of bisphenol A (BPA) from water by various nanofiltration (NF) and reverse osmosis (RO) membranes. *Journal of Hazardous Materials*, 263, Part 2, 307-310.
- ZAZOULI, M. A., SUSANTO, H., NASSERI, S. & ULBRICHT, M., 2009. Influences of solution chemistry and polymeric natural organic matter on the removal of aquatic pharmaceutical residuals by nanofiltration. *Water Research*, 43, 3270-3280.

- ZHAN, Y., LIN, J. & ZHU, Z., 2011. Removal of nitrate from aqueous solution using cetylpyridinium bromide (CPB) modified zeolite as adsorbent. *Journal of Hazardous Materials*, 186, 1972-1978.
- ZHANG, L. & WONG, M. H., 2007. Environmental mercury contamination in China: sources and impacts. *Environment International*, 33, 108-121.
- ZHANG, L., XU, T., LIU, X., ZHANG, Y. & JIN, H., 2011. Adsorption behavior of multi-walled carbon nanotubes for the removal of olaquinox from aqueous solutions. *Journal of Hazardous Materials*, 197, 389-396.
- ZHANG, X., FAN, L. & RODDICK, F. A., 2013. Understanding the fouling of a ceramic microfiltration membrane caused by algal organic matter released from *Microcystis aeruginosa*. *Journal of Membrane Science*, 447, 362-368.
- ZHANG, Y., LI, C., WANG, X., GUO, H., FENG, Y. & CHEN, J., 2012. Rush-hour aromatic and chlorinated hydrocarbons in selected subway stations of Shanghai, China. *Journal of Environmental Sciences*, 24, 131-141.
- ZHENG, L., LIU, G. & CHOU, C.-L., 2007. The distribution, occurrence and environmental effect of mercury in Chinese coals. *Science of The Total Environment*, 384, 374-383.
- ZHOU, S., SHAO, Y., GAO, N., LI, L., DENG, J., TAN, C. & ZHU, M., 2014. Influence of hydrophobic/hydrophilic fractions of extracellular organic matters of *Microcystis aeruginosa* on ultrafiltration membrane fouling. *Science of The Total Environment*, 470-471, 201-207.
- ZHOU, Y., YU, S., GAO, C. & FENG, X., 2009. Surface modification of thin film composite polyamide membranes by electrostatic self deposition of polycations for improved fouling resistance. *Separation and Purification Technology*, 66, 287-294.
- ZI-WEI, Y., GUI-BIN, J. & HENG-ZHEN, X., 2002. Distribution of organochlorine pesticides in seawater of the Bering and Chukchi Sea. *Environmental Pollution*, 116, 49-56.
- ZOU, L., VIDALIS, I., STEELE, D., MICHELMORE, A., LOW, S. P. & VERBERK, J. Q. J. C., 2011. Surface hydrophilic modification of RO membranes by plasma polymerization for low organic fouling. *Journal of Membrane Science*, 369, 420-428.
- ZULARISAM, A. W., ISMAIL, A. F., SALIM, M. R., SAKINAH, M. & OZAKI, H., 2007. The effects of natural organic matter (NOM) fractions on fouling characteristics and flux recovery of ultrafiltration membranes. *Desalination*, 212, 191-208.

## THESIS RELATED PUBLICATION

### Journal papers

1. Altalyan, H.N., B. Jones, J. Bradd, L.D. Nghiem and Y.M. Alyazichi, *Removal of volatile organic compounds (VOCs) from groundwater by reverse osmosis and nanofiltration*. Journal of Water Process Engineering, 2015. Manuscript in submission.
2. Altalyan, H.N., B. Jones, J. Bradd, M. Panhuis and S.F. Ralph, *Synthesis, characterisation and water permeability of MWNT buckypapers*. Manuscript will be submitted to Journal of Membrane Science, 2015.

### Conference papers and posters

1. Altalyan, H.N., B. Jones, J. Bradd and L.D. Nghiem, *Removal of organic contaminants from surface and groundwater by reverse osmosis and nanofiltration*. 2nd International Conference on Desalination using Membrane Technology, 2015, Singapore Expo Convention Centre, Singapore.
2. Alyazichi, Y.M., B. Jones, E. Mclean, H.N. Altalyan and A. Alnasrawi, *Risk Assessment of trace element pollution in Gynea Bay, NSW, Australia*. International Conference on Environmental and Water Resource Engineering, 2015, Melbourne, Australia.

## Appendix A : ILLUSTRATES WEATHER DATA FOR RUSSELL VALE AND BOTANY BAY AREAS.

**Table A-1:** Illustrates daily maximum temperature for Russell Vale area [Bellambi AWS (68228)] <sup>a</sup>.

2012	Jan	Feb	Mar	Apr	May	Jun	Jul	Aug	Sep	Oct	Nov	Dec
1st	24	18	26.3	23	21.8	18.7	15.7	14.4	15.9	17.9	28.7	28.3
2nd	24.5	18.2	20	23.1	23.3	16.5	15.9	14.5	17	22.9	17.6	21
3rd	23.6	21.2	21.2	26.6*	19.2	15.3	15.1	18.1	18.8	30.6	17.7	21.4
4th	23.8	24	23	24.6	19	20	15	19.8	20.6	31.6	21.4	28.3
5th	23.9	25.2	23.3	24.4	18.9	16	14.1	20.8	26.9	31.6	21.6	24.9
6th	21.4	22.4	20.7	24.8	19.5	12.9	14.6	16.3	26.8	16.7	22.5	19.6
7th	23.7	21.2	20.4	26	18	15.7	15.2	16.1	20.2	17.2	21.6	21.1
8th	24.2	21.1	20.1	23.1	22.4	15.2	16.9	21.1	19.8	16.7	22	23.8
9th	24.5	23.1	25.4	23.4	24.3	16.5	17.8	18.4	18.9	16.7	23.4	19.5
10th	26.3	23.8	22.4	17.1	26.8	16.1	17.5	14.8	21.3	21.2	18.1	18.7
11th	26.5	22.8	22.7	18.9	23.5	16.5	20	15.6	17.8*	17.7	19.5	20
12th	20.7*	23.9	22.5	19.9	18.5	17.4	17.5	14.7	20.1	15.5	22.1	22.6
13th	24.1	23.3	23.8	22.4	17.8	16.6	21.3	16	21.3	17	18.3	23.5
14th	21.3	23.7	23.9	22.8	16.6	17*	19.1	17.5	16.3	18.7	19.3	23.3
15th	23.2	24	24.3	23.1	18.1	19.8	17.2	19.5	16.7	23.7	22.2	24.4
16th	24.2	25.7	24.4	23	18	14.6	18.3	18	19.3	30.9	17.6	26.1
17th	24.9	25.2	20.3	21.4	18.7	18	19.4	19.8	17.1	19.3	20.4	21.7
18th	25.6	24.1	20.5	21.7	21.6	18.2	18.2	18.5	18.8	19.9	21.3	23.8
19th	24	25.7	21.9	22.2	20.4	19.1	13.7	17.2	19.1	25.7	18.3	30.3
20th	25	24.6	23.4	22.9	16.7	16.4	15.3	16.1	19.3	21.5	20.1	30.6
21st	25	22.9	23.7	23	21	18	14.8	18.2	24.3	26.8	22.8	22.6
22nd	23.9	22.8	18.8	24.6	20.7	17.2	15.3	23.8	18.8	15.5	18.8	23.7
23rd	23.5	25	24.1	21.5	21.2	15.8	14.8	26.7	21.1	17.9	21.1	26.6
24th	23.7	25.7	22.4	24.1	21	18	14.8	18.6	22.5	22.3	22.2	24.6
25th	22.9	24.6	20.7	18.1	18.1	18.8	17.7	18.7	18.4	23.6	24.6	19.9
26th	24.9	24	22.7	20.5	16.6	13.8	18.6	19.5	20.6	19.9	22.8	20.7
27th	23.5	24.9	22.6	20	16.8	14.5	17.2	18	22.7	17.1	21.2	22.9
28th	25.2	27.8	21.4	23.4	17.4	16.9	17.5	18.8	32.2	19.2	21.1	23.7
29th	25.7	20.8	23.1	17.4	17.1	19.1	14.7	20.4	21.7	20.5	24.1	22.6
30th	30.9		22.5	19	17.8	19.1	14.6	20.3	20.3		26.6	22.6
31st	23.5		24.7		17.4		14.3	18.1				25
Highest daily	30.9	27.8	26.3	26.6	26.8	20	21.3	26.7	32.2	31.6	28.7	30.6
Lowest daily	20.7	18	18.8	17.1	16.6	12.9	13.7	14.4	15.9	15.5	17.6	18.7
Monthly mean	24.3	23.4	22.5	22.2	19.6	16.9	16.5	18.3	20.5	21.2	21.3	23.5

Annual mean maximum temperature for 2012 = 20.5 °C

<sup>a</sup> Australian Government - Bureau of Meteorology.

\* Days of sample collection.

**Appendix A Illustrates weather data for Russell Vale and Botany Bay areas.**

**Table A-2:** Illustrates area daily maximum temperature for Botany Bay [Sydney Airport AMO (66037) -2011] <sup>a</sup>.

2011	Jan	Feb	Mar	Apr	May	Jun	Jul	Aug	Sep	Oct	Nov	Dec
1st	33.3	40.8	34.4	25	20.5	19.9	15.5	21.9	19.1	19	20.4	18.8*
2nd	25.4	32	22.9	21.5	19.8	19	19	22.5	16.8	16.9	22.3	18.7
3rd	21.2	36.7	31.7	23.7	18.5	20.6	20.8	25.9	20.7	16.2	18.4	22.3
4th	21.4	33.2	28.1	21	19.3	19.7	21.2	25.4	21.7	17.3	21.9	19.2
5th	23.9	42.2	21.9	20.7	17.6	18.2	17.9	25.2	22.6	19.1	24.8	17.7
6th	23.3	35	22.4	21.5	17.5	17.5	18.3	24.5	27	20.6	32.3	18.5
7th	26.2	21.8	24.8	22.2	21.3	15.3	17	20.5	18.1	21.8	28.9	20.5
8th	27.8	24.8	28.1	22.5	21.8	14.3	18	17.4	17.8	19.2	30.7	22.2
9th	27.7	25.4	32.1	27.5	16.4	17.2	17	16.9	12.9	24.1	32.4	23.9
10th	26.9	27	29.2	27.7	16.4	15.6	17.2	19.1	17	20.9	29.4	23.6
11th	26.8	33.9	25.7	22.6	17.1	15.7	17.3	16.2	19.4	20.4	23.7	28.2
12th	29.2	22.5	28.2	22.6	17	15.5	19.1	15.2	17.2	19.8	25.6	19
13th	27.4	22.3	29.8	24.8	21.4	16.9	13.6	18.4	23.6	19.7	25.1	22
14th	29.9	23.8	27.2	24.4	16.1	17.3	13.4	15.3	27.2	19.5	37.9	20.3
15th	30.5	25.5	23.4	20.8	19.4	18	12.8	17.1	20	23.5	27	22.3
16th	28.8	27.6	26.2	19.7	19.3	16.6	16.4	17.9	24.6	20.8	21.2	22.3
17th	29.9	30.2	24.4	21.4	17.5	19.1	16.5	17.7	23.9	18	22.3	22.5
18th	25.8	26.1	23.6	23.6	19.4	18	19.3	18.4	31.1	19.7	26	24.5
19th	25.6	32.5	23.4	24.7	21.6	18.8	15.2	17.2	25.9	23.2	31.4	24.4
20th	27.9	32.1	24.9	22.6	22.7	20.3	16.8	18.4	29.3	26.2	28.8	21.8
21st	29.1	25.1	26.8	26	24.1	21.6	14.4	17.7	21	30.7	23.6	22.7
22nd	30	20.6	29.7	25.7	23	16.4	14.1	17.5	22.7	25.8	22.3	22.6
23rd	30.1	23.5	31.5	18.6	24.2	19.5	13.9	16.8	32.1	25.6	18.6	25.6
24th	36.7	27.7	28	21.1	18.8	18.7	14.7	19.9	17.8	34.6	18.5	26.7
25th	29.6	29.5	25.5	19.9	14.3	19.4	18.6	21.6	17.3	18.4	20.2	28.2
26th	31.4	29.6	19.9	21	17.2	20.5	18.7	19.4	18.8	18.9	28	28.4
27th	29.4	32.2	20.3	19.4	17.6	18.1	15.3	20.1	21.2	20.4	28.5	21.7
28th	24.6	29	23.1	19.9	16.8	16.9	19.6	19.6	18.8	23.7	28.2	21.9
29th	26		26.7	19.8	16.4	18	19.9	21.9	22.8	28.9	27.6	22.7
30th	30.5		28.8	22.1	18.8	16.8	20.7	17.4	21.3	26.4	32.4	24.7
31st	35.6		21.2		20		20.4	18.8		19		23.9
Highest daily	36.7	42.2	34.4	27.7	24.2	21.6	21.2	25.9	32.1	34.6	37.9	28.4
Lowest daily	21.2	20.6	19.9	18.6	14.3	14.3	12.8	15.2	12.9	16.2	18.4	17.7
Monty mean	28.1	29	26.3	22.5	19.1	18	17.2	19.4	21.7	21.9	25.9	22.6

Annual mean maximum temperature for 2011 = 22.6 °C

<sup>a</sup> Australian Government - Bureau of Meteorology.

\* Days of sample collection.

**Appendix A Illustrates weather data for Russell Vale and Botany Bay areas.**

**Table A-3:** Illustrates area daily maximum temperature for Botany Bay [Sydney Airport AMO (66037) -2012] <sup>a</sup>.

2012	Jan	Feb	Mar	Apr	May	Jun	Jul	Aug	Sep	Oct	Nov	Dec
1st	27.6	22	30.6	25.1	23	18.3	17.1	14.3	15.7	20.1	34.2	36.2
2nd	28.5	20.2	21.2	24.5	25.5	16.6	16.4	15.2	20.2	20	19.1	22.8
3rd	29	21.2	22.6	28.6	20.7	15.7	15.4	19.2	19.7	30.9	18.4	22.9
4th	34.1	25.3	28.1	27.3*	21.1	20.5	14.7	21	22.8	33.6	23.8	30.3
5th	26.1	29.1	24.9	28	18.9	16.5	14	22.6	29	35.6	27	26.1
6th	21.9	22.9	21.9	27.1	21.8	15.4	14.2	18.2	28.6	19.8	28.2	22.1
7th	26.5	24.4	21.1	27.4	19	15.9	14.5	19	22.9	18.4	25.5	23.9
8th	28	23.7	21.6	25	22	16	17	22.1	21.1	18.3	25.5	28.4
9th	26.2	26.4	28.1	25	26.9	17.2	18.6	20	19.7	18	27	24.3
10th	28.6	27	24.7	17.4	27.5	14.7	19.4	14.3	24.7	25.1	19.9	20.5
11th	29.3	24.3	24.4	18.3	27.3	17.2	20.8	14.6	19.1	20	21.7	20.5
12th	21.3	25.7	25.4	20.6	20.4	18.9	18.4	14	22.9*	15.8	25.2	26.2
13th	27.1	25.6	27.2	25.9	18.1	15.3*	23.7	17.1	24.2	18.3	20.5	28.4
14th	22.7	25.1	26.5	26.1	16.5	19.1	20.8	20.1	17.2	19.4	22	27.9
15th	24.2	25.7	28.5	25.6	18.2	21.5	18.6	22.1	17.3	27.4	26.5	28.2
16th	24.9	28.4	31.3	22.5	18.6	14.8	18.9	19.8	21.9	34.7	17.9	34.1
17th	26.9	28.7	21	21.6	21.3	19.3	21.3	22.6	19.7	21.6	21.4	23.7
18th	29.3	25	22	21.7	22.8	18.8	21.3	19.1	22.2	23.7	25.1	26.9
19th	24.9	28.7	24.4	24.9	22.2	19.3	14.2	17.9	23	28.8	19	32.9
20th	26.4	25.3	24.9	27	16	18.4	15.3	19.7	22.4	30.2	22.5	34.6
21st	25.5	23.7	26.5	23.6	21.4	19.2	14.8	22.3	25.8	28.3	25.5	24.6
22nd	26.4	24	19.9	25.2	21.4	18.7	16.4	25.1	20.8	16.9	19.9	28
23rd	25.6	29.7	26	21	22.9	17.1	17.3	30	25.3	19.2	22	31.6
24th	24.3	29.3	23.7	26	17.3	18.3	14.4	20.5	24.4	24	26.7	31.6
25th	26	28.6	22.3	20	19.6	20.4	19.7	20.2	20	28.9	33.1	20.7
26th	27.7	28.6	25.1	19.9	17.8	14.1	20	18.9	22.3	22.9	25	22.3
27th	25.9	30.3	26.3	20.5	17.1	15.1	18.6	20.3	25.1	19.4	23.9	24.7
28th	27	34.3	23.5	24.1	16.8	18.5	17.9	20.5	34.1	20.2	23.4	31.3
29th	28.9	22.5	26.2	18.8	16.6	20.5	15	23.4	23.6	23	29.4	24.5
30th	34.6		23.2	20.3	17.3	20.6	14.2	23.3	21.2	24.7	32.8	24.8
31st	27.4		28.2		17.5		13.9	19.3		28.9		29.3
Highest daily	34.6	34.3	31.3	28.6	27.5	21.5	23.7	30	34.1	35.6	34.2	36.2
Lowest daily	21.3	20.2	19.9	17.4	16	14.1	13.9	14	15.7	15.8	17.9	20.5
Monthly mean	26.9	26.1	24.9	23.6	20.4	17.7	17.3	19.9	22.7	23.7	24.4	26.9

Annual mean maximum temperature for 2012 = 22.1 °C

<sup>a</sup> Australian Government - Bureau of Meteorology.

\* Days of sample collection.



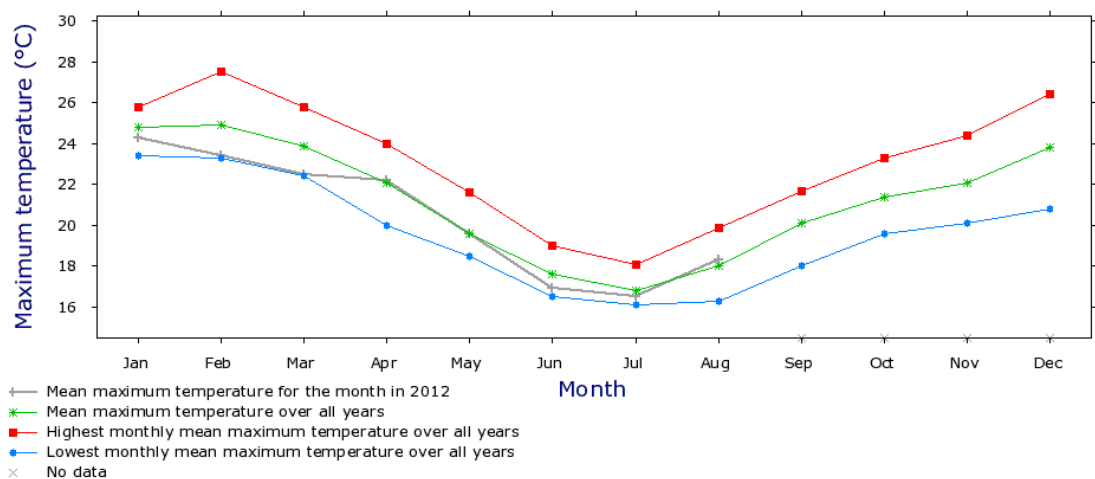


**Figure A-1:** Illustrates monthly maximum temperature for Russell Vale area [Bellambi AWS (68228) - 2012].

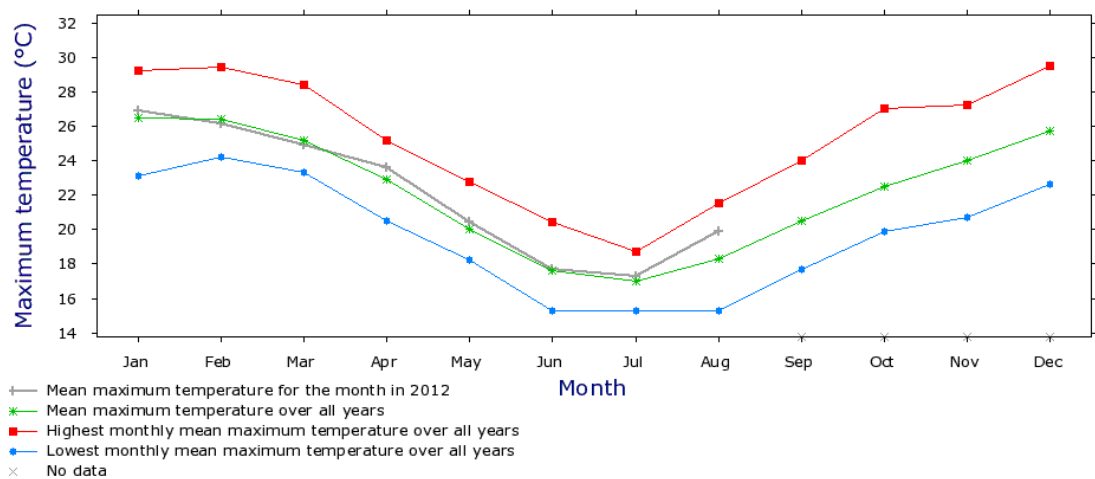


**Figure A-2:** Illustrates monthly maximum temperature for Botany Bay area [Sydney Airport AMO (66037) -2012].

**Appendix A Illustrates weather data for Russell Vale and Botany Bay areas.**

**Table A-4:** Illustrates daily rainfall for Russell Vale area [Bellambi AWS (68228)] <sup>a</sup>.

2012	Jan	Feb	Mar	Apr	May	Jun	Jul	Aug	Sep	Oct	Nov	Dec
1st	0	16.4	88.6	0	0	0	0	0	3.4	0		2
2nd	0	20.2	20	10.4	0	0.2	0	0	0	0	0	0
3rd	0	36.4	3	0*	5.8	17.2	0	0	0	0	3.8	2.8
4th	0	22.6	5.4	0	0	3.4	0	0	0	0	2.8	0
5th	0	0	5	0	0	0.4	0.2	0	0	0	0	0
6th	1.4	0	2.8	0	0.8	24.4	19.8	0	0	4	0	0
7th	0	0.4	8.2	0	0	6.2	0.4	0	0	11.8	3	0
8th	0.4	1.4	78.6	0	0	0	0	0	0.2	0	1	0
9th	8.8	20.2	16.2	4.6	0	0	0	0	0	3.4	14.8	0
10th	0	35.2	0.4	1.2	0	0	0	0	0	0	0.6	0.6
11th	0	17.8	0	0	0	50.4	8	0	0*	1	0	0.6
12th	0*	2	0	11.8	0	18.2	0	0.2	0	19	0	1.8
13th	0	5.8	0.2	0	0	10.2	0.2	0	0	30.4	0	0
14th	7.6	16	0	0	0	10.8*	0	0	7.2	11.2	1.2	0
15th	33.2	4.4	0	0	0	0	0	0	0	0	0.2	0
16th	17.8	0	0	0	0	0	0	0	0	0	0.8	0
17th	1.2	0	10.6	2.4	0	12	0	0	0	0	8	0
18th	0	4.4	1.2	54.4	0	0	0	0	0	0	0	0
19th	0	0	0.4	53.8	0	0	0	0	0	0	0	0
20th	0	28	0	3.2	1	0	0	0	0	0	3.6	0
21st	0.2	16.6	0	0	0	0	0	0	0.2	0	0	0
22nd	0	0	0	0	0.6	0	0.8	0	0	2.4	0	0.2
23rd	3.2	0	1.4	0	0	0	6.6	0.6	0	9.2	0	0
24th	0.2	0	0	0	0	0	4.6	5.4	0	0	0	0
25th	5	0	0	2.4	8.6	0	0	0	0	0	0	14.8
26th	31	0	0	0	0	0.4	0	0	0	0	0	9
27th	10.4	0	0	0	0	10	7.6	0	0	0	0	0
28th	0.4	0	0.2	0	0	0.8	0.4	0	0.4	0	10.8	0
29th	0	64	1.4	0.6		0	0	0	7.6	0	0	0
30th	0.6		0	1	0	0.2	0	0	0	0	0	0.6
31st	0		0		0		0	0				1.8
Highest Daily	33.2	64	88.6	54.4	8.6	50.4	19.8	5.4	7.6	30.4	14.8	14.8
Monthly Total	121.4	311.8	243.6	145.8	16.8	164.8	48.6	6.2	19	92.4	50.6	34.2

Annual total for 2012 = 1255.2 mm

<sup>a</sup> Australian Government - Bureau of Meteorology.

\* Days of sample collection.

**Appendix A Illustrates weather data for Russell Vale and Botany Bay areas.**

**Table A-5:** Illustrates daily rainfall for Botany Bay area [Sydney Airport AMO (66037) -2011] <sup>a</sup>.

2011	Jan	Feb	Mar	Apr	May	Jun	Jul	Aug	Sep	Oct	Nov	Dec
1st	0	0	0.6	1.4	1	7.8	2.2	0	0	0	0	9.8*
2nd	0	0	0	0	0	0.6	4.6	0	0	7	0	4
3rd	2.4	0	0	0	0.2	0	0	0	0	6.4	12.2	0
4th	3	0	0	0	0.4	0	0	0	0	0.6	4	0
5th	0	0	0.8	19.6	0	0.8	0	0	0	0	0	2.4
6th	0	0	0.2	8.2	0	0	0	0	0	0	0	6.2
7th	2.8	0.6	0	5.8	0	0	0	0.2	1	1.4	0	0.2
8th	5.6	0	0	0	0	0	0	3	0	3.2	1.8	21.2
9th	11.4	0.8	0	0	0	0	0	0	2.8	0	29	1
10th	5	0	0	0	3.6	0	0	0	2.2	0	0.4	0
11th	3.4	0	0	6.8	0	5.6	0	0	0	0	0.2	0
12th	1.8	1	1.6	0	0	10.4	0	9	0.2	0	0	37.8
13th	0	10.4	0	0	0	5.8	0	1.6	0	2.2	0	4.2
14th	0	0	0	0	0	2.2	0	3.2	0	0	0	0.2
15th	0.2	0.6	0.2	0	0	6.6	0.6	0.2	0	18.4	0	0.6
16th	0	0	0.4	40.8	0	4.8	4.6	0	0	0	0	0
17th	0	0	1.2	17.8	0	0	1.8	4	0	2.2	10.6	0
18th	0	0	0.6	0	0	0	0	6.4	0	0	1.6	0
19th	0.4	0	14.4	0	1.2	0	0	0.6	0	0	0	0
20th	0	0	106	0	0	0	60.2	11.8	0	0	0	9
21st	2.2	0.2	18.6	0	0	0	36.8	0	0	0	3	0
22nd	0	0	17.6	0	0	0	91	0	0	0	5.2	0.8
23rd	0	0.4	6.4	4.2	0.8	0	47.4	0.2	0	0	37.4	4
24th	0	0	0	12.8	0	0	1	0.6	0.2	0	11.4	9.8
25th	0	0	0	4.6	8.8	0	0	0	22.8	1.6	7	0
26th	0	0	0	3	9.2	0	0.2	0	19.8	3.2	23.6	0
27th	0	0	1.8	4.6	0	0	0	0	0	1.2	4.4	0.2
28th	0	0.4	5.2	30.2	0	0	0	0	0	0	0	0
29th	0		6.2	16.4	0	1.4	0	0	5	0	0	0
30th	0		0	34.8	22.4	2	0	0	1.2	0	0	1.8
31st	0		1.6		49.6		0	0		0.2		0.2
Highest Daily	11.4	10.4	106	40.8	49.6	10.4	91	11.8	22.8	18.4	37.4	37.8
Monthly Total	38.2	14.4	183.4	211	97.2	48	250.4	40.8	55.2	47.6	151.8	113.4

Annual total for 2011 = 1251.4 mm

<sup>a</sup> Australian Government - Bureau of Meteorology.

\* Days of sample collection.

**Appendix A Illustrates weather data for Russell Vale and Botany Bay areas.**

**Table A-6:** Illustrates daily rainfall for Botany Bay area [Sydney Airport AMO (66037) -2012] <sup>a</sup>

2012	Jan	Feb	Mar	Apr	May	Jun	Jul	Aug	Sep	Oct	Nov	Dec
1st	0	8	23.6	0	0	0	0	0	0.6	0	0	1.2
2nd	0	3	8.4	1.2	0	0.2	0	0	1	1.4	0	0
3rd	0	40.2	8	0	0	32.2	0	0	0	0	6.2	1
4th	0	5.8	2.4	0*	0	11.8	0	0	0	0	0.8	0.6
5th	0	0	13.4	0	0	0	3.4	0	0	0	0	0
6th	5	0	0	0	0	20.2	21	0	0	0	0	0
7th	0	1.8	0	0	0	4.8	1.2	0	0	1.6	0	0
8th	0	0.6	83.6	0	0	0	0	0	0	0	0	0
9th	8.2	0.6	12.4	5	0	0	0	0	0	4	7.6	0
10th	0	1.8	0	0	0	2.8	0	0	0	0	4.4	0.2
11th	0	9.4	0	0	0	50.4	8.2	3.2	0	7.2	0	0
12th	0	3.8	0	3.8	0	41.6	0	3	0*	3.2	0	2.2
13th	0	2	0	0	0	12.2*	0	0.2	0	4.4	0	0
14th	0.8	0	0	0	0	6.2	0	0	2	0	2.8	0
15th	32.2	0.6	0	0	0	0	0	0	0	0	0	0
16th	8.8	0	0	0	0	0.2	0	0	0	0	1	0
17th	2.6	0	26.2	11.2	0	8.8	0	0	0	0	6.2	0
18th	0.2	1.4	3.4	31	0	0	0	0	0	0	0	0
19th	0	0	5	63.2	0	0	0	0	3	0	0	0
20th	0	53.6	4.8	2.2	0	0	0	0	0	0	3	0
21st	0	1.6	0	0.2	11	0	0.2	0	0	0	0	0
22nd	7.4	0	0	0	0	0	6	0	1.4	0	0	0.2
23rd	0.2	0	2.2	0.6	0	0	0.6	0	0	1.6	0	0
24th	0	0	0	2.6	0	0	6.6	6.2	0	0	0	0
25th	4.8	0	0	0	10.2	0	3.4	0	0.2	0	0	4.4
26th	35.2	0	0.6	0	0	0.6	0	0	0.2	0	0	16.8
27th	3.6	0	0	0	0	5.6	0	0	0	0	0.4	0
28th	0	0	0	0	0	0	0	0	0	0	8.6	0
29th	0	3.8	5.4	0	7.2	0.6	0	0	11.6	0	0	0
30th	1.6		0	0	0.8	0	0	0	0	0	0	0
31st	0		0		0		2.8	0		0		0
Highest Daily	35.2	53.6	83.6	63.2	11	50.4	21	6.2	11.6	7.2	8.6	16.8
Monthly Total	110.6	138	199.4	121	29.2	198.2	53.4	12.6	20	23.4	41	26.6

Annual total for 2012 = 973.4 mm

<sup>a</sup> Australian Government - Bureau of Meteorology.

\* Days of sample collection.

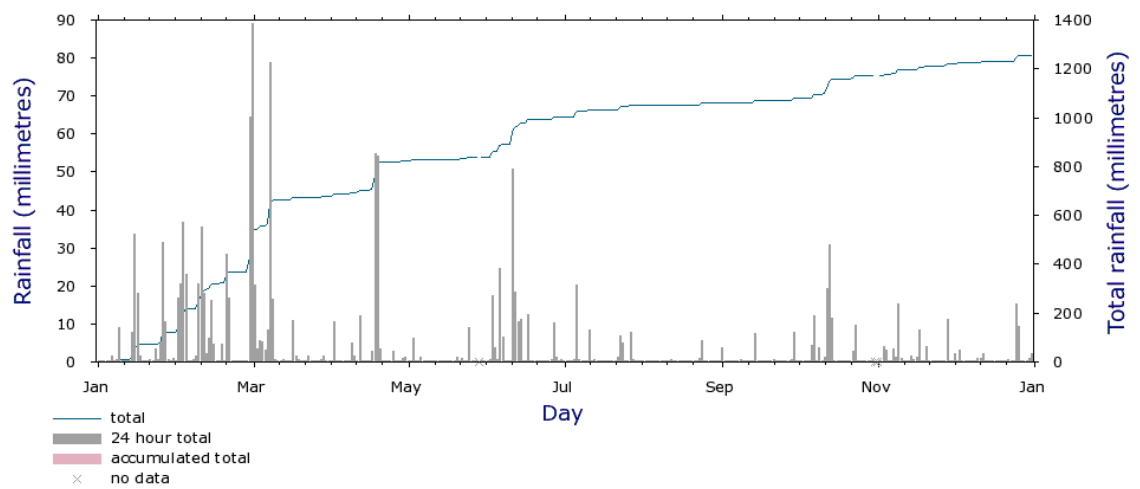


**Figure A-3:** Illustrates monthly rainfall for Russell Vale area [Bellambi AWS (68228) - 2012].

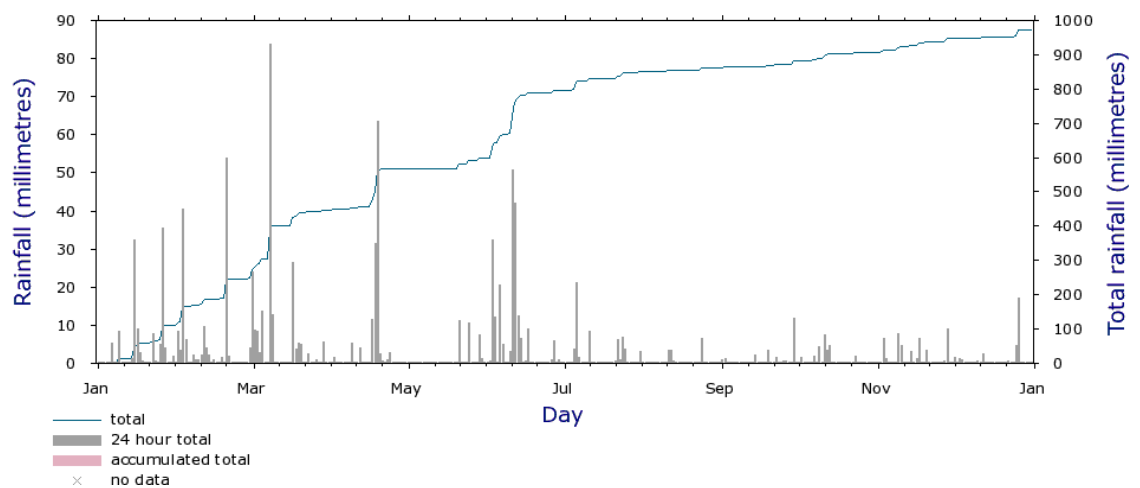


**Figure A-4:** Illustrates monthly rainfall for Botany Bay area [Sydney Airport AMO (66037) -201

**Appendix B : IMAGES OF THE NF-90 AND ESPA2 MEMBRANES FOULED BY LEACHATE POND AT RUSSELL VALE AND WGB32 AT BOTANY BAY IN DIFFERENT SEASONS.**



**Figure B-1:** Image of the NF-90 membrane surface fouled by leachate pond at Russell Vale-autumn

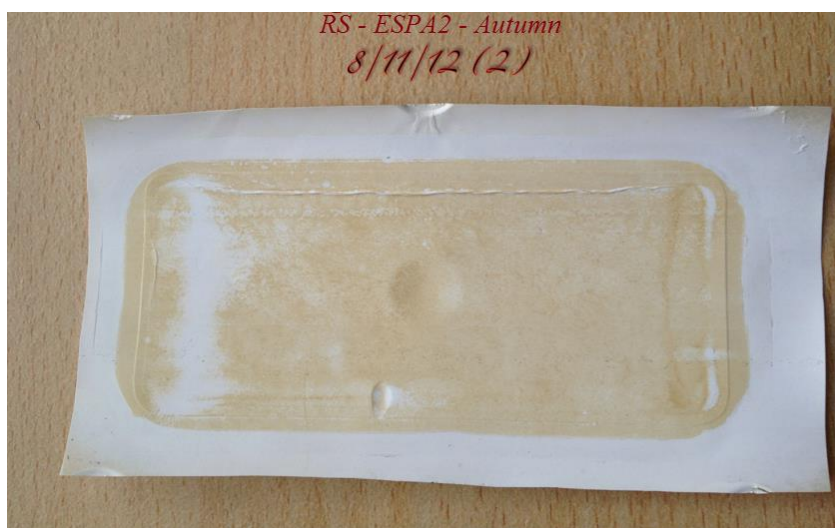


**Figure B-2:** Image of the ESPA2 membrane surface fouled by leachate pond at Russell Vale-autumn.

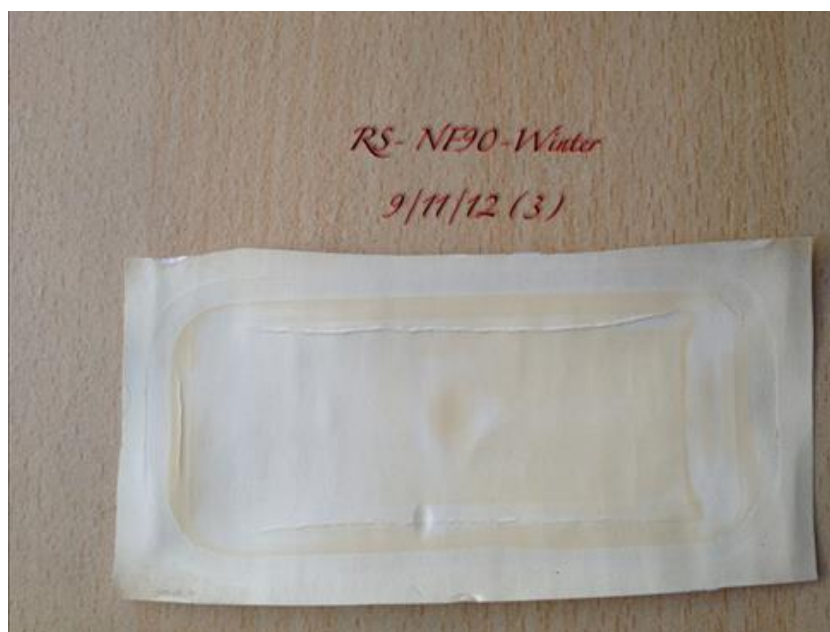


**Figure B-3:** Image of the NF-90 membrane surface fouled by leachate pond at Russell Vale-winter.

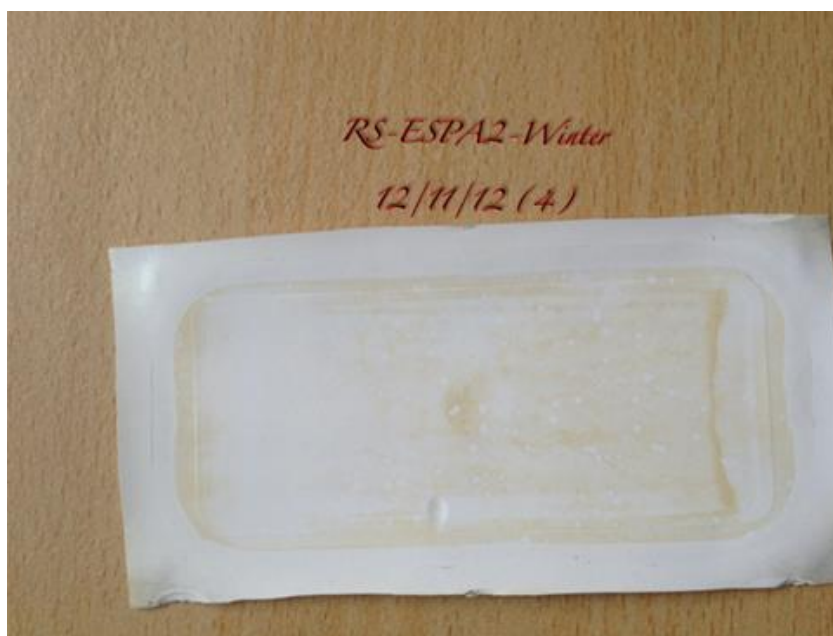


**Figure B-4:** Image of the ESPA2 membrane surface fouled by leachate pond at Russell Vale-winter.



**Figure B-5:** Image of the NF-90 membrane surface fouled by leachate pond at Russell Vale-spring.

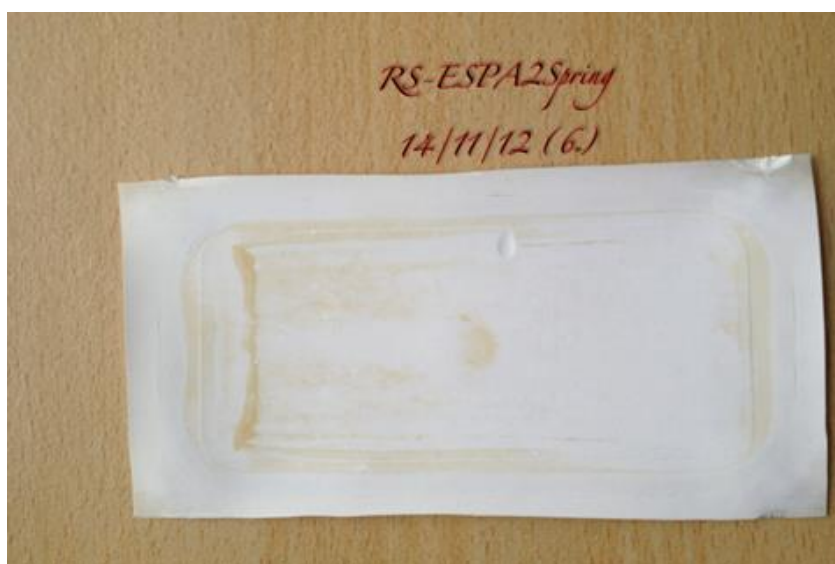


**Figure B-6:** Image of the ESPA2 membrane surface fouled by leachate pond at Russell Vale-spring.



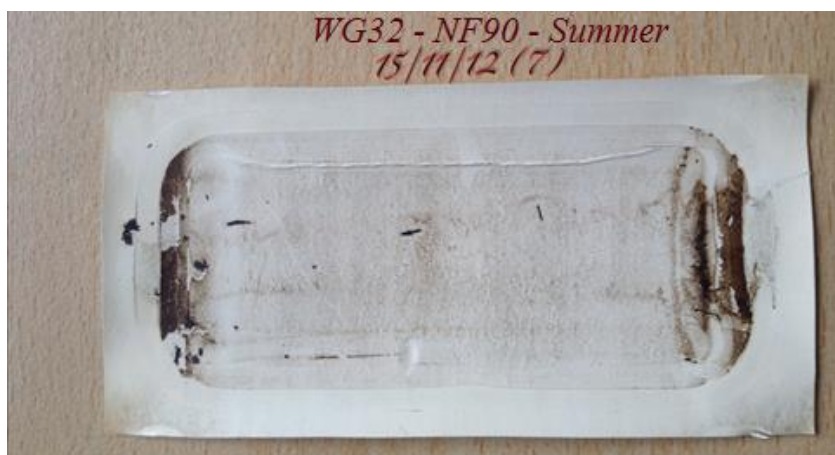


**Figure B-7:** Image of the NF-90 membrane surface fouled by WG32 at Botany Bay-summer.



**Figure B-8:** Image of the NF-90 membrane surface fouled by WG32 at Botany Bay-autumn.



**Figure B-9:** Image of the ESPA2 membrane surface fouled by WG32 at Botany Bay-autumn.



**Figure B-10:** Image of the NF-90 membrane surface fouled by WG32 at Botany Bay-winter.



**Figure B-11:** Image of the ESPA2 membrane surface fouled by WG32 at Botany Bay-winter



**Figure B-12:** Image of the ESPA2 membrane surface fouled by WG32 at Botany Bay-summer.

**Appendix C : IMAGES OF FIELD EMISSION SCANNING ELECTRON MICROSCOPY (SEM).**

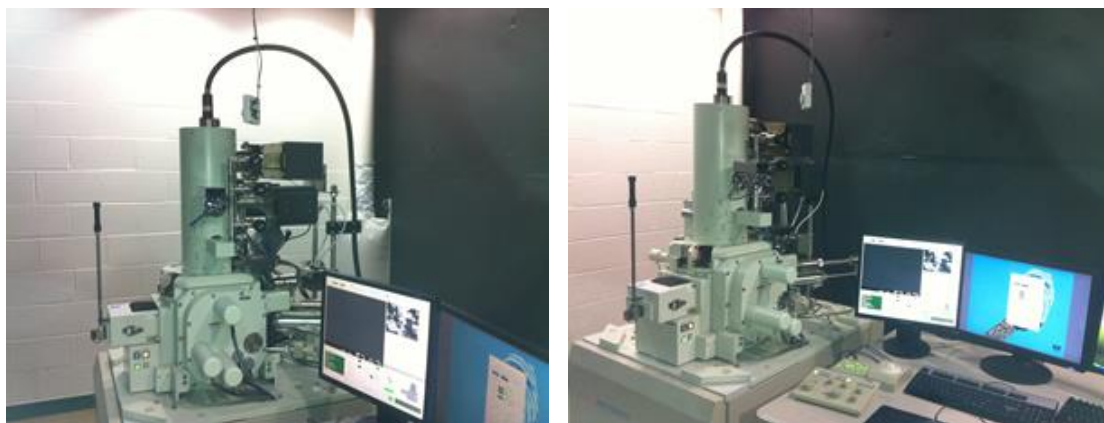


**Figure C-1:** Images of Field Emission Scanning Electron Microscopy (SEM) using a JEOL JSM-7500FA - (BRUKER-QUANTAX 400).